AD NUMBER

AD908453

LIMITATION CHANGES

TO:

Approved for public release; distribution is unlimited.

FROM:

Distribution authorized to U.S. Gov't. agencies only; Test and Evaluation; 23 MAR 1973. Other requests shall be referred to Army Missile Command, Redstone Arsenal, AL.

AUTHORITY

DARPA Itr, 27 Jun 1973

191300-1-P

Semiannual Technical Report

INVESTIGATIONS OF CHEMICAL LASER PROCESSES

1 January 1972 Through 30 June 1972

GEORGE H. LINDQUIST
ROBERT E. MEREDITH
CHARLES B. ARNOLD
FREDERICK G. SMITH
ROBERT L. SPELLICY
Infrared and Optics Division

FEBRUARY 1973

ENVIRONMENTAL
RESEARCH INSTITUTE
OF MICHIGAN
FORMERLY WILLOW RUN LABORATORIES,
THE UNIVERSITY OF MICHIGAN

Sponsored by the Advanced Research Projects Agency,
Department of Defense, Washington, D. C.

ARPA Order No. 1180

Contract No. DAAH01-72-C-0573

NOTICES

Sponsorship. The work reported herein was conducted by the Environmental Research Institute of Michigan (formerly Willow Run Laboratories of the University of Michigan) for the Advanced Research Projects Agency, Department of Defense, Washington, D.C. 20301. Contracting Officer is Dr. Fred Haak of the ARPA Support Office, Army Missile Command, Huntsville, Alabama under Contract No. DAAH01-72-C-0573, ARPA Order No. 1108. Technical Monitor is Edward T. Gerry. Contracts and grants to the Institute for the support of sponsored research are administered through the Office of Contracts Administration.

Distribution. Initial distribution is indicated at the end of this document.

DDC Availability. Qualified requesters may obtain copies of this document from:

Defense Documentation Center
Cameron Station
Alexandria, Virginia 22314

Final Disposition. After this document has served its purpose, it may be destroyed. Please do not return it to the Environmental Research Institute of Michigan.

191300-1-P

Semiannual Technical Report

INVESTIGATIONS OF CHEMICAL LASER PROCESSES

1 January 1972 Through 30 June 1972

GEORGE H. LINDQUIST
ROBERT E. MEREDITH
CHARLES B. ARNOLD
FREDERICK G. SMITH
ROBERT L. SPELLICY
Infrared and Optics Division

FEBRUARY 1973

ENVIRONMENTAL
RESEARCH INSTITUTE
OF MICHIGAN
FORMERLY WILLOW RUN LABORATORIES,
THE UNIVERSITY OF MICHIGAN

FOREWORD

An investigation of fundamental molecular processes in support of laser system design was begun at the Environmental Research Institute of Michigan, formerly the Willow Run Laboratories of the Institute of Science and Technology, The University of Michigan for the Advanced Research Projects Agency under Contract No. DAHC-15-67-C-0062. The current effort is a continuation of this work performed under Contract No. DAAH01-72-C-0573. This current work concerns transition probabilities for several molecules and the transfer of vibrational and rotational energy between HF molecules. The work was performed with R. E. Meredith as Principal Investigator for approximately six months. Dr. Meredith left The University of Michigan on 1 June 1972, and at this time Mr. George Lindquist became Principal Investigator. Director of the program is R. R. Legault. Contracting Officer is Dr. Fred Haak of the ARPA Support Office, Army Missile Command, Huntsville, Alabama. The Institute number for this report is 191300-1-P.

The authors wish to thank Robert Turner for his contributions. The authors of Section 5 wish to acknowledge the cooperation of The University of Michigan Physics Department. Particular thanks are due to Professor C. W. Peters for his interest and helpful discussion.

The contract expired 31 December 1972.

ABSTRACT

A complete set of electric dipole transition probabilities for HCl has been computed by means of a numerical procedure developed previously. To produce these computations, the dipole moment and internuclear potential for the HCl molecule were modeled with the available experimental data. The results are presented in tabular form for vibrational quantum states from 0 to 12, for changes in vibrational states between 0 and 5, and for all rotational states between 0 and 35. Progress on experimental measurements of the intensity of the v = 0 to v' = 4 band of CO are included as well as progress on an experiment to measure rotational relaxation in an excited cell of HF.

Measurements of the strengths and widths of lines in the v = 0 to v' = 3 band of HF are reported. This work was begun under an earlier contract with the Advanced Research Projects Agency, and was completed under the current contract. The electric dipole matrix element for the band has been determined from the measured strengths to be 1.628×10^{-21} esu-cm. The rotational dependence of the measured half widths agrees with the Anderson theory of collision broadening if off-resonant collisions are taken into account. A complete code has been written to compute line widths resulting from collision broadening. A section describing this program is included. Sample calculations which show good agreement with available experimental data are presented.

CONTENTS

FIGURES

TABLES

SYMBOLS

A	area
A_{uf}	coefficient for spontaneous emission
A_{vi}	elements of 2 dimensional matrix A, equal to $\int \psi_0 \rho^i \psi_v r^2 dr$
b	impact parameter
b_0	impact parameter where $\mathcal{P}(b) = 1$
b_{min}	radius corresponding to the minimum cross section
$B_{jvv'}$	elements of 3 dimensional matrix B, equal to $\int \psi_{v'} \rho^j \psi_v r^2 dr$
B_{fu}	coefficient for stimulated absorption of radiation
B_{uf}	coefficient for stimulated emission of radiation
B_v	vibrationally dependent rotational constant
B_0	rotational constant in the v = 0 state
B_1	rotational constant in the v = 1 state
c	velocity of light
C_λ^κ	constant in the expression for collision Hamiltonian
$C_{iv'v}$	elements of 3 dimensional matrix C, equal to $\sum_j B_{jv'v} A_{ji}^{-1}$
C_s	coefficients for multipole-multipole interactions
C_v	linear coefficient for F factor
D^*	dimensionless detectivity $\left(\text{cm}\sqrt{\text{sec}^{-1}}/\text{watt}\right)$
D_e	energy difference between the dissociation limit and the bottom of the potential well
D_0	energy difference between the dissociation limit and the v = 0 level
D_v	quadratic coefficient for F factor
E_a	energy of state a
E_{uf}	energy difference between upper and lower state
$f_s(k_{st})$	resonance factor
$F^{v'v}(J)$	vibration-rotation interaction factor (Herman and Wallis F factor)
g_2	degeneracy of the state of the perturbing molecule
g_f	degeneracy of the lower state
g_{fs}	degeneracy of lower level of stimulating transition
g_{st}	transition factors
g_u	degeneracy of the upper state
g_{u_s}	degeneracy of upper level of stimulating transition

G_J	rotational energy in cm^{-1}
G_v	vibrational energy in cm^{-1}
$G(v, J)$	vibration-rotation energy in cm^{-1}
h	Planck's constant
$\hbar$	$h/2\pi$
H	collision Hamiltonian
H_C	time dependent collision Hamiltonian
H_I	interaction Hamiltonian
H_{IR}	Hamiltonian for interaction between radiating molecule and radiation field
H_0	unperturbed Hamiltonian
H_R	radiation Hamiltonian
H_1	Hamiltonian for radiating molecule
H_2	Hamiltonian for perturbing molecule
J	initial rotational quantum number of absorbing or emitting molecule
J'	final rotational quantum number of absorbing or emitting molecule
J_s	rotational level of lower state of stimulating laser
$J_,$	quantum numbers of absorbing molecule in lower state after a collision with a perturber
$J'_,$	quantum numbers of absorbing molecule in upper state after a collision with a perturber
J_2	rotational quantum number of perturber before collision
$J_{2'}$	rotational quantum number of perturber after collision
k	Boltzmann's constant
k_{st}	dimensionless energy defect of a near resonant collision
$\bar{k}_\Omega$	unit vector in Ω direction
k_0	k_{st} evaluated at b_0
K^P	peak absorption coefficient
$K(\nu)$	spectral absorption coefficient
ℓ	path length in cm
$\bar{\ell}$	unit vector normal to area element dA
L	radiance (photons/sec cm^2 sr)
L_ν	spectral radiance (photons/sec cm^2 sr sec^{-1})
L^*	dimensionless length, $xG\eta(0, x)$
L^*_T	L^* associated with x_T
m	rotational index, -J for P branch, +J' for R branch
M_l	dipole moment expansion coefficients

$\mathcal{M}$	molecular mass
M	initial magnetic quantum number of absorbing or emitting molecule before collision
M_1	initial magnetic quantum number of absorbing or emitting molecule after collision
M'	final magnetic quantum number of absorbing or emitting molecule before collision
M_1'	final magnetic quantum number of absorbing or emitting molecule after collision
M_2	magnetic quantum number of perturber before collision
$M_{2'}$	magnetic quantum number of perturber after collision
n_{J_i}	population of molecules in rotational state J_i
n_{J_2}	population of perturber molecules with the J_2 state state
n_ℓ	population of lower state ($1/cm^3$)
n_{ℓ_ν}	spectral population of lower state ($1/cm^3\ sec^{-1}$)
n_u	population of upper state ($1/cm^3$)
n_{u_ν}	spectral population of upper state ($1/cm^3\ sec^{-1}$)
n_s	state density
N	sum of n_ℓ and n_u
N_ν	sum of n_{ℓ_ν} and n_{u_ν}
P	absorbing gas pressure in atmospheres
P_{ab}	probability of transition from state a to state b
P_0	total laser pulse photon density per unit area (photons/cm^2)
P^*	dimensionless laser pulse energy per unit area $P_0 H/N_\nu \Delta\nu c$
$P^*_{.1}$	dimensionless energy per unit area required to drive η at far end of cell to 0.1 its original value
Q	quadrupole moment of radiating molecule
Q_2	quadrupole moment of perturbing molecule
r	internuclear distance
r_e	equilibrium internuclear distance
ρ	position vector of the field point
ρ'	position vector of the source point
$R_{v'v} = R^{v'v}$	rotationless dipole matrix elements
s_ℓ	Doppler spectral distribution of n_{ℓ_ν}
s_u	Doppler spectral distribution of n_{u_ν}

S	line strength ($atm^{-1}\ cm^{-2}$)
$S_{vv'}(m)$	line strength corresponding to rotational index m in the $v \rightarrow v'$ band
$\mathscr{S}(b)$	collision amplitude
$\mathscr{S}_0, \mathscr{S}_1, \mathscr{S}_2$	0-th, first and second order terms in expansion for $\mathscr{S}$
S	$U(+\infty, -\infty)$
t	time
t	index for the various possible collision combinations
T	temperature
T	transition operator
T_0, T_1, T_2	0-th, first and second order terms in expansion of T
u	relative velocity
$\bar{u}$	mean relative velocity
U	unitary time operator
v	initial vibrational quantum number of radiating molecul
v'	final vibrational quantum number of radiating molecule
v_D	vibrational quantum number associated with the dissociation limit
V	volume
V	interaction potential
w	general transition rate
w_{ba}	transition rate from state a to state b
x	distance along laser line of sight in active medium
x_T	cell length
Y_{ij}	Dunham coefficients for energy levels
Y_λ^k	spherical harmonics
z	vibration-rotation partition function
Z_1	$N_\nu g_\ell B_{\ell u}$
Z_2	$cN_\nu(B_{\ell u} + B_{u\ell})$
α^P	peak absorptance for a line
$\alpha(\nu')$	spectral absorptance
γ	line half width in cm^{-1}
γ_D	Doppler line halfwidth
Γ_v	one-dimensional matrix containing overtone matrix elements
ΔE	energy change of radiating molecule because of collision
ΔE_2	energy change of perturber because of collision
Δt	pulse duration
η	dimensionless number density difference $\left(\frac{n_\ell}{g_\ell}_\nu - \frac{n_u}{g_u}_\nu\right)/N_\nu$

κ	general wave number
$\lambda_1, \lambda_2, \lambda_1, \lambda_2$	internal coordinates of the collision partners
$\mu(r)$	dipole moment
μ_2	dipole moment of perturber
μ_0	dipole moment at $r = r_e$
ν	spectral frequency (sec^{-1})
ν'	spectral wavenumber (cm^{-1})
ν_0	spectral frequency of line center (sec^{-1})
ρ'	deviation of spectral directional photon density from equilibrium value
ρ_ν	spectral photon density (photons/cm^3 sec^{-1})
$\rho_{\nu,\Omega}$	spectral, directional photon density (photons/cm^3 sec^{-1} sr)
$\rho^\bullet_{\nu,\Omega}$	equilibrium (blackbody) spectral, directional photon density
σ	collision cross section
σ_r, σ_i	real and imaginary parts of the collision cross section
$\tau(\nu')$	spectral transmittance
Φ	dimensionless photon density, ρ_ν / N_ν
ψ_v	radial wave function for state v, J = 0
$\psi_{v'}$	radial wave function for v', J = 0
$\psi_{v,J}$	radial wave function for state v, J
ψ	quantum mechanical wave function
$\mathcal{N}$	radiation field vector
Ω	two dimensional angular direction

INVESTIGATIONS OF CHEMICAL LASER PROCESSES

1 January 1972 Through 30 June 1972

1
INTRODUCTION AND SUMMARY

The primary tasks of the current program have been: (1) to increase the knowledge of the transition probabilities for the hydrogen halide and for carbon monoxide molecules (Task I); and (2) to measure the relaxation rates in an excited cell of HF (Task II).

1.1 TASK I: MATRIX ELEMENT DETERMINATIONS

In earlier work electric dipole moment matrix elements were calculated for HF and DF for transitions expected to be important in HF and DF lasers [1]. CO lasers show promise of high output, and hence matrix elements are to be computed for this molecule. Other hydrogen halides have also shown lasing action in their vibration-rotation bands and are thus also worthy of consideration. The present effort consists of:

(1) Modeling the electric dipole moment for CO and for hydrogen halides and computing their electric dipole matrix elements for the vibration-rotation transitions expected in lasing action.

(2) Making absorption line-strength measurements in the second and third overtone bands of CO ($v = 0 \rightarrow v = 3$ and $v = 0 \rightarrow v = 4$) to be used in refining the dipole moment model for CO in (1) (v is the vibrational quantum number).

To date, we have completed the dipole moment modeling and matrix-element calculations on HCl only. General results of these calculations are summarized below and more specific details are presented in Section 2.

We modeled the HCl potential and dipole moment using existing spectroscopic data. These models produce matrix elements and hence transition probabilities which result in agreement within experimental accuracy with the measured transition probabilities. The latter are available only for vibrational levels up to $v = 3$. These models were used to calculate the transition probabilities for transitions involving vibrational levels up to $v = 12$. The accuracy of the results of these calculations are undetermined for vibrational levels above $v = 3$ because the relationship between the dipole moment expansion used and the actual dipole moment at the large internuclear separations, which occur at the higher v levels, is unknown. However, the transition probabilities for levels somewhat above $v = 3$ (e.g., $v = 4$, 5, and 6) are probably reasonably accurate extrapolations.

An original objective was to measure absorption line strengths (or, equivalently, electric dipole matrix elements) in the second overtone band of CO. However, since results have been published for this band for near-Doppler lines [2], we will perform measurements primarily on the third overtone band, returning to the second overtone to determine Lorentz widths if scheduling permits it.

Present plans are to determine individual vibration-rotation line strengths and Lorentz half widths in the $v = 0 \rightarrow v = 4$ band of CO for gas pressures near 2 atm. Path lengths on the order of 200 m will be used. The experimental preparations are going well and we expect to encounter no problems in the completion of this portion of the program. The progress of this effort is reported in detail in Section 2.3.

The CO molecule will be modeled during the second half of the contract period when we have the outcome of the experimental intensity measurements. The results of the experimental strength and matrix-element determinations and the calculations for CO will be included in the final report.

1.2. TASK II: MOLECULAR ENERGY TRANSFER RATES

Because of the various processes which compete with a laser action, in the design and operation of chemical lasers, it is necessary to know the rates at which energy in the various degrees of freedom is transferred among molecules. Molecular collisions with the cavity walls, molecular diffusion into and out of the active region, and collisions between molecules in the active gas medium all produce changes in the population of the various energy states. In Task II, we are concerned with the redistribution and loss to translation of rotational and vibrational energy, as the result of collisions among the gas molecules within the active medium.

The primary objective of these studies is to determine experimentally the populations of HF molecules as functions of (1) time and (2) their vibrational and rotational state in cells containing excited HF and in the absence of diffusion and wall effects. Once radiative processes are accounted for, experimental transfer rates resulting from collision processes can be determined. From these, energy-transfer cross sections for the various processes can be determined.

In the experiment presently being prepared, the stimulation in the HF cell is to be produced by an HF laser operating on a single HF vibration-rotation line. This will produce an excitation condition in which the molecules in all but one particular rotational state will have a Boltzmann distribution of rotational energy. A fraction of those molecules in the selected rotational state will be raised from the $v = 0$ to the $v = 1$ level by absorption of the energy from the monochromatic HF laser beam.

The relaxation of this excitation condition is expected to occur primarily by collisional processes, first by equilibration of the rotational energy of the molecules excited to the v = 1 level and then by equilibration of the vibrational energy back to the original state. We will monitor the relaxation process by monitoring the absorption of the beam from a second HF laser of very low power. This laser will also operate on a single HF line. The rotational relaxation will be monitored by observation of the absorption of the probe laser operating in a v = 1 to v = 2 transition either at the same, or at a different rotational state from that pumped by the stimulating laser. By monitoring the absorption of this probe laser as a function of time, the variation in the population of a given vibration-rotation state with time can be determined. The details of the rotational relaxation process can be determined from a series of such measurements in which the stimulating transition is not changed but the transition of the probe laser is varied.

A set of computations showing the feasibility of such an experiment is presented in Sections 3.1 through 3.4. Some of the requirements on the stimulating and probe lasers are discussed and the effect of radiative relaxation on the measurements is considered. Some alternate means of monitoring the relaxation process are discussed and the choice of probe laser absorption measurements over fluorescence measurements is justified. The apparatus to perform the experiment is being assembled. The progress made to date is reported in Section 3.5.

1.3 ADDITIONAL EFFORT

We expended some effort to write and test a code for computing collision-broadened line widths using Anderson's theory of collision broadening [3].

The variation in the gain of the laser medium with frequency is a very important factor when the mode structure of the laser is a consideration. Line broadening resulting from collisions is important as a homogeneous broadening mechanism in gas lasers which operate at or near atmospheric pressure. Hence, knowledge of the collision-broadened widths can be an important parameter in some laser-design situations. Yet measurements of collision-broadened widths are difficult and have been performed only for a relatively small number of active gas-perturber combinations. In particular, determinations of the collisional broadening of the transitions of the active gases in gas-laser media are largely nonexistent. Measurements of the broadening in such cases would be very difficult because of the complex, nonequilibrium nature of the gas in the cavity. Theoretical computer codes to perform such calculations are hence a useful tool for predicting such effects. The code which we have generated provides a useful beginning although it is limited to diatomic and linear molecules.

The technique used in the code is described in detail in Section 4. Some sample calculations are also presented. Some of these calculations represent the conditions under which collision-broadened half widths were obtained experimentally in other programs. The agreement between the half widths predicted by the computer code and the experimental half widths is very good.

Section 5 includes the measurements of the $v = 0 \rightarrow v = 3$ dipole matrix elements of HF performed partially under a previous chemical laser study contract, Contract No. DAHC-15-67-C-0062. This work was not completed under that contract and hence was not reported. However, because of its connection to the present effort it was completed under the present contract and we feel it appropriate to report it here. The measurements performed during that effort were successful and complete; the results obtained were utilized in the complete set of matrix elements calculated for HF under the previous contract [1].

Appendix I presents a derivation of the equations governing the interactions of radiation with matter described by the Einstein coefficients and is supplemental to Section 3. Appendix II contains the detailed results of the matrix element calculations performed for HCl.

2
MATRIX ELEMENT CALCULATIONS AND INTENSITY MEASUREMENTS

F. G. Smith, G. H. Lindquist, and R. L. Spellicy

2.1. MATRIX ELEMENT CALCULATIONS

Consider a gas having a nonequilibrium population of vibrational and rotational states so that a known population inversion exists. In order to determine the ability of that gas to produce stimulated emission and hence lasing action in its vibration-rotation bands, it is necessary to know the transition probability for stimulated emission for the states involved in the inversion.

For a particular change of state, the three Einstein coefficients represent transition probabilities for spontaneous emission, stimulated emission, and stimulated absorption of radiation. These Einstein coefficients are a molecular property and, in the case of vibration and rotation, can be related to a quantum mechanical description of the vibrational and rotational motion of that molecule and its dipole moment. It has been shown that the three Einstein coefficients are each directly proportional to the quantum mechanical electric dipole matrix element for that transition [4]. Hence, determination of such matrix elements is extremely useful in the determination of the required transition probabilities.

The most accurate method of determining transition probabilities is by measuring absorption under equilibrium conditions in which the population of states is well known. However, such measurements cannot be made on many of the transitions of interest in laser studies because the states involved are not significantly populated at reasonable temperatures. The computation of the electric dipole matrix elements associated with such transitions provides a powerful tool for the estimation of the transition probabilities.

2.1.1. THE DIPOLE MOMENT AND CALCULATED MATRIX ELEMENTS FOR HCl

The electric dipole matrix element for the v, J → v', J' transition is defined by the following [1]:

$$\langle v, J|\mu(r)|v', J'\rangle = \int \psi_{v',J'}\mu(r)\psi_{v,J}r^2 dr$$

where $\psi_{v',J'}$ = the radial wavefunction for the upper state of the transition
$\psi_{v,J}$ = the radial wavefunction for the lower state of the transition
$\mu(r)$ = the dipole moment as a function of r
r = the internuclear separation
v, v' = the lower-and upper-state vibrational quantum numbers
J, J' = the lower- and upper-state rotational quantum numbers

Calculation of the matrix-element integral requires initial and final state wavefunctions and the molecular electric dipole moment function. Once the form of the potential function is known, the wavefunctions are calculated by numerical integration of the Schrödinger equation. Our procedure allows any functional form for the dipole moment function, but experimental intensity data are required to determine the values of the coefficients of the dipole moment function. The procedure used to establish the potential and dipole moment functions is described below and the results are used to calculate HCl matrix elements.

2.1.2. DETERMINATION OF THE INTERMOLECULAR POTENTIAL: GENERAL CONSIDERATIONS

The three most commonly used potential functions are the Dunham (or polynomial) potential, the Ryberg-Klein-Rees (RKR) potential, and the Morse potential. The Dunham potential defines the energy as a power series in $(r - r_e)$ where r is the internuclear coordinate and r_e is the equilibrium value of internuclear distance. In his original paper, Dunham shows that the coefficients of the series expansion may be obtained directly from spectroscopic constants [5]. The Dunham potential allows analytic solution of the radial Schrödinger equation and evaluation of the dipole moment integral by a standard, but tedious, application of perturbation theory. Recently, Toth, Hunt, and Plyler [6] have used this method to obtain vibration-rotation interaction factors for $0 \rightarrow 1$, $0 \rightarrow 2$, and $0 \rightarrow 3$ bands of CO. The Dunham potential is not very useful for numerical calculations, however, since the Dunham expansion is not constrained to approach realistic forms in the limits of large and small internuclear separations.

The Morse potential is an analytic function containing three parameters which may be chosen to obtain agreement with the vibrational and rotational energy levels of the molecules. The primary advantage of the Morse oscillator over other analytic forms is that it is simple, yet its wavefunctions are analytic. It predicts accurate eigenvalues over a fairly wide range of oscillations.

The RKR potential is simply a tabulation of energy versus internuclear distance, constructed to reproduce the observed energy levels of the molecule. The RKR potential is constructed by determining the turning points of the molecular oscillations with the Wentzel-Kramer-Brillouin (WKB) approximation [7, 8, 9]. The procedure requires only the spectral line positions.

Whatever the form of the function, if it is to realistically represent the potential for a diatomic molecule, it must fulfill certain minimal conditions, as pointed out by LeRoy and Burns [10]. The conditions are that:

(1) the outer branch of the function should asymptotically approach the known dissociation limit of the electronic state of the molecule.

(2) the slope of the inner-branch of the potential must be negative.

(3) The inner branch of the potential must become steeper with decreasing internuclear distance, i.e., its second derivative must be positive in that region.

The Dunham potential does not fulfill condition (1) since finite polynomial series diverge at infinity. Analytic functions generally are constructed to fulfill all three conditions but may fail in other respects e.g. in the prediction of energy levels. Since the RKR potential may be constructed to fulfill all conditions, we have chosen to use it in this study.

2.1.3. THE RKR POTENTIAL

The generation of an RKR potential requires a knowledge of the vibrational energy levels and rotational energy constants of the molecule in its various vibrational states. From spectroscopic data, Dunham coefficients $Y_{i,j}$ can be determined which describe the value of the quantities by a power series in v, the vibrational quantum number. The vibrational energy levels are given by

$$G_v \quad \sum_{i=0}^{n} Y_{i,0}(v + 1/2)^i \qquad (1)$$

and the rotational constants are

$$B_v \quad \sum_{i=0}^{m} Y_{i,1}(v + 1/2)^i \qquad (2)$$

The number of constants are chosen to fit the data within the measurement error. The G_v and B_v values, or equivalently the Y coefficients, provide input data which uniquely define the RKR potential. The method used to determine the potential is described in a paper by Vanderslice et.al. [9]. For the actual calculation presented later in this report we have used a computer program written by Zare [11] modified to run in FORTRAN IV on an IBM 360/67 computer.

The necessary Y coefficients for HCl have been obtained by Rank, et al. using v = 0 through v = 5 line and band position data [12, 13]. The vibrational and rotational constants which they obtained are given in column (a) of Tables 1 and 2 respectively. Using these constants to generate an RKR potential, we obtained curve a of Fig. 1. The dissociation energy corresponding to the accepted D_0 value of 4.43 eV [14] is 37217 cm^{-1} and is also indicated on that figure as D_e (D_0 is the energy difference between the dissociation limit and the v = 0 level). It may be seen that, for a realistic potential function conditions (1) and (3) are violated by the constructed potential. This is not surprising since the Y's used were determined only from data on the six lowest vibration states of the molecule. Since we are interested in transitions involving v as high as 12, the potential must be upgraded.

TABLE 1. VIBRATIONAL CONSTANTS FOR HCl

	(a) From Rank et al. [12] (cm^{-1})	(b) Adjusted Constants (cm^{-1})
Y_{10}	2990.9463	2990.9270
Y_{20}	-52.8185	-52.7842
Y_{30}	0.2243	0.199160
Y_{40}	-0.0121	-0.004536
Y_{50}	0.0	-0.000806

TABLE 2. ROTATIONAL ENERGY CONSTANTS FOR HCl

	(a) From Rank et al. [12] (cm^{-1})	(b) Adjusted Constants (cm^{-1})
Y_{01}	10.593416	10.593246
Y_{11}	-0.307181	-0.305812
Y_{21}	0.001772	0.000670175
Y_{31}	-0.0001201	0.000171434
Y_{41}	0.0	-0.0000231052

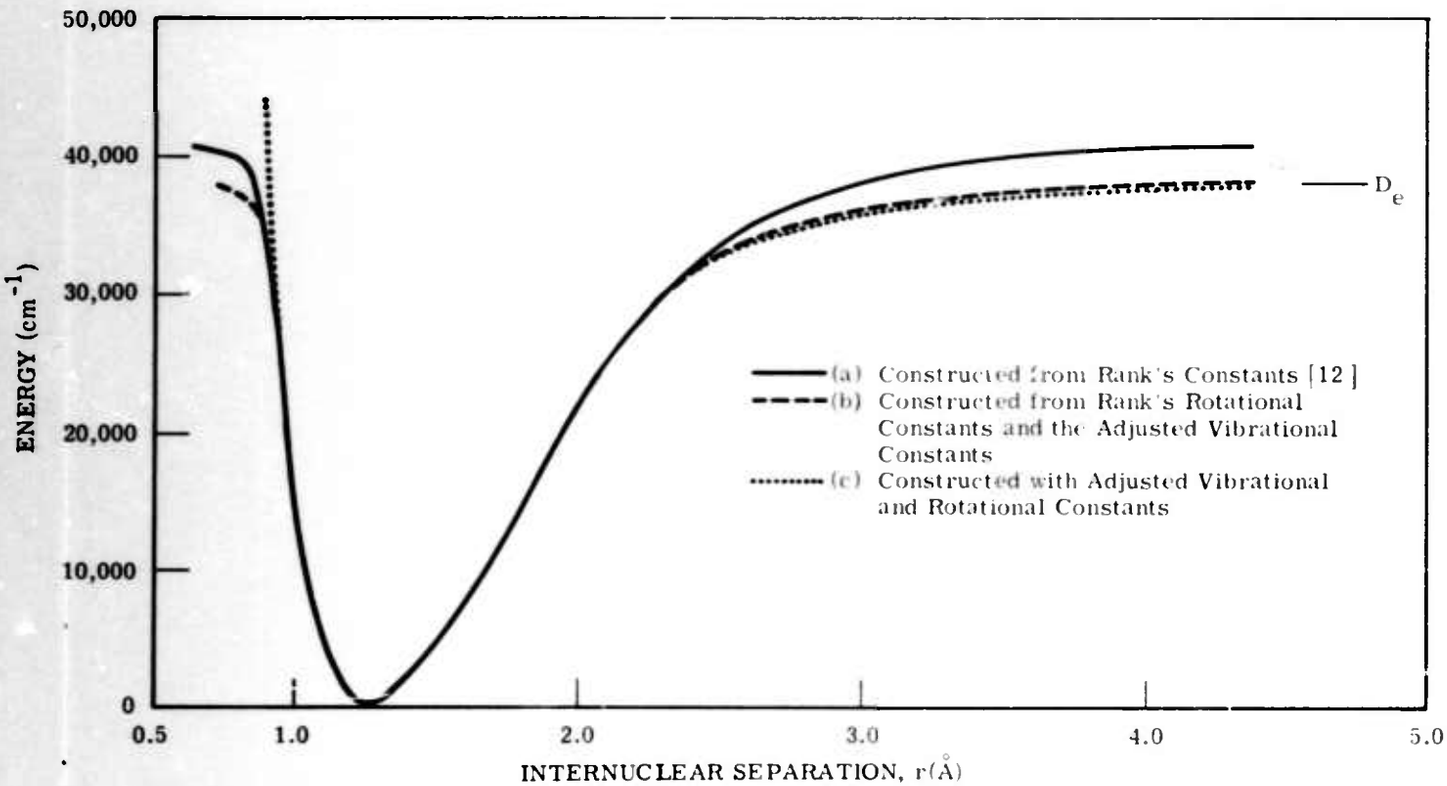

FIGURE 1. RKR POTENTIAL FOR HCl

2.1.4. CONSTRUCTION OF THE RKR POTENTIAL

In order to construct an RKR potential which fulfills the minimum requirements of LeRoy and Burns, we have followed a procedure outlined by them for adjusting the Y's to obtain a better potential function. This is a two-step procedure. First the vibrational constants are modified to fulfill condition (1) and second, the rotational constants are adjusted until conditions (2) and (3) are met.

Condition (1), that the dissociation energy be asymptotically approached at large internuclear separations, is equivalent to two constraints on the energy-level curve:

$$\left(\frac{dG}{dv}\right)_{v_D} = 0 \tag{3}$$

where v_D is the vibrational quantum level corresponding to dissociation and

$$G_v(v_D) = D_e \tag{4}$$

where D_e is the energy difference between the dissociation limit and the bottom of the potential well. Equation (1) for G, with the vibrational constants of Rank inserted into Eq. (3) gives $v_D = 27.834$. The value of D_e obtained from this value of v_D is 40600 cm^{-1}. This result can be compared with the accepted dissociation energy of 37217 cm^{-1}, and it confirms what Fig. 1 has indicated; i.e., Rank's vibrational constants do not properly represent the energy levels of HCl near dissociation. If an additional constant, in the present case, Y_{50}, is added to the vibrational energy expansion, then Eqs. (3) and (4) may be fulfilled and a good fit to the experimental data also maintained.

A FORTRAN program incorporating an iterative procedure was used to calculate such a consistent set of $Y_{i,0}$ constants. The first step in this procedure was the solution of Eq. (3) with Rank's constants for an initial value of v_D. This value for v_D was then used to define a linear system of equations consisting of Eq. (4) and four equations relating the polynomial for G_v to experimental values of G_v. The complete system used for the HCl case was

$$\sum_{i=1}^{5} Y_{i,0}(v_D + 1/2)^i = D_0$$

and

$$\sum_{i=1}^{5} Y_{i,0}(v + 1/2)^i = G_v \quad \text{for } v = 1, 2, 3, 4 \tag{5}$$

The values of G_v used on the right-hand sides of the latter equations were calculated from Rank's constants. The linear system was solved to obtain a new set of $Y_{i,0}$ constants which

were then used in Eq. (3) and iterated values of v_D were obtained. The iteration was contained until successive iterates of v_D varied by less than 0.001. The corresponding values of the $Y_{i,0}$ constants at that point in the iteration were taken as the adjusted vibrational constants and are given in Column b of Table 1. The G(v) curve determined from this set of constants is plotted in Fig. 2.

Columns (a) and (b) of Table 5 compare the observed band origins with those calculated with the adjusted set of constants. Finally, an RKR potential was generated from these adjusted vibrational constants and Rank's rotational constants; it is curve 2 of Fig. 1. As expected this function exhibits the correct behavior at large internuclear separations. However, it does not fulfill the requirements at small separations.

In order to construct a potential which fulfills conditions (2) and (3) on the form of this function, we varied an additional Dunham coefficient, $Y_{4,1}$, in the expansion for B_v while simultaneously adjusting the lower-order coefficients to maintain the least-square fit to the measured B_v values. Table 4 contains some sets of rotational constants which were tested, and Fig. 3 shows the upper sections of the inner branch of the RKR functions resulting from these sets of rotational constants. Inspection of that figure shows that none of these potentials fulfill condition (2) all the way to the dissociation limit. This could be corrected by the addition of another adjustable constant. We chose, however, not to add another constant but simply to use Function b of Fig. 3 up to 36,500 cm^{-1} and a 12-deg polynomial extrapolation above that point. We believe this is more than justified since the effect of this portion of the potential should be insignificant for vibration states below v = 12 which are of primary interest here. The final potential form which we have used in all the calculations that follow is curve c of Fig. 1. In Table 5, the observed B_v values are compared with the values defined by the adjusted rotational constants and Fig. 4 gives B_v for all the vibrational states predicted.

The final RKR turning points for the bound vibrational levels are tabulated in Table 6. In the actual calculation, the potential is determined at 199 values of internuclear separation and a cubic spline interpolation is used to interpolate between those points [15]. The numerical solutions of the radial Shrödinger equation determine the vibrational energy levels. The band origins calculated from the numerical solutions are given in Column c of Table 3.

2.2. THE DIPOLE MOMENT FUNCTION

2.2.1. THE POLYNOMIAL APPROXIMATION

The most important consideration in the calculation of the electric dipole matrix elements is the determination of the dipole moment parameters. For a diatomic molecule, it may be assumed that the vector dipole moment function is directed along the internuclear axis and thus the function can be represented as a scalar function of the internuclear separation. The stan-

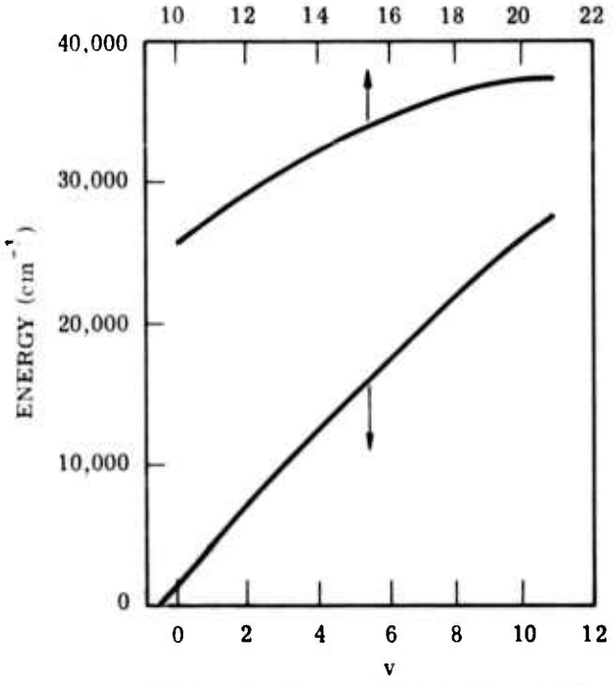

FIGURE 2. VIBRATIONAL ENERGY LEVELS FOR HCl DETERMINED BY THE MODIFIED DUNHAM COEFFICIENTS USED TO GENERATE THE RKR POTENTIAL

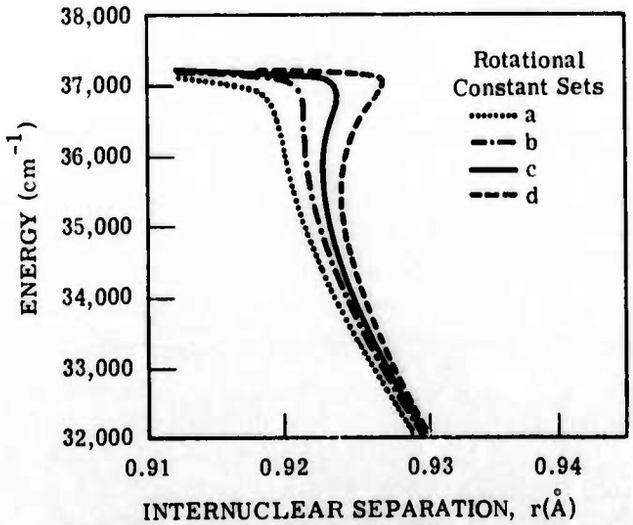

FIGURE 3. INNER BRANCH OF RKR POTENTIALS CALCULATED BY MEANS OF THE TRIAL ROTATIONAL CONSTANTS IN TABLE 3

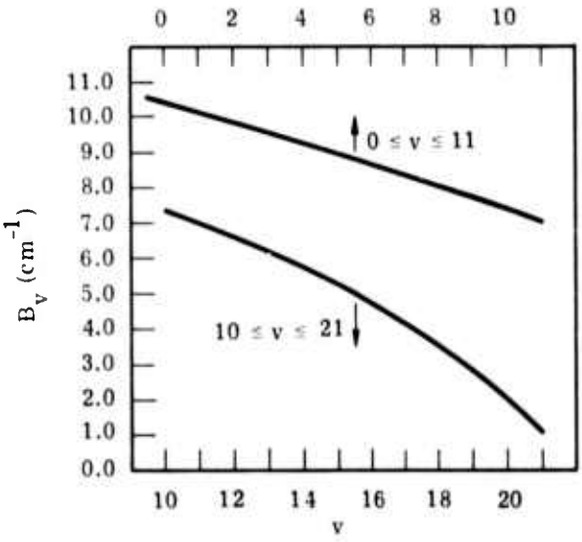

FIGURE 4. ROTATIONAL CONSTANTS FOR HCl AS DETERMINED BY THE MODIFIED DUNHAM COEFFICIENTS USED TO GENERATE THE RKR POTENTIAL

TABLE 3. OBSERVED AND CALCULATED BAND ORIGINS FOR HCl

	(a) Observed (Rank et al.) [12] (cm^{-1})	(b) Calculated (Adjusted Constants of Table 1) (cm^{-1})	(c) Calculated (Numerical Schrödinger Solution) (cm^{-1})
1-0	2885.978	2885.974	2886.891
2-0	5667.984	5667.974	5669.352
3-0	8346.782	8346.775	8348.559
4-0	10922.803	10922.789	10925.289
5-0	13396.217	13396.009	13400.008
3-1	5460.804	5460.801	5461.668
4-2	5254.856	5254.815	5255.937
5-3	5049.503	5049.234	5051.449

TABLE 4. TRIAL ROTATIONAL CONSTANT VALUES
(cm^{-1})

	(a)	(b)	(c)	(d)
Y_{01}	10.5932490	10.5932460	10.5932440	10.5932410
Y_{11}	-0.3059344	-0.3059118	-0.305889	-0.305867
Y_{21}	0.0006909	0.0006702	0.0006494	0.0006287
Y_{31}	0.0001655	0.0001714	0.0001774	0.0001833
Y_{41}	-0.0000225	-0.0000231	-0.0000236	-0.0000242

TABLE 5. OBSERVED AND CALCULATED ROTATIONAL CONSTANTS FOR HCl

	(a) Observed (Rank et al.) [12] (cm^{-1})	(b) Calculated (Adjusted Constants of Table 2) (cm^{-1})
B_0	10.440254	10.44047
B_1	10.136228	10.13634
B_2	9.834665	9.834431
B_3	9.534845	9.534647
B_4	9.236010 (4-2 data) 9.2363 (4-0 data)	9.236362
B_5	8.93743 (5-3 data) 8.9395 (5-0 data)	8.938385

TABLE 6. RKR POTENTIAL FOR HCl

V	Energy (cm^{-1})	r_{min} (Å)	r_{max} (Å)
0	1482.292	1.177068	1.393102
1	4368.266	1.117050	1.496985
2	7150.270	1.080607	1.578597
3	9829.070	1.053586	1.652208
4	12405.080	1.031951	1.722040
5	14878.300	1.0139810	1.789915
6	17248.130	0.9986415	1.857172
7	19513.380	0.9853323	1.924772
8	21672.090	0.9736691	1.993561
9	23721.480	0.9634037	2.064413
10	25657.840	0.9543734	2.138287
11	27476.430	0.9464760	2.216341
12	29171.380	0.9396601	2.300038
13	30735.610	0.9339066	2.391312
14	32160.720	0.9292040	2.492930
15	33436.890	0.9256439	2.608497
16	34552.790	0.9231968	2.744314
17	35495.490	0.9218721	2.910449
18	36250.340	0.9215231	3.126173
19	36800.920	0.9214401	3.436183
20	37128.870	0.9178123	3.996376

dard functional form chosen is a polynomial:

$$\mu(r) = \sum_i M_i (r - r_e)^i$$

where M_i are the coefficients of this dipole moment expansion. The M_i coefficients can be determined either by theoretical calculations or through reference to experimental data. Experience has generally shown that ab-initio calculations are only reliable for determining the M_0 and M_1 coefficients accurately; therefore, for a better determination of the dipole moment, reference to experimental data is necessary. The usual procedure for determination of the M_i coefficients from experimental data is by solution of the following set of linear equations:

$$\sum_{i=0}^{n} M_i \int \psi_0 (r - r_e)^i \psi_v r^2 dr = \langle 0 | \mu(r) | v \rangle \quad \text{for } v = 0, 1, \ldots n \tag{6}$$

where the $\langle 0 | \mu(r) | n \rangle$ is the highest overtone matrix element which has been measured. Once the M_i have been determined for the above equations, any other matrix elements can be approximated as follows:

$$\langle v' | \mu(r) | v \rangle = \sum_{i=0}^{n} M_i \int \psi_{v'} (r - r_e)^l \psi_v r^2 dr \tag{7}$$

It may be seen that the relationship between the various matrix elements is somewhat obscured by the interposition of M_i's. In a previous report [1], we derived expressions which define any matrix element as a linear combination of the overtone matrix elements. We repeat the derivation here with slightly different notation and in a more general form to allow direct comparison with similar relationships derived by Trischka and Salwen from the wavefunction expansion method [16].

2.2.2. DERIVATION OF RELATIONSHIPS BETWEEN VARIOUS MATRIX ELEMENTS

In this section, we deviate from the standard notation and designate a matrix by a capital letter and elements of that matrix by simply attaching subscripts to that capital letter. Thus, the dipole moment coefficients M_i can be written as a one-dimensional matrix M. Let us define a one-dimensional matrix Γ which contains the overtone matrix elements by:

$$\Gamma_v = \langle v | \mu | 0 \rangle \quad v = 0, \ldots n \tag{8}$$

we also need the $n \times n$ moment matrix A defined by:

$$A_{v,l} = \int \psi_0 (r - r_e)^l \psi_v r^2 dr \tag{9}$$

If these relations are used, Eq. (5) can be written in matrix form as:

$$AM = \Gamma \tag{10}$$

If A^{-1} exists then (1) can be solved for M giving:

$$M = A^{-1}\Gamma \tag{11}$$

We define a n × xm matrix B by:

$$B_{j,v,v'} = \int \psi_{v'} \rho^j \psi_v r^2 dr \qquad \begin{matrix} j = 0, \ldots n \\ v = 0, \ldots m \\ v' = 0, \ldots m \end{matrix}$$

and an m × m matrix R containing the dipole matrix elements between the m bound states of the molecule:

$$R_{v',v} = \langle v' | \mu | v \rangle \tag{13}$$

Equation (7) can then be written:

$$R = BM \tag{14}$$

The substitution of Eq. (11) into (14) gives:

$$R = BA^{-1}\Gamma \tag{15}$$

This can be rewritten in terms of the elements of the matrices as:

$$R_{v',v} = \sum_{j,l=0}^{n} B_{j,v',v} A^{-1}_{j,i} \Gamma_i \tag{16}$$

If we define the n × m × m matrix C by

$$C_{i,v',v} = \sum_{j=0}^{n} B_{j,v',v} A^{-1}_{j,i} \tag{17}$$

then

$$R_{v',v} = \sum_{i=0}^{n} C_{i,v',v} \Gamma_i \tag{18}$$

This expression gives a set of linear equations relating the overtone matrix elements to all other matrix elements. These are not exact relationships but approximations determined by n, the degree of the polynomial approximation used. Coefficients calculated with the cubic polynomial approximation are given in Table 7. The coefficients can be compared with those in Table 8 which contains similar coefficients calculated by Kaiser, who used the wavefunction approximation [17]. It can be seen that the polynomial and the wavefunction approximations

TABLE 7. SELECTED $C_{i,v',v}$ COEFFICIENTS FOR HCl WITH A CUBIC POLYNOMIAL APPROXIMATION

i	$C_{i,0,0}$	$C_{i,1,1}$	$C_{i,2,2}$	$C_{i,0,1}$	$C_{i,1,2}$	$C_{i,1,3}$
0	1.0	1.0	1.0	0.0	0.0	0.0
1	0.0	0.5838	1.233	1.0	1.5148	1.9915
2	0.0	1.515	3.892	0.0	1.2337	3.4093
3	0.0	0.000394	2.111	0.0	1.9916	7.2681

TABLE 8. SELECTED $C_{i,v',v}$ COEFFICIENTS FOR HCl CALCULATED WITH THE WAVEFUNCTION APPROXIMATION

i	$C_{i,0,0}$	$C_{i,1,1}$	$C_{i,2,2}$	$C_{i,0,1}$	$C_{i,1,2}$	$C_{i,2,3}$
0	1.0	1.0	1.0	0.0	0.0	0.0
1	0.0	0.5839	1.234	1.0	1.5148	1.9914
2	0.0	1.55	4.001	0.0	1.2335	3.4305
3	0.0	0.000417	3.430	0.0	1.994	7.7752

are nearly equivalent when the $R_{v,v'}$'s are calculated with these tabulated $C_{j,v,v'}$ coefficients. These coefficients will be valuable later for comparing various types of experimental data. In the remainder of the paper, the notation of Trischka and Salwen is used, i.e., the initial and final states are written as superscripts.

2.2.3. EXPERIMENTAL HCl MATRIX ELEMENTS

Numerous line-strength measurements have been performed on HCl. The most complete work appears to be that of Benedict, Herman, Moore, and Silverman (BHMS) [18]. They measured the HCl overtone matrix elements $R^{1,0}$, $R^{2,0}$, and $R^{3,0}$ as well as $R^{2,1}$, and $R^{3,2}$. More recently Toth, Hunt, and Plyler (TRP) [19] have measured the fundamental and first overtone bands. They have also included a table of the overtone band strengths measured by other laboratories. We have calculated experimental matrix elements corresponding to these tabulated strengths. They are given in Table 9. Inspection of Table 9 shows that the errors quoted by the different laboratories do not, in general, overlap.

Since the band intensity is proportional to the square of the dipole matrix element, additional information is necessary to determine the sign of the $R^{v,0}$ matrix elements. For HCl, when $R^{0,0}$ is assumed positive, it has been shown that the $R^{1,0}$ and $R^{3,0}$ matrix elements are greater than zero and the $R^{2,0}$ matrix element is less than zero. We will not repeat the arguments, but Kaiser has shown that only this choice of signs is compatible with his high-precision measurements of R_{11} and R_{22}. Similarly, THP have concluded that the above signs give the best agreement between their calculated and measured vibration-rotation intensity measurements for the 0-1 and 0-2 bands of HCl.

A comparison of matrix elements determined in different laboratories [20, 21, 22] is presented in Fig. 5 where fundamental and first overtone matrix elements are represented as dimensions in a two-dimensional space. In that figure, the fundamental and first overtone matrix-element determinations have been represented by a slash on the horizontal or vertical axes, respectively. In the three cases in which both matrix elements were measured by one laboratory, the measurements are represented by a point in the space. A point representing the average of the results of all the infrared intensity measurements is also plotted.

In addition to the directly determined experimental matrix elements, some additional points are also shown. The point labeled K represents the choice made by Kaiser [17] as being the most probable value of the $R^{1,0}$ and $R^{2,0}$ matrix elements. In essence, he assumed that the BHMS value of $R^{3,0}$ was correct. He then solved Eq. (18) for $R^{1,0}$ using his measured value of $R^{0,0} - R^{1,1}$ and using the coefficients in Table 8.

TABLE 9. VARIOUS DETERMINATIONS OF THE OVERTONE MATRIX ELEMENTS FOR HCl

	$R^{0,1}$ (esu-cm)	$R^{0,2}$ (esu-cm)	$R^{0,3}$ (esu-cm)
Used in Present Calculations	7.12×10^{-20}	-7.75×10^{-21}	5.15×10^{-22}
Average	7.02	-7.74	5.15
Derived from Kaiser's Data (KD)	7.23	-7.78	5.15
Kaiser's Choice (K) [17]	7.00 ± 0.10	-7.00 ± 0.50	
Benedict et al. (BHMS) [18]	6.70 ± 0.12	-7.02 ± 0.28	5.15 ± 0.21
Toth et al. (THP) [19]	6.80 ± 0.13	-8.00 ± 0.15	
Penner and Weber (PW) [20]	7.41 ± 1.01	-7.94	
Babrov et al. (B) [21]	7.17 ± 0.16		
Jaffe et al. (J) [22]		-7.94	

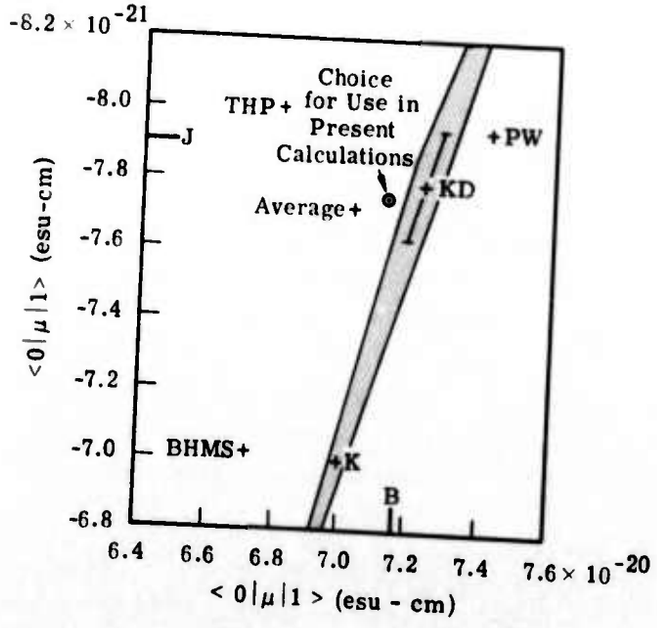

FIGURE 5. EXPERIMENTAL DETERMINATIONS OF $<0|\mu|1>$ AND $<0|\mu|2>$

We have calculated the point marked KD by solving Eq. (18) using the $C_{j,0,0}$, $C_{j,1,1}$, and $C_{j,2,2}$ coefficients from Table 7 and using Kaiser's difference measurements. This gives two equations in the three unknowns $R^{1,0}$, $R^{2,0}$, and $R^{3,0}$:

$$0.5838\ R^{1,0} + 1.515\ R^{2,0} + 0.000394\ R^{3,0} = R^{1,1} - R^{0,0}$$
$$1.233\ R^{1,0} + 3.892\ R^{2,0} + 2.111\ R^{3,0} = R^{2,2} - R^{0,0} \qquad (19)$$

If we assume that $R^{3,0}$ is known from BHMS's measurement, the $R^{1,0}$ and $R^{2,0}$ may be determined. The results are as follow:

$$R^{1,0} = 7.23 \times 10^{-20}$$
$$R^{2,0} = -7.79 \times 10^{-21}$$

That is the point marked KD in Fig. 5. Two sources of experimental error are expected in the point KD: one arises from error in Kaiser's measurement of matrix-element differences and the other arises from the error in the BHMS $R^{3,0}$ determinations. We have calculated the effect of these two errors on the solution to Eq. (19). The solid error bar shown on the KD point represents the error in the $R^{1,0}$ and $R^{2,0}$ matrix elements assuming a ±10% error in the BHMS $R^{3,0}$ value. The larger, shaded region shows the error bounds expected from the error estimate given by Kaiser for his matrix element difference measurements.

Best estimates of $R^{1,0}$ and $R^{2,0}$ are not obvious from Fig. 5. However, we chose as the best values, a point halfway between the average of the infrared measurements and the value determined from Kaiser's data. If we assign a ±3% error to this choice, there is overlap between all of the measurements and our choice except for the data of BHMS. It appears, as Kaiser has also concluded, that their overtone measurements are systematically low.

Our final choices for the best experimental overtone matrix elements are given in Table 10. The $R^{0,0}$ matrix element is again from Kaiser's work. The choice of the $R^{1,0}$ and $R^{2,0}$ was explained above. BHMS have reported the only measurement of $R^{3,0}$ for HCl so we have taken their value and assigned it ±10% error. Using this set of matrix elements and the errors given, we have computed the corresponding M_i. These are tabulated in column (a) of Table 11. Our calculated M_i are quite close to the THP values, except for the M_3 coefficient, but they do not overlap. The comparison with Kaiser's values for the M_i show overlap between the present calculation for M_0 and M_1, but not for the higher coefficients. It appears to us that either Kaiser has used the negative sign for the $R^{0,3}$ matrix elements, contrary to his paper or that the procedure he has used to determine polynomial coefficients by fitting to the wavefunction expansion has introduced the differences. The first suggestion seems more likely for several reasons. First, we have calculated a set of M_i using the set of matrix elements in Table 12. By setting $R^{4,0}$ equal to zero, we have created a set of M_i somewhat analogous to

TABLE 10. OVERTONE MATRIX ELEMENTS USED IN THE PRESENT WORK

v	$R^{v,0}$ (esu-cm)
0	$1.10847 \pm 0.0005 \times 10^{-18}$
1	$7.12 \pm 0.21 \times 10^{-20}$
2	$-7.75 \pm 0.23 \times 10^{-21}$
3	$5.15 \pm 0.52 \times 10^{-22}$

TABLE 11. DIPOLE MOMENT COEFFICIENTS FOR HCl

	Present Work (a)	Toth et al. [19] (b)	Kaiser [17] (c)	Calculation using $R^{i,0}$ of Table 12 (d)
M_0 (esu-cm) $\times 10^{18}$	1.0935 ± 0.0007	1.095	1.0933 ± 0.0005	1.0923
M_1 (esu-cm/cm) $\times 10^{10}$	0.947 ± 0.023	0.9031 ± 0.017	0.925 ± 0.02	0.930
M_2 (esu-cm/cm^2) $\times 10^{2}$	0.015 ± 0.041	-0.06 ± 0.025	0.08 ± 0.055	0.25
M_3 (esu-cm/cm^3) $\times 10^{-6}$	-0.814 ± 0.116	-0.73 ± 0.07	-1.277 ± 0.3	-1.057
M_4 (esu-cm/cm^4) $\times 10^{-14}$	0.0	0.0	-1.9 ± 1.2	-2.9

TABLE 12. $R^{i,0}$ USED TO COMPUTE COLUMN d OF TABLE 11

i	$R^{i,0}$ (esu-cm)
0	1.10847×10^{-18}
1	7.00×10^{-20}
2	-7.00×10^{-21}
3	-5.15×10^{-22}
4	0.0

the wavefunction approximation Kaiser used in which all the $R^{0,v}$ overtones greater than those measured are assumed to be zero. The M_i coefficients from this calculation are listed in column (d) of Table 11, and they are very similar to the values reported by Kaiser. Second, when Kaiser's M_i are compared with the M_i determined by THP for various sign combinations of $R^{2,0}$ and $R^{3,0}$ we have found that the best agreement is obtained between Kaiser's M_i and the M_i's given by THP for the combination $R^{0,0}$, $R^{1,0} > 0$ and $R^{2,0}$, $R^{3,0} < 0$. Thus, while we agree with the signs determined by Kaiser for the $R^{v,0}$ matrix elements, we believe that an error has been made in his determination of the M_i's.

2.2.4. THE VIBRATIONAL MATRIX ELEMENTS

In Figs. 6 to 9, the calculated vibrational matrix elements are shown for the sequences $\Delta v = 0$, 1, and 3. In addition to the data considered in previous sections of this report, the only experimental data are the BHMS measurements of the $R^{1,2}$ and $R^{2,3}$ matrix elements. In Table 13, the results of our calculation of those matrix elements are compared with the BHMS data and with those from a similar calculation in which the BHMS set of $R^{0,v}$ overtone matrix elements were used. The calculated matrix elements in which we used our new $R^{0,v}$ give better agreement with BHMS's $\Delta v = 1$ data than do the calculations in which the BHMS overtone matrix elements were used.

In Figs. 6 and 7, we have also indicated error estimates for the various $R^{v,v'}$. As explained in our previous report [1], we know of no way to predict the error involved in approximating the dipole by a cubic polynomial; we can however, determine the approximate error introduced through use of the experimental overtone data to determine the polynomial coefficients. Thus, the error indicated on the figures as well as the previously assigned error in the M_i's is measurement-induced error rather than dipole approximation error. Unfortunately, the latter error will be most significant for high Δv transitions and, for a given set of Δv transitions, will be most important when higher vibrational levels are involved. We have no way of estimating these additional uncertainties. The dipole moment used (with the coefficients of Table 11) is plotted in Fig. 10. The experimental information includes values for matrix elements involving only v levels from 0 to 3. Thus, the dipole moment expansion can be considered strictly valid only for that range of internuclear separations encompassed by the wavefunctions for $v \leq 3$. This corresponds approximately to the range between 1 and 1.6 Å. Although the dipole moment function has a reasonable form both above and below these values, there is no way of determining its quantitative uncertainty at the larger internuclear separations encountered at high vibrational levels and, therefore, no way to assign total accuracy values to the matrix elements involving the higher v levels. This situation unfortunately limits the usefulness of these calculations for predictions of laser performance at the higher vibrational levels.

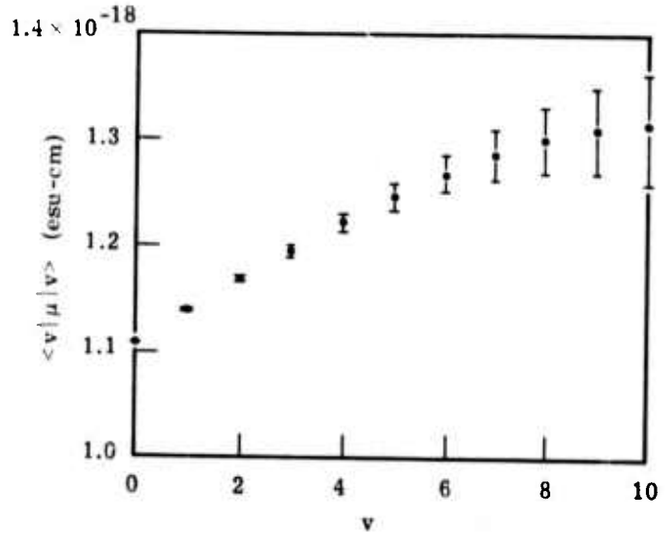

FIGURE 6. Δv = 0 MATRIX ELEMENTS FOR HCl

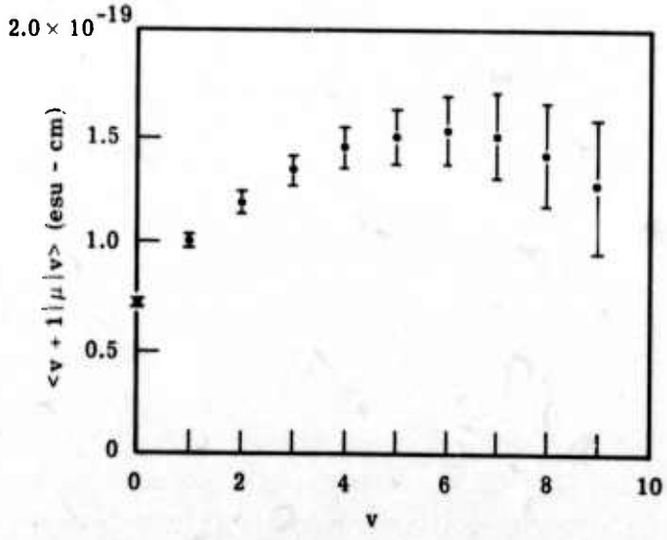

FIGURE 7. Δv = 1 MATRIX ELEMENTS FOR HCl

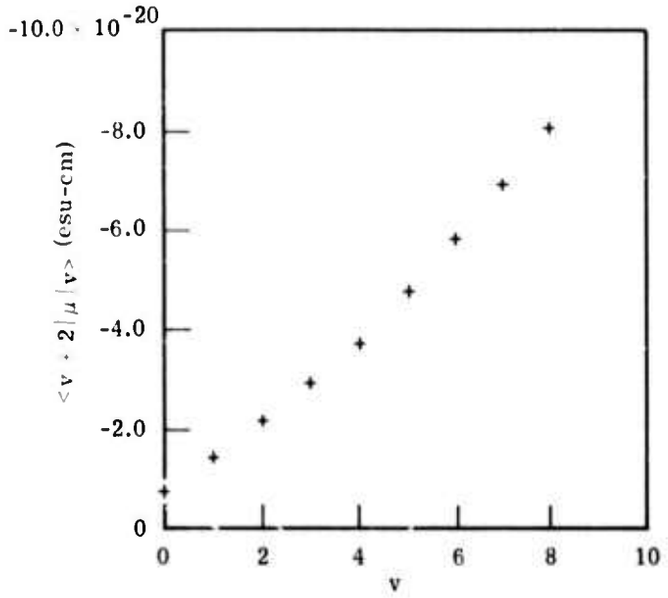

FIGURE 8. Δv = 2 MATRIX ELEMENTS FOR HCl

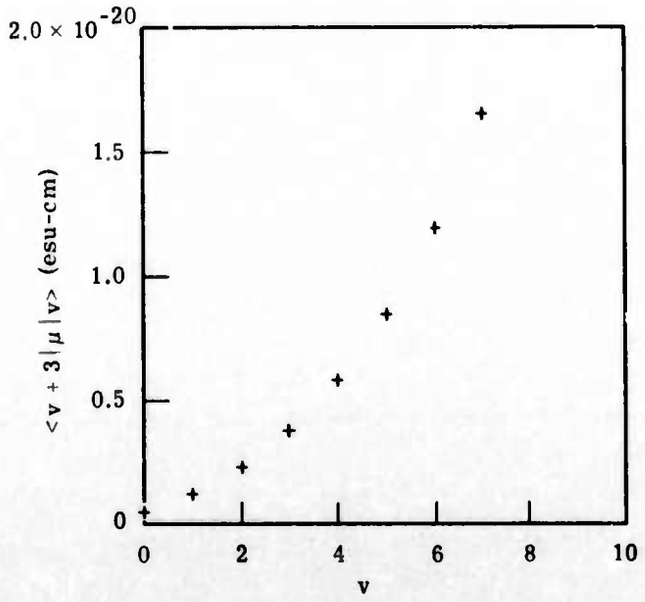

FIGURE 9. Δv = 3 MATRIX ELEMENTS FOR HCl

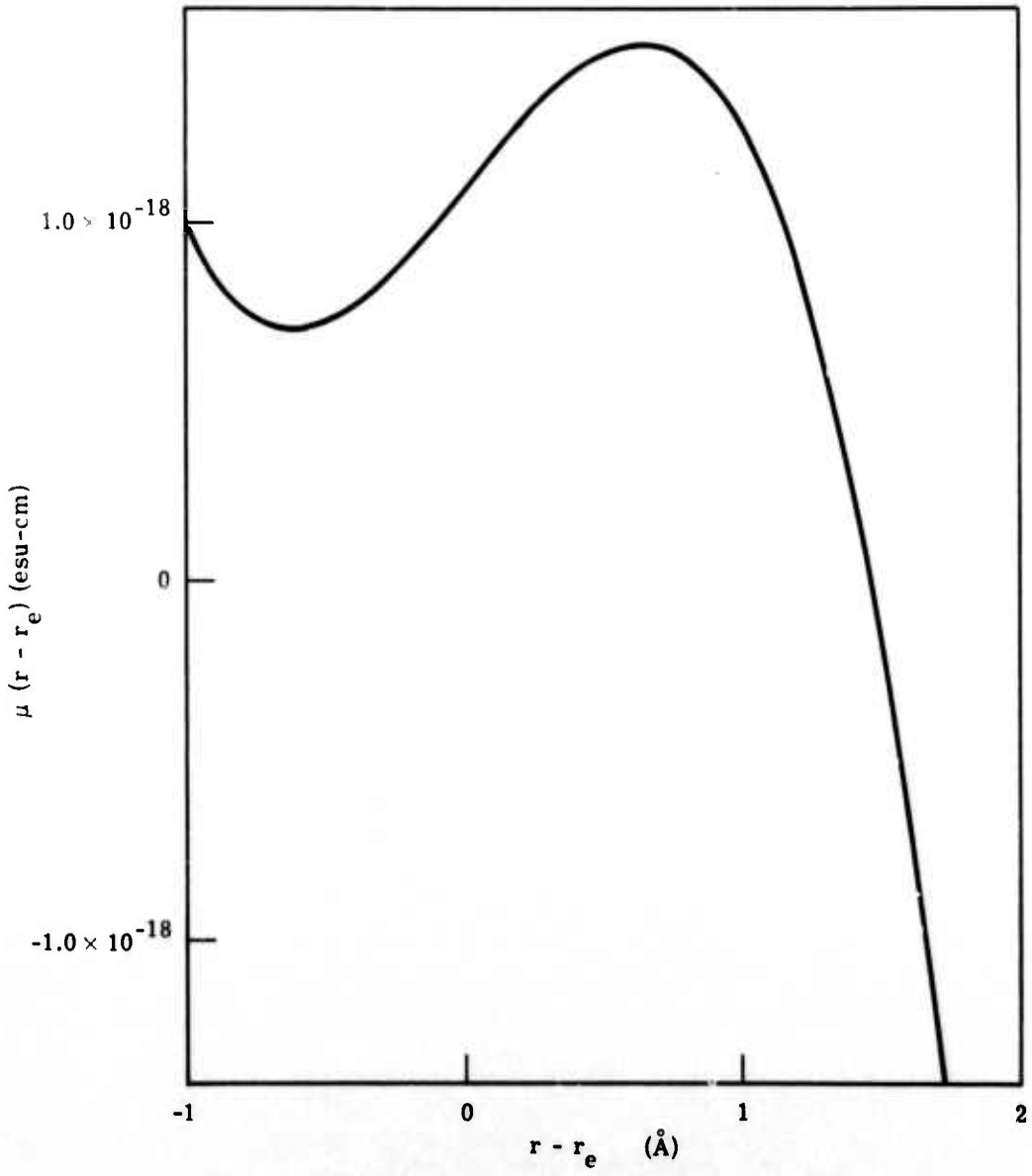

FIGURE 10. DIPOLE MOMENT FUNCTION FOR HCl USED IN THE PRESENT CALCULATIONS

2.2.5. ROTATIONAL DEPENDENCE OF THE MATRIX ELEMENTS

Once we had obtained an expansion for the dipole moment which satisfied the known experimental information (the M_i's shown in Table 11), we were able to compute the J-dependent matrix elements. The procedure used is identical to that used to compute the rotationless matrix elements except that an effective J-dependent potential was obtained by adding a centrifugal force term to the potential [14]:

$$\frac{hJ(J+1)}{8\pi^2 c\mu r^2}\ (cm^{-1})$$

Here, h is Planck's constant and c is the velocity of light. Energy eigenvalues which include both the vibrational and rotational contributions were then used to obtain rotationally dependent wavefunctions. Matrix elements for a specific v and J change were computed with the previously determined dipole moment expansion.

A complete set of the results from these calculations is presented in Appendix II. Vibrational levels as high as 12 are included for $0 \le \Delta v \le 5$ and for J going from 0 to 35. Both the P and R branches of the vibration-rotation bands as well as the pure rotation bands are included.

These results, though presented completely, are also of undetermined accuracy for vibrational levels substantially above 4 for the reasons discussed in the previous paragraph. The rotation-dependent matrix elements contain uncertainties resulting from measurement inaccuracies comparable to those presented in Figs. 6 and 7 for similar v and Δv. Again, we have no way of estimating the additional uncertainties that are present at higher v's because of uncertainties in the dipole moment at large separations.

The rotational dependence of the matrix elements for the $0 \rightarrow 1$, $0 \rightarrow 2$, and $0 \rightarrow 3$ bands can be compared to results obtained by THP [19]. Rather than treating the matrix elements themselves, this representation treats the vibration-rotation interaction factors, F, defined by:

$$\langle v', J'|u(r)|v, J\rangle^2 = \langle v'|\mu(r)|v\rangle^2 \cdot F^{v'v}(J) = (R^{v'v})^2 F^{v'v}(m)$$

where m has the value -J for the P branch and +J' for the R branch; $m = 0$ corresponds to the rotationless transition so that $F^{v'v}(0) \equiv 1$. THP have determined quadratic expressions for F^{10}, F^{20}, and F^{30} in the following form

$$F^{v0}(m) = 1 + C_v m + D_v m^2$$

THP have determined analytical expressions for C_v and D_v using a cubic representation for the dipole moment, a quantic power series for the internuclear potential and third order perturbation theory [6]. In addition, they have determined experimental values for C_1 and C_2 and D_1 and D_2 based on $0 \rightarrow 1$ and $0 \rightarrow 2$ absorption measurements [19]. An experimental value was also obtained for C_3 from the data of BHMS. These values are presented in the first and second columns of Table 14. Values of F(m) were determined from the rotation-dependent matrix elements calculated during the present program and presented in Appendix II. These

TABLE 13. COMPARISON OF MEASURED AND CALCULATED $R^{1,2}$ AND $R^{2,3}$

	Experimental (BHMS)	Present Calculation	Calculations for BHMS $R^{0,1}$, $R^{0,2}$, and $R^{0,3}$
$R^{1,2}$	$9.71 \pm 0.48 \times 10^{-2}$	$9.67 \pm 0.35 \times 10^{-2}$	$9.38 \pm 0.22 \times 10^{-2}$
$R^{2,3}$	$11.88 \pm 0.59 \times 10^{-2}$	$11.55 \pm 0.9 \times 10^{-2}$	$11.32 \pm 0.32 \times 10^{-2}$

TABLE 14. F-FACTOR COEFFICIENTS FOR HCl

	THP Observed	THP Calculated	Present Calculations
C_1	-0.0260 ± 0.002	-0.0279 ± 0.0006	-0.0269
C_2	-0.0086 ± 0.0015	-0.0066 ± 0.0005	-0.0061
C_3	0.017	0.011 ± 0.003	0.011
D_1	$4.5 \pm 2.0 \times 10^{-4}$	$2.8 \pm 0.2 \times 10^{-4}$	2.65×10^{-4}
D_2	$4.1 \pm 2.0 \times 10^{-4}$	$2.7 \pm 0.3 \times 10^{-4}$	3.76×10^{-4}
D_3		$3.3 \pm 0.5 \times 10^{-4}$	1.03×10^{-3}

were fit by least squares to a quadratic polynomial as a function of m to obtain values for C_1, C_2, C_3 and D_1, D_2, D_3 corresponding to the present work. These coefficients are presented in the third column of Table 14.

As one would expect, the results of the present calculations are very close to the calculated values of THP. However, they are not so close that the present calculations overlap with the THP uncertainties. The agreement with the experimental results is similar to that of the calculations of THP and is not improved by the present calculations. There is quite a substantial difference in the values for D_3. Since both values shown are computed values, this difference must represent either the differences in the calculational techniques or the differences in the M_i used in the two cases. We cannot reconcile this difference without recomputing C_v and D_v using the expressions of THP with the dipole moment function used in the present work. We have not included error limits on the results for C_v and D_v because of the complexity of the dependence of C_v and D_v on the dipole moment coefficients through the numerical calculations. General comparisons of our techniques with the analytical techniques of THP would be a useful future exercise to show the range of validity of the approximations of THP. The present technique, though less sophisticated, is potentially more accurate than that of THP.

In conclusion, the matrix elements for HCl computed herein and presented here and in Appendix II provide a good characterization of HCl molecule to the degree that the dipole moment function accurately represents the molecule. The use of a completely numerical technique means that the results are free of any truncation errors introduced by the representation of the potential by a power series.

2.3. PROGRESS ON THE OVERTONE ABSORPTION MEASUREMENTS OF CO

The original work statement calls for measurement of absorption line strengths (or equivalently electric dipole matrix elements) in the second overtone band of carbon monoxide. However, results have been published for this band for near Doppler lines by Toth, Hunt and Plyler [2]. Measurements will therefore be made primarily on the third overtone band, returning to the second overtone to determine Lorentz widths if scheduling permits it.

Present plans are to determine individual vibration-rotation line strengths and Lorentz half widths in the $v = 0 \rightarrow v' = 4$ band of carbon monoxide for gas pressures near two atmospheres: path lengths will be on the order of 200 m. Our data and data from other investigators will be used for the fundamental through second overtone bands to determine the coefficients of the dipole moment expansion for CO through fourth order. Line strengths will be determined by integrating the area under the observed absorption coefficient curve. Line strengths will also be obtained from the data by use of the Lorentz relation and the peak absorption coefficients and half widths. Line half widths will be measured directly from the observed data and com-

pared with those predicted by the Anderson theory. Distortion of the spectral lines introduced by the spectrometer slit function will be corrected by means of a modified direct measurement method [23].

2.3.1. MEASUREMENT FEASIBILITY

To determine the feasibility of observing the third overtone band of CO with path lengths obtainable in the laboratory, we must estimate the strength of the band by calculating the ratio of the squares of the rotationless dipole moment matrix elements which are proportional to the band strengths S:

$$\langle 0|\mu(r)|4\rangle^2 / \langle 0|\mu(r)|3\rangle^2 \propto \frac{S(0 \rightarrow 4)}{S(0 \rightarrow 3)}$$

Since the matrix elements are defined as

$$R^{v,0} = \langle 0|\mu(r)|v\rangle = \int \psi_0 \mu(r) \psi_v r^2 dr$$

they may be evaluated through numeric integration by means of wavefunctions obtained by numeric solution of the radial Schrödinger equation and the polynomial expansion for $\mu(r)$ known through third degree from previous experimental work. This was done by means of the existing matrix element calculation program. The value obtained in this manner is:

$$S(0 \rightarrow 4)/S(0 \rightarrow 3) \cong 0.0045$$

Once the ratio is known, estimates of line strengths in the third overtone band are obtained from those observed in the second overtone band [2]. We can then calculate approximate peak absorptions for the lines by assuming Lorentz line shapes and using the expression:

$$\alpha^P(m) = 1 - \exp\left[-K^P(m) P \ell\right] = 1 - \exp\left[-S(m) P \ell / \gamma\pi\right]$$

where $\alpha^P(m)$ = peak absorptances for the line
$S(m)$ = strength of the line
$K^P(m)$ = peak absorption coefficient
P = pressure of the gas (atm)
ℓ = path length in cm
γ = Lorentz half width
m = line index, $-J$ in the P branch, $+J'$ in the R branch
J, J' = initial and final rotational quantum numbers of the transition

Calculations of this type for a path length of 200 m and a constant half width of 0.05 cm^{-1} at 1 atm give the results presented in Table 15. This table shows that with path lengths of the

TABLE 15. RESULTS OF CALCULATIONS OF PEAK ABSORPTIONS

Line	$S(0-4) \times 10^6$ ($atm^{-1}\ cm^{-2}$)	$\alpha^P(\nu_6)$ (200-m Path at 2 atm)	Line	$S(0-4) \times 10^6$ ($atm^{-1}\ cm^{-2}$)	$\alpha^P(\nu_7)$ (200-m Path at 2 atm)
R(0)	0.62	7	P(1)	0.6	7
R(1)	1.2	13	P(2)	1.1	12
R(2)	1.7	18	P(3)	1.6	16
R(3)	2.0	21	P(4)	1.9	19
R(4)	2.6	26	P(5)	2.0	21
R(5)	2.7	27	P(6)	2.1	22
R(6)	2.9	28	P(7)	2.1	22
R(7)	2.9	28	P(8)	2.0	21
R(8)	2.9	28	P(9)	1.9	20
R(9)	2.6	26	P(10)	1.8	19
R(10)	2.4	24	P(11)	1.5	16
R(11)	2.2	22	P(12)	1.4	14
R(12)	1.9	20	P(13)	1.0	11
R(13)	1.6	17	P(14)	0.8	9
R(14)	1.3	14	P(15)	0.6	7
R(15)	1.0	11	P(16)	0.5	6
R(16)	0.8	9	P(17)	0.3	4
R(17)	0.6	7	P(18)	0.3	4
R(18)	0.4	5	P(19)	0.2	3
R(19)	0.3	4	P(20)	0.1	2
R(20)	0.2	3			

order of 200 m, we should be able to determine line parameters in the third overtone band for all lines between P16 and R18.

To minimize instrumental distortion of the observed spectra, spectral lines which are broad compared to the spectral resolution of the instrument are required. It is always possible to increase the pressure of the gas under observation to obtain broad lines; however, this also has the effect of overlapping the wings of adjacent lines and increasing the difficulty of data reduction. To determine the seriousness of these problems in the present study, the amount of line overlap for the pressures to be used during observation must be estimated.

Since CO has a very small dipole moment, quadrupole transitions dominate the pressure broadening. We therefore expect only slight variations in Lorentz half widths between second and third overtone bands. Previous experimental data [24] give widths of the order of 0.053 cm^{-1} atm^{-1} for R(17) and P(18) lines and values of 0.071 cm^{-1} atm^{-1} for R(1) or P(2) lines. Since the spectral resolution of the instrument being used is of the order of 0.05 cm^{-1}, to obtain resolution to line width ratios of 0.5, pressures of approximately two atmospheres should be used for the higher J lines, and, pressures of one to one-and-a-half atmospheres for lines near band center. To determine the amount of overlap evident at these pressures, we assume a Lorentz line shape, distorted by the instrumental slit function, and then evaluate the distance from line center at which a specified absorptance is observed.* With a resolution-to-line width ratio of 0.5, a distorted line with a peak absorption of 30% has an absorptance of 0.1% at a distance of 18.8 half widths from line center or approximately 1.9 cm^{-1}. Since the CO lines are separated by 4 cm^{-1}, overlap effects are not serious at these pressures.

2.3.2. APPARATUS

The long path lengths required for observation of the third overtone band are obtained with a 5-m White cell**. A photograph of the cell chamber is shown in Fig. 11. Entrance and exit windows are seen on the front bell housing and the turbo-molecular pump used for evaluation of the system is visible in the background. The optical system of the cell consists of three accurately ground, spherical mirrors placed one radius of curvature apart. Long path lengths are obtained by successively imaging the light intercepted by the pair of back mirrors onto the surface of the single front mirror. Figure 12 shows the light path for eight passes. The number of traversals of the cell is set by rotating the two back mirrors about vertical axes, causing the distance between successive images on the single mirror to decrease. A single rotation adjustment for this purpose has been incorporated into the cell design. Figure 13 is a photograph

*For a detailed discussion of the methods and tabulations of results, see Ref. [23].

**Cell designed and constructed under Contract DAHC-15-67-C-0062.

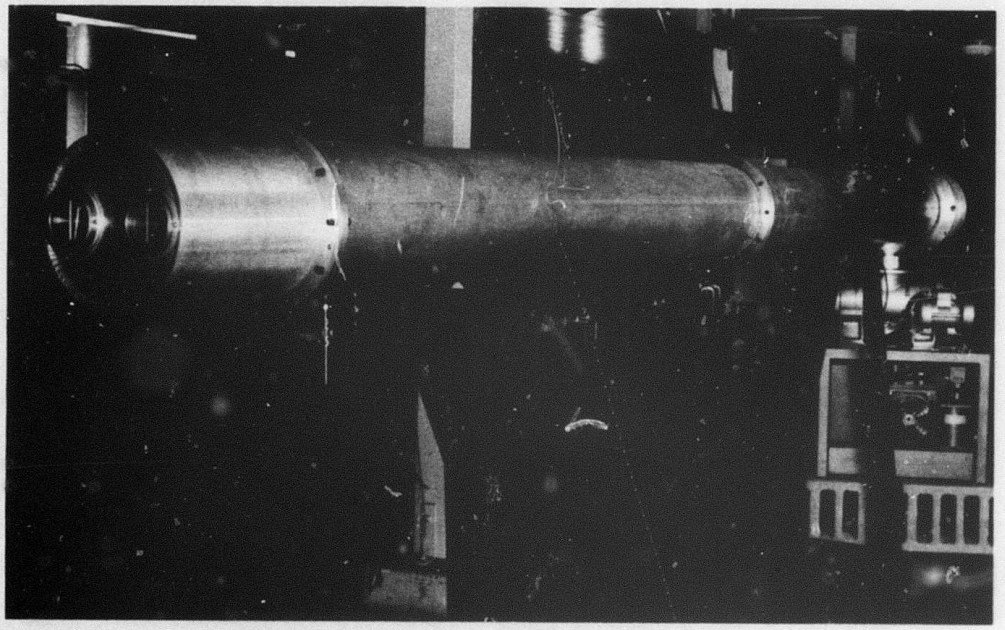

FIGURE 11. FIVE-METER WHITE CELL FOR OBSERVANCE OF THE THIRD OVERTONE BAND OF CO

of the optical system removed from its vacuum chamber. Visible in this figure is the path followed by 6328 Å radiation from a He:Ne laser with the cell set for 16 traverses.

The spectrometer used is a 1.8-m focal length Ebert Vacuum Spectrometer with a 190-mm × 135-mm Bausch and Lomb replica grating. Resolution of approximately 0.05 cm^{-1} over the third overtone CO band is obtainable with a 3-μm blaze grating in third order, double passed. To insure stability of the spectrometer wavelength drive, the room temperature is held constant to within 0.5°C.

Since the spectrometer operates at f/10 and the White cell at f/45, vacuum f-number matching optics are required to couple the two systems. A schematic of the optics built for this purpose is shown in Fig. 14. A photograph of the entire optical system consisting of the White cell, matching optics, and vacuum spectrometer is presented in Fig. 15.

During data collection, the CO pressure in the White cell is continuously monitored with an MKS Baratron capacitance bridge-pressure gauge. This gauge permits observation of pressure variations of 0.06 torr at two atmospheres. Although thermal effects alone may cause variations of this magnitude, pressure stability is expected to be better than 0.1%.

The infrared energy will be detected with a selected PbS photoconductive detector and a Princeton Applied Research lock-in amplifier. The detector is operated at -79°C and has a measured dimensionless detectivity (D^*) of 1.4×10^{11} cm $Hz^{1/2}$ W^{-1}. In the complete optical system, with a chopping frequency of 510 Hz, a signal-to-noise ratio of 200 has been observed with the White cell set for a 16-pass operation. The analog signal from the lock-in amplifier is digitized and integrated with a digital voltmeter and the result is fed to an IBM card punch.

2.4. DATA REDUCTION

Two major computer codes have been written to handle the data reduction. The first of these determines the strength of the spectral lines through numeric integration using:

$$S = \frac{1}{P}\int K(\nu')\,d\nu' = -\frac{1}{P\ell}\int \log_e \tau(\nu')\,d\nu'$$

where S = strength of the spectral line
P = pressure of gas under observation (atm)
ℓ = path length (cm)
$\tau(\nu')$ = spectra transmittance = $1 - \alpha(\nu')$
$K(\nu')$ = spectral absorption coefficient
ν' = spectral wavenumber (cm^{-1})

The same program evaluates the peak absorption coefficient and the Lorentz half width for each line. All of these values are distorted by the spectrometer slit function however, and

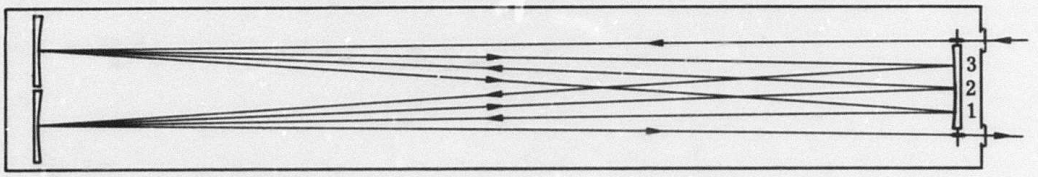

FIGURE 12. WHITE CELL OPTICAL PATH: EIGHT TRAVERSAL OPERATION

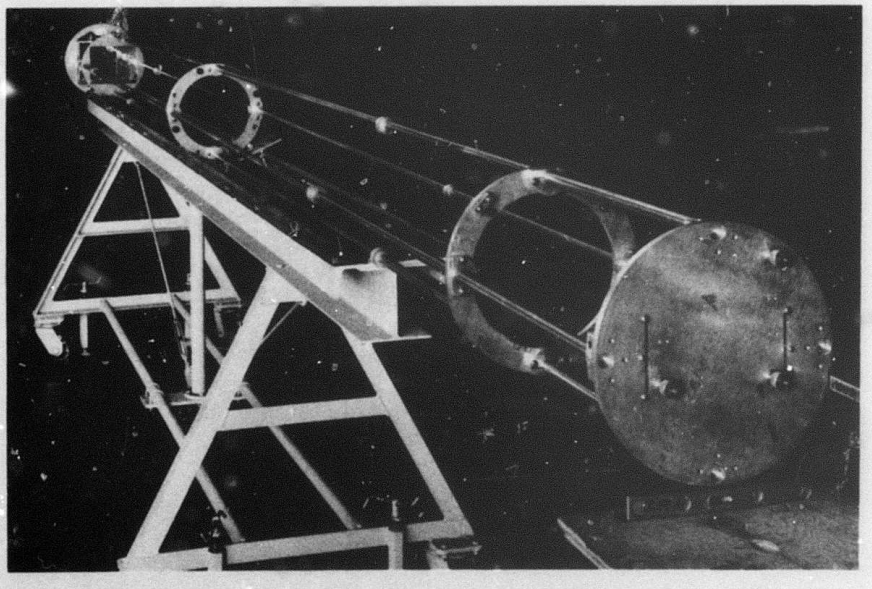

FIGURE 13. OPTICAL SYSTEM OF FIVE-METER WHITE CELL REMOVED FROM ITS VACUUM CHAMBER. Path lines are for 6328 Å radiation from the He:Ne laser with cell set for 16 traversals.

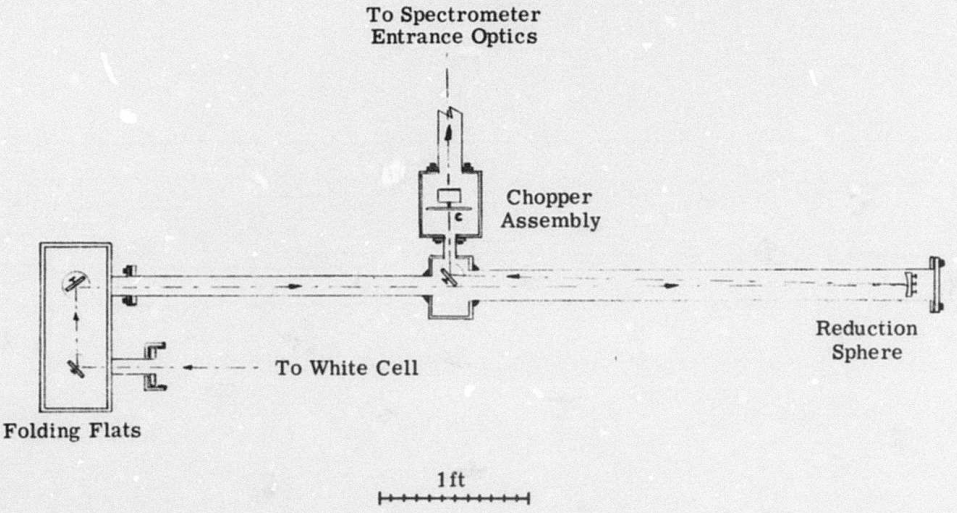

FIGURE 14. REDUCTION OPTICS FOR WHITE CELL

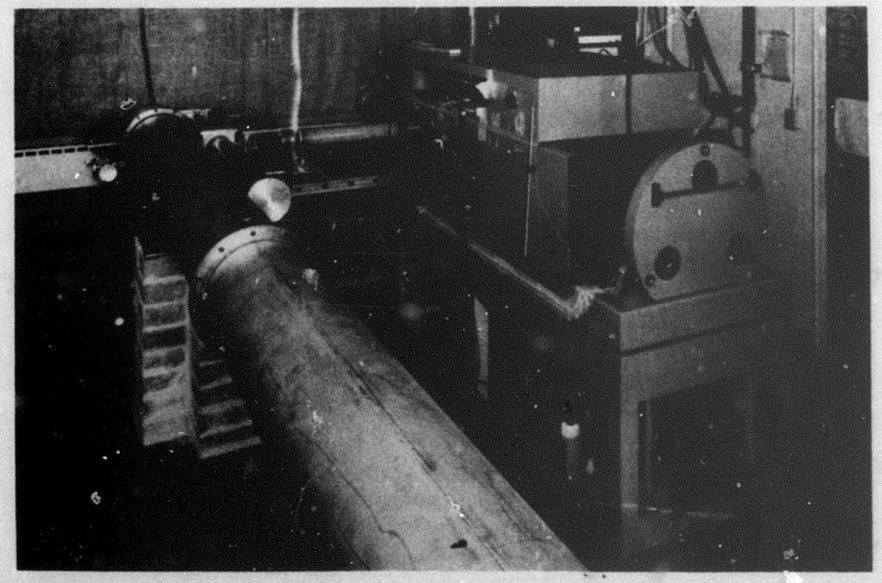

FIGURE 15. WHITE CELL, MATCHING OPTICS AND VACUUM SPECTROMETER

correction procedures must be used to obtain the true line parameters. Therefore, we use a second program which follows the procedures of a direct measurement method [23] and corrects these values for instrumental distortion yielding the true strengths, widths, and peak absorption coefficients.

Calculation of the dipole moment coefficients and matrix elements has been discussed earlier, and Anderson theory pressure broadened widths is presented in Section 4.

3
INFRARED DIAGNOSTIC STUDIES

G. H. Lindquist and C. B. Arnold

3.1. INTRODUCTION

In the design and operation of chemical lasers, it is necessary to know the rates of creation and loss of molecules in the energy states involved resulting from the various processes which compete with laser action. Molecular collisions with the cavity walls, molecular diffusion into and out of the active region, and collisions between molecules in the active gas medium all produce such changes in the population. This portion of the program is concerned with the redistribution and loss to translation of rotational and vibrational energy. Such redistribution and loss are the result of collisions among the gas molecules within the active medium.

The primary objective of the studies is to determine experimentally the populations of HF molecules as a function of time and of their vibrational and rotational state in a cell of excited HF and in the absence of diffusion and wall effects. Once radiative processes are accounted for, experimental transfer rates resulting from collision processes can be determined. From these, energy-transfer cross sections for the various processes can be determined.

3.2. EXPERIMENTAL DESIGN

3.2.1. EXCITATION TECHNIQUE

It would be most realistic if energy-transfer cross sections could be determined under the chemical excitation conditions existing in a HF laser cavity. However, because of the large number of different excited states that exist in such a case, it would be difficult to trace the flow of the excitation energy during relaxation. To make the interpretation of the experiment simpler, we have decided instead to excite the HF gas with a monochromatic beam from an HF laser operating on a single vibration-rotation line. This procedure would excite only those HF molecules in the cell with rotational energy coinciding with the lower state of the vibration-rotation line upon which the laser is operating. The relaxation from this relatively simple departure from equilibrium can then be studied in one of the ways described below.

Further, a number of investigators are currently studying the vibrational relaxation of excited HF molecules [25, 26, 27]. Although it would be interesting to study vibrational relaxation under our particular excitation conditions, it is our opinion that more useful and unique results can be obtained by concentrating on rotational energy relaxation. The decision to study rotational energy transfer in itself precludes the use of a realistic laser cavity, because the cell

pressure required to yield rotational relaxation times on the order of 1 μsec are about 0.01 torr, much lower than typical cavity pressures (the relaxation time must be long enough to be observed with typical infrared detectors).

The excitation technique described above, although allowing simple interpretation, has several limitations which stem from its failure to reproduce the real situation. The most severe of these limitations is related to the possible rotational levels that can be studied. Under chemical excitation, it appears that substantial energy initially goes into high rotational levels as evidenced by Deutsch's success in building a pure rotational laser at low pressures (~ 1 torr) operating at high rotational levels and by the calculations of Wilkins [28, 29]. At the usual pressures at which chemical lasers operate (10 to ~ 100 torr), rotational equilibrium occurs fast enough that little or no rotational disequilibrium is apparent [30]. The current experimental design precludes the possibility of studying the high rotational levels because such levels cannot be populated in a cell at or near room temperature. There are essentially no molecules available to absorb the energy from a vibration-rotation laser operating at high rotational levels. At present, we can visualize no method whereby the ease of interpretation of the presently planned experiment can be retained and in which higher rotational levels can be excited.

3.2.2. RELAXATION MONITORING TECHNIQUE

Once the cell of gas has been excited, a means must be devised whereby the history of the populations of the various states involved can be observed during the relaxation process. All of the techniques considered are optical techniques whereby the interaction of the excited gas with optical radiation in either the vibration-rotation region or the pure rotation region is monitored by infrared detectors. The relaxation of the excited gas can be monitored by observation of either emission or absorption. In addition, the monitoring can be performed in either the vibration-rotation bands or pure rotation bands. Both techniques have been used in the vibration-rotation region [30, 31]; however, observations in the pure rotation region have never been used.

Observations of emission from the active gas generally yield signals large enough to be visible above detector noise in the vibration-rotation region. However, calculations for emission in the pure rotation region indicate that only marginal signal-to-noise ratios are available.

Observations of absorption are not practical in the vibration-rotation region when spectrally continuous sources (e.g., incandescent lamps) are used because, at low pressures, the absorption is very small and the spectral slit width of any practical observing instrument is large compared to the true line width. Thus, the observed absorption is even lower than the true peak-line absorption. However, if the source used in the absorption measurement is an HF laser, operating at the peak of one of the HF vibration-rotation transitions, the absorption of

such a monocromatic source can be high enough to be easily measured. We have chosen this technique as the primary monitoring technique for this experiment. Absorption measurements are also feasible in the pure rotation portion of the spectrum where absorption is greater. However, there is increased operating difficulty involved in this region. The analysis in Section 3.3 indicates that the use of absorption measurements in the pure rotation region allows relaxation measurements to be made for a greater range of rotational energies than are possible in the vibration-rotation region provided that pure rotation lasers can be obtained for the desired lines.

To summarize, the relaxation of the excitation produced in a low-pressure cell of HF and possible dilutents are to be monitored by measuring the absorption (as a function of time) of the energy from a second or probe laser operating in a single line in the HF vibration-rotation band. Absorption histories obtained for a number of different vibration-rotation transitions (corresponding to the operation of the probe laser on different lines) will yield histories of the populations of the different states. Section 3.3 presents estimates of the emission and absorption signal levels available in both the vibration-rotation region and the pure rotation region and discusses the basis upon which the above monitoring technique was chosen.

3.3. COMPUTATION OF EXPECTED RESULTS

The following describes an analysis, based on radiative considerations only, of both the excitation techniques and the various possible monitoring techniques. No collision or diffusion processes are accounted for.

It is necessary to determine the approximate cell conditions necessary in order for rotational relaxation to be observed. First, for observation with a system having about a 0.1-μsec rise time, the pressure must be low so that the relaxation will be slow enough to be seen. This rise time is about the shortest that can be obtained without use of specially constructed high-speed infrared detectors and preamps. We estimated the collision cross section for rotational energy transfer between HF molecules to be between 3 and 30 Å from calculations based on the theory of Sharma and Brau [32]. We assumed a cross section of 15 Å and obtained a relaxation time at 373^{o}K of about 0.035 μsec at 1-mm pressure. Pressures of ~ 0.01 mm are therefore required to obtain relaxation times of the order of 1 μsec. The temperature of 373^{o}K was used since it is necessary to heat the HF to about 100^{o}C to prevent polymerization of the HF. Cell lengths longer than about 50 cm are difficult to accommodate in the experimental apparatus. Therefore, cell lengths of 5, 30, and 50 cm were considered.

3.3.1. EXCITATION

The excitation is to be stimulated by directing a pulse of monochromatic radiation into the cell containing the HF mixture. The stimulating beam will be generated by a pulsed HF laser

operating on one of the vibration-rotation transitions of HF. Since the cell will be at equilibrium before the stimulating pulse occurs, most of the molecules will be in the v = 0 vibrational state (v is the vibrational quantum number).

Thus, to obtain maximum excitation, the stimulating beam should operate in the v = 0 → v' = 1 band. The HF laser used to generate the stimulating pulse will operate with only a partial population inversion; therefore its output will be largely limited to the P branch of that band. Only those molecules in the cell can be stimulated which are in rotational level J, (J is the rotational quantum number) corresponding to the lower level of the stimulating transition and which have v = 0. Those molecules will be stimulated to the v' = 1, J' = J - 1 level.

We can treat the excitation quantitatively, using the equations for laser amplification. In this case, where the only radiation of interest (the stimulating radiation) is collimated or unidirectional, the conservation equations for photons and molecules can be given by:*

photon conservation
$$\frac{\partial \rho_\nu}{\partial t} + c\,\frac{\partial \rho_\nu}{\partial x} = -\rho_\nu c\left(n_{\ell_\nu} B_{\ell u} - n_{u_\nu} B_{u\ell}\right) \tag{20}$$

molecule conservation
$$\frac{\partial n_{\ell_\nu}}{\partial t} = -\rho_\nu c\left(n_{\ell_\nu} B_{\ell u} - n_{u_\nu} B_{u\ell}\right) \tag{21}$$

$$\frac{\partial n_{\ell_\nu}}{\partial t} = +\rho_\nu c\left(n_{\ell_\nu} B_{\ell u} - n_{u_\nu} B_{u\ell}\right) \tag{22}$$

Note that the number densities have been written as spectral quantities to account for the fact that the photon density of the stimulating beam, ρ_ν, has a spectral distribution associated with it and that the molecules, by virtue of their random thermal velocities, are ready to absorb energy in a distribution of frequencies corresponding to a Doppler profile.

No terms are included for relaxation by spontaneous emission, or by any other mechanism for that matter, since the stimulation pulse is assumed to occur much faster than any relaxation process. These equations can be reduced to dimensionless form by defining the following dimensionless variables. A dimensionless number density difference η is defined as:

$$\eta(x, t) = \frac{\dfrac{n_{\ell_\nu}}{g_\ell} - \dfrac{n_{u_\nu}}{g_u}}{N_\nu}$$

*See also Appendix I and Ref. [33].

where g_ℓ and g_u are the degeneracies of the lower and upper states and where $N_\nu = n_{\ell_\nu} + n_{u_\nu}$, the sum of the molecules in the upper and lower state ready to absorb energy at frequency ν. The spectral populations, n_{ℓ_ν} and n_{u_ν} can be written as:

$$n_{\ell_\nu} = n_\ell s_\ell(\nu - \nu_0)$$

$$n_{u_\nu} = n_u s_u(\nu - \nu_0)$$

where s_ℓ and s_u are the Doppler distributions of n_ℓ and n_u about the center frequency of the transition ν_0. Also, $n_u + n_\ell = N$, a constant by molecular conservation in the absence of other processes that create or destroy molecules. Further, if we assume that the stimulated absorption or emission does not affect the translational energy of the molecule, and if the spectral width of the incident laser pulse is larger than the Doppler width in the HF cell, then

$$n_{u_\nu} + n_{\ell_\nu} = N_\nu \tag{23}$$

and

$$s_\ell = s_u$$

Also, we define a dimensionless photon density

$$\Phi(x, t) = \frac{\rho_\nu}{N_\nu} \tag{24}$$

Equations (21) and (22) can now be added to obtain:

$$\frac{\partial \eta}{\partial t} = -\Phi\eta[cN_\nu(B_{\ell u} + B_{u\ell})] \tag{25}$$

Equation (20) becomes

$$\frac{\partial \Phi}{\partial t} + c\frac{\partial \Phi}{\partial x} = -\Phi\eta(cN_\nu g_\ell B_{\ell u}) \tag{26}$$

Equations (25) and (26) can be simply solved (e.g., see Ref. [33] to give:

$$\eta(x, t) = \frac{\eta(x, 0) \exp\left[Z_1 \int_0^x \eta(x', 0)\,dx'\right]}{\exp\left[Z_2 \int_0^{t-x/c} \Phi(0, t')\,dt'\right] + \exp\left[Z_1 \int_0^x \eta(x', 0)\,dx'\right] - 1} \tag{27}$$

and

$$\Phi(x, t) = \frac{\Phi\left(0, t - \frac{x}{c}\right)}{1 - \left\{1 - \exp\left[Z_1 \int_0^x \eta(x', 0)\,dx'\right]\right\}\left\{\exp\left[-Z_2 \int_0^{t-x/c} \Phi(0, t')\,dt'\right]\right\}} \tag{28}$$

where $Z_1 = N_\nu g_\ell B_{\ell u}$

$Z_2 = cN_\nu(B_{\ell u} + B_{u\ell})$

If we now let the input flux be a laser pulse having an integrated energy per unit area of P_0 distributed uniformly over a spectral width, $\Delta\nu$, then

$$P_0 = \int \rho_\nu \Delta\nu c\,dt = \int_{\Delta t} N_\nu \Phi(0, t)(\Delta\nu)c\,dt \quad \text{photons/cm}^2$$

where Δt is the pulse duration. For a rectangular pulse

$$P_0 = \Phi_0 \Delta t \Delta\nu c N_\nu \tag{29}$$

The total flux passing through a position $x \geq 0$ is

$$P(x) = \int_{x/c}^{x/c+\Delta t} cN_\nu \Phi(x, t')\,dt' = cN_\nu \int_{x/c}^{x/c+\Delta t} \frac{\Phi_0\,dt}{1 - \left\{1 - \exp\left[Z_1 \int_0^x \eta(x', 0)\,dx'\right]\right\}\left\{\exp\left[Z_2 \int_0^{t-x/c} \Phi_0\,dt\right]\right\}}$$

This can be reduced to the following expression

$$\frac{P(x)}{P_0} = 1 + \frac{1}{P^*} \log \frac{1 - \exp(-P^*) + \exp(L^* - P^*)}{\exp L^*} \tag{30}$$

where P^* is a dimensionless energy input given by

$$P^* = \frac{P_0 Z_2}{N_\nu \Delta\nu c} = \frac{P_0}{\Delta\nu}(B_{u\ell} + B_{\ell u}) \tag{31}$$

and L^* is a dimensionless length

$$L^* = Z_1 x \eta(0, x) = g_\ell B_{\ell u} x \left(n_{\ell_\nu} - n_{u_\nu}\right) t = 0 \tag{32}$$

L^* is a spectrally varying quantity. In order to get substantial power from the HF lasers we constructed, we had to use relatively high pressures and high cavity losses (low mirror reflectivities). The high cavity losses indicate that the effective spectral width of our stimulating pulse could be wider than the Doppler width corresponding to absorption in the cell. In such a case P^* can be taken as constant over the Doppler profile and L^* will vary both with x and with the spectral distance from line center, $\nu - \nu_0$. At the line center

$$n_{u_\nu} = \frac{n_u}{\sqrt{\pi}\gamma_D} \text{ and } n_{\ell_\nu} = \frac{n_\ell}{\sqrt{\pi}\gamma_D}$$

where γ_D is the Doppler half width of the gas absorption line.

$$\gamma_D = \frac{\nu_0}{c}\sqrt{\frac{2kT}{\mathcal{M}}}$$

where $\mathcal{M}$ = the molecular mass
k = the Boltzmann constant
T = the temperature

Before stimulation $n_\ell \gg n_u$ since n_u is a state where v = 1 and n_ℓ is a v = 0 state. Thus

$$\left(n_{\ell_\nu} - n_{u_\nu}\right)_{t=0} \approx \frac{\left(n_\ell\right)_{t=0}}{\sqrt{\pi}\gamma_D}$$

$$\text{so that } L^* = \frac{(\eta_f)_{t=0}}{\sqrt{\pi}\,\gamma_D}\, g_f B_{fu} x \tag{33}$$

at line center. If the value of η at $t = 0$ is constant for all x and equal to η_0, then the expression for $\eta(x)$ after the passage of the pulse is

$$\eta\left(x,\ \Delta t + \frac{x}{c}\right) = \frac{\eta_0 \exp\left(Z_1 \eta_0 x\right)}{\exp\left(Z_2 \int_0^{\Delta t} \Phi_0\, dt'\right) + \exp\left(Z_1 \eta_0 x\right) - 1} \tag{34}$$

or

$$\frac{\eta(x)}{\eta_0} = \frac{\exp L^*}{\exp P^* + \exp L^* - 1}$$

Note that the limiting value for η after the passage of an infinitely strong pulse is zero. This corresponds to the inversion boundary and is the state in which a stimulated absorption event is equally as probable as a stimulated emission event. Henceforth $\eta = 0$ will be referred to as the bleached condition. It is of primary interest in this program to determine, for a cell of total length x_T, the energy required per pulse to reduce η to some arbitrarily small value at the far end of the cell, i.e., at $x = x_T$ (η will always be closer to zero for other $x < x_T$). We have assumed that a 90% change in η at the far end of the cell will yield a sufficiently stimulated cell for our purposes. Thus, the condition may be written

$$\eta(x_T) \text{ (after pulse)} \leq 0.1\, \eta_0$$

We would like to find P^* so that for $L^* = L_T^*$ (corresponding to $x = x_T$) the above condition is satisfied. We write:

$$\frac{\eta(x_T)}{\eta_0}(0.1) = \frac{\exp\left(L_T^*\right)}{\exp\left(P_{0.1}^*\right) + \exp\left(L_T^*\right) - 1}$$

or

$$P_{0.1}^* = \ln\left[9.\ \exp\left(L_T^*\right) + 1\right] \tag{35}$$

$P_{0.1}^*$ is the dimensionless power required to drive the value of η at the far end of the cell to 0.1, its original value. The value of η in the remainder of the cell is even lower; we computed

L_T^* for the line center using Eq. (33). Values of $B_{u\ell}$ and $B_{\ell u}$ for the stimulating laser transition were obtained from the values of the Einstein coefficient for spontaneous emission, $A_{u\ell}$, given in Ref. [1], using the relations

$$B_{u\ell} = \frac{A_{u\ell}}{8\pi\nu'^2} \frac{cm^2}{sec} \tag{36}$$

and

$$B_{\ell u} = \frac{g_u}{g_\ell} B_{u\ell}$$

where ν' is the wavenumber of the transition: $B_{\ell u}$ and $B_{u\ell}$ are in photon units.

The degeneracies of the lower and upper states, g_ℓ and g_u, are given by

$$g_\ell = 2J_s + 1$$

$$g_u = 2J_s - 1$$

where J_s is the rotational designation of the stimulating laser transition. This particular relation between g_ℓ and g_u appears because the laser operates in the P branch. Table 16 shows the energy required per unit cross-sectional area to excite the cell so that 90% of the possible stimulation is obtained at the far end of cell, for 0.01 torr pressure, 373°K, and cell length of 5, 30, and 50 cm. This calculation assumes that the equivalent spectral width of the laser pulse is equal to its upper limit, 0.025 cm^{-1}. This value is approximate and was obtained by assuming that the pressure in the laser cavity would be about 30 torr and that collisional broadening of the transitions by H_2 and SF_6 would be nearly identical. Broadening by H_2 was assumed to be about 1/5 as effective as broadening by HF. These considerations yield a collisional half width of about 0.01 cm^{-1}. This half width, in combination with a Doppler half width of about 0.006 cm^{-1}, should yield a full width for the laser transition (assuming that the laser is operated without a front mirror) of about 0.025 cm^{-1} neglecting narrowing due to stimulated emission. The levels required are very modest and are well within the capability of the stimulation laser already constructed.

3.3.2. RELAXATION MONITORING

As mentioned earlier, optical monitoring of the relaxation process can be accomplished in either absorption or emission and either in the vibration-rotation or pure rotation region. The purpose of this section is to determine expected levels for all four types of monitoring and to present conclusions covering the most appropriate means of measurement. Since absorption is the simplest to model, it is discussed first.

TABLE 16. POWER REQUIREMENT PER UNIT CELL AREA TO PRODUCE 90% OF MAXIMUM POSSIBLE CHANGE IN CELL POPULATION

(a) 5 cm Cell Length

Cell Pressure: 0.010 torr
Cell Temperature: 373.0 deg K
Laser Line Width: 0.0250 cm^{-1}

Stimulating Laser Line	L_T^*	$P_{.1}^*$	Energy Required (J/cm^2)
P 1(1-0)	0.1134	2.4052	0.2102E-03
P 2(1-0)	0.1739	2.4604	0.2551E-03
P 3(1-0)	0.1705	2.4573	0.2512E-03
P 4(1-0)	0.1268	2.4174	0.2379E-03
P 5(1-0)	0.0753	2.3706	0.2234E-03
P 6(1-0)	0.0366	2.3356	0.2104E-03
P 7(1-0)	0.0148	2.3159	0.1993E-03
P 8(1-0)	0.0050	2.3071	0.1897E-03
P 9(1-0)	0.0014	2.3038	0.1810E-03
P10(1-0)	0.0003	2.3029	0.1731E-03
P11(1-0)	0.0001	2.3026	0.1656E-03
P12(1-0)	0.0	2.3026	0.1585E-03
P13(1-0)	0.0	2.3026	0.1518E-03
P14(1-0)	0.0	2.3026	0.1455E-03
P15(1-0)	0.0	2.3026	0.1395E-03

TABLE 16. POWER REQUIREMENT PER UNIT CELL AREA TO PRODUCE 90% OF MAXIMUM POSSIBLE CHANGE IN CELL POPULATION
(Continued)

(b) 30 cm Cell Length

Cell Pressure: 0.010 torr
Cell Temperature: 373.0 deg K
Laser Line Width: 0.0250 cm^{-1}

Stimulating Laser Line	L_T^*	$P_{.1}^*$	Energy Required (J/cm^2)
P 1(1-0)	0.6801	2.9321	0.2563E-03
P 2(1-0)	1.0435	3.2791	0.3400E-03
P 3(1-0)	1.0233	3.2597	0.3332E-03
P 4(1-0)	0.7606	3.0084	0.2961E-03
P 5(1-0)	0.4519	2.7174	0.2561E-03
P 6(1-0)	0.2197	2.5024	0.2254E-03
P 7(1-0)	0.0886	2.3826	0.2050E-03
P 8(1-0)	0.0298	2.3295	0.1916E-03
P 9(1-0)	0.0084	2.3102	0.1815E-03
P10(1-0)	0.0020	2.3044	0.1732E-03
P11(1-0)	0.0004	2.3029	0.1656E-03
P12(1-0)	0.0001	2.3026	0.1585E-03
P13(1-0)	0.0	2.3026	0.1518E-03
P14(1-0)	0.0	2.3026	0.1455E-03
P15(1-0)	0.0	2.3026	0.1395E-03

TABLE 16. POWER REQUIREMENT PER UNIT CELL AREA TO PRODUCE 90% OF MAXIMUM POSSIBLE CHANGE IN CELL POPULATION
(Concluded)

(c) 50 cm Cell Length

Cell Pressure: 0.010 torr

Cell Temperature: 375.0 deg K

Laser Line Width: 0.0250 cm^{-1}

Stimulating Laser Line	L_T^*	$P^*_{.1}$	Energy Required (J/cm^2)
P 1(1-0)	1.1335	3.3659	0.2942E-03
P 2(1-0)	1.7391	3.9557	0.4102E-03
P 3(1-0)	1.7055	3.9227	0.4009E-03
P 4(1-0)	1.2676	3.4957	0.3441E-03
P 5(1-0)	0.7531	3.0013	0.2828E-03
P 6(1-0)	0.3662	2.6376	0.2376E-03
P 7(1-0)	0.1476	2.4364	0.2097E-03
P 8(1-0)	0.0497	2.3474	0.1930E-03
P 9(1-0)	0.0140	2.3152	0.1819E-03
P10(1-0)	0.0033	0.3056	0.1733E-03
P11(1-0)	0.0007	2.3032	0.1656E-03
P12(1-0)	0.0001	2.3027	0.1585E-03
P13(1-0)	0.0	2.3026	0.1518E-03
P14(1-0)	0.0	2.3026	0.1455E-03
P15(1-0)	0.0	2.3026	0.1395E-03

3.3.3. ABSORPTION

Once the cell is stimulated, it can then be probed with a second, lower power laser. The absorption of energy from this second laser can be monitored. To keep the experimental results as independent of the degree of stimulation provided by the stimulating laser as possible, it is desirable to have the cell as bleached as possible. Therefore, as high an energy as possible per pulse, within reasonable limits, is necessary from the stimulating laser. For the remainder of this section the cell will be assumed to have been completely bleached by the monochromatic stimulating pulse. That is, the following condition will be assumed to exist throughout the cell immediately after stimulation

$$\frac{n_{u_s}}{g_{u_s}} = \frac{n_{\ell_s}}{g_{\ell_s}} \tag{37}$$

where the subscript s refers to the stimulating transition (such a subscript is needed because we now plan to introduce a probe transition).

The same equations developed earlier for the absorption of the stimulating pulse apply to the absorption of the probe pulse, except that the initial conditions are now the conditions after stimulation.

The absorption of a probe laser is given by Eq. (30). However, that relation indicates that the absorption is a function of probe laser energy, P^*, as well as the length L^*. If we consider small probe laser energies only, however, the exponentials involving P^* and the logarithm can be replaced by the first two terms in series expansions so that, for small P^*

$$\frac{P}{P_0} = \exp\left(-L_T^*\right) \tag{38}$$

the usual law of absorption. From Eq. (32), L_T^* is related to η of the gas before the incidence of a pulse, in this case the probe laser pulse; η for this case is

$$\eta(t=0) = \frac{\left(\frac{n_{\ell_p}^P}{g_\ell^P} - \frac{n_{u_p}^P}{g_u^P}\right)_0}{N_p^P} \tag{39}$$

where the P superscript refers to the probe laser and the 0 signifies initial conditions. Thus, the absorption is dependent on the populations of the upper and lower states before the incidence of the probe laser pulse. We have computed the absorption of the probe laser for three condi-

tions: (a) immediately after the passage of the stimulating pulse; (b) after rotational relaxation (assuming that rotational relaxation occurs before any vibrational relaxation); and (c) after complete relaxation.

Immediately after stimulation in a $v = 0 \rightarrow v' = 1$ P-branch line, the number densities in cm^{-3} are given by the following relations:

$v = 1$

$$J = J_s - 1: \quad \frac{P}{kT} \frac{(2J_s - 1)(2J_s + 1)}{4J_s} \frac{hcB_0}{kT} \exp\left[-\frac{hcB_0}{kT} J_s(J_s + 1)\right]$$

$$J \neq J_s - 1: \quad \sim 0$$

$v = 0$ (40)

$$J = J_s: \quad \frac{P}{kT} \frac{(2J_s + 1)^2}{4J_s} \frac{hcB_0}{kT} \exp\left[-\frac{hcB_0}{kT} J_s(J_s + 1)\right]$$

$$J \neq J_s: \quad \frac{P}{kT}(2J + 1) \frac{hcB_0}{kT} \exp\left[-\frac{hcB_0}{kT} J(J + 1)\right]$$

where B_0 is the rotational constant for HF in the $v = 0$ state. These relations correspond to a Boltzmann distribution of energies except for those levels affected by the stimulating pulse. The populations of the levels affected by the stimulating pulse are determined from Eq. (37). For this calculation, the population of the $v = 1$ state at equilibrium is assumed to be zero (at $100^{\circ}C$ far less than 1% of the total number density are in the $v = 1$ level).

Using Eqs. (32), (38), and (39), we computed the absorption of a probe laser operating in the P branch of the $v = 1 \rightarrow v' = 2$ band for probe laser transitions having various J values after stimulation by a laser pulse. The results of these tabulations are shown in Table 17. Each of the five parts of Table 17 corresponds to a particular J value for the stimulating laser line. The absorption before any relaxation occurred was computed by use of Eq. (21) for the required number densities. The results of these computations are shown in the first column of each part of Table 17.

The L^* values and hence the absorption, were computed for the peak of the Doppler absorption line. (Only Doppler broadening is important at the low cell pressures being used.) The calculated absorption values are therefore only realized in practice if the spectral width of the

TABLE I7. ABSORPTION OF COMPLETELY STIMULATED CELL BY PROBE LASER

(a)

Stimulating Line: P3 (1-0)
Cell Temperature: 373.0 deg K
Cell Pressure: 0.010 torr of HF
Cell Length: 50.0 cm in Probe Dimension

J of Probe Laser	Absorption of 2-1 Laser			Absorption of 1-1 Rotational Laser		
	Before Relaxation	After Rotational Relaxation	After Complete Relaxation	Before Relaxation	After Rotational Relaxation	After Complete Relaxation
1	0.0	0.1792	0.0	0.0	1.0	0.0
2	0.7083	0.2618	0.0	1.0	1.0	0.0001
3	0.0	0.2578	0.0	0.0	1.0	0.0001
4	0.0	0.1991	0.0	0.0	1.0	0.0001
5	0.0	0.1237	0.0	0.0	1.0	0.0
6	0.0	0.0623	0.0	0.0	0.9994	0.0
7	0.0	0.0256	0.0	0.0	0.9469	0.0
8	0.0	0.0087	0.0	0.0	0.6174	0.0
9	0.0	0.0025	0.0	0.0	0.2315	0.0
10	0.0	0.0006	0.0	0.0	0.0589	0.0
11	0.0	0.0001	0.0	0.0	0.0117	0.0
12	0.0	0.0	0.0	0.0	0.0019	0.0
13	0.0	0.0	0.0	0.0	0.0003	0.0
14	0.0	0.0	0.0	0.0	0.0	0.0
15	0.0	0.0	0.0	0.0	0.0	0.0

TABLE 17. ABSORPTION OF COMPLETELY STIMULATED CELL BY PROBE LASER
(Continued)

(b)

Stimulating Line: P4 (1-0)
Cell Temperature: 373.0 deg K
Cell Pressure: 0.010 torr of HF
Cell Length: 50.0 cm in Probe Dimension

J of Probe Laser	Absorption of 2-1 Laser			Absorption of 1-1 Rotational Laser		
	Before Relaxation	After Rotational Relaxation	After Complete Relaxation	Before Relaxation	After Rotational Relaxation	After Complete Relaxation
1	0.0	0.1318	0.0	0.0	0.9999	0.0
2	0.0	0.1953	0.0	0.0	1.0	0.0001
3	0.6306	0.1922	0.0	1.0	1.0	0.0001
4	0.0	0.1469	0.0	0.0	1.0	0.0001
5	0.0	0.0902	0.0	0.0	1.0	0.0
6	0.0	0.0450	0.0	0.0	0.9952	0.0
7	0.0	0.0184	0.0	0.0	0.8776	0.0
8	0.0	0.0062	0.0	0.0	0.4973	0.0
9	0.0	0.0018	0.0	0.0	0.1718	0.0
10	0.0	0.0004	0.0	0.0	0.0425	0.0
11	0.0	0.0001	0.0	0.0	0.0084	0.0
12	0.0	0.0	0.0	0.0	0.0014	0.0
13	0.0	0.0	0.0	0.0	0.0002	0.0
14	0.0	0.0	0.0	0.0	0.0	0.0
15	0.0	0.0	0.0	0.0	0.0	0.0

TABLE 17. ABSORPTION OF COMPLETELY STIMULATED CELL BY PROBE LASER
(Continued)

(c)

Stimulating Line: P5 (1-0)
Cell Temperature: 373.0 deg K
Cell Pressure: 0.010 torr of HF
Cell Length: 50.0 cm in Probe Dimension

J of Probe Laser	Absorption of 2-1 Laser			Absorption of 1-1 Rotational Laser		
	Before Relaxation	After Rotational Relaxation	After Complete Relaxation	Before Relaxation	After Rotational Relaxation	After Complete Relaxation
1	0.0	0.0773	0.0	0.0	0.9964	0.0
2	0.0	0.1163	0.0	0.0	1.0	0.0001
3	0.0	0.1143	0.0	0.0	1.0	0.0001
4	0.4613	0.0864	0.0	1.0	1.0	0.0001
5	0.0	0.0523	0.0	0.0	0.9983	0.0
6	0.0	0.0258	0.0	0.0	0.9521	0.0
7	0.0	0.0105	0.0	0.0	0.6973	0.0
8	0.0	0.0036	0.0	0.0	0.3237	0.0
9	0.0	0.0010	0.0	0.0	0.1017	0.0
10	0.0	0.0002	0.0	0.0	0.0244	0.0
11	0.0	0.0	0.0	0.0	0.0048	0.0
12	0.0	0.0	0.0	0.0	0.0008	0.0
13	0.0	0.0	0.0	0.0	0.0001	0.0
14	0.0	0.0	0.0	0.0	0.0	0.0
15	0.0	0.0	0.0	0.0	0.0	0.0

TABLE 17. ABSORPTION OF COMPLETELY STIMULATED CELL BY PROBE LASER
(Continued)

(d)

Stimulating Line: P6 (1-0)
Cell Temperature: 373.0 deg K
Cell Pressure: 0.010 torr of HF
Cell Length: 50.0 cm in Probe Dimension

J of Probe Laser	Absorption of 2-1 Laser			Absorption of 1-1 Rotational Laser		
	Before Relaxation	After Rotational Relaxation	After Complete Relaxation	Before Relaxation	After Rotational Relaxation	After Complete Relaxation
1	0.0	0.0367	0.0	0.0	0.9266	0.0
2	0.0	0.0558	0.0	0.0	0.9978	0.0001
3	0.0	0.0549	0.0	0.0	0.9986	0.0001
4	0.0	0.0411	0.0	0.0	0.9932	0.0001
5	0.2660	0.0247	0.0	1.0	0.9478	0.0
6	0.0	0.0121	0.0	0.0	0.7564	0.0
7	0.0	0.0049	0.0	0.0	0.4261	0.0
8	0.0	0.0017	0.0	0.0	0.1632	0.0
9	0.0	0.0005	0.0	0.0	0.0486	0.0
10	0.0	0.0001	0.0	0.0	0.0114	0.0
11	0.0	0.0	0.0	0.0	0.0022	0.0
12	0.0	0.0	0.0	0.0	0.0004	0.0
13	0.0	0.0	0.0	0.0	0.0001	0.0
14	0.0	0.0	0.0	0.0	0.0	0.0
15	0.0	0.0	0.0	0.0	0.0	0.0

TABLE 17. ABSORPTION OF COMPLETELY STIMULATED CELL BY PROBE LASER
(Concluded)

(e)

Stimulating Line: P7 (1-0)
Cell Temperature: 373.0 deg K
Cell Pressure: 0.010 torr of HF
Cell Length: 50.0 cm in Probe Dimension

J of Probe Laser	Absorption of 2-1 Laser			Absorption of 1-1 Rotational Laser		
	Before Relaxation	After Rotational Relaxation	After Complete Relaxation	Before Relaxation	After Rotational Relaxation	After Complete Relaxation
1	0.0	0.0143	0.0	0.0	0.6343	0.0
2	0.0	0.0219	0.0	0.0	0.9051	0.0001
3	0.0	0.0215	0.0	0.0	0.9202	0.0001
4	0.0	0.0160	0.0	0.0	0.8536	0.0001
5	0.0	0.0096	0.0	0.0	0.6793	0.0
6	0.1193	0.0047	0.0	1.0	0.4195	0.0
7	0.0	0.0019	0.0	0.0	0.1925	0.0
8	0.0	0.0006	0.0	0.0	0.0676	0.0
9	0.0	0.0002	0.0	0.0	0.0190	0.0
10	0.0	0.0	0.0	0.0	0.0044	0.0
11	0.0	0.0	0.0	0.0	0.0009	0.0
12	0.0	0.0	0.0	0.0	0.0001	0.0
13	0.0	0.0	0.0	0.0	0.0	0.0
14	0.0	0.0	0.0	0.0	0.0	0.0
15	0.0	0.0	0.0	0.0	0.0	0.0

probe laser is small compared to the Doppler line width. The realization of this condition is discussed in 3.5.

Similar calculations were performed for the condition existing after rotational relaxation. For this condition, the molecules stimulated to the v = 1 level were allowed to distribute themselves in a Boltzmann rotational distribution; the number densities corresponding to this case are as follows:

$$v = 1: \quad \frac{p}{kT} \frac{(2J_s + 1)(2J_s - 1)}{4J_s} \frac{hcB_0}{kT} \exp\left[-\frac{hcB_0}{kT} J_s(J_s + 1)\right] - \left\{\frac{hcB_f}{kT} \exp\left[-\frac{hcB_f}{kT} J(J + 1)\right]\right\}$$

where B_f is the rotational constant for HF in the v = 1 level. (41)

$$v = 0: \quad \frac{p}{kT}\left\{1 - \frac{(2J_s + 1)(2J_s - 1)}{4J_s} \frac{hcB_0}{kT} \exp\left[-\frac{hcB_0}{kT} J_s(J_s + 1)\right]\frac{hcB_0}{kT} \exp\left[-\frac{hcB_0}{kT} J(J + 1)\right]\right\}$$

for any J. The calculated absorptions for this case are shown in the second column of the parts of Table 17.

To compute the absorption calculations for the completely relaxed gas, we assumed a Boltzmann distribution for the number densities in both vibration and rotation. For this case, the number density in the v = 1 state was determined with use of the vibrational partition function for a harmonic oscillator. These values are shown in the third column of each of the parts of Table 17. Similar calculations were made for a probe laser operating in the v = 1 → v' = 1 pure rotation band. The corresponding results are shown in the fourth, fifth, and sixth columns of the various entries of Table 17.

It is expected that the experimental apparatus will not be able to detect absorptions less than ~ 5%. We have seen operation of the stimulating laser only on the P4 through P9 lines in the v = 0 → v' = 1 band. From Table 17, it can be seen that at a pressure of 0.01 torr, a temperature of 373°K, and a cell length of 50 cm, there is enough absorption before any relaxation takes place to be easily seen with a v = 1 to v' = 2 probe laser provided that we operate the stimulating laser on one of the P4 through P7 lines. After rotational relaxation, except for a few transitions with a lower state population near the Boltzmann peak, there will not be enough absorption to be observed. This is not expected to be a serious problem, however, because observation of the absorption after rotational relaxation would be in conjunction with observation of vibrational relaxation. This has a longer time constant than rotational relaxation; and the cell pressure, and hence the absorption, could be raised to observe these events.

Very substantial absorption of a pure rotational laser pulse is expected so that the line is completely absorbing in the center. Probing with a pure rotation laser should therefore be useful for probing after stimulation at high J levels at which few excited molecules will be created. Since we have not yet built a pure rotation laser, it is expected that all efforts on this contract will be limited to probing with a v = 1 to v' = 2 laser.

3.3.4. MONITORING RELAXATION BY FLUORESCENCE

Use of the fluorescence produced by the gas within the cell in its nonequilibrium state is an attractive alternative means of monitoring the relaxation of the excited gas. No alignment or timing difficulties such as those which exist in probe laser absorption measurements are present to complicate the measurements.

The calculation of the radiance levels expected from this fluorescence is necessary for judging the feasibility of fluorescence measurements at the low pressures to be used. Such calculations are also important because fluorescence and accompanying absorption also provide a means for relaxation to occur in the nonequilibrium gas. Usually, the time constant of this relaxation is taken to be $A_{u\ell}^{-1}$, i.e., the radiative relaxation occurs solely by spontaneous emission. This time constant is much larger than the time constants we expect for collisional deactivation in the current experiment and thus might be ignored. However the effects of stimulated emission and absorption on the radiative relaxation must also be accounted for.

The equations of fluorescence have been derived in Appendix I also. They are more complex than the equations governing the stimulation of the cell because there are photons present corresponding to all possible transitions rather than to one transition only. Hence, the changes in population of all the states must be considered. For each transition, there is a photon conservation equation which depends on the populations of only the upper and lower states for that transition. In addition, there is a conservation equation for the population of each state in the gas. Each of these equations contains terms corresponding to spontaneous emission and stimulated emission and absorption from and to each state having a transition in common with the state in question. To correctly determine the fluorescence as a function of time, it is necessary to solve these equations simultaneously. Because of the large number of variables involved, analytical solutions to these equations are available only in the simplest of situations.

Solutions to simple cases, involving only a few states, which ignore stimulated emission and absorption yield the usual optically thin solution with a decay having a time constant of $A_{u\ell}^{-1}$. To assess the importance of stimulated processes and hence to determine whether they can be ignored in the present situation, consider a photon conservation equation for one of the transitions involved. From Appendix I, Eq. (101) we write directly:

$$\frac{\partial \rho_{\nu,\Omega}}{\partial t} + c \nabla_{\Omega} \rho_{\nu,\Omega} = c\rho_{\nu,\Omega}\left(n_{u_\nu} B_{u\ell} - n_{\ell_\nu} B_{\ell u}\right) + n_{u_\nu} \frac{A_{u\ell}}{4\pi} \tag{42}$$

where ∇_{Ω} is simply a symbol for the gradient in the Ω direction.

Since no easily available measuring device can hope to resolve the detail of a fluorescence line, we can integrate over frequency. Further, the measuring device will compare the fluorescence output with the ambient radiation level. Hence, it is reasonable to substitute for $\rho_{\nu,\Omega}$, the sum of a constant ambient equilibrium (blackbody) photon density, ρ^*_ν, and a deviation from this equilibrium value, ρ', i.e.,

$$\rho_{\nu,\Omega} = \rho^*_{\nu,\Omega} + \rho'$$

Substitution of this value into Eq. (42) and integration over frequency yields

$$\frac{\partial \rho'}{\partial t} + c \nabla_{\Omega} \rho' = c\rho^*_{\nu,\Omega}\left(n_u B_{u\ell} - n_\ell B_{\ell u}\right) + c\int \rho'\left(n_{u_\nu} B_{u\ell} - n_{\ell_\nu} B_{\ell u}\right) d\nu + n_u \frac{A_{u\ell}}{4\pi} \tag{43}$$

Assuming that ρ' is not large compared to the ambient equilibrium photon density, we assessed the importance of stimulated emission and absorption in the fluorescence compared to spontaneous emission by taking the ratio of the first to third terms on the RHS of Eq. (43). Under equilibrium conditions, ρ' is constant and zero so that the above mentioned ratio must be -1. The ratio must be zero in cases in which stimulated processes can be ignored. The ambient photon density is given by

$$\rho^*_{\nu,\Omega} = \frac{2\nu^2}{c^3}\left[\exp\left(\frac{h\nu}{kT}\right) - 1\right]^{-1} \frac{\text{photons}}{\text{cm}^3\,\text{sr}(1/\text{sec})} \tag{44}$$

With this substitution, the ratio between the first and third right hand terms becomes

$$\left(1 - \frac{n_\ell}{n_u}\frac{g_u}{g_\ell}\right)\left[\exp\frac{h\nu}{kT} - 1\right]^{-1} \tag{45}$$

where the relation between the $A_{u\ell}$ and $B_{u\ell}$ coefficient has also been introduced.

This ratio has been computed for the present situation (i.e., for the conditions existing immediately after the HF cell has been stimulated or pumped by monochromatic light from an HF laser) for both R-branch fluorescence and pure rotation fluorescence from the upper level stimulated by the pump laser. The upper level and lower level number densities given by

Eq. (40) were used. The results are shown in Table 18 for stimulation by different P-branch lines. It can be seen that, for the pure rotation transition, the ratio is substantially greater than zero, indicating that stimulated emission is as important as spontaneous emission. If the cell is long so that ρ' becomes comparable to $\rho^*_{\nu,\Omega}$, stimulated emission becomes proportionately more important. The ratio is near zero for R-branch fluorescence from the stimulated state indicating that stimulated emission might be neglected in the R branch. The P branch has not been included since the observation of the P-branch fluorescence is difficult in the presence of the stimulating pulse.

Because of the difficulty of including stimulated processes, initial calculations of the fluorescent radiance to be expected from the experimental situation neglected stimulated terms even though, as shown above, stimulated emission cannot be neglected in the case of pure rotation. Directly after stimulation, the fluorescent radiance from spontaneous emission alone (i.e., the optically thin radiance) from the state pumped by the stimulating laser can be determined from Eq. (43) with the first and second terms on the right hand side set to zero: $\partial\rho'/\partial t$ can also be neglected in comparison to $c(\partial\rho'/\partial x)$ since the smallest time increment of interest is much larger than the time it takes a photon to travel the largest distance of interest. Under these assumptions, Eq. (43) can be integrated to yield

$$\rho' = \frac{n_u A_{uf}}{c(4\pi)} \cdot x$$

where ρ' is the partial photon density per unit solid angle in the direction x within the cell immediately after stimulation; and n_u is the photon density of the upper state immediately after stimulation. The fluorescent radiance (L) is correspondingly given by:

$$L = \frac{n_u A_{uf}}{4\pi} \cdot x \qquad (46)$$

We have calculated radiance values using this expression and the expressions for the upper level population density given in Eq. (40) as a function of cell length and the J level of the stimulating line. These radiances are plotted in Fig. 16 for the R branch of the vibration-rotation band and in Fig. 17 for the pure rotation band as functions of the J value of the stimulating line. These values are for fluorescence from the state pumped by the stimulating laser and hence are the maximum fluorescence values expected during the relaxation process based on the optically thin assumption.

Since we do not currently have a means of solving the full set of equations governing fluorescence and the accompanying radiative relaxation, we have used the fluorescent radiance values in Figs. 16 and 17 to judge the feasibility of using fluorescence to monitor the relaxation.

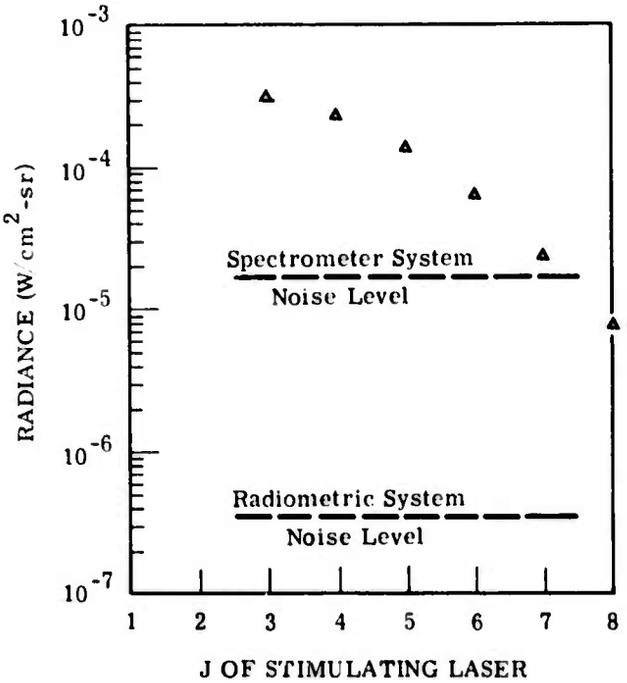

FIGURE 16. R-BRANCH FLUORESCENCE IN THE 0 → 1 LINE PUMPED BY THE STIMULATION LASER, BEFORE RELAXATION AND IN AN OPTICALLY THIN APPROXIMATION

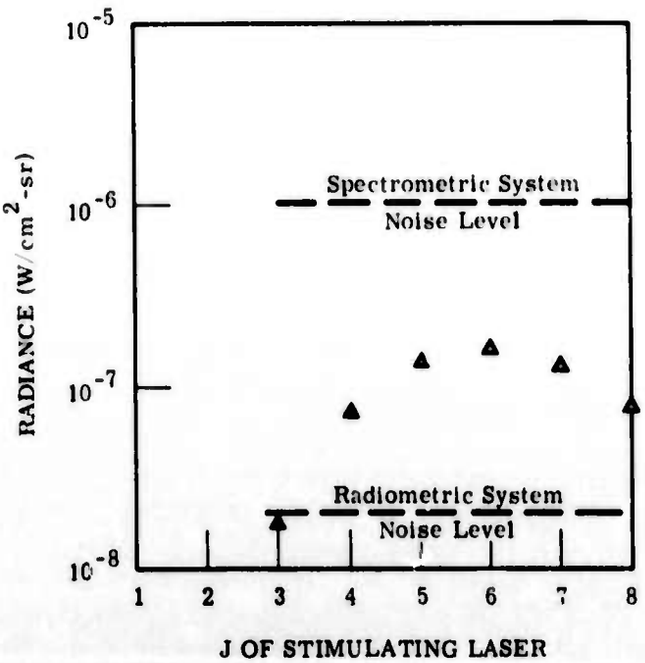

FIGURE 17. PURE ROTATION FLUORESCENCE IN THE 1 → 1 LINE PUMPED BY THE STIMULATING LASER, BEFORE RELAXATION AND IN AN OPTICALLY THIN APPROXIMATION

These radiative values do not include the effects of stimulated emission and absorption which have been shown to be important in at least the case of pure rotation. The relaxation time constants associated with the values shown on Figs. 16 and 17 are of course the reciprocals of the A_{ul} values (taken from Ref. [1]) which are all greater than a few milliseconds. When stimulated processes are included, however, the radiance values are sure to increase in the pure rotation region because of stimulated emission, and the time constants will correspondingly decrease. While these effects are important for predicting the nature of the relaxation process, they are less important for predicting measurement feasibility. Stimulated emission is made important primarily by the discontinuous nature of the rotational distribution produced by the stimulating laser. There are a large number of molecules in the pumped state and essentially none in the adjacent rotational state. Stimulated emission is likely to be important for only the pure rotation transition from the pumped state. Since fluorescence measurements from a number of states are required to determine the nature of the relaxation process occurring in the gas, possible high fluorescence rates from one transition cannot be used to judge the feasibility of fluorescence measurements as a monitoring process. Therefore the radiance values shown in Figs. 16 and 17 are taken to be conservative estimates of possible fluorescent radiance values to be expected during the relaxation process.

To determine the feasibility of measuring these radiance values, noise-equivalent radiance values for typical state-of-the-art radiometric systems were determined and compared to the values shown in Figs. 16 and 17. Two systems were considered for each spectral region, a spectrometric and radiometric system. For the R branch, the detection system was assumed to be a detector having a spectral dimensionless detectivity (D*) of 3×10^{10} cm$\sqrt{\text{Hz}}$/W in the vibration-rotation region. For the pure rotation region, the detector was assumed to be background noise limited and shielded from all ambient background except that between 20 and 28 μm in the solid angle viewed by the optical system. This allows observation of the transitions only between J = 9 → J = 8 and J = 13 → J = 12, but inclusion of the longer wavelengths required to observe lower J values would increase the noise of the system further. In any real experiment, the cooled filter used to eliminate the background need only be wide enough to observe one or several transitions at a time and should be capable of being changed to observe others at will.

The optical parameters for the spectrometer were assumed to be: a 1/2- × 12-mm entrance slit; a collection angle corresponding to f/4.5 and an efficiency of 25%. The radiometric system in each case was assumed to consist of a 2-mm square detector and an f/1 viewing system with an 80% efficiency. All systems were assumed to have a 0.1-μsec time constant. Table 19 gives the noise equivalent radiance for all of these systems. The noise equivalent radiances are also shown on Figs. 16 and 17.

TABLE 18. RATIO OF STIMULATED FLUORESCENCE TERMS TO SPONTANEOUS FLUORESCENCE TERM IN EQUATION (45)

Stimulating Line in 0 → 1 Band	R-Branch Fluorescence in the 0 → 1 Line (Pumped by the Stimulating Laser)	Pure Rotation Fluorescence in the 1 → 1 Line (Pumped by the Stimulating Laser)
P3	-4.78×10^{-7}	2.81
P4	-6.55×10^{-7}	1.73
P5	-8.57×10^{-7}	1.19
P6	-1.10×10^{-6}	0.88
P7	-1.39×10^{-6}	0.675
P8	-1.76×10^{-6}	0.532

TABLE 19. NOISE EQUIVALENT RADIANCES FOR PRACTICAL RADIOMETRIC AND SPECTROMETRIC SYSTEMS IN BOTH THE VIBRATION-ROTATION REGION AND THE SHORT WAVELENGTH END OF THE PURE ROTATION REGION FOR HF

	Spectrometric System (1/2 × 12-mm Slits, f/4.5)	Radiometric System (2-mm Square Detector, f/1)
Vibration-Rotation Region (2.5 μm) $D^*_\lambda = 3 \times 10^{10} \left(\frac{cm\sqrt{Hz}}{W}\right)$	1.7×10^{-5} W/cm^2-sr	3.4×10^{-7} W/cm^2-sr
Pure Rotation Region (20-28 μm, Background-Noise Limited Detector)	1.0×10^{-6} W/cm^2-sr	2.0×10^{-8} W/cm^2-sr

Since radiometric techniques do not allow the separation of contributions from different rotational levels, spectrometric measurements are far more desirable for use in this experiment. An examination of Figs. 16 and 17 reveals that sufficient fluorescence radiation is available from the R branch to be observed spectrometrically at least through a J value of six for the stimulating laser. On the other hand, pure rotation fluorescence could only be observed spectrometrically if some form of pulse integration technique using a waveform eductor or boxcar integrator were available. The fluorescence radiance is so low that at least 5000 pulses would need to be integrated to yield a signal-to-noise ratio of 10. Moreover, the results of Fig. 17 are for fluorescence from the pumped level. The results for fluorescence from other levels populated during the relaxation process would be lower. Thus, the measurement of rotational fluorescence is considered unfeasible as a means of monitoring rotational relaxation; R-branch fluorescence measurement appears to be a feasible means however.

3.4. CHOICE OF A MEASUREMENT SCHEME

It appears that measurement of either absorption of a probe laser operating at one of several lines, or of R-branch fluorescence will be suitable for monitoring rotational relaxation. The choice of the probe laser absorption technique was made in light of the following considerations:

(1) In order to realize the calculated fluorescence output, the cell design must be such that no ray from the spectrometric measurement apparatus intersects the side walls of the cell and that no ray passes through an unstimulated region of the cell. These requirements dictate a great deal of expansion of the stimulating laser beam, which, in turn, requires a relatively large, well collimated stimulating laser output and a very high quality infrared beam expander.

(2) It will be necessary to insure that the probe laser oscillates only in a single longitudinal mode and is relatively stable in frequency in order to insure that the spectral width of the emitted radiation is narrow compared to the Doppler line width and that its output remains close to line center.

(3) The dimensions of the cell must be smaller than the dimensions of the stimulated region and, in addition, the volume of the monitored region must be smaller than the stimulated region. These relationships are required to insure that wall effects and the diffusion of unstimulated molecules into the monitoring region have no effect on the measurements. A molecule is typically expected to travel a fraction of a centimeter during one experimental event. In the case of a laser absorption measurement, the size of the stimulated region need thus only be of the order of 1 cm (which is

easily obtained) if the beam of the probe laser is very small. On the other hand, in the case of fluorescence measurement, this requirement would significantly increase the required expansion of the stimulating beam.

(4) Figure 16 indicates that measurement of R-branch fluorescence would yield a maximum signal-to-noise ratio of 10. This is considered to be minimal for good data interpretation. Figure 17 assumes that the measurement system is detector-noise limited. Thus, it appears that a boxcar integrator and associated low-noise preamp would be desirable even for R-branch fluorescence measurements. The budget for this contract could not support this capital expenditure in addition to the others required. Furthermore, the maintenance of a detector noise limited condition in the presence of the electrical interference produced by the laser power supply is a difficult task.

(5) The timing and alignment requirements will be more stringent with probe laser absorption measurements.

It is our opinion that the two monitoring schemes are probably about equivalent when both advantages and disadvantages are compared. Although the choice of the probe laser absorption technique was made before all the above considerations became apparent, it appears that the choice will meet with reasonable success.

3.5. TECHNIQUES TO BE USED IN THE MEASUREMENT OF RELAXATION TIMES

3.5.1. EXPERIMENTAL ARRANGEMENT

The measurement of the relaxation rates of excited HF molecules will be made with two HF pulsed lasers. The first laser is the stimulating or pumping laser and its output is a short pulse (duration < 500 nsec) on one of the P_5-P_8 lines of the HF 1 → 0 vibration band. The pumping laser's output is directed through a cell containing pure HF at low pressure (P ~ 0.01 torr). The output energy of the pumping laser is of sufficient energy (~ 0.5 mJ) to excite at least 80% of the molecules in the HF cell. After a suitable time delay (0 → 50 μsec), a second pulsed HF laser, the probe laser, is triggered. The probe laser produces short (t < 200 nsec) pulses of low energy (~ 0.01 mJ) on one of the P_4-P_6 lines of the HF 2 → 1 band. The probe laser beam is directed coaxially through the HF cell with the pumping laser, and the intensity of the probe laser beam is measured before and after it traverses the HF cell. The ratio of the intensities gives the absorption of the excited HF molecules, and a plot of absorption versus delay time between the pump and probe laser pulses yields the relaxation time of the excited HF.

The requirements on the components of the experimental apparatus and the present state of development of these components are discussed below. A block diagram of the apparatus is shown in Fig. 18.

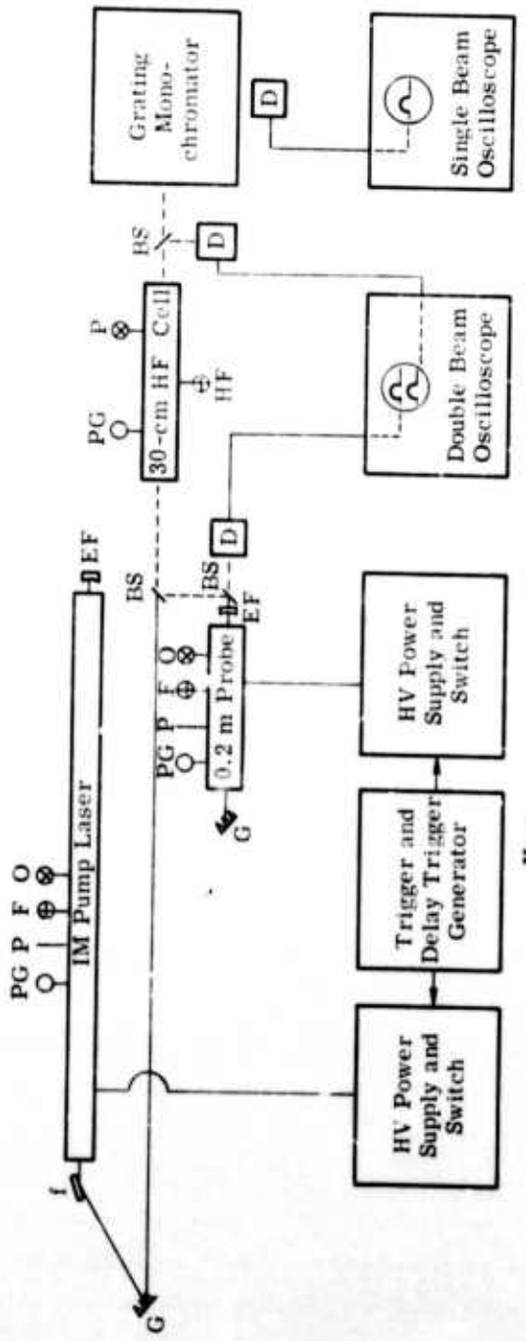

FIGURE 18. BLOCK DIAGRAM OF HF RELAXATION RATE APPARATUS

The pump laser is shown in Fig. 19. The optical path length is 1 m, and ninety-eight 300-Ω, 2-W ballast resistors are arranged in a linear array with the resistor leads pointed to form the anodes. The premixed fuel and oxidizer gases are admitted into the inlet manifold and the gases flow around the pin anodes and down into the optical cavity. Spent gases flow out of the optical cavity through a slot, into the exhaust manifold, and hence to the vacuum pump. The exhaust manifold is electrically grounded and the slot serves as a cathode. Typical operation parameters for the pump laser are as given in Table 20. The pump laser is usually operated super-radiantly with no front-end reflector. When a front-end reflector is used (infinite radius of curvature, reflectivity between 0.9 and 0.75), the P_3 and P_8 lines of the $1 \rightarrow 0$ band can be made to oscillate weakly. The strength of the P_4-P_7 $1 \rightarrow 0$ lines is reduced from the values shown in Table 20, however. The maximum output on any one line is obtained with fuel type H_2 or CH_4, fuel pressure, oxidizer pressure, and high voltage unique to that line.

The 1-m pump laser exhibits a variation in output energy of ~ ±10% from pulse to pulse. The reason for this variation is not known but is suspected to be the result of variations in the gas discharges along the cavity which produce the F atoms. The output energy variations are more pronounced at low output energy. Further efforts are being made to reduce the output energy variations so that the number of $1 \rightarrow 0$ HF lines available for pumping may be increased beyond the four (P_4-P_7) lines available at present.

The 1-m pump laser exhibits sufficient gain to super-radiate when no cavity mirrors are used. When the fuel and oxidizer pressures are lowered to reduce gain, the output energy is also reduced. Initial plans to operate the pump laser on a single line have been abandoned in favor of allowing the laser to oscillate at will and to select the desired output line by means of a monochromator. An additional advantage is obtained by operating the pump laser with a single-end reflector; the absence of a high-cavity Q allows the laser to operate over the full gain curve of a given line. This should provide pumping energy over the entire Doppler width of the HF transition.

The beam pattern of the pump laser has been observed with an infrared quenching phosphor positioned ~ 30 cm in front of the laser. No front-end reflector was used and the beam image appeared uniformly intense over the cross sectional area of the sensor.

The probe laser is similar to one reported by Pettipiece [34] and is shown in Fig. 20. It consists of a 0.2-m long Lucite tube with a 1.2-cm bore and a 3.17-mm wall thickness. The tube ends are cut at the Brewster angle, and sapphire windows are used to close the tube. Premixed fuel and oxidizer gases are admitted at each end of the tube, and an exhaust port is located in the center. Forty 910-Ω 1-W carbon resistors are arranged in a single-turn helix along the tube's circumference, with the pointed lead of each resistor passing through the tube wall and forming an anode. A set of cathodes is also arranged in a single-turn helix so that

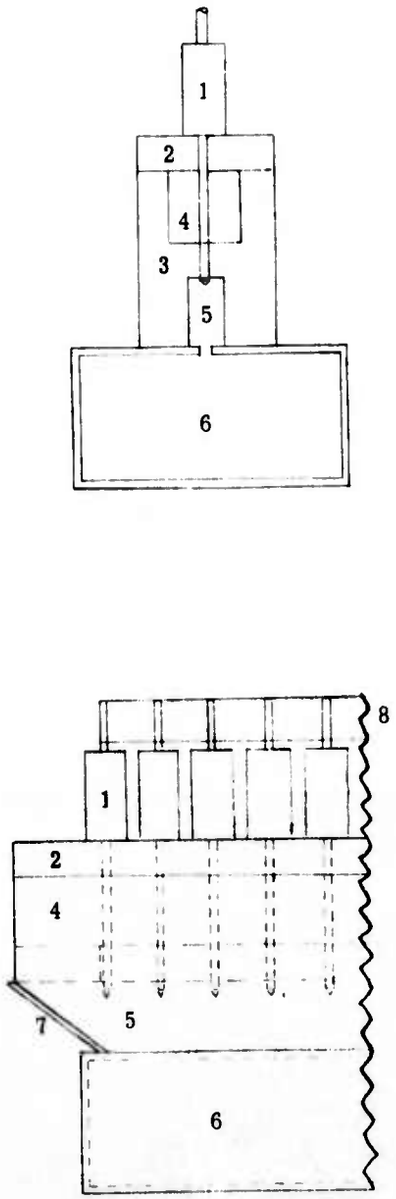

Key

1. Ballast Resistor and Pin Electrode
2. Lucite Top Cover
3. Lucite Body
4. Gas Inlet Manifold
5. Optical Cavity
6. Exhaust Manifold and Cathode
7. Sapphire Window
8. HV Anode Buss

FIGURE 19. IM PUMP LASER

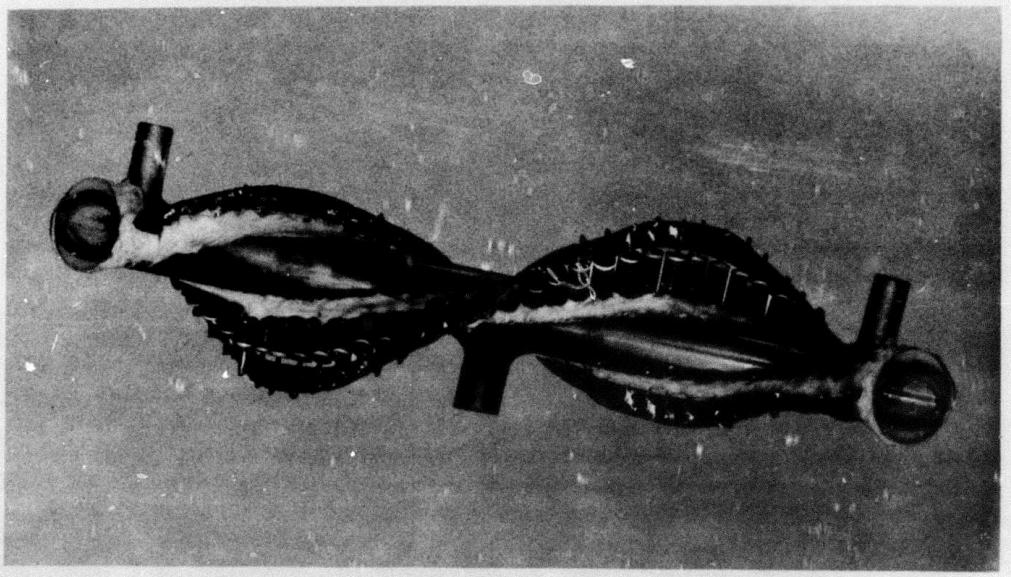

FIGURE 20. INTERIOR VIEW OF 1-m PUMP LASER. Lucite tube is 0.2 m long with a 1.2-cm bore. Tube ends are cut at the Brewster angle and closed with sapphire windows. Forty 910-Ω 1-W carbon resistors are arranged in a single-turn helix.

each cathode is directly opposite one of the anodes. Typical operating parameters are given in Table 21.

The probe laser is required to operate on a single line and also in the TEM_{00} mode; however, the required output energy is very low (~0.01 mJ). A high-Q cavity is required for this type of operation, and consists of a plane grating on one end ($r \approx 0.95$), and a spherical mirror (1-m radius of curvature, 0.75 reflectivity) on the other end. The spherical mirror is made of fused quartz which is transparent to the output wavelengths of the laser, and the laser output passes through the mirror. The mirror is equipped with a 3.3-mm aperture stop which provides a Fresnel number of 4 which, in conjunction with the helical resistor arrangement, is low enough to control transverse modes.

The high Q cavity of the probe laser operates at a mode number of ~200,000 and is quite sensitive to mechanical vibrations. The laser has been isolated from the vacuum pump by a 6-ft long rubber tube to reduce cavity vibrations caused by the pump. Pulse-to-pulse amplitude variations are encountered with the probe laser which are similar to those observed with the pump laser. Variations in the population inversion resulting from variations in the discharge are again believed to be the reason for this. If further efforts to eliminate the problem are unsuccessful, to reduce the uncertainty in the measurements we will have to average over many pulses during the measurement of relaxation rates.

Another problem encountered with the operation of the pulsed lasers is the electromagnetic interference (EMI) caused by the electrical discharge. The discharge consists of high voltage (up to 20 kV) and high current (up to 5 kamp) pulses and causes EMI with the low level (~ 20 mV) signals from the infrared detectors. All components of the power supply and laser heads have been shielded by metal enclosures. The most troublesome interference is not caused by the de/dt or di/dt of the storage capacitor since the interference appears as a damped oscillation with a frequency of 50 to 100 MHz. The only process that might contain frequency components this high is the sequential breakdown of the laser electrodes. The EMI level is high in amplitude and of long duration when the resulting laser output pulse is low in amplitude. We feel, therefore, that when the electrodes discharge almost simultaneously, the population inversion builds up faster and to a higher level than when the electrodes discharge over a longer period of time.

The beam pattern of the probe laser has been measured for multiple line operation. This was done in the near field with a 1.0 mm diameter PbSe detector which was traversed in the vertical and horizontal directions across the laser beam. The results are shown in Fig. 21.

The circuit diagram of the pump laser power supply is shown in Fig. 22. The probe laser power supply uses a higher voltage-power transformer and energy-storage capacitor but is otherwise the same. Trigger pulses for the pump laser are supplied by a H-P 211A square-wave

TABLE 20. TYPICAL OPERATING PARAMETERS FOR THE 1-m PUMP LASER

Output pulse energy (all lines)	4.4 mJ
Pulse length	300 to 500 nsec (may be detector limited)
Fuel pressure (H_2 or CH_4)	1 to 10 torr
Oxidizer pressure (SF_6)	10 to 50 torr
Gas flow rate	120 l/sec
HV pulse amplitude	8 to 14 kV
HV pulse energy	6.4 to 19.6 J
HV pulse duration	300 nsec
Pulse repetition frequency	1 to 10 Hz
Rear-end reflector	4-m radius sphere; 100% Au coated
Front-end reflector	None used

TABLE 21. TYPICAL OPERATING PARAMETERS FOR THE 0.2-m PROBE LASER

Output pulse energy (all lines)	0.5 mJ
Pulse length	200 to 400 nsec (may be detector limited)
Fuel pressure (H_2 or CH_4)	1 to 4 torr
Oxidizer pressure (SF_6)	10 to 20 torr
Gas flow rate	120 l/sec
HV pulse amplitude	10 to 20 kV
HV pulse energy	1 to 25 J
HV pulse duration	200 nsec
Pulse repetition frequency	1 to 10 Hz
Rear-end reflector	625 l/mm grating
Front-end reflector	4-m radius sphere; 95% Au coated

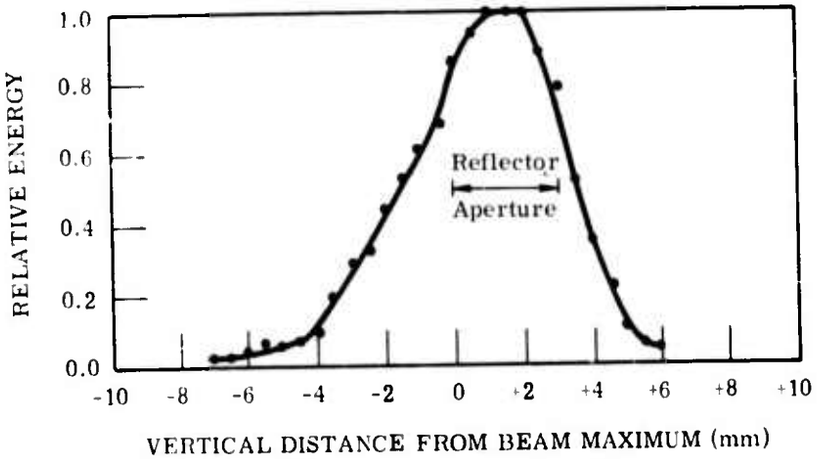

(a) Vertical

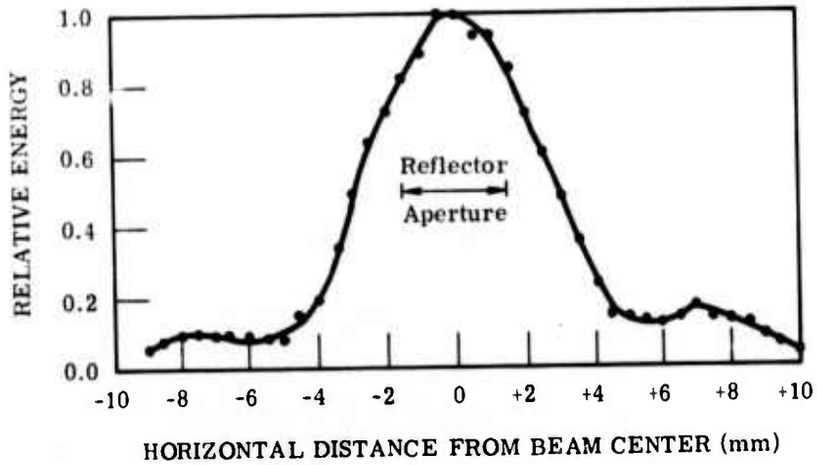

(b) Horizontal

FIGURE 21. NEAR-FIELD BEAM PATTERN OF 0.2-m PROBE LASER

generator. Delayed pulses for the probe laser are supplied by the delaying sweep gate output of a Tektronix 535A oscilloscope. The output of a pump laser beam sampler is displayed on the oscilloscope. The outputs from the beam samplers for the probe laser are displayed on a Tektronix 556 dual beam oscilloscope; one beam displays the amplitude of the probe laser beam incident on the HF sample cell and the other beam displays the difference between the incident and transmitted probe laser beam amplitudes. The time base of the dual-beam oscilloscope is initiated by the pump laser pulse and indicates the time delay between the pump laser and probe laser pulses. The data are recorded by photographing the 556 oscilloscope screen. Typical data expected are shown in Fig. 23. Many pulses (~ 100) may be required to average out the effects or variations in the probe laser beam.

The HF cell used for the experiment was made for a previous study.* It is 30-cm long and has a clear aperture of 5.7 cm. Sapphire windows are sealed to the cell with Viton O-rings, and the cell is made of Inconel X. The cell is heated with an electrical heater tape to 80°C to prevent HF polymerization. The cell is HF passivated before use. Purified HF from a supply cylinder flows through the cell at a low rate to avoid any remaining absorption effects on the cell and piping walls. The cell pressure is measured with a capacitance manometer.

The infrared detectors presently in use are all dewar-mounted InSb and InAs detectors. Both types require liquid nitrogen cooling, and none of them are designed for detection of short pulses. We believe that the detectors on hand have longer rise times than the laser pulses and that the displayed pulse shape is distorted. A new detector is on order which will have a maximum rise time of 10 nsec, and when pulse waveforms from it are compared with those from the present detectors, the adequacy of the detectors' response time can be determined.

A Perkin-Elmer type 98-G monochromator with a 3-μm blaze grating is used to identify and monitor the various lines of the lasers. Figure 24 shows the pump laser and its associated optical bench inside the fume hood; the small object mounted on a ring stand to the right of the laser is used for measuring the laser beam pattern. The monochromator is outside the fume hood, and infrared energy passes through a hole in the fume-hood wall to reach the monochromator. The compressed gas cylinders contain fuel, oxidizer, and diluent gases used with the lasers.

3.5.2. DATA REDUCTION AND ANALYSIS

The amplitudes on the photographic outputs typified by Fig. 23 are to be digitized on a curve digitizer, and absorption as a function of time will be determined for the transition involved.

*See 0-3 HF measurement, Section 5.

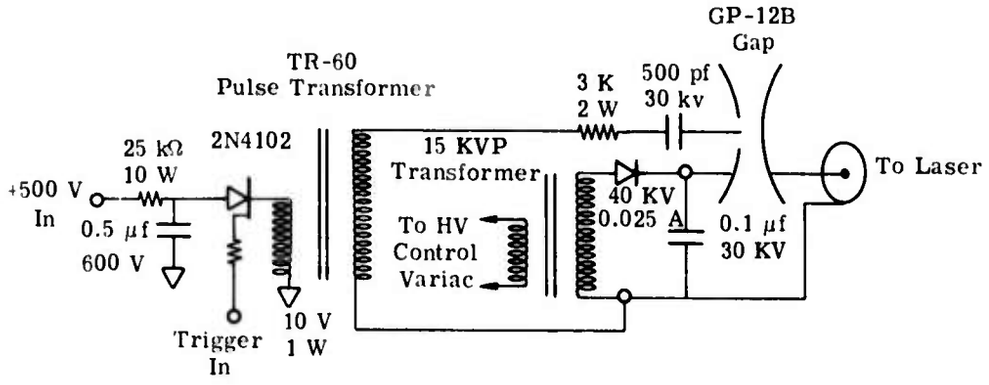

FIGURE 22. PUMP LASER POWER SUPPLY CIRCUIT

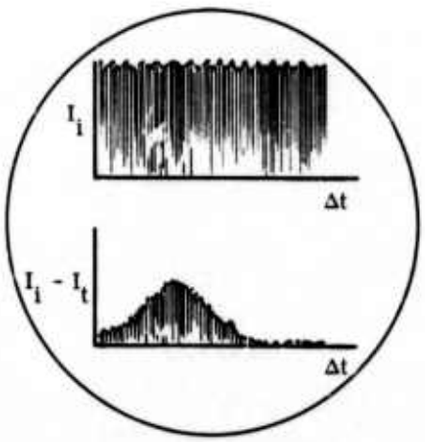

PHF Cell = 0.01 Torr
Pump = P_5 1 → 0
Probe = P_4 2 → 1

FIGURE 23. EXPECTED DATA AS DISPLAYED ON DUAL BEAM OSCILLOSCOPE

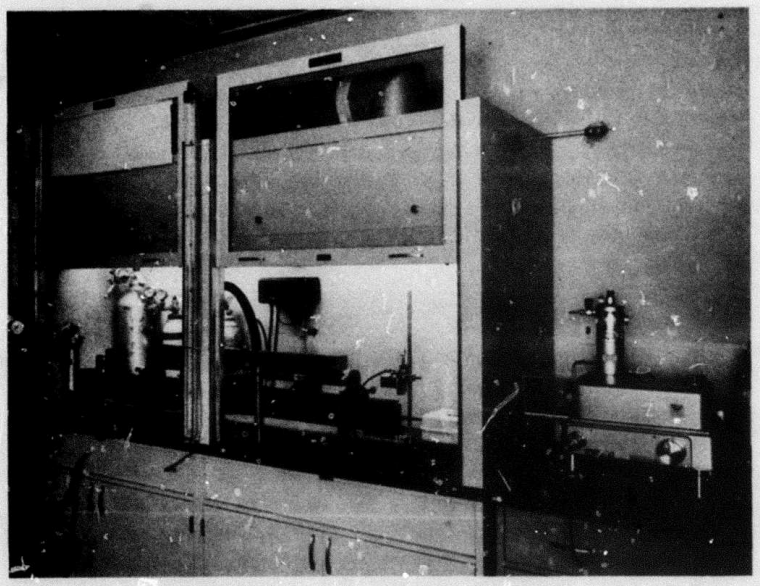

FIGURE 24. PUMP LASER AND ITS ASSOCIATED OPTICAL BENCH INSIDE THE FUME HOOD

The time constant of these curves is a measure of the relaxation time within the cell. Assuming that rotational relaxation occurs before any vibrational relaxation occurs, the time constant is a measure of rotational relaxation.

We expect to perform a detailed analysis of the absorption versus time curves however. Absorption histories for various probe laser transitions and hence populations of different rotational-vibrational states will have been obtained from the experiment. The set of equations governing radiative relaxation described in Section 5 will be modified to include a model for vibrational and rotational energy transfer by collisional processes. These equations will then be solved numerically for various collisional rates and from the solutions, theoretical absorption histories will be computed. By comparison of these histories with the experimental absorption histories, best values for the collisional rates can be inferred. It is recognized that simplifying assumptions will be needed to accomplish the modeling of the collisional deactivation to limit the number of rates considered.

A more straightforward and satisfying way to analyze the data would be to obtain absorption histories for enough transitions so that we can determine the population history of each vibrational-rotational state after stimulation. These histories would give a complete picture of the relaxation process. However, we have not been able to operate the probe laser on more than 5 lines in each of the 0 – 1 and the 1 – 2 bands and these lines will probably not be enough to provide complete, unambiguous population histories.

4
COMPUTATION OF THE WIDTH OF COLLISION-BROADENED SPECTRAL LINES

(R. E. Meredith and R. E. Turner)

A verbal understanding between R. E. Meredith and the technical monitor allowed the current contract to support the development of a code to compute collision-broadened half widths of vibration-rotation transitions by Anderson's method [3]. This section describes this work.

4.1. INTRODUCTION

Collision theory has been developed along two lines: the stationary-state theory in which the time-independent Schrödinger wave equation is solved and the time-dependent theory, in which the initial and final states of the system are connected by a linear, unitary time-translation operator. In the latter, the Hamiltonian is divided into two parts, i.e.:

$$H = H_0 + V \tag{47}$$

where H_0 is the unperturbed Hamiltonian which describes the system at times in the infinite past and infinite future. As the colliding parts interact with each other, the change in the energy manifests itself through the interaction potential V. If $|\phi_a>$ is the eigenket or state vector for the unperturbed state a, then we have

$$H_0|\phi_a> = E_a|\phi_a> \tag{48}$$

where E_a is the corresponding eigenvalue (energy). Likewise, if we let $|\psi_a^->$ and $|\psi_a^+>$ be the eigenkets for the incoming and outgoing states respectively for the general system, then

$$H|\psi_a^\pm> = E_a|\psi_a^\pm> \tag{49}$$

It can be shown [35], [36] that these states satisfy the Lippmann-Schwinger equation, i.e.:

$$|\psi_a^+> = |\phi_a> + \lim_{\epsilon \to 0+} \frac{1}{E_a - H_0 + i\epsilon} V|\psi_a^+> \tag{50}$$

$$|\psi_a^-> = |\phi_a> + \lim_{\epsilon \to 0+} \frac{1}{E_a - H_0 - i\epsilon} V|\psi_a^-> \tag{51}$$

when ϵ is an infinitesimal. Now, the eigenstate at any time t is $|\psi_a(t)>$ and is related to the eigenstate in the infinite past by a unitary operator U(t, $-\infty$):

$$|\psi_a(t)> = U(t, -\infty)|\psi_a(-\infty)> \tag{52}$$

As $t \to +\infty$, the final state, then

$$|\psi_a(+\infty)\rangle = U(+\infty, -\infty)|\psi_a(-\infty)\rangle \tag{53}$$

where $S = U(+\infty, -\infty)$. The time development operator can be found by solving the Schrödinger equation in the interaction picture:

$$U(t, t_0) = 1 - \frac{i}{\hbar}\int_{t_0}^{t} H_I(t')U(t', t_0)\,dt' \tag{54}$$

where $H_I(t)$ is the interaction Hamiltonian in the Dirac picture. Therefore, the transition rate per unit time is given by

$$w_{ba} = \frac{2\pi}{\hbar}|\langle\psi_b|S|\psi_a\rangle|^2 n(E_b) \tag{55}$$

where $n(E_b)$ is the number density of final states and $\langle\psi_b|$ is the bra vector corresponding to the final state b.

A completely analogous solution can be found by use of the stationary-state method. Here, one starts by solving the integral equation

$$\psi(\vec{s}) = e^{i\vec{K}\cdot\vec{s}} - \frac{1}{4\pi}\int \frac{\exp(i\kappa|\vec{s} - \vec{s}'|)}{|\vec{s} - \vec{s}'|} V(\vec{s}')\psi(\vec{s}')\,d\vec{s}' \tag{56}$$

where κ $(= \sqrt{2mE}/\hbar)$ is the wave number and $V(\vec{s})$ is the potential. In Eq. (56), $\vec{s}$ is the position vector of the field point and $\vec{s}'$ is the position vector of the source point. Iteration of this equation allows one to find an approximate solution called the Born approximation. It is especially valid for weak collisions and therefore it has been used extensively in spectral line-broadening theory. This is the approach used by Anderson [3] which we shall now describe.

4.2. ANDERSON'S THEORY OF SPECTRAL LINE BROADENING

Let us consider two molecules, a radiating molecule 1, and the perturbing molecule 2. For a gas in statistical equilibrium, the number of molecules which are radiating relative to the total number is quite small, and therefore it is very unlikely that both molecules will be radiating simultaneously. For classical trajectories of the molecules, the complete Hamiltonian is then given by

$$H = H_1 + H_2 + H_c(t) + H_R + H_{1R} \tag{57}$$

where $H_0 (= H_1 + H_2)$ is the unperturbed molecular Hamiltonian, $H_c(t)$ is the time-dependent collision Hamiltonian, H_R is the Hamiltonian of the pure radiation field, and H_{1R} is the interaction between the radiating molecule and the radiation field. Since our goal is to find the

transition probability per unit time between molecular states a and b, we must consider the initial and final state vectors $|\psi_a(t_0)\rangle$ and $|\psi_b(t)\rangle$. Thus

$$|\psi_a(t_0)\rangle = |\psi_a(t_0)\chi_{n_k}\rangle \tag{58}$$

and

$$|\psi_b(t)\rangle = |\psi_b(t)\chi_{n_{k-1}}\rangle \tag{59}$$

where χ's are the vectors for the radiation field with photon occupation number indices n_k and n_{k-1}. The general time-dependent state at time t is simply related to the original state at time t_0 by the linear unitary time development operator, i.e.:

$$|\psi_a(t)\rangle = U(t, t_0)|\psi_a(t_0)\rangle \tag{60}$$

Operator Eq. (54) can be solved by successive iterations to yield

$$U(t, t_0) = \exp\left[\frac{i}{\hbar}\int_{t_0}^{t} \boldsymbol{H}_i(t')\,dt'\right] \tag{61}$$

where $\boldsymbol{H}_1 = \boldsymbol{H}_0 + \boldsymbol{H}_c(t)$. The transition probability for going from state a to b is

$$P_{ba} = |\langle\psi_b(t)|\psi_a(t)\rangle|^2 \tag{62}$$

or, making use of the time-development operator of Eq. (60), we get

$$P_{ba} = |\langle\psi_b(t)|U(t, t_0)|\psi_a(t_0)\rangle|^2 \tag{63}$$

Using these principles, and the assumption that the duration of collisions is small compared to the time interval between collisions, Anderson was able to derive the following expression for the average transition rate per unit time for dipole interactions:

$$w = \frac{8\pi^2\nu}{hc}\sum_{J_iJ_f}\frac{n_{J_i}}{2J_i+1}\sum_{M_iM_f}|\langle vJM|\mu_z|v'J'M'\rangle|^2 \times\left\{\frac{\left(\frac{nu\sigma_r}{2\pi}\right)}{\left[\nu-\nu_{fi}+\left(\frac{nu\sigma_i}{2\pi}\right)\right]^2+\left(\frac{nu\sigma_r}{2\pi}\right)^2}\right\} \tag{64}$$

where ν is the frequency, n is the number density of the absorbing molecule, and u is the relative velocity of the two molecules. The v, J, and M indices denote the vibrational, rotational, and magnetic quantum numbers respectively, and $\langle vJM|\mu_z|v'J'M'\rangle$ is the dipole matrix element for the transition. The σ_r and σ_i are the real and imaginary parts of the total collision cross section σ. If we denote the wave number by $\nu'(=\nu/c)$, then the line half width is

$$\gamma = \frac{nu\sigma_r}{2\pi c} \tag{65}$$

and the line-shift is

$$\Delta\nu' = -\frac{nu\sigma_i}{2\pi c} \tag{66}$$

Now, if T is the transition operator and we make use of the assumption that the time interval between collisions is greater than the duration, then the cross-section for a given perturber molecule is [37]:

$$\sigma_{J_2} = \int\left[1 - \sum_{\substack{\text{all} \\ M\text{'s}}}\sum_{J_2'} \frac{<J'LM'M\,|\,JM><JLM'M\,|\,JM>}{(2J+1)(2J_2+1)} \times <J'M'J_2M_2|T^{-1}|J'M'J_2'M_2'><JMJ_2'M_2'|T|JMJ_2M_2>\right]d\sigma \tag{67}$$

The transition operator T is similar to the unitary operator $U(t, t_0)$ defined earlier, except that we now consider $t \to +\infty$ and $t_0 = 0$ and let U transform the collision Hamiltonian $H_c(t)$ into the Dirac picture. Thus,

$$T = \exp\left[-\frac{i}{\hbar}\int_0^\infty U^{-1}H_c(t)U\,dt\right] \tag{68}$$

or, by expanding the exponential we get the various terms

$$T = T_0 - iT_1 - \frac{1}{2}T_2 + \ldots \tag{69}$$

where

$$T_0 = 1 \tag{70}$$

$$T_1 = \frac{1}{\hbar}\int_{-\infty}^{\infty} U^{-1}H_c(t)U\,dt \tag{71}$$

$$T_2 = \left[\frac{1}{\hbar}\int_{-\infty}^{\infty} U^{-1}H_c(t)U\,dt\right]^2 \tag{72}$$

Since the differential cross-section $d\sigma$ of Eq. (67) is given by

$$d\sigma = 2\pi b\,db \tag{73}$$

where b is the classical impact parameter, we can write for the cross-section of Eq. (67)

$$\sigma_{J_2} = \int_0^\infty 2\pi b \mathcal{S}(b)\, db \tag{74}$$

where $\mathcal{S}(b)$ is everything contained within the braces of Eq. (67). Making use of the approximation, Eq. (69), we see that

$$\mathcal{S}(b) = \mathcal{S}_0(b) + \mathcal{S}_1(b) + \mathcal{S}_2(b) + \cdots \tag{75}$$

It can be shown that in the zero-th order case, $\mathcal{S}_0(b) = 0$, and that for the first order case $\mathcal{S}_1(b)$ is pure imaginary and hence will contribute only to the line shift, but not to the line width. Thus, the first real, non-zero term which contributes to the half width is $\mathcal{S}_2(b)$.

$$\mathcal{S}_2(b) = -\left[\sum_{M,M_2} \frac{\langle JMJ_2M_2 | T_2 | JMJ_2M_2\rangle}{(2J+1)(2J_2+1)} + \sum_{M',M_2} \frac{\langle J'M'J_2M_2 | T_2 | J'M'J_2M_2\rangle}{(2J'+1)(2J_2+1)}\right]$$

$$+ \sum_{\substack{\text{all} \\ M\text{'s}}} \sum_{J_2} \frac{\langle J'LM'M | JM\rangle \langle J'LM'M | JM\rangle}{(2J+1)(2J_2+1)}$$

$$\langle J'M'J_2M_2 | T_1 | J'M'J_2'M_2'\rangle \langle JMJ_2'M_2' | T_1 | JMJ_2M_2\rangle \tag{76}$$

The quantities $\langle\ |\ \rangle$ are scalar quantities, called Clebsch-Gordan coefficients and represent the vector addition of two angular moments to give a resultant angular momentum. Tables exist which allow one to evaluate these quantities for many values of angular momenta.

The collision Hamiltonian H_c can be expressed as the product of the spherical harmonics Y_λ^κ of the internal coordinates of the two molecules, i.e.:

$$H_c = C_{\lambda_1\lambda_2}^{\kappa_1\kappa_2} Y_{\lambda_1}^{\kappa_1}(1) Y_{\lambda_2}^{\kappa_2}(2) \tag{77}$$

where C_λ^κ are constants in the expansion of the collision Hamiltonian. One can write the interaction potential for dipole-dipole, dipole-quadrupole, quadrupole-quadrupole or for all possible multipole-multipole interactions. The angular coordinates can then be expressed in terms of the spherical harmonics and the matrix elements evaluated. Limiting ourselves to the first three multipole interactions, we get

$$\mathcal{S}(b) = \sum_t C_1 b^{-4} g_{1t} f_1(k_{1t}) + C_2 b^{-6} g_{2t} f_2(k_{2t}) + C_3 b^{-8} g_{3t} f_3(k_{3t}) \tag{78}$$

where the indices 1, 2, and 3 refer to the first three multipole interactions given above. The subscript t refers to the various possible collision combinations. The g_{st} are functions of the Clebsch-Gordan coefficients and are tabulated by Benedict and Herman* [38]. The functions $f_s(k_{st})$ are dependent upon the energy defect of a particular collision and are tabulated by Tsao and Curnutte [37]. The parameter k_{st} is given by

$$k_{st} = \frac{2\pi bc}{u}(\Delta E - \Delta E_2) \tag{79}$$

where ΔE and ΔE_2 are the energy level spacings between the transitions made by the radiating and perturbing molecule, respectively, as the result of the collision. The constants C_s are expressed in terms of the dipole moments μ and μ_2 and the quadrupole moments Q and Q_2, i.e.:

$$C_1 = \frac{4}{9}\frac{\mu^2\mu_2^2}{(\hbar u)^2}$$

$$C_2 = \frac{4}{45}\frac{\mu^2 Q_2^2}{(\hbar u)^2} \text{ or } \frac{4}{45}\frac{\mu^2 Q^2}{(\hbar u)^2}$$

$$C_3 = \frac{1}{25}\frac{Q^2 Q_2^2}{(\hbar u)^2}$$

The approximation used for these calculations is basically the Born approximation, that is, one which holds only for weak collisions. If, however, we include all impact parameters, then strong collisions will be considered for which the approximation breaks down. Anderson assumed that the theory was valid for all b for $\mathcal{S}(b) < 1$, that is, for all impact parameters such that the radiation does not have a complete change of phase. When b was less than or equal to b_0, a phase change of 2π was assumed. Thus

*Some discrepancy was noted in the g_{st} factors tabulated in Ref. 38. The authors have confirmed that the values of g_{35}, g_{36}, and g_{37} are incorrect as they appear in Ref. 38. We have derived the following functions for the above quantities:

$$g_{35} = \frac{(4m^4 - m^2 - 9)J_2(J_2 + 1)}{(4m^2 - 1)(4m^2 - 9)(2J_2 - 1)(2J_2 + 3)}$$

$$g_{36} = \frac{3(4m^4 - m^2 - 9)J_2(J_2 - 1)}{2(4m^2 - 1)(4m^2 - 9)(2J_2 - 1)(2J_2 + 1)}$$

$$g_{37} = \frac{3(4m^4 - m^2 - 9)(J_2 + 1)(J_2 + 2)}{2(4m^2 - 1)(4m^2 - 9)(2J_2 + 1)(2J_2 + 3)}$$

$$\sigma_{J_2} = \int_0^{b_0} 2\pi b \mathscr{S}(b)\, db + \int_{b_0}^{\infty} 2\pi b \mathscr{S}(b)\, db \tag{80}$$

This equation can be integrated and the result is

$$\sigma_{J_2} = \pi b_0^2 \left[1 + C_1 b_0^{-4} \sum_t g_{1t} F_1(k_0) + C_2 b_0^{-6} \sum_t g_{2t} F_2(k_0) + C_3 b_0^{-8} \sum_t g_{3t} F_3(k_0) \right] \tag{81}$$

where the functions $F_i(k_0)$ are tabulated [1], and k_0 is the value of k at $b = b_0$. The value b_0 is determined by setting $\mathscr{S}(b_0) = 1$ and solving Eq. (78) for b_0.

4.3. HALF-WIDTH CALCULATIONS

To calculate the half widths, one must use Eq. (65), in which σ_r is the real part of the total cross-section σ. This cross-section σ is the summation of all cross sections for the angular momentum states of the perturbing molecule weighted according to the population of the states of the perturber, i.e.:

$$\sigma = \sum_{J_2} n_{J_2} \sigma_{J_2} \tag{82}$$

and, where σ_{J_2} is determined from Eqs. (74) and (78). Since the $f_s(k_{st})$ are known functions of k_{st}, it is important to see how the half widths depend on k_{st}. Now

$$|\Delta E + \Delta E_2| = \left| E_{vJ'} - E_{vJ} + E_{v_2 J_2'} - E_{v_2 J_2} \right| \tag{83}$$

or

$$|\Delta E + \Delta E_2| = \left| E_{v'J'} - E_{v'J''} + E_{v_2 J_2'} - E_{v_2 J_2} \right| \tag{84}$$

One can illustrate the effect of the self broadening of highly polar molecules by considering the R(1) line of HF as shown in Fig. 25. Usually, only one of the intermediate levels contributes to a significant extent. The $J = 1$ level can interact with the $J_2 = 0$ or the $J_2 = 2$ levels (dashed arrows), and the $J' = 2$ level can interact with the $J_2 = 1$ or the $J_2 = 3$ level (wavy arrows). Here we include only dipole interactions, i.e., those cases in which $\Delta J = \pm 1$. By considering higher order terms in the collision Hamiltonian, one can consider the quadrupole interactions, $\Delta J = \pm 2$, octupole interactions, $\Delta J = \pm 3$, and all higher multipole interactions. As an example, if $\Delta E_2 = \Delta E$ where ΔE_2 is the energy difference between $J_2 = 3$ and $J_2 = 2$, and ΔE is the energy difference between $J = 2$ and $J = 0$, then a dipole-quadrupole interaction can occur. The closer these levels are to each other the stronger the resonance. Details of the hard-core effect are treated in Section 5.

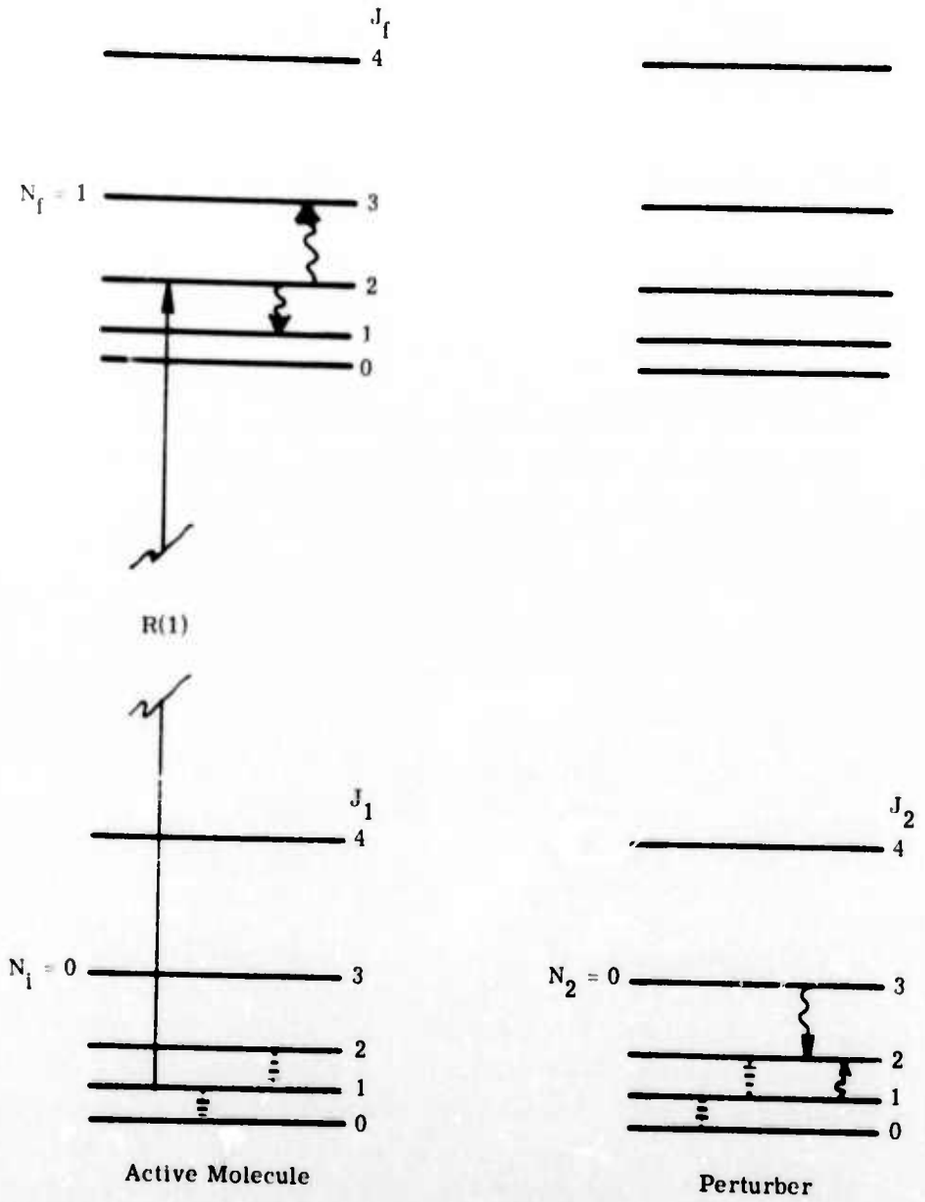

FIGURE 25. SELF-BROADENING ASPECT OF HIGHLY POLAR MOLECULES. Usually, only one of the intermediate levels contributes to a significant level. The closer these levels are to each other, the stronger the resonance.

The present calculations are presented in Figs. 26-29. The figures show a comparison of measurement and theory for the pure rotation, fundamental and first overtone bands of self-broadened HF. Figures 26 and 26 give the fundamental linewidths for two temperatures, 373°K and 390°K. Figures 27 and 29 show the largest discrepancy between theory and measurement, possibly because the data were taken at lower resolution than the others, and because the pure rotation data were obtained at 306°K, where polymerization effects might be significant. Tables 22 through 26 give tabulated widths for self-broadened widths in the fundamental series: $v = 0 \rightarrow 1$, $1 \rightarrow 2$, $2 \rightarrow 3$, $3 \rightarrow 4$, and $4 \rightarrow 5$. It is assumed that the absorber molecules are in a bath of perturber molecules maintained at a temperature of 373°K. The results are qualitatively as one would expect. For greater vibrational levels of the active molecule, the widths are smaller in general because of the greater resonance defect between the rotational levels of the upper v states and the rotational levels of the perturber molecules, assumed to be the $v = 0$ state. Also, as the defect becomes larger the influence of more than 1 dipole-dipole interaction becomes greater, as do the shorter range forces. This tends to make the width versus m curve flatten out, for lines involving larger v.

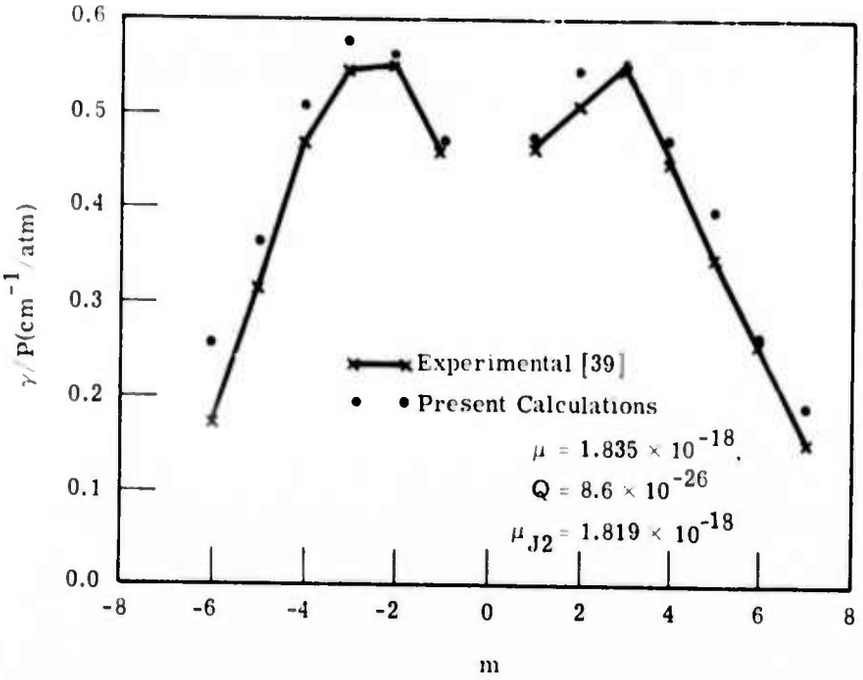

FIGURE 26. COMPARISON OF MEASUREMENT AND THEORY FOR THE FUNDAMENTAL BAND OF SELF-BROADENED HF. Temperature is 373°K, v = 0 → 1 [39].

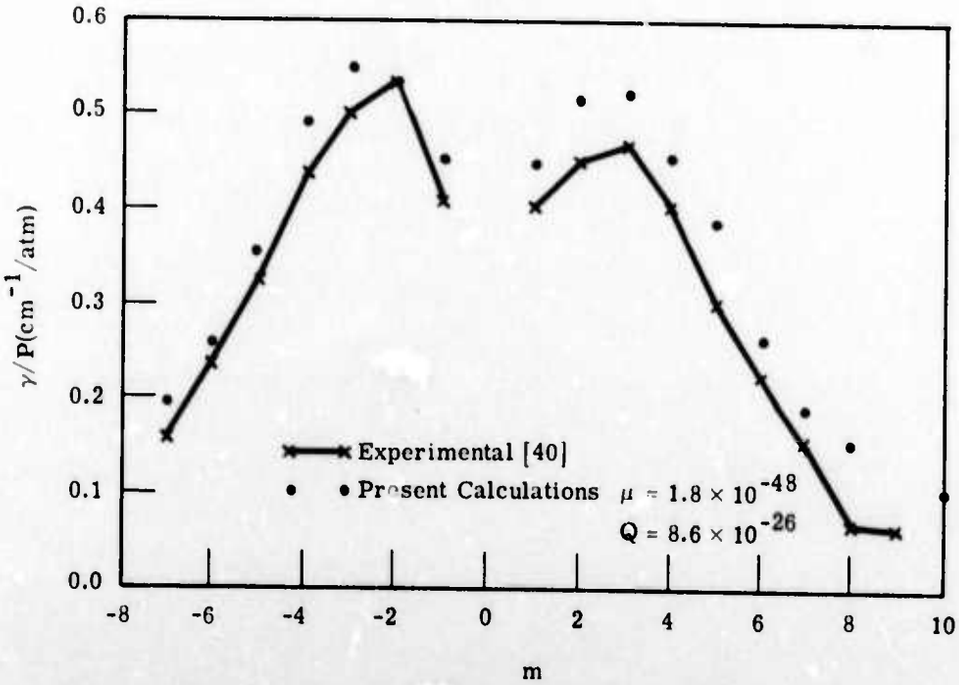

FIGURE 27. COMPARISON OF MEASUREMENT AND THEORY FOR THE FUNDAMENTAL BAND OF SELF-BROADENED HF. Temperature is 390°K, v = 0 → 1 [40].

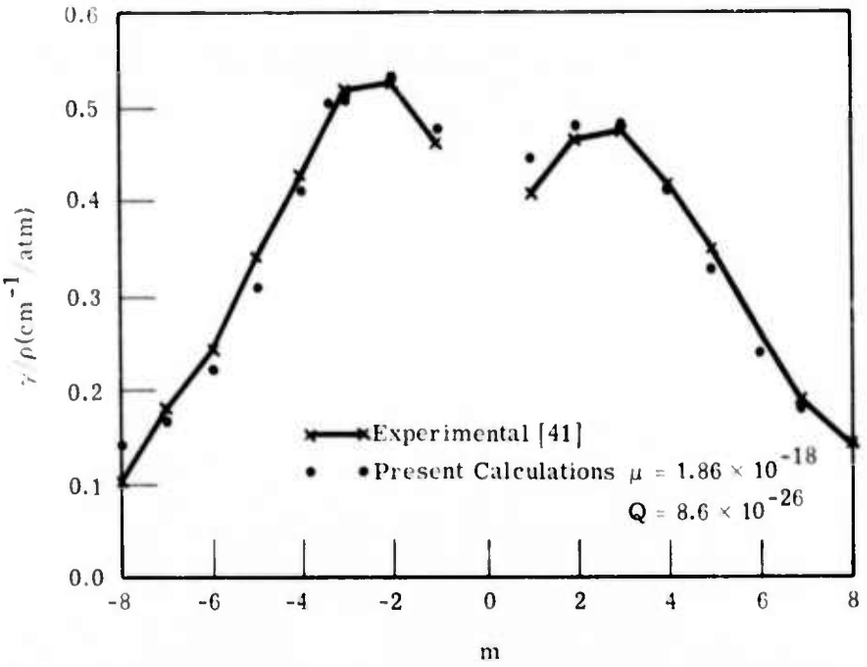

FIGURE 28. COMPARISON OF MEASUREMENT AND THEORY FOR THE FIRST OVERTONE BAND OF SELF-BROADENED HF. Temperature is 373°K, v = 0 → 2 [41].

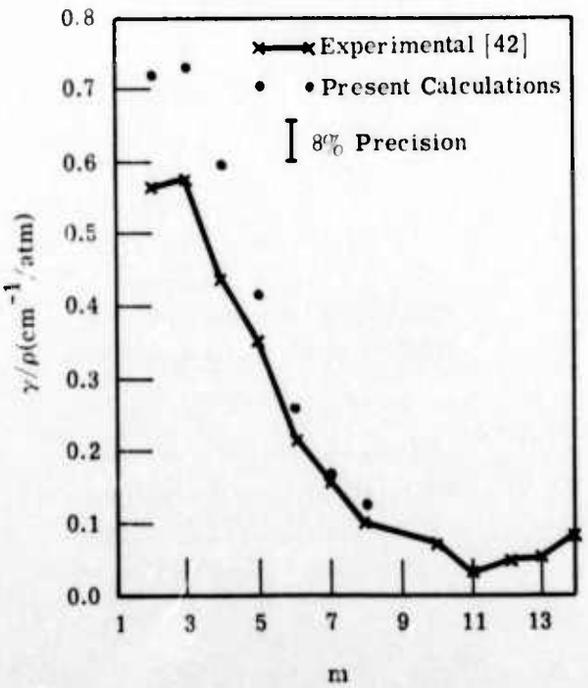

FIGURE 29. COMPARISON OF MEASUREMENT AND THEORY FOR THE PURE ROTATION BAND OF SELF-BROADENED HF. Temperature is 306°K, v = 0 → 0 [42].

TABLE 22. CALCULATED HALF WIDTHS FOR HF(v = 0 → v' = 1) PERTURBED BY HF(v = 0) AT 373.0 DEG K

Input Constants:

B_0 = 20.56 B_1 = 19.79 B_e(Perturber) = 20.56

μ(v = 1) = 1.835E-18 μ(v = 0) = 1.819E-18

Q(v = 1) = 5.000E-26 Q(v = 0) = 5.000E-26

b_{min} = 3.100E-08 cm

Line (m)	Half Width (cm^{-1})	Cross Section (cm^{-2})
-10	6.458068E-02	5.900998E-15
-9	9.805483E-02	1.047799E-14
-8	1.091869E-01	1.166756E-14
-7	1.581954E-01	1.690453E-14
-6	2.482012E-01	2.652241E-14
-5	3.461167E-01	3.698552E-14
-4	4.664320E-01	4.984224E-14
-3	5.604853E-01	5.989263E-14
-2	5.428386E-01	5.800693E-14
-1	4.599256E-01	4.914697E-14
1	4.566365E-01	4.879551E-14
2	5.394523E-01	5.764508E-14
3	5.431765E-01	5.804303E-14
4	4.536538E-01	4.847677E-14
5	3.687319E-01	3.940215E-14
6	2.409441E-01	2.574693E-14
7	1.558045E-01	1.664904E-14
8	1.196923E-01	1.279015E-14
9	9.616441E-02	1.027599E-14
10	6.029395E-02	6.442922E-15

TABLE 23. CALCULATED HALF WIDTHS FOR HF(v = 1 → v' = 2) PERTURBED BY HF(v = 0) AT 373.0 DEG K

Input Constants:

B_1 = 19.79 B_2 = 19.03 B_e(Perturber) = 20.56

μ(v = 1, v = 2) = 1.888E-18 μ(v = 0) = 1.819E-18

Q(v = 1, v = 2) = 5.000E-26 Q(v = 0) = 5.000E-26

b_{min} = 3.100E-08 cm

Line (m)	Half Width (cm^{-1})	Cross Section (cm^{-2})
-15	6.056339E-02	6.471715E-15
-14	6.608039E-02	7.061256E-15
-13	7.197571E-02	7.691222E-15
-12	8.030647E-02	8.581436E-15
-11	8.920157E-02	9.531953E-15
-10	8.696866E-02	9.293347E-15
-9	1.166320E-01	1.246313E-14
-8	1.510004E-01	1.613568E-14
-7	2.555299E-01	2.730555E-14
-6	1.778305E-01	1.900271E-14
-5	2.960820E-01	3.163888E-14
-4	3.675299E-01	3.927371E-14
-3	4.797472E-01	5.126507E-14
-2	5.206271E-01	5.563345E-14
-1	4.683717E-01	5.004951E-14
1	4.382111E-01	4.682659E-14
2	4.857581E-01	5.190739E-14
3	4.679816E-01	5.000782E-14
4	3.856282E-01	4.120766E-14
5	2.776271E-01	2.966682E-14
6	1.886207E-01	2.015573E-14
7	1.497991E-01	1.600731E-14
8	1.142144E-01	1.220479E-14
9	1.041594E-01	1.113032E-14
10	8.753276E-02	9.353626E-15
11	7.639092E-02	8.163026E-15
12	7.357877E-02	7.862519E-15
13	6.507319E-02	6.953629E-15
14	6.160619E-02	6.583147E-15
15	5.900751E-02	6.305456E-15

TABLE 24. CALCULATED HALF WIDTHS FOR HF(v = 2 → v' = 3) PERTURBED BY HF(v = 0) AT 373.0 DEG K

Input Constants:

B_2 = 19.03 B_3 = 18.30 B_e(Perturber) = 20.56

μ(v = 2, v = 3) = 1.931E-18 μ(v = 0) = 1.819E-18

Q(v = 2, v = 3) = 5.000E-26 Q(v = 0) = 5.000E-26

b_{min} = 3.100E-08 cm

Line (m)	Half Width (cm^{-1})	Cross Section (cm^{-2})
-15	5.720191E-02	6.112512E-15
-14	5.724202E-02	6.116798E-15
-13	5.613416E-02	5.998413E-15
-12	6.311947E-02	6.744859E-15
-11	5.885377E-02	6.289027E-15
-10	6.792086E-02	7.257924E-15
-9	1.166134E-01	1.246114E-14
-8	9.010297E-02	9.628274E-15
-7	6.380910E-02	6.818547E-15
-6	1.912177E-01	2.043324E-14
-5	2.119154E-01	2.264497E-14
-4	2.565911E-01	2.741895E-14
-3	2.527246E-01	2.700579E-14
-2	4.150084E-01	4.434718E-14
-1	2.644687E-01	2.826074E-14
1	3.669097E-01	3.920743E-14
2	4.013655E-01	4.288932E-14
3	3.466491E-01	3.704241E-14
4	3.526849E-01	3.768739E-14
5	1.958660E-01	2.092995E-14
6	1.136313E-01	1.214248E-14
7	1.258485E-01	1.344799E-14
8	1.048915E-01	1.120855E-14
9	7.242495E-02	7.739225E-15
10	6.685930E-02	7.144489E-15
11	5.218943E-02	5.576885E-15
12	7.083857E-02	7.569710E-15
13	4.839763E-02	5.171699E-15
14	6.362098E-02	6.798446E-15
15	6.258583E-02	6.687830E-15

TABLE 25. CALCULATED HALF WIDTHS FOR HF(v = 3 → v' = 4) PERTURBED BY HF(v = 0) AT 373.0 DEG K

Input Constants:

B_3 = 18.30 B_4 = 17.58 B_e(Perturber) = 20.56

μ(v = 3, v = 4) = 1.973E-18 μ(v = 0) = 1.819E-18

Q(v = 3, v = 4) = 5.000E-26 Q(v = 0) = 5.000E-26

b_{min} = 3.100E-08 cm

Line (m)	Half Width (cm^{-1})	Cross Section (cm^{-2})
-15	3.660505E-02	3.911561E-15
-14	4.923180E-02	5.260837E-15
-13	6.160534E-02	6.583055E-15
-12	7.554555E-02	8.072692E-15
-11	6.648064E-02	7.104028E-15
-10	8.061868E-02	8.614796E-15
-9	9.220731E-02	9.853138E-15
-8	1.444248E-01	1.543302E-14
-7	2.127870E-01	2.273810E-14
-6	1.467471E-01	1.568118E-14
-5	1.381717E-01	1.476483E-14
-4	1.961167E-01	2.095674E-14
-3	1.385143E-01	1.480143E-14
-2	2.562874E-01	2.738650E-14
-1	2.081543E-01	2.224306E-14
1	3.157854E-01	3.374437E-14
2	3.242705E-01	3.465106E-14
3	1.563498E-01	1.670731E-14
4	2.428266E-01	2.594809E-14
5	2.885888E-01	3.083817E-14
6	1.743240E-01	1.862800E-14
7	1.561589E-01	1.668691E-14
8	1.147209E-01	1.225891E-14
9	7.256985E-02	7.754712E-15
10	6.383151E-02	6.820946E-15
11	7.895076E-02	8.436563E-15
12	4.543156E-02	4.854749E-15
13	7.631880E-02	8.155318E-15
14	5.062404E-02	5.409610E-15
15	4.792231E-02	5.120907E-15

TABLE 26. CALCULATED HALF WIDTHS FOR HF(v = 4 → v' = 5) PERTURBED BY HF(v = 0) AT 373.0 DEG K

Input Constants:

B_4 = 17.58 B_5 = 16.88 B_e(Perturber) = 20.56

μ(v = 4, v = 5) = 2.012E-18 μ(v = 0) = 1.819E-18

Q(v = 4, v = 5) = 5.000E-26 Q(v = 0) = 5.000E-26

b_{min} = 3.100E-08 cm

Line (m)	Half Width (cm^{-1})	Cross Section (cm^{-2})
-15	5.034163E-02	5.379432E-15
-14	5.535909E-02	5.915590E-15
-13	7.611191E-02	8.133210E-15
-12	7.832700E-02	8.369912E-15
-11	4.893632E-02	5.229263E-15
-10	5.115712E-02	5.466574E-15
-9	1.139505E-01	1.217658E-14
-8	1.190719E-01	1.272385E-14
-7	2.561160E-01	2.736818E-14
-6	2.717257E-01	2.903620E-14
-5	2.175332E-01	2.324527E-14
-4	2.013538E-01	2.151637E-14
-3	9.152400E-02	9.780124E-15
-2	2.802700E-01	2.994924E-14
-1	2.122521E-01	2.268095E-14
1	2.998384E-01	3.204029E-14
2	2.800925E-01	2.993028E-14
3	2.623007E-01	2.802907E-14
4	2.671228E-01	2.854435E-14
5	3.556556E-01	3.800483E-14
6	1.493846E-01	1.596302E-14
7	2.021505E-01	2.160150E-14
8	1.609575E-01	1.719968E-14
9	7.349074E-02	7.853114E-15
10	7.011849E-02	7.492762E-15
11	6.331491E-02	6.765740E-15
12	5.155549E-02	5.509143E-15
13	6.930453E-02	7.405782E-15
14	6.410170E-02	6.849817E-15
15	5.575894E-02	5.958318E-15

5

MEASUREMENTS OF INTENSITIES AND WIDTHS IN THE SECOND OVERTONE OF HF*

(R. L. Spellicy, R. E. Meredith, and F. G. Smith)

Collision-broadened molecular vibration-rotation line parameters continue to be of importance for a variety of applications. For example, strength and width parameters are required for analytical predictions of radiative transfer within complex gaseous mixtures. Also, the electric dipole matrix element of a molecular transition may be determined from line strengths measured by absorption spectroscopy, and the electric dipole moment function may be empirically modeled by means of the matrix elements [41, 43, 44]. Determination of the dipole moment permits the calculation of radiative lifetimes and absorption strengths of lines not measurable in the laboratory, e.g., fundamental and overtone vibration-rotation lines involving levels for which $v > 0$, and for which J is not sufficiently populated to permit observation. Collision-broadened line half widths supply information about molecular collision processes particularly with regard to the validity of collision broadening and collision-deactivation theories. Also, measured line half widths may yield molecular electric multipole parameters of the active specie and its collision partners.

In the present investigation, line strengths and self-broadened half widths in the second overtone band of hydrogen fluoride have been measured. The primary motivation of the investigation was to obtain a better definition of the HF dipole moment [1] for the calculation of radiative lifetimes of vibration-rotation lines lying well above the ground state. These lifetimes must be known for an understanding of HF chemical laser performance as well as for other applications for which radiative strengths of excited HF are required.

5.1. MATRIX ELEMENT CALCULATIONS

The connection between the strength of a vibration-rotation spectral absorption line and its electric dipole matrix element for a diatomic molecule is

$$S_{v',v}(m) = \frac{8\pi^3 |m|\nu' \exp\left[-G(v, J)\frac{hc}{kT}\right]|\langle v'J'|\mu(r)|vJ\rangle|^2}{3hckTz} \times 1.0135 \times 10^6 \qquad (85)$$

*Contract No. DAHC-15-67-C-0062 supported previous work in chemical laser studies at the Willow Run Laboratories. Part of this effort involved the measurement of line strengths, and hence, matrix elements in the $v = 0 \rightarrow v' = 3$ vibration-rotation band of HF. This work was not reported under the previous contract and is therefore described here.

The matrix element $|\langle v'J'|\mu(r)|vJ\rangle|$ is given by the expression

$$|\langle v'J'|\mu(r)|vJ\rangle| = \int \psi_{v',J'} \mu(r) \psi_{v,J} r^2 dr \tag{86}$$

where S = line strength $(atm\text{-}cm^2)^{-1}$

ν' = wave number of the transition

z = vibration-rotation partition function

$G(\nu, J)$ = term value of lower level

k = Boltzmann's constant

T = temperature (deg K)

$\mu(r)$ = radial electric dipole moment function

m = $-J$ for P branch; $+J'$ for R branch

The matrix elements are functions of the internuclear potential through the wavefunction $\psi(r)$, and they are functions of the form of the electric dipole moment $\mu(r)$. The most commonly used function $\mu(r)$ is the truncated polynomial expansion $\mu(np)$:

$$\mu(np) = \sum_n M_n (r - r_e)^n \tag{87}$$

The matrix elements $\pm\langle v'J'|\mu(r)|vJ\rangle_{exp}$ may be determined from individual line strengths $S(m)$ from Eq. (85). The line strengths may be obtained from the measured absorption coefficient of the transition $K(\nu)$ through the relationship:

$$S(m) = \frac{1}{P} \int_{line} K(\nu') d\nu' \tag{88}$$

where P is the pressure of the absorbing gas. On the other hand, the matrix elements (and hence the line strengths) may be calculated if the polynomial coefficients for the dipole moment M_i and the wavefunctions ψ are known [1].

In the present investigation, the parameters M_l have been determined from line-strength measurements in various overtone bands through simultaneous solution of equations of the form:

$$\langle v|\mu(r)|0\rangle = \sum_{i=0}^{v_{max}} M_l \int \psi_v (r - r_e)^i \psi_0 r^2 dr \quad \text{for } v = 0, 1 \ldots v_{max} \tag{89}$$

where v_{max} is the upper vibrational quantum number of the highest overtone measurement available. The matrix elements have been calculated by numerical integration of Eq. (86). We obtained wavefunctions $\psi_{v,J}$ by solving Schrödinger's equation using finite difference equations. The RKR potential function, including the vibration-rotation interaction term $J(J+1)/r^2$, was used.

5.2. LINE-WIDTH CALCULATIONS

The Anderson theory has been used with considerable success to calculate self-broadened half widths of spectral lines of simple molecules [3, 38, 41]. In this theory, the half width (γ) is related to the real part of the total cross section (σ) through the relation:

$$\gamma(m) = \frac{N\bar{u}}{2c}\frac{\sigma}{\pi} \tag{90}$$

where $\bar{u}$ is the mean relative collision velocity and N is the number density at one atmosphere and at temperature T. The cross section is written as the statistical average of the partial cross sections of each rotational state (J_2) of the perturbing molecule:

$$\frac{\sigma}{\pi} = \frac{1}{z}\sum_{J_2}\frac{\sigma(J_2)}{\pi} g_2 \exp\left(-\frac{G_{J_2} hc}{kT}\right) \tag{91}$$

where g is the degeneracy of the perturbing state. The partial cross sections are in turn related to the impact parameters $b(J_2)$ and $\mathscr{S}(b)$ which contain the details of the collision through the relationship

$$\frac{\sigma(J_2)}{\pi} = 2\int_0^\infty \mathscr{S}(b) b\, db \tag{92}$$

In what follows, the functional dependence of $b(J_2)$ on J_2 will not be discussed in the interest of brevity.

The collision amplitude $\mathscr{S}(b)$ may be expressed in terms of multipole interactions for $b > 0$ as

$$\mathscr{S}(b) = \sum_{J'J}\left[\sum_{s=1}^{3}\sum_{t} C_s b^{-2(s+1)} g_{st} f_s(k_{st})\right] \tag{93}$$

s = 1, 2, and 3 represent the dipole-dipole, dipole-quadrupole, and quadrupole-quadrupole contributions, respectively. The subscript t refers to the various collision combinations. The $g_{s,t}$ are products of Clebsch-Gordan coefficients, and the $f_s(k)$ are resonance factors [37, 38]. The parameter k is essentially the dimensionless energy defect of a near resonant collision. The coefficients C_s and the parameter k are as follows:

$$C_1 = \frac{4}{9}\left[\frac{\mu_0^4}{(\hbar u)^2}\right]$$

$$C_2 = \frac{4}{45}\left[\frac{\mu_0^2 Q^2}{(\hbar u)^2}\right] \tag{94}$$

$$C_3 = \frac{1}{25}\left[\frac{Q^4}{(\hbar u)^2}\right]$$

$$k_{s,t} = \frac{2\pi c b}{u}\left|\Delta E - \Delta E_2\right|_{s,t}$$

For polar molecules such as HF, Anderson's approximation No. 2 [3] is appropriate:

$$\mathcal{S}(b) = 1 \text{ for } b \leq b_0$$

$$\mathcal{S}(b) < 1 \text{ for } b > b_0 \tag{95}$$

Integration of Eq. (92) then gives

$$\frac{\sigma(J_2)}{\pi} = b_0^2 + \sum_{t,s} C_s b_0^{-2s} g_{st} f_s(k_0) \tag{96}$$

where k_0 is the k_{st} evaluated at $b(J_2) = b_0(J_2)$, and where Eq. (95) has been applied to Eq. (93) to determine $b_0(J_2)$.

In practice, Eq. (96) can be used only for collision partners J_2 for which the long range forces dominate. If this is not the case, b_0 must be determined empirically, or a model such as the resonant dipole billiard ball model must be used [45].

5.3. EXPERIMENTAL PROCEDURE

5.3.1. BACKGROUND

Measurements were performed with a 3-m focal length Ebert spectrometer constructed by H. W. Marshall [46]. A 600 groove/mm Bausch and Lomb replica grating blazed at 1.6 μm was used in second order, double passed. An average spectral resolution of 0.07 cm^{-1} across the second overtone band of HF was obtained.

We achieved wavelength calibration using the HF lines themselves since accurate line positions are well known [39, 47]. Resolution checks were made with Krypton and Xenon Geissler tube emission lines.

Determination of scattered light is particularly difficult in this spectral region (11,500 cm^{-1}) since molecular absorption strengths are too weak to permit observation of opaque lines without very long path lengths. The required extinction can be obtained from a 0.09 molar concentration of Neodymium (+3) in a 1-normal solution of nitric acid. Although the absorption lines of Nd^{+3} are broad, the strongest of the lines could be made sufficiently opaque while leaving sufficient window transmittance. Scattered light determined with this method was less than 1%.

A silicon photovoltaic detector, cooled to -79°C, was used for all measurements. Light from a 1000-W quartz iodine source was modulated at 90 Hz, and the signal was amplified by a Princeton Applied Research Corporation lock-in amplifier, Model HR8 and was displayed on a Leeds and Northrup chart recorder.

An absorption cell having an optical path length of 33 cm was used for all measurements. The cell was constructed of monel with sapphire windows and had a design identical to that reported in Ref. [41]. The gas handling system was also similar to that described in Ref. [41]. The cell, gas manifold, and a Teledyne pressure transducer were maintained at 100°C while the cell was filled with HF, and, during the measurements, the cell was immersed in a bath of gently boiling water. These and other gas-handling precautions were used to avoid the effects of polymerization of HF at room temperature, the absorption of HF by the cell walls, and the reaction of HF with exposed metal surfaces.

Observed line widths, peak values of absorption coefficients, and integrated absorption coefficients were taken directly from the chart recorder and corrected by the direct measurement method. The entire procedure was the same as described in an earlier publication [23].

5.3.2. EXPERIMENTAL STRENGTHS, WIDTHS, AND MATRIX ELEMENTS

Line strengths, widths, and peak absorption coefficients were determined by direct measurement with the use of correction factors tabulated in Ref. [23]. Table 27 shows the corrected values for pressures of 0.932 atm and 0.467 atm. We obtained dipole moment matrix elements by averaging the measured strengths and using Eq. (85).

TABLE 27. MEASURED LINE PARAMETERS

Line	Parameter	(0.467 atm)	(0.932 atm)
P(4)	S	-	0.0175
	γ/P	-	0.430
	K^P	-	0.0127
P(3)	S	0.0235	0.0232
	γ/P	0.503	0.502
	K^P	0.0149	0.0144
P(2)	S	0.0245	0.0235
	γ/P	0.506	0.509
	K^P	0.0154	0.0146
P(1)	S	0.0164	0.0164
	γ/P	0.447	0.488
	K^P	0.0116	0.0107
R(0)	S	0.0193	0.0188
	γ/P	0.397	0.430
	K^P	0.0154	0.0139
R(1)	S	0.0327	0.0310
	γ/P	0.443	0.427
	K^P	0.0234	0.0231
R(2)	S	0.0353	0.0308
	γ/P	0.453	0.400
	K^P	0.0248	0.0245
R(3)	S	0.0287	0.0299
	γ/P	0.412	0.434
	K^P	0.0222	0.0219
R(4)	S	0.0188	0.0159
	γ/P	0.331	0.295
	K^P	0.0182	0.0172
R(5)	S	0.0099	0.0103
	γ/P	0.254	0.256
	K^P	0.0124	0.0127
R(6)	S	0.0039	0.0038
	γ/P	0.164	0.167
	K^P	0.0074	0.0072

Since band-strength measurements determine only the square of the rotationless matrix elements (Table 28), the m dependence of the matrix elements must be used to remove the sign ambiguity. This is feasible in the case of HF since its vibration-rotation interaction is quite large. The signs determined in this manner are listed in Table 29 along with the present value of $\langle 3|\mu(r)|0\rangle_{exp}$ and the preferred dipole moment coefficients of $\mu(3P)$. The correctness of this choice of sign is indicated in Fig. 30, where we compared the experimental matrix elements with calculations using both the preferred $\mu(3P)$ and that based on the negative matrix element. We computed the wavefunctions used in the calculations numerically, using the RKR potential tabulated in Ref. [1]. This potential was calculated with a program written by Zare [11] using the spectroscopic data of Johns and Barrow [48] as input.

A comparison of the observed and calculated half widths is shown in Fig. 31. Listed also are the dipole and quadrupole moments used in the calculations. For the radiating molecule, μ was taken as a weighted average between its v = 0 and v = 3 values while the v = 0 dipole moment was used for the perturbing molecule. The same quadrupole moment was used in both cases. The lower curve shows the widths obtained from Eq. (89) when only dipole-dipole contributions were considered. The upper curve includes contributions through quadrupole-quadrupole. The comparison is quite good, indicating that the theory properly accounts for the energy defects. As predicted by the theory and verified with the fundamental band and first overtone band of HF [41], the R-branch lines are narrower than the corresponding P-branch lines for small |m|, and the line widths decrease progressively with increasing Δv. The tendency of the calculated values to lie below the experimental curve is not unexpected, since forces of shorter range than quadrupole have not been explicitly accounted for.

The m dependence of the line widths arises from the product of the J_2-dependent collision cross section and the Boltzmann factor. This is shown in Figs. 32 and 33. Figure 32 depicts the case in which the spectral line involves energy levels near the Boltzmann maximum. The Boltzmann distribution for the v = 0 levels of the colliding molecule and the partial cross sections contributed by the J_2 states are shown. The contributions for m = +2 and m = -2 are not identical and the Boltzmann distribution is more favorable for the P-branch line, causing it to be broader than the corresponding R-branch line.

Figure 33 describes the case of lines with energy levels far from the Boltzmann maximum. The partial cross sections for the two branches are more comparable in this case, and the Boltzmann distribution does not favor either branch. The resonant and near-resonant terms are eliminated by the Boltzmann factor and the dominant contributions are now the off-resonant terms. These terms are nearly equal and tend to a constant value as the energy defect ΔE increases. This condition produces nearly equal half widths for the P and R branches for large |m|. This is essentially the assumption of the resonant dipole billiard ball model (RDBBM) [45]

TABLE 28. EXPERIMENTAL MATRIX ELEMENTS $\langle v'J'|\mu(r)|vJ\rangle_{exp}$

	(esu-cm)
P(4)	1.738×10^{-21}
P(3)	1.677
P(2)	1.642
P(1)	1.639
R(0)	1.623
R(1)	1.613
R(2)	1.563
R(3)	1.615
R(4)	1.528
R(5)	1.574
R(6)	1.554

TABLE 29. DIPOLE MOMENT PARAMETERS AND EXPERIMENTAL MATRIX ELEMENTS

(a) (r_e = 0.91717 Å)

	$[\mu(1p)]$	$[\mu(2p)]$	$[\mu(3p)]$
M_0	1.819	1.819	1.819
M_1	1.494	1.511	1.522
M_2	-	-0.286	-0.136
M_3	-	-	-1.314

(b) $M_i = \left(\frac{10^8}{cm}\right)^i$ Debye

$\langle 0|\mu(r)|0\rangle_{exp} = 1.819 \times 10^{-18}$ esu-cm
$\langle 1|\mu(r)|0\rangle_{exp} = 9.850 \times 10^{-20}$ esu·cm (15)
$\langle 2|\mu(r)|0\rangle_{exp} = -1.253 \times 10^{-20}$ esu-cm (3)
$+\langle 3|\mu(r)|0\rangle_{exp} = +1.628 \times 10^{-21}$ esu-cm

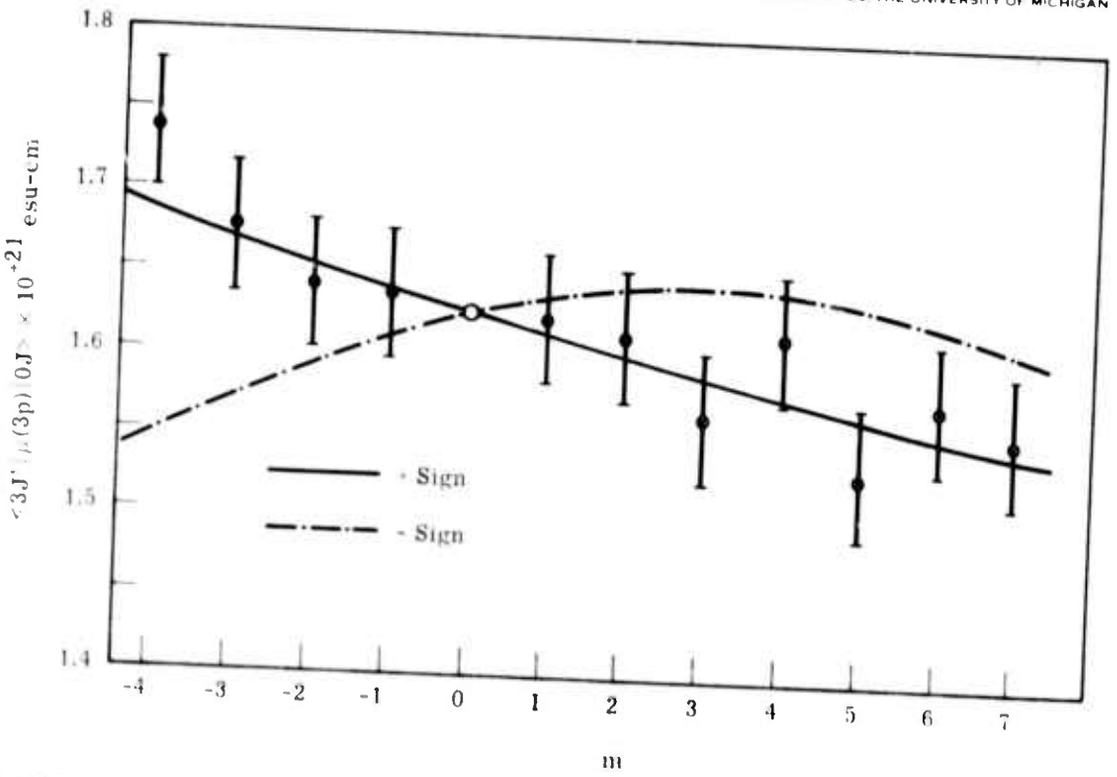

FIGURE 30. COMPARISON OF BOTH EXPERIMENTAL AND CALCULATED MATRIX ELEMENTS

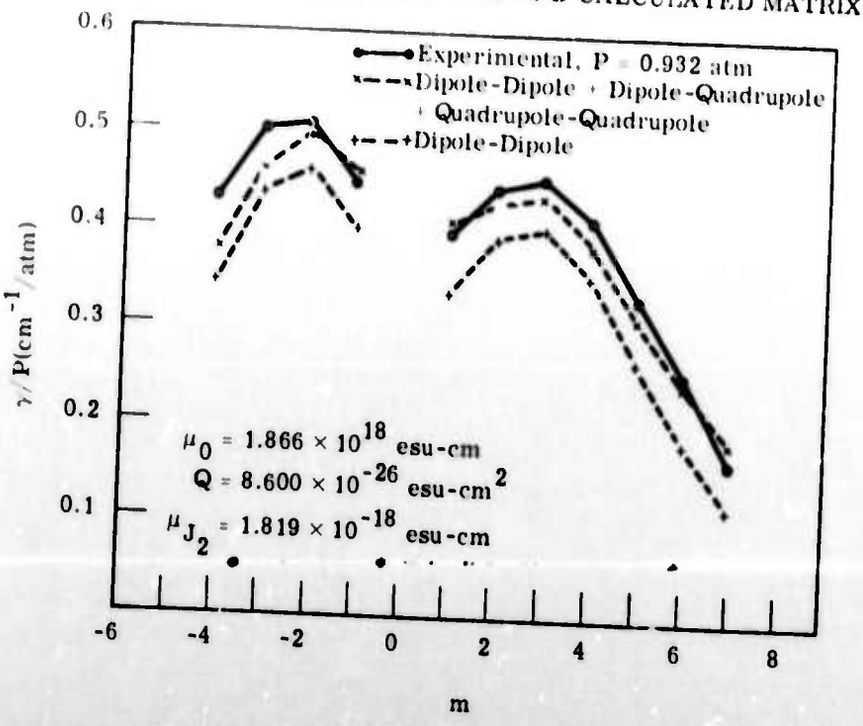

FIGURE 31. COMPARISON OF OBSERVED AND CALCULATED HALF WIDTHS

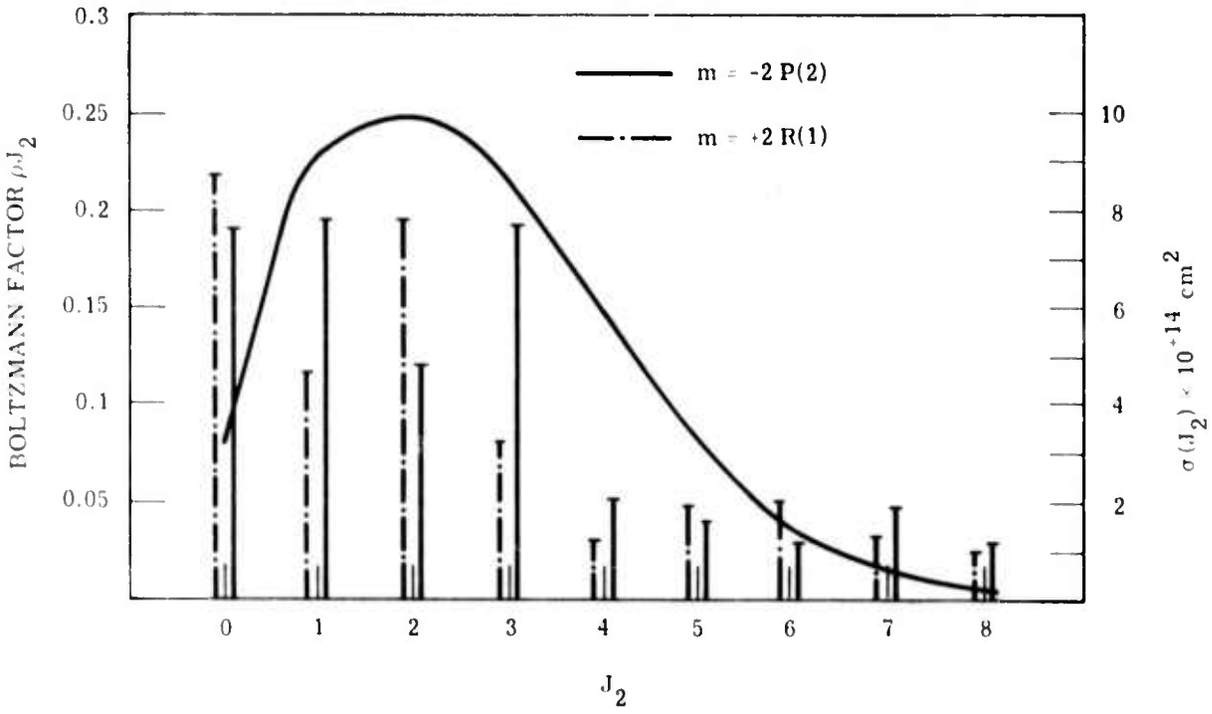

FIGURE 32. CASE IN WHICH SPECTRAL LINE INVOLVES ENERGY LEVELS NEAR THE THE BOLTZMANN MAXIMUM

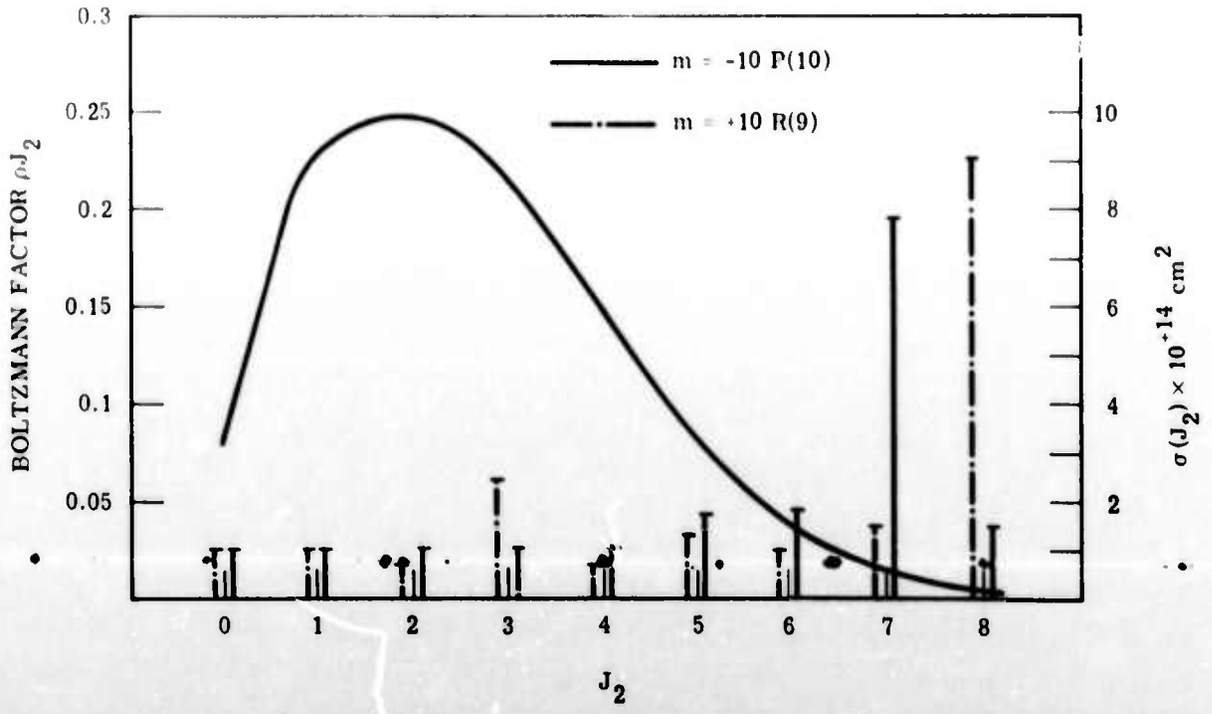

FIGURE 33. CASE IN WHICH SPECTRAL LINE INVOLVES ENERGY LEVELS FAR FROM THE BOLTZMANN MAXIMUM

and is in agreement with measured second overtone half widths. If it is assumed that the constant value of the cross section is given by $\sigma(J_2) = \pi b_{min}^2$, the calculations predict a value $b_{min} = 5.6 \times 10^{-8}$ cm. This compares well with the half widths reported in Ref. [41].

The contributions of the higher order terms (dipole-quadrupole, quadrupole-quadrupole) may be inferred from Fig. 31. Although these terms are not as large as the resonant or near-resonant dipole terms, they become increasingly significant as the stronger terms move into the wings of the Boltzmann distribution. Figure 34 clarifies this by showing the partial cross sections calculated from dipole-dipole interactions alone and those calculated from all interactions through quadrupole-quadrupole. The increase in $\sigma(1)$, $\sigma(2)$, $\sigma(3)$, and $\sigma(4)$ resulting from the higher order terms significantly alters the calculated half widths since these levels are heavily weighted by the Boltzmann factor.

5.4. CONCLUSIONS

The investigation reported here confirms earlier indications that we can reliably predict self-broadened, spectral line widths with theories like Anderson's using long range multipolar molecular interactions. Although the HF molecule represents the extreme case of small moment of inertia and large dipole moment, the pronounced agreement between theory and experiment indicates that line widths may be calculated accurately if proper account is taken of nonresonant effects. It is also confirmed that the effects of vibration-rotation interaction diminish with increasing Δv, in agreement with theory.

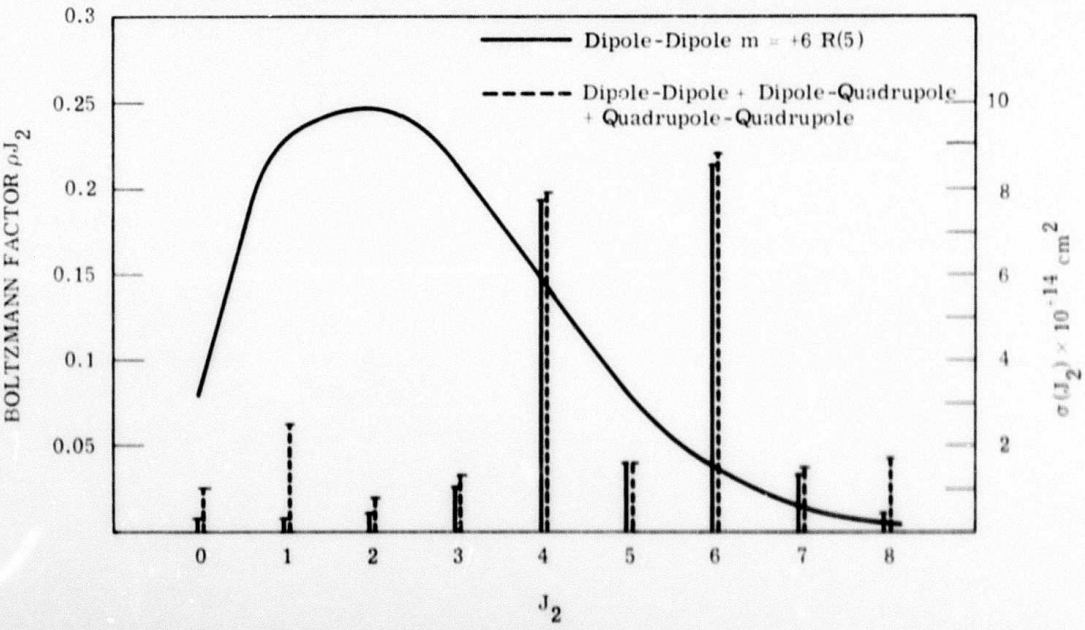

FIGURE 34. PARTIAL CROSS SECTIONS CALCULATED FROM DIPOLE-DIPOLE INTERACTIONS AND FROM ALL INTERACTIONS THROUGH QUADRUPOLE-QUADRUPOLE INTERACTIONS

Appendix I

The equations governing the interaction of gas molecules with radiation by means of the processes described by the Einstein coefficients for spontaneous emission and stimulated absorption and emission can be developed in the following way.

Consider from the standpoint of hydrodynamics, a volume (V) fixed in space with boundary surface A. Let us assume that this volume contains molecules in two states only and that Doppler broadening is the only broadening mechanism. The number density of molecules in the upper state is n_u, and of those in the lower state n_ℓ. Because of Doppler broadening, only a certain portion of the molecules, namely $n_{u_\nu}\, d\nu$ and $n_{\ell_\nu}\, d\nu$ are capable of absorbing or emitting at any one frequency ν. Consider also a density of photons, $\rho_{\nu,\Omega}$, at or near a frequency ν entering and leaving that volume and travelling between directions Ω and $\Omega + d\Omega$, where, $\vec{k}_\Omega$ is a unit vector in the Ω direction. The net time rate of change in photons within that volume is given by the first term on the left hand side of the following equation:

$$\frac{\partial}{\partial t}\int_V (\rho_{\nu,\Omega}\, d\nu\, d\Omega)\, dV + c\int_A (\rho_{\nu,\Omega}\, d\nu\, d\Omega)\vec{k}_\Omega \cdot \vec{\ell}\, dA = \left(\frac{d\rho_{\nu,\Omega}}{dt}\right)_{EA} dV \tag{97}$$

The remainder of the terms account for the means by which photons within the volume are gained or lost. The second term accounts for the change in $\rho_{\nu,\Omega}$ by the inward and outward flux of photons. The elemental area dA has the outward normal $\vec{\ell}$. The right hand side is a source term and $\left(d\rho_{\nu,\Omega}/dt\right)_{EA}$ is the rate of creation and loss of photons resulting from the processes described by the Einstein coefficients

$$\left(\frac{d\rho_{\nu,\Omega}}{dt}\right)_{EA} = \frac{n_{u_\nu} A_{u\ell}}{4\pi}\, d\Omega\, d\nu + n_{u_\nu}\rho_{\nu,\Omega} cB_{u\ell}\, d\Omega\, d\nu - n_{\ell_\nu}\rho_{\nu,\Omega} cB_{\ell u}\, d\Omega\, d\nu \tag{98}$$

The form of $\left(d\rho_{\nu,\Omega}/dt\right)_{EA}$ is determined by the definition of the Einstein coefficients (see for example, Ref. 49) where $A_{u\ell}$ is the coefficient for spontaneous emission, and $A_{u\ell}\Delta t$ is the probability that a molecule in the upper state will spontaneously emit a photon in any direction in time Δt; $B_{u\ell}$ and $B_{\ell u}$ are the coefficients for stimulated emission and absorption respectively; $B_{u\ell} L_\nu \Delta t$ is the probability that a molecule in the upper state will emit a photon by stimulated emission in time Δt when subjected to an incident spectral photon radiance of L_ν. This photon

will be in phase with and in the same direction as the incident photon. A similar definition holds for the absorption of a photon because of the stimulated absorption coefficient $B_{\ell u}$

The molecular number densities within the volume also change because of the absorption and emission of photons. The number density of molecules capable of emitting at frequency ν is $n_{u_\nu} d_\nu$, where n_{u_ν} is a spectral number density having a frequency distribution identical to the shape of the absorption coefficient for a Doppler broadened line. It is assumed here that collisional broadening is not important, an assumption which is certainly reasonable at the low cell pressures considered for this program. Assuming that the net flow of molecules across the surface of the volume is negligible, the equation for the change in molecular number densities can be written

$$\frac{\partial}{\partial t}\int_V \left(n_{\ell_\nu} d\nu\right) dV = \int_V \left(n_{u_\nu} A_{u\ell} d\nu\right) dV + \int_V \int_\Omega \rho_{\nu,\Omega} c \left[\left(n_{u_\nu} d\nu\right) B_{u\ell} - \left(n_{\ell_\nu} d\nu\right) B_{\ell u}\right] d\Omega\, dV \tag{99}$$

The first term on the right hand side is the gain of molecules in state ℓ capable of absorbing between ν and $\nu + d\nu$, because of spontaneous emission. The second term is the gain and loss of molecules in state ℓ because of stimulated emission and absorption. Both these terms involve integration over all directions to account for all changes in n_ℓ. The order of the integrations over solid angle and ν in the right hand side of Eq. (99) can be inverted and the time derivative on the left hand side can be brought inside the integrals. Since all terms are to be integrated over ν and V, the integrals can be dropped so that

$$\frac{\partial n_{\ell_\nu}}{\partial t} = n_{u_\nu} A_{u\ell} + \int_{4\pi} \rho_{\nu,\Omega} c \left[n_{u_\nu} B_{u\ell} - n_{\ell_\nu} B_{\ell u}\right] d\Omega \tag{100}$$

The integral over solid angle is really a two-dimensional integration.

Similar simplifications can be made to Eq. (98). The term representing photon flux through the surface of the volume can be transformed to an integral over the volume by Gauss' theorem so that Eq. (98) becomes

$$\frac{\partial}{\partial t}\int_V \left(\rho_{\nu,\Omega}\, d\nu\right) d\Omega\, dV + c\int_V \vec{k}_\Omega \cdot \nabla\left(\rho_{\nu,\Omega}\, d\nu\, d\Omega\right) dV = \int_V \left(\frac{\rho_{\nu,\Omega}}{dt}\right)_{EA} dV$$

Again, the integrals can be dropped so that Eq. (98) reduces to

$$\frac{\partial \rho_{\nu,\Omega}}{t} + c\vec{k}_\Omega \cdot \nabla \rho_{\nu,\Omega} = \frac{n_{u_\nu} A_{u\ell}}{4\pi} + \rho_{\nu,\Omega} c\left(n_{u_\nu} B_{u\ell} - n_{\ell_\nu} B_{\ell u}\right) \tag{101}$$

Thus, Eqs. (100) and (101) form two partial differential equations in the three unknowns, $\rho_{\nu,\Omega}$, n_{ℓ_ν}, n_{u_ν}. The third equation is the molecular conservation equation

$$n_u + n_\ell = N \tag{102}$$

where N is a known function of position. If no interaction between the photon field and translational energy occurs, then

$$n_{u_\nu} + n_{\ell_\nu} = N_\nu \tag{103}$$

where N_ν is a known function of position and has the characteristic Doppler variation with frequency. The quantities n_{u_ν}, n_{ℓ_ν}, and N_ν can also vary with direction, since the existence of a nonisotropic photon field having an arbitrary spectral shape could produce different spectral profiles in n_{ℓ_ν} and n_{u_ν} in different directions. The constraint on such variations must be such that the number density at any position and time, integrated over all frequencies must be the same from all directions, i.e.,

$$\int n_{\ell_\nu}(\vec{r}, t, \Omega, \nu)\, d\nu = n_\ell(\vec{r}, t)$$

and similarly (104)

$$\int n_{u_\nu}(\vec{r}, t, \Omega, \nu)\, d\nu = n_u(\vec{r}, t)$$

In other words, n_ℓ and n_u cannot be functions of Ω.

Equation (101) yields the blackbody photon density when thermodynamic equilibrium is assumed. This can be seen by inserting the relationship between $A_{u\ell}$, $B_{u\ell}$, and $B_{\ell u}$ and noting that at equilibrium $\partial\rho_{\nu,\Omega}/\partial t = \nabla\rho_{\nu,\Omega} = 0$. The relationship between $A_{u\ell}$, $B_{u\ell}$, and $B_{\ell u}$ are given by Eq. (36). At equilibrium, the relationship between n_u and n_ℓ must be

$$\frac{n_{u_\nu}}{n_{\ell_\nu}} = \frac{n_u}{n_\ell} = \frac{g_u}{g_\ell} \exp\left[\frac{E_{u\ell}}{kT}\right] \tag{105}$$

where g_u and g_ℓ are the statistical weights of the upper and lower levels respectively and $E_{u\ell}$ is the energy difference between the two levels and is equal to $h\nu$; h is Planck's constant. Substituting these relationships into Eq. (101) yields

$$\rho_{\nu,\Omega} = \frac{2\nu^2}{c^3}\left[\exp\left(\frac{h\nu}{kT}\right) - 1\right]^{-1} \tag{106}$$

the blackbody spectral photon density per unit solid angle.

If all photons of interest are traveling in one direction only, and the ambient radiation can be ignored, and if spontaneous emission is ignored, then Eqs. (100) and (101) can be reduced to the laser amplifier equations:

$$\frac{\partial \rho_\nu}{\partial t} + c\frac{\partial \rho_\nu}{\partial x} = \rho_\nu c\left(n_{u_\nu} B_{u\ell} - n_{\ell_\nu} B_{\ell u}\right)$$

$$\frac{\partial n_{\ell_\nu}}{\partial t} = -\frac{\partial n_{n_\nu}}{\partial t} = \rho_\nu c\left(n_{u_\nu} B_{u\ell} - n_{\ell_\nu} B_{\ell u}\right) \tag{107}$$

In the case of a simple laser amplifier, the radiation of interest comes from one transition only, so that the two-level picture above is sufficient. However, when fluorescence and radiative relaxation are to be considered, many different transitions and states participate in the relaxation process. Thus, it is necessary to consider a photon-density conservation equation like (101) for each transition involved. There must also be an equation like (100) for each of the states involved. Since each state can gain or lose molecules by several transitions, e.g., pure rotation, P-branch and R-branch transitions, terms must be added to the right hand side of each of these equations for each of the possible transitions in which that state participates.

The resulting equations contain such a large number of terms that it is not practical to solve them, even by numerical means. Even a general solution to the two-level case is complex because of the large number of dependent variables involved (three position variables, two direction variables, time, and frequency). However, as has been noted, it will be necessary to assess the effects of radiative rotational relaxation by stimulated emission. This assessment necessitates the solution of these equations for some simplified case and will be attempted during the second half of the contract period.

Appendix II

The detailed results of the matrix element calculations for HCl are included in this appendix. The matrix elements used to determine the dipole moment function were:

$$\langle 0|\mu(r)|0\rangle = 1.10847 \times 10^{-18} \text{ esu-cm}$$
$$\langle 1|\mu(r)|0\rangle = 7.12 \times 10^{-20} \text{ esu-cm}$$
$$\langle 2|\mu(r)|0\rangle = -7.75 \times 10^{-21} \text{ esu-cm}$$
$$\langle 3|\mu(r)|0\rangle = 5.15 \times 10^{-22} \text{ esu-cm}$$

The dipole moment coefficients determined from these matrix elements are:

$$M_0 = 1.0935 \pm 0.0007 \times 10^{-18} \text{ esu-cm}$$
$$M_1 = 0.947 \pm 0.023 \times 10^{-10} \text{ esu-cm/cm}$$
$$M_2 = 0.015 \pm 0.041 \times 10^{-2} \text{ esu-cm/cm}^2$$
$$M_3 = -0.814 \pm 0.116 \times 10^{6} \text{ esu-cm/cm}^3$$

The first three pages of tabulated values lists the rotationless matrix elements computed, the corresponding Einstein A's and the computed band positions. The following pages list the rotation dependent matrix elements and Einstein A's. The transitions covered in the tabulation include vibrational transitions for which $0 < \Delta\nu \leq 5$ for all vibrational levels between 0 and 12. All rotational states between 0 and 35 are included.

Tabulated values for transitions involving vibrational states substantially greater than 3 should be used with caution, however. Such transitions represent extrapolation of the polynomial dipole moment function to internuclear distances beyond those distances represented by available experimental measurements and hence are subject to unknown inaccuracies. The tabulated values for transitions involving $v > 5$ states exhibit unusual and unexplained variations with rotational quantum number J. These variations cannot be defended because of this extrapolation and should be treated with some skepticism.

VIBRATIONAL MATRIX ELEMENTS FOR HCL USING THE 3KR POTENTIAL FUNCTION

ESU-CM

V	0	1	2	3	4	5	6	7	8	9	10
V'											
0	1.109E-18										
1	7.120E-20	1.130E-18									
2	-7.750E-21	9.933E-20	1.167E-18								
3	5.150E-22	-1.430E-20	1.193E-19	1.195E-18							
4	4.083E-23	1.243E-21	-2.149E-20	1.340E-19	1.221E-18						
5	-4.547E-23	3.414E-23	2.322E-21	-2.939E-20	1.445E-19	1.245E-18					
6	2.280E-23	-9.350E-23	-4.568E-23	3.874E-21	-3.807E-20	1.509E-19	1.267E-18				
7	-1.026E-23	5.428E-23	-1.392E-22	-2.494E-22	5.852E-21	-4.757E-20	1.530E-19	1.285E-18			
8	4.549E-24	-2.695E-23	9.428E-23	-1.576E-22	-6.474E-22	9.532E-21	-5.789E-20	1.503E-19	1.299E-18		
9	-2.053E-24	1.285E-23	-5.032E-23	1.318E-22	-1.119E-22	1.421E-21	1.198E-20	-6.897E-20	1.419E-19	1.308E-18	
10	9.439E-25	-5.917E-24	2.472E-23	-7.569E-23	1.502E-22	4.120E-23	-2.378E-21	1.638E-20	-8.072E-20	1.269E-19	1.309E-18

EINSTEIN COEFFICIENTS A(V',V) FOR HCL

SEC-1

V	0	1	2	3	4	5	6	7	8	9	10
V'											
0	0.0										
1	3.826E 01	0.0									
2	3.433E 00	6.667E 01	0.0								
3	4.841E-02	1.044E 01	9.581E 01	0.0							
4	6.819E-04	2.519E-01	2.101E 01	9.641E 01	0.0						
5	1.561E-03	4.249E-04	7.812E-01	3.492E 01	9.932E 01	0.0					
6	6.357E-04	5.869E-03	6.751E-04	1.877E 00	5.179E 01	9.549E 01	0.0				
7	1.941E-04	3.218E-03	1.152E-02	1.779E-02	3.876E 00	7.111E 01	8.602E 01	0.0			
8	5.359E-05	1.185E-03	8.574E-03	1.300E-02	1.053E-01	7.214E 00	9.187E 01	7.210E 01	0.0		
9	1.461E-05	3.774E-04	3.435E-03	1.471E-02	5.725E-03	3.925E-01	1.236E 01	1.128E 02	5.532E 01	0.0	
10	3.971E-06	1.046E-04	1.224E-03	7.197E-03	1.663E-02	6.747E-04	1.070E 00	1.984E 01	1.318E 02	3.743E 01	0.0

BAND POSITIONS FOR HCL

CM-1

V	0	1	2	3	4	5	6	7	8	9
V°										
0	0.0									
1	2887.027	0.0								
2	5669.637	2782.609	0.0							
3	8348.965	5461.939	2679.328	0.0						
4	10925.928	8039.801	5256.191	2576.863	0.0					
5	13400.742	10513.715	7731.105	5051.777	2474.914	0.0				
6	15773.809	12886.781	10104.172	7424.844	4847.990	2373.066	0.0			
7	18044.820	15157.793	12375.184	9695.855	7119.002	4644.078	2271.012	0.0		
8	20211.797	17324.770	14542.160	11862.832	9235.969	6811.055	4437.988	2166.977	0.0	
9	22272.680	19385.652	16603.043	13923.715	11346.852	8871.939	6498.871	4227.859	2060.883	0.0
10	24227.602	21335.574	18552.365	15873.637	13296.773	10821.859	8448.793	6177.791	4010.805	1949.922

MATRIX ELEMENTS, EINSTEIN A'S AND ENERGIES FOR V= 0 TO 0 TRANSITIONS OF HCL

Pure Rotation

J	<V J'M'|/V" J+1>	A	F
	ESU-CM	SEC-1	CM-1
0	1.1085E-18	1.1707E-03	20.9
1	1.1087E-18	1.1230E-02	41.8
2	1.1090E-18	4.0576E-02	62.6
3	1.1094E-18	9.0559E-02	83.4
4	1.1100E-18	1.5857E-01	104.2
5	1.1106E-18	3.4773E-01	124.9
6	1.1114E-18	5.5673E-01	145.5
7	1.1123E-18	8.3555E-01	166.0
8	1.1134E-18	1.1933E 00	186.5
9	1.1145E-18	1.6401E 00	206.8
10	1.1158E-18	2.1835E 00	227.0
11	1.1172E-18	2.8324E 00	247.0
12	1.1187E-18	3.5944E 00	266.9
13	1.1204E-18	4.4782E 00	286.7
14	1.1221E-18	5.4887E 00	306.3
15	1.1240E-18	6.6344E 00	325.6
16	1.1261E-18	7.9223E 00	344.8
17	1.1282E-18	9.3541E 00	363.8
18	1.1305E-18	1.0930E 01	382.6
19	1.1329E-18	1.2676E 01	401.1
20	1.1354E-18	1.4575E 01	419.5
21	1.1381E-18	1.6635E 01	437.5
22	1.1409E-18	1.8859E 01	455.3
23	1.1438E-18	2.1248E 01	472.8
24	1.1468E-18	2.3807E 01	490.1
25	1.1500E-18	2.6531E 01	507.1
26	1.1533E-18	2.9424E 01	523.7
27	1.1568E-18	3.2481E 01	540.1
28	1.1603E-18	3.5704E 01	556.1
29	1.1640E-18	3.9089E 01	571.9
30	1.1679E-18	4.2633E 01	587.3
31	1.1719E-18	4.6333E 01	602.3
32	1.1760E-18	5.0183E 01	617.0
33	1.1802E-18	5.4174E 01	631.3
34	1.1846E-18	5.8309E 01	645.3
35	1.1891E-18	6.2573E 01	658.9

MATRIX ELEMENTS, EINSTEIN A'S AND ENERGIES FOR V= 0 TO 1 TRANSITIONS OF HCL

J	R-BRANCH <V J/MU/V' J+1> ESU-CM	R-BRANCH A SEC-1	R-BRANCH E CM-1	P-BRANCH <V J/MU/V' J-1> ESU-CM	P-BRANCH A SEC-1	P-BRANCH E CM-1
0	7.0255E-20	1.2681E 01	2907.3			
1	6.9315E-20	1.5116E 01	2927.0	7.2152E-20	3.9445E 01	2866.1
2	6.8381E-20	1.6071E 01	2946.0	7.3110E-20	2.5728E 01	2844.7
3	6.7452E-20	1.6522E 01	2964.4	7.4074E-20	2.3222E 01	2822.6
4	6.6528E-20	1.6734E 01	2982.1	7.5047E-20	2.2159E 01	2800.0
5	6.5609E-20	1.6810E 01	2999.1	7.6026E-20	2.1565E 01	2776.8
6	6.4695E-20	1.6798E 01	3015.5	7.7013E-20	2.1173E 01	2753.0
7	6.3786E-20	1.6722E 01	3031.2	7.8009E-20	2.0884E 01	2728.8
8	6.2882E-20	1.6599E 01	3046.2	7.9013E-20	2.0648E 01	2704.0
9	6.1983E-20	1.6438E 01	3060.4	8.0025E-20	2.0440E 01	2678.7
10	6.1089E-20	1.6244E 01	3073.9	8.1045E-20	2.0246E 01	2652.9
11	6.0199E-20	1.6022E 01	3086.7	8.2075E-20	2.0058E 01	2626.7
12	5.9315E-20	1.5776E 01	3098.8	8.3114E-20	1.9868E 01	2600.0
13	5.8436E-20	1.5508E 01	3110.1	8.4162E-20	1.9675E 01	2572.8
14	5.7563E-20	1.5219E 01	3120.6	8.5219E-20	1.9474E 01	2545.2
15	5.6696E-20	1.4912E 01	3130.4	8.6287E-20	1.9266E 01	2517.2
16	5.5833E-20	1.4589E 01	3139.4	8.7364E-20	1.9047E 01	2488.7
17	5.4977E-20	1.4248E 01	3147.6	8.8451E-20	1.8817E 01	2459.9
18	5.4126E-20	1.3894E 01	3154.9	8.9548E-20	1.8577E 01	2430.7
19	5.3282E-20	1.3526E 01	3161.5	9.0655E-20	1.8324E 01	2401.1
20	5.1970E-20	1.3145E 01	3167.3	9.1772E-20	1.8061E 01	2371.2
21	5.1042E-20	1.2753E 01	3172.2	9.2900E-20	1.7786E 01	2340.9
22	5.0107E-20	1.2349E 01	3176.3	9.4038E-20	1.7499E 01	2310.3
23	4.9164E-20	1.1936E 01	3179.5	9.5187E-20	1.7201E 01	2279.3
24	4.8211E-20	1.1513E 01	3182.0	9.6346E-20	1.6893E 01	2248.1
25	4.7248E-20	1.1083E 01	3183.5	9.7517E-20	1.6573E 01	2216.6
26	4.6274E-20	1.0645E 01	3184.2	9.8697E-20	1.6244E 01	2184.8
27	4.5288E-20	1.0201E 01	3184.0	9.9888E-20	1.5904E 01	2152.7
28	4.4287E-20	9.7512E 00	3183.0	1.0109E-19	1.5556E 01	2120.4
29	4.3271E-20	9.2972E 00	3181.1	1.0230E-19	1.5199E 01	2087.8
30	4.2239E-20	8.8400E 00	3178.2	1.0353E-19	1.4833E 01	2055.0
31	4.1186E-20	8.3800E 00	3174.6	1.0476E-19	1.4460E 01	2021.9
32	4.0115E-20	7.9189E 00	3170.0	1.0600E-19	1.4080E 01	1988.7
33	3.9021E-20	7.4572E 00	3164.4	1.0726E-19	1.3693E 01	1955.3
34	3.7903E-20	6.9965E 00	3158.1	1.0852E-19	1.3301E 01	1921.6
35	3.6759E-20	6.5375E 00	3150.7	1.0979E-19	1.2903E 01	1887.8

MATRIX ELEMENTS, EINSTEIN A'S AND ENERGIES FOR V= 0 TO 2 TRANSITIONS OF HCL

	P-BRANCH			P-BRANCH		
J	<V J/MU/V' J+1>	A	E	<V J/MU/V' J-1>	A	E
	ESU-CM	SEC-1	CM-1	ESU-CM	SEC-1	CM-1
0	-7.72875E-21	1.15[illegible]E 00	5688.3			
1	-7.71015E-21	1.29695E 00	5707.8	-7.7730E-21	3.4166E 00	5648.8
2	-7.69479E-21	1.40335E 00	5725.0	-7.8009E-21	2.2668E 00	5626.7
3	-7.68156E-21	1.5564E 00	5740.9	-7.8305E-21	2.0302E 00	5603.4
4	-7.67009E-21	1.59965E 00	5755.6	-7.8620E-21	1.9242E 00	5579.0
5	-7.66033E-21	1.63235E 00	5769.1	-7.8986E-21	1.8619E 00	5553.3
6	-7.65192E-21	1.65875E 00	5781.2	-7.9369E-21	1.8193E 00	5526.6
7	-7.64558E-21	1.68910E 00	5792.1	-7.9784E-21	1.7874E 00	5498.7
8	-7.64061E-21	1.7006E 00	5801.6	-8.0229E-21	1.7620E 00	5469.7
9	-7.63709E-21	1.71983E 00	5809.9	-8.0704E-21	1.7408E 00	5439.6
10	-7.63446E-21	1.7343E 00	5816.9	-8.1211E-21	1.7224E 00	5408.4
11	-7.63286E-21	1.7494E 00	5822.4	-8.1753E-21	1.7063E 00	5376.1
12	-7.63233E-21	1.7636E 00	5826.6	-8.2335E-21	1.6916E 00	5342.8
13	-7.63267E-21	1.7771E 00	5829.5	-8.2931E-21	1.6780E 00	5308.4
14	-7.63425E-21	1.7899E 00	5831.1	-8.3572E-21	1.6654E 00	5273.0
15	-7.63710E-21	1.8023E 00	5831.3	-8.4250E-21	1.6536E 00	5236.6
16	-7.64121E-21	1.8143E 00	5830.1	-8.4962E-21	1.6424E 00	5199.2
17	-7.64657E-21	1.8258E 00	5827.6	-8.5712E-21	1.6316E 00	5160.8
18	-7.65321E-21	1.8372E 00	5823.6	-8.6501E-21	1.6214E 00	5121.4
19	-7.66109E-21	1.8480E 00	5818.3	-8.7326E-21	1.6113E 00	5081.1
20	-7.67021E-21	1.8585E 00	5811.6	-8.8196E-21	1.6017E 00	5039.9
21	-7.68064E-21	1.8689E 00	5803.5	-8.9109E-21	1.5923E 00	4997.7
22	-7.69236E-21	1.8786E 00	5793.9	-9.0058E-21	1.5830E 00	4954.6
23	-7.70718E-21	1.8882E 00	5783.0	-9.1059E-21	1.5741E 00	4910.6
24	-8.01356E-21	1.8974E 00	5770.7	-9.2102E-21	1.5652E 00	4865.8
25	-8.05756E-21	1.9060E 00	5756.9	-9.3195E-21	1.5565E 00	4820.0
26	-8.10406E-21	1.9142E 00	5741.7	-9.4339E-21	1.5479E 00	4773.5
27	-8.15246E-21	1.9220E 00	5725.1	-9.5533E-21	1.5394E 00	4726.1
28	-8.20496E-21	1.9292E 00	5707.0	-9.6780E-21	1.5310E 00	4677.9
29	-8.25896E-21	1.9358E 00	5687.5	-9.8086E-21	1.5227E 00	4628.8
30	-8.31566E-21	1.9419E 00	5666.6	-9.9451E-21	1.5145E 00	4579.0
31	-8.37416E-21	1.9471E 00	5644.2	-1.0087E-20	1.5062E 00	4528.4
32	-8.43566E-21	1.9518E 00	5620.4	-1.0236E-20	1.4981E 00	4477.0
33	-8.49936E-21	1.9556E 00	5595.1	-1.0392E-20	1.4899E 00	4424.9
34	-8.56506E-21	1.9584E 00	5568.3	-1.0554E-20	1.4818E 00	4372.0
35	-8.63336E-21	1.9604E 00	5540.1	-1.0725E-20	1.4737E 00	4318.4

MATRIX ELEMENTS, EINSTEIN A'S AND ENERGIES FOR V= 0 TO 3 TRANSITIONS OF HCL

	P-BRANCH			P-BRANCH		
J	<V J/MU/V' J+1>	A	E	<V J/MU/V' J-1>	A	E
	ESU-CM	SEC-1	CM-1	ESU-CM	SEC-1	CM-1
0	5.1801E-22	1.6439E-02	8368.1			
1	5.2149E-22	2.0117E-02	8385.3	5.1243E-22	4.7574E-02	8328.1
2	5.2545E-22	2.2003E-02	8400.7	5.1049E-22	3.1218E-02	8305.4
3	5.3025E-22	2.3349E-02	8414.2	5.0910E-22	2.7499E-02	8280.9
4	5.3519E-22	2.4429E-02	8425.9	5.0784E-22	2.6000E-02	8254.7
5	5.4077E-22	2.5413E-02	8435.9	5.0739E-22	2.4977E-02	8226.7
6	5.4701E-22	2.6367E-02	8443.7	5.0732E-22	2.4251E-02	8196.9
7	5.5391E-22	2.7322E-02	8449.9	5.0770E-22	2.3701E-02	8165.4
8	5.6126E-22	2.8278E-02	8453.9	5.0843E-22	2.3256E-02	8132.2
9	5.6925E-22	2.9266E-02	8456.2	5.0977E-22	2.2910E-02	8097.3
10	5.7787E-22	3.0294E-02	8456.5	5.1156E-22	2.2626E-02	8060.7
11	5.8718E-22	3.1374E-02	8454.9	5.1380E-22	2.2394E-02	8022.4
12	5.9706E-22	3.2498E-02	8451.4	5.1650E-22	2.2206E-02	7982.5
13	6.0773E-22	3.3694E-02	8445.9	5.1973E-22	2.2061E-02	7941.0
14	6.1921E-22	3.4968E-02	8439.5	5.2341E-22	2.1949E-02	7897.8
15	6.3114E-22	3.6281E-02	8429.2	5.2743E-22	2.1857E-02	7853.0
16	6.4398E-22	3.7687E-02	8417.9	5.3214E-22	2.1811E-02	7806.6
17	6.5764E-22	3.9180E-02	8404.6	5.3724E-22	2.1792E-02	7758.7
18	6.7200E-22	4.0746E-02	8389.4	5.4281E-22	2.1776E-02	7709.2
19	6.8719E-22	4.2402E-02	8372.3	5.4902E-22	2.1806E-02	7658.2
20	7.0321E-22	4.4150E-02	8353.1	5.5569E-22	2.1853E-02	7605.7
21	7.2033E-22	4.6023E-02	8332.0	5.6292E-22	2.1924E-02	7551.6
22	7.3807E-22	4.7963E-02	8308.9	5.7054E-22	2.2004E-02	7496.1
23	7.5690E-22	5.0031E-02	8283.8	5.7894E-22	2.2121E-02	7439.1
24	7.7674E-22	5.2215E-02	8256.7	5.8787E-22	2.2255E-02	7380.7
25	7.9757E-22	5.4515E-02	8227.6	5.9738E-22	2.2407E-02	7320.8
26	8.1919E-22	5.6902E-02	8196.6	6.0743E-22	2.2572E-02	7259.5
27	8.4212E-22	5.9447E-02	8163.5	6.1836E-22	2.2774E-02	7196.8
28	8.6621E-22	6.2126E-02	8128.5	6.2990E-22	2.2991E-02	7132.7
29	8.9135E-22	6.4925E-02	8091.4	6.4204E-22	2.3220E-02	7067.3
30	9.1778E-22	6.7877E-02	8052.4	6.5493E-22	2.3469E-02	7000.5
31	9.4546E-22	7.0972E-02	8011.3	6.6864E-22	2.3741E-02	6932.3
32	9.7432E-22	7.4197E-02	7968.2	6.8308E-22	2.4028E-02	6862.8
33	1.0047E-21	7.7604E-02	7923.1	6.9852E-22	2.4345E-02	6792.0
34	1.0364E-21	8.1138E-02	7876.0	7.1470E-22	2.4672E-02	6719.9
35	1.0697E-21	8.4864E-02	7826.8	7.3203E-22	2.5033E-02	6646.5

MATRIX ELEMENTS, EINSTEIN A'S AND ENERGIES FOR V= 0 TO 4 TRANSITIONS OF HCL

J	R-BRANCH <V J/MU/V' J+1> ESU-CM	R-BRANCH A SEC-1	R-BRANCH F CM-1	P-BRANCH <V J/MU/V' J-1> ESU-CM	P-BRANCH A SEC-1	P-BRANCH F CM-1
0	4.0558E-23	2.2545E-04	10944.3			
1	4.1127E-23	2.4588E-04	10960.4	4.1002E-23	4.8381E-04	10904.9
2	4.0713E-23	2.8018E-04	10973.9	4.1147E-23	4.5619E-04	10881.7
3	4.0103E-23	2.9227E-04	10985.1	4.1071E-23	4.0615E-04	10856.0
4	3.9379E-23	2.7904E-04	10993.8	4.1056E-23	3.8353E-04	10827.9
5	3.7652E-23	2.7375E-04	11000.0	4.0993E-23	3.6972E-04	10797.5
6	3.6794E-23	2.6388E-04	11003.7	4.0720E-23	3.5387E-04	10764.7
7	3.5422E-23	2.4963E-04	11005.0	4.0416E-23	3.4079E-04	10729.7
8	3.4564E-23	2.3652E-04	11003.8	4.0192E-23	3.3033E-04	10692.2
9	3.3280E-23	2.2030E-04	11000.0	3.9673E-23	3.1594E-04	10652.5
10	3.1805E-23	2.0163E-04	10993.8	3.9179E-23	3.0272E-04	10610.6
11	3.0262E-23	1.8279E-04	10985.0	3.8742E-23	2.9091E-04	10566.7
12	2.8586E-23	1.6307E-04	10973.7	3.8069E-23	2.7610E-04	10519.8
13	2.6656E-23	1.4162E-04	10959.9	3.7294E-23	2.6044E-04	10471.1
14	2.4473E-23	1.1913E-04	10943.6	3.6560E-23	2.4596E-04	10420.1
15	2.2279E-23	9.9413E-05	10924.7	3.5808E-23	2.3178E-04	10367.0
16	1.9836E-23	7.7701E-05	10903.3	3.4393E-23	2.1611E-04	10311.7
17	1.7126E-23	5.7527E-05	10879.3	3.3950E-23	2.0081E-04	10254.2
18	1.4311E-23	4.0005E-05	10852.8	3.2908E-23	1.8509E-04	10194.6
19	1.1191E-23	2.4299E-05	10823.8	3.1691E-23	1.6830E-04	10132.9
20	7.8770E-24	1.1947E-05	10792.2	3.0600E-23	1.5376E-04	10069.1
21	4.2911E-24	3.5157E-06	10758.1	2.9371E-23	1.3873E-04	10003.2
22	4.2687E-25	3.5102E-08	10721.3	2.8019E-23	1.2355E-04	9935.2
23	-3.6273E-24	2.6638E-06	10682.1	2.6630E-23	1.0916E-04	9865.2
24	-8.0132E-24	1.1803E-05	10640.2	2.5060E-23	9.4476E-05	9793.2
25	-1.2788E-23	2.6935E-05	10595.8	2.3504E-23	8.1167E-05	9719.1
26	-1.7705E-23	5.6661E-05	10548.8	2.1928E-23	6.8947E-05	9643.0
27	-2.2086E-23	9.4219E-05	10499.3	2.0071E-23	5.6331E-05	9565.0
28	-2.8789E-23	1.4569E-04	10447.2	1.8123E-23	4.4752E-05	9485.0
29	-3.4843E-23	2.1020E-04	10392.5	1.6241E-23	3.4995E-05	9403.1
30	-4.1169E-23	2.9878E-04	10335.2	1.4245E-23	2.6193E-05	9319.2
31	-4.8239E-23	3.8983E-04	10275.3	1.1960E-23	1.7949E-05	9233.4
32	-5.5327E-23	5.0373E-04	10212.8	9.9007E-24	1.1947E-05	9145.6
33	-6.3142E-23	6.4392E-04	10147.6	7.3671E-24	6.4188E-06	9056.0
34	-7.1353E-23	8.0625E-04	10079.8	4.9061E-24	2.7599E-06	8964.4
35	-8.0119E-23	9.9577E-04	10009.6	2.2068E-24	5.4091E-07	8871.0

MATRIX ELEMENTS, EINSTEIN A'S AND ENERGIES FOR V= 0 TO 5 TRANSITIONS OF HCL

	R-BRANCH			P-BRANCH		
J	<V J/MU/V' J+1>	A	E	<V J/MU/V' J-1>	A	E
	ESU-CM	SEC-1	CM-1	ESU-CM	SEC-1	CM-1
0	-4.5740E-23	5.2652E-04	13418.6			
1	-4.5950E-23	6.4049E-04	13433.4	-4.5188E-23	1.5341E-03	13379.9
2	-4.6125E-23	6.9512E-04	13445.2	-4.5010E-23	1.0093E-03	13356.0
3	-4.6275E-23	7.3013E-04	13452.9	-4.4719E-23	8.9122E-04	13329.1
4	-4.6401E-23	7.5140E-04	13459.6	-4.4398E-23	8.3104E-04	13299.2
5	-4.6710E-23	7.7091E-04	13462.2	-4.4222E-23	7.9566E-04	13266.4
6	-4.6855E-23	7.8303E-04	13461.7	-4.3898E-23	7.6357E-04	13230.6
7	-4.6921E-23	7.9212E-04	13458.1	-4.3625E-23	7.3791E-04	13191.8
8	-4.7103E-23	8.0232E-04	13451.4	-4.3387E-23	7.1609E-04	13150.2
9	-4.7173E-23	8.0737E-04	13441.7	-4.3039E-23	6.9239E-04	13105.6
10	-4.7169E-23	8.0825E-04	13428.8	-4.2753E-23	6.7188E-04	13058.2
11	-4.7271E-23	8.1178E-04	13412.8	-4.2553E-23	6.5480E-04	13007.9
12	-4.7256E-23	8.1031E-04	13393.7	-4.2109E-23	6.3359E-04	12954.8
13	-4.7207E-23	8.0674E-04	13371.5	-4.1858E-23	6.1329E-04	12898.8
14	-4.7104E-23	8.0059E-04	13346.1	-4.1598E-23	5.9575E-04	12840.1
15	-4.6980E-23	7.9283E-04	13317.7	-4.1317E-23	5.7790E-04	12778.5
16	-4.6787E-23	7.8213E-04	13286.1	-4.0990E-23	5.5904E-04	12714.3
17	-4.6586E-23	7.7060E-04	13251.4	-4.0722E-23	5.4205E-04	12647.7
18	-4.6327E-23	7.5660E-04	13213.5	-4.0340E-23	5.2228E-04	12577.4
19	-4.5957E-23	7.3960E-04	13172.5	-3.9989E-23	5.0366E-04	12504.9
20	-4.5527E-23	7.1875E-04	13129.4	-3.9713E-23	4.8717E-04	12429.8
21	-4.5154E-23	6.9583E-04	13081.1	-3.9415E-23	4.7035E-04	12351.9
22	-4.4570E-23	6.7463E-04	13030.7	-3.8998E-23	4.5101E-04	12271.4
23	-4.3953E-23	6.4979E-04	12977.1	-3.8693E-23	4.3458E-04	12188.2
24	-4.3314E-23	6.2217E-04	12920.4	-3.8287E-23	4.1619E-04	12102.5
25	-4.2543E-23	5.9234E-04	12960.5	-3.7953E-23	3.9974E-04	12014.1
26	-4.1607E-23	5.5866E-04	12797.4	-3.7541E-23	3.8198E-04	11923.2
27	-4.0696E-23	5.2657E-04	12731.1	-3.7144E-23	3.6495E-04	11829.6
28	-3.9568E-23	4.9049E-04	12661.7	-3.6708E-23	3.4759E-04	11733.6
29	-3.8345E-23	4.5254E-04	12589.1	-3.6306E-23	3.3130E-04	11634.9
30	-3.7152E-23	4.1742E-04	12513.3	-3.5917E-23	3.1568E-04	11533.7
31	-3.5582E-23	3.7595E-04	12434.3	-3.5369E-23	2.9776E-04	11430.0
32	-3.4103E-23	3.3861E-04	12352.1	-3.5015E-23	2.8363E-04	11323.8
33	-3.2417E-23	2.9978E-04	12266.6	-3.4486E-23	2.6714E-04	11215.0
34	-3.0506E-23	2.5998E-04	12177.9	-3.3972E-23	2.5149E-04	11103.7
35	-2.8504E-23	2.2186E-04	12085.9	-3.3509E-23	2.3714E-04	10990.0

MATRIX ELEMENTS, EINSTEIN A'S AND ENERGIES FOR V= 1 TO 1 TRANSITIONS OF HCL

Pure Rotation

J	<V J/MU/V' J+1>	A	E
	ESU-CM	SEC-1	CM-1
0	1.1384E-18	1.1309E-03	20.3
1	1.1385E-18	1.0935E-03	40.5
2	1.1388E-18	2.9164E-03	60.9
3	1.1393E-18	9.5113E-03	81.0
4	1.1398E-18	1.9156E-01	101.1
5	1.1405E-18	3.2534E-01	121.2
6	1.1412E-18	5.3721E-01	141.2
7	1.1421E-18	8.3589E-01	161.2
8	1.1432E-18	1.1512E 00	181.3
9	1.1443E-18	1.5813E 00	200.7
10	1.1456E-18	2.1049E 00	220.3
11	1.1469E-18	2.7209E 00	239.8
12	1.1485E-18	3.4635E 00	259.1
13	1.1501E-18	4.3139E 00	278.2
14	1.1518E-18	5.2964E 00	297.2
15	1.1537E-18	6.3879E 00	316.0
16	1.1557E-18	7.6238E 00	334.6
17	1.1578E-18	8.9995E 00	353.0
18	1.1601E-18	1.0519E 01	371.2
19	1.1624E-18	1.2187E 01	389.2
20	1.1648E-18	1.4005E 01	406.9
21	1.1675E-18	1.5976E 01	424.4
22	1.1703E-18	1.8105E 01	441.6
23	1.1731E-18	2.0360E 01	458.4
24	1.1761E-18	2.2821E 01	475.3
25	1.1792E-18	2.5433E 01	491.7
26	1.1825E-18	2.8196E 01	507.8
27	1.1858E-18	3.1007E 01	523.6
28	1.1893E-18	3.4167E 01	539.0
29	1.1929E-18	3.7373E 01	554.2
30	1.1967E-18	4.0729E 01	569.1
31	1.2006E-18	4.4230E 01	583.6
32	1.2046E-18	4.7862E 01	597.7
33	1.2087E-18	5.1629E 01	611.5
34	1.2129E-18	5.5520E 01	624.9
35	1.2173E-18	5.9524E 01	638.0

MATRIX ELEMENTS, EINSTEIN A'S AND ENERGIES FOR V= 1 TO 2 TRANSITIONS OF HCL

J	R-BRANCH <V J/MU/V° J+1>	R-BRANCH A	R-BRANCH E	P-BRANCH <V J/MU/V° J-1>	P-BRANCH A	P-BRANCH E
	ESU-CM	SEC-1	CM-1	ESU-CM	SEC-1	CM-1
0	9.7948E-20	2.2073E 01	2802.3			
1	9.6577E-20	2.6280E 01	2821.3	1.0071E-19	6.7052E 01	2762.3
2	9.5212E-20	2.7007E 01	2839.8	1.0210E-19	4.4911E 01	2741.5
3	9.3860E-20	2.8650E 01	2857.5	1.0350E-19	4.0567E 01	2720.0
4	9.2494E-20	2.8375E 01	2874.7	1.0490E-19	3.8736E 01	2698.0
5	9.1141E-20	2.8061E 01	2891.1	1.0632E-19	3.7719E 01	2675.4
6	8.9791E-20	2.8090E 01	2906.9	1.0774E-19	3.7054E 01	2652.3
7	8.8443E-20	2.8806E 01	2922.0	1.0917E-19	3.6563E 01	2628.7
8	8.7097E-20	2.8638E 01	2936.5	1.1061E-19	3.6162E 01	2604.5
9	8.5751E-20	2.8300E 01	2950.2	1.1206E-19	3.5807E 01	2579.9
10	8.4405E-20	2.7904E 01	2963.1	1.1352E-19	3.5474E 01	2554.8
11	8.3058E-20	2.7359E 01	2975.4	1.1499E-19	3.5147E 01	2529.2
12	8.1709E-20	2.6868E 01	2986.9	1.1647E-19	3.4816E 01	2503.1
13	8.0357E-20	2.6338E 01	2997.7	1.1796E-19	3.4476E 01	2476.6
14	7.9001E-20	2.5772E 01	3007.7	1.1947E-19	3.4120E 01	2449.6
15	7.7641E-20	2.5172E 01	3016.9	1.2098E-19	3.3747E 01	2422.2
16	7.6273E-20	2.4542E 01	3025.4	1.2251E-19	3.3354E 01	2394.4
17	7.4900E-20	2.3885E 01	3033.0	1.2404E-19	3.2940E 01	2366.3
18	7.3517E-20	2.3201E 01	3039.9	1.2559E-19	3.2505E 01	2337.7
19	7.2125E-20	2.2493E 01	3046.0	1.2715E-19	3.2047E 01	2308.8
20	7.0721E-20	2.1764E 01	3051.2	1.2872E-19	3.1567E 01	2279.5
21	6.9305E-20	2.1014E 01	3055.7	1.3030E-19	3.1066E 01	2249.9
22	6.7875E-20	2.0247E 01	3059.3	1.3190E-19	3.0542E 01	2219.9
23	6.6429E-20	1.9464E 01	3062.0	1.3350E-19	2.9997E 01	2189.7
24	6.4969E-20	1.8665E 01	3064.0	1.3512E-19	2.9432E 01	2159.1
25	6.3492E-20	1.7855E 01	3065.0	1.3675E-19	2.8847E 01	2128.2
26	6.1997E-20	1.7034E 01	3065.3	1.3839E-19	2.8241E 01	2097.0
27	6.0485E-20	1.6205E 01	3064.6	1.4004E-19	2.7619E 01	2065.6
28	5.8957E-20	1.5370E 01	3063.1	1.4170E-19	2.6978E 01	2033.9
29	5.7411E-20	1.4530E 01	3060.7	1.4338E-19	2.6322E 01	2002.0
30	5.5850E-20	1.3687E 01	3057.4	1.4506E-19	2.5651E 01	1969.8
31	5.4272E-20	1.2846E 01	3053.2	1.4675E-19	2.4965E 01	1937.4
32	5.2678E-20	1.2005E 01	3048.1	1.4846E-19	2.4266E 01	1904.8
33	5.1066E-20	1.1170E 01	3042.1	1.5017E-19	2.3557E 01	1872.0
34	4.9436E-20	1.0341E 01	3035.2	1.5189E-19	2.2837E 01	1838.9
35	4.7788E-20	9.5219E 00	3027.4	1.5363E-19	2.2108E 01	1805.7

MATRIX ELEMENTS, EINSTEIN A'S AND ENERGIES FOR V= 1 TO 3 TRANSITIONS OF HCL

J	P-BRANCH <V J/MU/V' J-1> ESU-CM	P-BRANCH A SEC-1	P-BRANCH E CM-1	<V J/MU/V' J-1> ESU-CM	A SEC-1	E CM-1
0	-1.4253E-20	3.4972E 00	5481.0			
1	-1.4215E-20	4.2153E 00	5498.9	-1.4343E-20	1.0398E 01	5441.7
2	-1.4182E-20	4.5364E 00	5515.5	-1.4396E-20	6.9009E 00	5420.2
3	-1.4154E-20	4.7249E 00	5530.9	-1.4454E-20	6.1825E 00	5397.5
4	-1.4130E-20	4.8534E 00	5545.0	-1.4517E-20	5.8614E 00	5373.7
5	-1.4112E-20	4.9403E 00	5557.8	-1.4585E-20	5.6725E 00	5348.8
6	-1.4098E-20	5.0256E 00	5569.4	-1.4659E-20	5.5438E 00	5322.6
7	-1.4088E-20	5.0893E 00	5579.7	-1.4738E-20	5.4474E 00	5295.4
8	-1.4082E-20	5.1440E 00	5588.7	-1.4823E-20	5.3704E 00	5267.0
9	-1.4080E-20	5.1927E 00	5596.5	-1.4913E-20	5.3063E 00	5237.6
10	-1.4080E-20	5.2365E 00	5602.9	-1.5009E-20	5.2505E 00	5207.1
11	-1.4082E-20	5.2765E 00	5607.9	-1.5111E-20	5.2009E 00	5175.5
12	-1.4113E-20	5.3136E 00	5611.7	-1.5220E-20	5.1560E 00	5142.8
13	-1.4128E-20	5.3482E 00	5614.1	-1.5334E-20	5.1144E 00	5109.1
14	-1.4151E-20	5.3805E 00	5615.1	-1.5455E-20	5.0756E 00	5074.4
15	-1.4179E-20	5.4111E 00	5614.8	-1.5582E-20	5.0389E 00	5038.6
16	-1.4209E-20	5.4400E 00	5613.1	-1.5716E-20	5.0038E 00	5001.9
17	-1.4245E-20	5.4671E 00	5610.1	-1.5857E-20	4.9701E 00	4964.2
18	-1.4285E-20	5.4929E 00	5605.7	-1.6005E-20	4.9379E 00	4925.5
19	-1.4330E-20	5.5174E 00	5599.9	-1.6161E-20	4.9063E 00	4885.9
20	-1.4379E-20	5.5401E 00	5592.7	-1.6324E-20	4.8756E 00	4845.3
21	-1.4433E-20	5.5615E 00	5584.2	-1.6495E-20	4.8458E 00	4803.8
22	-1.4490E-20	5.5812E 00	5574.2	-1.6674E-20	4.8163E 00	4761.5
23	-1.4551E-20	5.5993E 00	5562.8	-1.6862E-20	4.7874E 00	4718.2
24	-1.4617E-20	5.6159E 00	5550.0	-1.7059E-20	4.7591E 00	4674.0
25	-1.4687E-20	5.6306E 00	5535.8	-1.7264E-20	4.7309E 00	4629.0
26	-1.4761E-20	5.6434E 00	5520.1	-1.7479E-20	4.7030E 00	4583.1
27	-1.4839E-20	5.6544E 00	5503.1	-1.7704E-20	4.6756E 00	4536.4
28	-1.4921E-20	5.6636E 00	5484.5	-1.7940E-20	4.6481E 00	4488.8
29	-1.5007E-20	5.6694E 00	5464.6	-1.8186E-20	4.6209E 00	4440.4
30	-1.5097E-20	5.6733E 00	5443.2	-1.8443E-20	4.5938E 00	4391.3
31	-1.5191E-20	5.6744E 00	5420.3	-1.8712E-20	4.5668E 00	4341.3
32	-1.5288E-20	5.6727E 00	5396.0	-1.8994E-20	4.5399E 00	4290.6
33	-1.5388E-20	5.6681E 00	5370.2	-1.9288E-20	4.5129E 00	4239.0
34	-1.5492E-20	5.6599E 00	5342.9	-1.9596E-20	4.4859E 00	4186.8
35	-1.5598E-20	5.6482E 00	5314.1	-1.9919E-20	4.4589E 00	4133.7

MATRIX ELEMENTS, EINSTEIN A'S AND ENERGIES FOR V= 1 TO 4 TRANSITIONS OF HCL

J	P-BRANCH <V J/MU/V' J+1> ESU-CM	P-BRANCH A SEC-1	P-BRANCH E CM-1	P-BRANCH <V J/MU/V' J-1> ESU-CM	P-BRANCH A SEC-1	P-BRANCH E CM-1
0	1.2495E-21	8.5383E-02	8057.3			
1	1.2571E-21	1.0436E-01	8073.9	1.2376E-21	2.4767E-01	8018.5
2	1.2657E-21	1.1397E-01	8089.7	1.2331E-21	1.6258E-01	7996.5
3	1.2756E-21	1.2063E-01	8101.7	1.2298E-21	1.4423E-01	7972.6
4	1.2864E-21	1.2599E-01	8112.8	1.2272E-21	1.3548E-01	7947.0
5	1.2985E-21	1.3077E-01	8122.1	1.2260E-21	1.3010E-01	7919.6
6	1.3118E-21	1.3533E-01	8129.5	1.2257E-21	1.2627E-01	7890.5
7	1.3262E-21	1.3979E-01	8135.0	1.2262E-21	1.2330E-01	7859.6
8	1.3420E-21	1.4425E-01	8138.6	1.2279E-21	1.2093E-01	7827.1
9	1.3590E-21	1.4879E-01	8140.3	1.2305E-21	1.1898E-01	7792.8
10	1.3774E-21	1.5350E-01	8140.1	1.2342E-21	1.1737E-01	7756.9
11	1.3969E-21	1.5835E-01	8138.0	1.2388E-21	1.1598E-01	7719.3
12	1.4180E-21	1.6342E-01	8134.0	1.2445E-21	1.1482E-01	7680.1
13	1.4406E-21	1.6874E-01	8128.0	1.2514E-21	1.1386E-01	7639.2
14	1.4646E-21	1.7432E-01	8120.2	1.2591E-21	1.1303E-01	7596.7
15	1.4900E-21	1.8011E-01	8110.3	1.2677E-21	1.1233E-01	7552.6
16	1.5173E-21	1.8629E-01	8098.5	1.2779E-21	1.1183E-01	7506.9
17	1.5459E-21	1.9270E-01	8084.9	1.2887E-21	1.1140E-01	7459.7
18	1.5763E-21	1.9948E-01	8069.1	1.3010E-21	1.1114E-01	7410.9
19	1.6085E-21	2.0661E-01	8051.5	1.3144E-21	1.1097E-01	7360.6
20	1.6424E-21	2.1409E-01	8031.8	1.3289E-21	1.1090E-01	7308.7
21	1.6783E-21	2.2200E-01	8010.3	1.3447E-21	1.1096E-01	7255.4
22	1.7158E-21	2.3022E-01	7986.7	1.3617E-21	1.1109E-01	7200.6
23	1.7556E-21	2.3891E-01	7961.1	1.3802E-21	1.1136E-01	7144.2
24	1.7976E-21	2.4810E-01	7933.5	1.4001E-21	1.1173E-01	7086.5
25	1.8413E-21	2.5760E-01	7904.0	1.4211E-21	1.1215E-01	7027.3
26	1.8875E-21	2.6764E-01	7872.4	1.4440E-21	1.1273E-01	6966.6
27	1.9360E-21	2.7817E-01	7838.8	1.4682E-21	1.1337E-01	6904.6
28	1.9869E-21	2.8916E-01	7803.2	1.4940E-21	1.1411E-01	6841.1
29	2.0401E-21	3.0067E-01	7765.6	1.5216E-21	1.1496E-01	6776.2
30	2.0961E-21	3.1274E-01	7726.0	1.5510E-21	1.1591E-01	6710.0
31	2.1546E-21	3.2527E-01	7684.3	1.5823E-21	1.1696E-01	6642.4
32	2.2161E-21	3.3842E-01	7640.5	1.6156E-21	1.1812E-01	6573.4
33	2.2804E-21	3.5209E-01	7594.7	1.6510E-21	1.1937E-01	6503.0
34	2.3479E-21	3.6637E-01	7546.9	1.6888E-21	1.2076E-01	6431.3
35	2.4186E-21	3.8124E-01	7496.8	1.7289E-21	1.2224E-01	6358.3

MATRIX ELEMENTS, EINSTEIN A'S AND ENERGIES FOR V= 1 TO 5 TRANSITIONS OF HCL

	P-BRANCH			P-BRANCH		
J	<V J/MU/V' J+1>	A	E	<V J/MU/V' J-1>	A	E
	ESU-CM	SEC-1	CM-1	ESU-CM	SEC-1	CM-1
0	3.3088E-23	1.3371E-04	10531.6			
1	3.1767E-23	1.4854E-04	10547.0	3.4983E-23	4.4354E-04	10493.4
2	3.0388E-23	1.4619E-04	10560.0	3.5722E-23	3.0631E-04	10470.8
3	2.8962E-23	1.3338E-04	10570.6	3.6053E-23	2.7981E-04	10445.7
4	2.7500E-23	1.1951E-04	10578.6	3.6464E-23	2.6948E-04	10418.2
5	2.6052E-23	1.0180E-04	10584.3	3.6423E-23	2.5917E-04	10388.4
6	2.1740E-23	8.2101E-05	10587.4	3.6316E-23	2.5063E-04	10356.3
7	1.8012E-23	6.2666E-05	10588.1	3.6076E-23	2.4172E-04	10321.8
8	1.5744E-23	4.3690E-05	10586.3	3.5614E-23	2.3084E-04	10285.0
9	1.2346E-23	2.6375E-05	10582.0	3.5068E-23	2.1965E-04	10245.9
10	8.5010E-24	1.2821E-05	10575.1	3.4208E-23	2.0528E-04	10204.6
11	4.3431E-24	3.3806E-06	10565.9	3.3254E-23	1.9060E-04	10160.9
12	-1.0914E-25	2.1147E-09	10554.0	3.2112E-23	1.7465E-04	10115.1
13	-5.1507E-24	4.7196E-06	10539.6	3.0685E-23	1.5668E-04	10067.0
14	-1.0572E-23	1.9763E-05	10522.7	2.9312E-23	1.4044E-04	10016.7
15	-1.6224E-23	4.6382E-05	10503.3	2.7739E-23	1.2349E-04	9964.2
16	-2.2579E-23	8.9436E-05	10481.3	2.5720E-23	1.0421E-04	9909.5
17	-2.9384E-23	1.5044E-04	10456.8	2.3793E-23	8.7492E-05	9852.7
18	-3.6609E-23	2.3236E-04	10429.8	2.1651E-23	7.1031E-05	9793.7
19	-4.4350E-23	3.3854E-04	10400.2	1.9149E-23	5.4451E-05	9732.6
20	-5.2709E-23	4.7593E-04	10368.0	1.6483E-23	3.9506E-05	9669.4
21	-6.1799E-23	6.4616E-04	10333.3	1.3770E-23	2.6987E-05	9604.1
22	-7.1344E-23	8.5273E-04	10296.0	1.0725E-23	1.6012E-05	9536.7
23	-8.1640E-23	1.1047E-03	10256.1	7.4363E-24	7.5225E-06	9467.3
24	-9.2743E-23	1.4091E-03	10213.7	4.0168E-24	2.1436E-06	9395.8
25	-1.0435E-22	1.7617E-03	10168.6	4.0853E-25	2.1638E-08	9322.3
26	-1.1696E-22	2.1798E-03	10121.0	-3.6065E-24	1.6443E-06	9246.8
27	-1.3011E-22	2.6639E-03	10070.7	-7.7579E-24	7.4136E-06	9169.2
28	-1.4432E-22	3.2285E-03	10017.8	-1.2311E-23	1.8176E-05	9089.6
29	-1.5940E-22	3.8754E-03	9962.3	-1.7031E-23	3.3835E-05	9008.1
30	-1.7551E-22	4.6189E-03	9904.1	-2.2152E-23	5.5629E-05	8924.5
31	-1.9264E-22	5.4655E-03	9843.3	-2.7580E-23	8.3732E-05	8839.0
32	-2.1084E-22	6.4236E-03	9779.8	-3.3265E-23	1.1816E-04	8751.5
33	-2.3017E-22	7.5047E-03	9713.6	-3.9422E-23	1.6084E-04	8662.1
34	-2.5090E-22	8.7327E-03	9644.8	-4.6058E-23	2.1258E-04	8570.6
35	-2.7280E-22	1.0099E-02	9573.1	-5.2886E-23	2.7110E-04	8477.2

MATRIX ELEMENTS, EINSTEIN A'S AND ENERGIES FOR V= 1 TO 6 TRANSITIONS OF HCL

	P-BRANCH			P-BRANCH		
J	<V J/MU/V' J+1>	A	E	<V J/MU/V' J-1>	A	E
	ESU-CM	SEC-1	CM-1	ESU-CM	SEC-1	CM-1
0	-9.3900E-23	1.9808E-03	12904.0			
1	-9.4242E-23	2.4022E-03	12918.2	-9.3111E-23	5.7922E-03	12866.5
2	-9.4422E-23	2.6014E-03	12929.4	-9.2766E-23	3.8121E-03	12843.2
3	-9.4851E-23	2.7150E-03	12937.4	-9.2259E-23	3.3727E-03	12816.9
4	-9.5150E-23	2.7983E-03	12942.4	-9.1812E-23	3.1593E-03	12787.6
5	-9.5315E-23	2.8525E-03	12944.3	-9.1317E-23	3.0155E-03	12755.3
6	-9.5459E-23	2.8922E-03	12943.1	-9.0853E-23	2.9065E-03	12720.1
7	-9.5533E-23	2.9181E-03	12938.9	-9.0303E-23	2.8091E-03	12681.8
8	-9.5594E-23	2.9360E-03	12931.5	-8.9826E-23	2.7263E-03	12640.7
9	-9.5642E-23	2.9412E-03	12921.0	-8.9274E-23	2.6453E-03	12596.7
10	-9.5625E-23	2.9375E-03	12907.4	-8.8759E-23	2.5707E-03	12549.8
11	-9.5190E-23	2.9222E-03	12890.7	-8.8181E-23	2.4952E-03	12500.0
12	-9.4941E-23	2.9026E-03	12870.9	-8.7596E-23	2.4217E-03	12447.4
13	-9.4500E-23	2.8679E-03	12848.0	-8.6956E-23	2.3468E-03	12391.9
14	-9.3989E-23	2.8262E-03	12822.0	-8.6383E-23	2.2769E-03	12333.6
15	-9.3354E-23	2.7748E-03	12792.9	-8.5751E-23	2.2052E-03	12272.6
16	-9.2624E-23	2.7157E-03	12760.5	-8.5105E-23	2.1338E-03	12208.7
17	-9.1825E-23	2.6546E-03	12725.1	-8.4377E-23	2.0593E-03	12142.2
18	-9.0650E-23	2.5630E-03	12686.5	-8.3795E-23	1.9931E-03	12072.9
19	-8.9516E-23	2.4788E-03	12644.8	-8.3023E-23	1.9188E-03	12000.8
20	-8.8045E-23	2.3753E-03	12599.9	-8.2194E-23	1.8433E-03	11926.1
21	-8.6532E-23	2.2706E-03	12551.8	-8.1527E-23	1.7763E-03	11848.7
22	-8.4740E-23	2.1541E-03	12500.6	-8.0665E-23	1.7020E-03	11768.6
23	-8.2904E-23	2.0310E-03	12446.2	-7.9871E-23	1.6321E-03	11685.8
24	-8.0683E-23	1.9031E-03	12388.7	-7.9086E-23	1.5538E-03	11600.4
25	-7.8233E-23	1.7644E-03	12327.9	-7.8174E-23	1.4922E-03	11512.4
26	-7.5609E-23	1.6236E-03	12263.8	-7.7331E-23	1.4248E-03	11421.7
27	-7.2749E-23	1.4795E-03	12196.6	-7.6409E-23	1.3563E-03	11328.4
28	-6.9490E-23	1.3274E-03	12126.1	-7.5362E-23	1.2852E-03	11232.5
29	-6.5980E-23	1.1757E-03	12052.3	-7.4375E-23	1.2184E-03	11134.0
30	-6.2152E-23	1.0239E-03	11975.2	-7.3308E-23	1.1510E-03	11032.8
31	-5.7807E-23	8.6841E-04	11894.8	-7.2134E-23	1.0927E-03	10929.0
32	-5.3269E-23	7.2229E-04	11811.0	-7.1043E-23	1.0193E-03	10822.6
33	-4.8223E-23	5.7918E-04	11723.9	-6.9736E-23	9.5230E-04	10713.5
34	-4.2643E-23	4.4268E-04	11633.4	-6.8449E-23	8.8867E-04	10601.8
35	-3.6744E-23	3.2090E-04	11539.4	-6.7155E-23	8.2764E-04	10487.5

MATRIX ELEMENTS, EINSTEIN A'S AND ENERGIES FOR V= 2 TO 2 TRANSITIONS OF HCL

Pure Rotation

I	<V J/MU/V' J+1>	A	E
	ESU-CM	SEC-1	CM-1
0	1.1[illegible]E-18	1.0945E-03	19.7
1	1.1[illegible]E-18	1.0411E-03	39.3
2	1.1[illegible]E-18	9.7579E-02	58.0
3	1.1[illegible]E-18	9.2225E-02	78.6
4	1.1[illegible]E-18	1.8301E-01	98.1
5	1.1[illegible]E-18	3.2203E-01	117.6
6	1.1701E-18	5.1547E-01	137.0
7	1.1710E-18	7.7348E-01	156.3
8	1.1720E-18	1.1045E 00	175.6
9	1.1731E-18	1.5163E 00	194.7
10	1.1743E-18	2.0194E 00	213.7
11	1.1757E-18	2.6173E 00	232.6
12	1.1771E-18	3.3137E 00	251.3
13	1.1787E-18	4.1137E 00	269.9
14	1.1804E-18	5.0637E 00	288.2
15	1.1822E-18	6.1165E 00	306.4
16	1.1842E-18	7.2983E 00	324.5
17	1.1862E-18	8.6105E 00	342.3
18	1.1884E-18	1.0061E 01	359.9
19	1.1907E-18	1.1650E 01	377.3
20	1.1931E-18	1.3382E 01	394.4
21	1.1957E-18	1.5258E 01	411.3
22	1.1983E-18	1.7281E 01	428.0
23	1.2011E-18	1.9450E 01	444.4
24	1.2040E-18	2.1765E 01	460.5
25	1.2070E-18	2.4229E 01	476.3
26	1.2101E-18	2.6833E 01	491.9
27	1.2134E-18	2.9582E 01	507.1
28	1.2167E-18	3.2471E 01	522.0
29	1.2202E-18	3.5494E 01	536.6
30	1.2238E-18	3.8651E 01	550.9
31	1.2275E-18	4.1936E 01	564.9
32	1.2313E-18	4.5334E 01	578.5
33	1.2352E-18	4.8856E 01	591.7
34	1.2392E-18	5.2477E 01	604.5
35	1.2434E-18	5.6196E 01	617.1

MATRIX ELEMENTS, EINSTEIN A'S AND ENERGIES FOR V= 2 TO 3 TRANSITIONS OF HCL

	P-BRANCH			R-BRANCH		
J	<V J/MU/V' J+1>	A	E	<V J/MU/V' J-1>	A	E
	ESU-CM	SEC-1	CM-1	ESU-CM	SEC-1	CM-1
0	1.1753E-19	2.8375E 01	2698.4			
1	1.1580E-19	3.3737E 01	2716.9	1.2100E-19	8.6403E 01	2659.7
2	1.1407E-19	3.5770E 01	2734.7	1.2275E-19	5.7932E 01	2639.4
3	1.1234E-19	3.6664E 01	2751.9	1.2450E-19	5.2377E 01	2618.6
4	1.1062E-19	3.7014E 01	2768.4	1.2626E-19	5.0054E 01	2597.2
5	1.0889E-19	3.7052E 01	2784.3	1.2802E-19	4.9776E 01	2575.2
6	1.0717E-19	3.6884E 01	2799.5	1.2980E-19	4.7945E 01	2552.7
7	1.0544E-19	3.6570E 01	2814.0	1.3158E-19	4.7332E 01	2529.7
8	1.0372E-19	3.6143E 01	2827.9	1.3336E-19	4.6836E 01	2506.2
9	1.0199E-19	3.5624E 01	2841.0	1.3516E-19	4.6389E 01	2482.1
10	1.0025E-19	3.5027E 01	2853.4	1.3697E-19	4.5969E 01	2457.6
11	9.8513E-20	3.4364E 01	2865.1	1.3878E-19	4.5553E 01	2432.6
12	9.6767E-20	3.3642E 01	2876.0	1.4061E-19	4.5126E 01	2407.2
13	9.5014E-20	3.2867E 01	2886.2	1.4244E-19	4.4683E 01	2381.3
14	9.3250E-20	3.2043E 01	2895.7	1.4428E-19	4.4216E 01	2354.9
15	9.1477E-20	3.1177E 01	2904.4	1.4614E-19	4.3723E 01	2328.2
16	8.9691E-20	3.0271E 01	2912.3	1.4800E-19	4.3201E 01	2301.0
17	8.7891E-20	2.9328E 01	2919.4	1.4987E-19	4.2647E 01	2273.4
18	8.6075E-20	2.8353E 01	2925.7	1.5176E-19	4.2063E 01	2245.5
19	8.4242E-20	2.7348E 01	2931.2	1.5365E-19	4.1446E 01	2217.2
20	8.2390E-20	2.6315E 01	2936.0	1.5555E-19	4.0798E 01	2188.5
21	8.0517E-20	2.5259E 01	2939.8	1.5747E-19	4.0118E 01	2159.5
22	7.8620E-20	2.4182E 01	2942.9	1.5939E-19	3.9408E 01	2130.2
23	7.6697E-20	2.3086E 01	2945.1	1.6132E-19	3.8666E 01	2100.5
24	7.4747E-20	2.1976E 01	2946.5	1.6326E-19	3.7896E 01	2070.5
25	7.2765E-20	2.0853E 01	2947.1	1.6521E-19	3.7099E 01	2040.3
26	7.0750E-20	1.9722E 01	2946.8	1.6717E-19	3.6273E 01	2009.7
27	6.8699E-20	1.8585E 01	2945.6	1.6914E-19	3.5423E 01	1978.9
28	6.6609E-20	1.7445E 01	2943.5	1.7112E-19	3.4550E 01	1947.8
29	6.4476E-20	1.6305E 01	2940.5	1.7310E-19	3.3654E 01	1916.4
30	6.2298E-20	1.5171E 01	2936.7	1.7509E-19	3.2737E 01	1884.8
31	6.0069E-20	1.4044E 01	2932.0	1.7708E-19	3.1801E 01	1853.0
32	5.7787E-20	1.2928E 01	2926.3	1.7908E-19	3.0847E 01	1820.9
33	5.5447E-20	1.1827E 01	2919.8	1.8108E-19	2.9876E 01	1788.6
34	5.3045E-20	1.0746E 01	2912.2	1.8309E-19	2.8897E 01	1756.1
35	5.0575E-20	9.6877E 00	2903.8	1.8509E-19	2.7902E 01	1723.4

MATRIX ELEMENTS, EINSTEIN A'S AND ENERGIES FOR V= 2 TO 4 TRANSITIONS OF HCL

J	R-BRANCH <V J/MU/V' J+1> ESU-CM	R-BRANCH A SEC-1	R-BRANCH E CM-1	P-BRANCH <V J/MU/V' J-1> ESU-CM	P-BRANCH A SEC-1	P-BRANCH E CM-1
0	-2.1402E-20	7.0323E 00	5274.7			
1	-2.1346E-20	8.4714E 00	5291.9	-2.1557E-20	2.0929E 01	5236.5
2	-2.1290E-20	9.1113E 00	5307.9	-2.1642E-20	1.8806E 01	5215.7
3	-2.1240E-20	9.4839E 00	5322.7	-2.1734E-20	1.7454E 01	5193.6
4	-2.1198E-20	9.7348E 00	5336.3	-2.1834E-20	1.1811E 01	5170.4
5	-2.1162E-20	9.9198E 00	5348.6	-2.1942E-20	1.1433E 01	5146.1
6	-2.1132E-20	1.0064E 01	5359.4	-2.2058E-20	1.1176E 01	5120.6
7	-2.1111E-20	1.0183E 01	5369.3	-2.2182E-20	1.0984E 01	5093.9
8	-2.1096E-20	1.0283E 01	5377.7	-2.2314E-20	1.0831E 01	5066.2
9	-2.1087E-20	1.0370E 01	5384.8	-2.2455E-20	1.0702E 01	5037.4
10	-2.1084E-20	1.0447E 01	5390.7	-2.2604E-20	1.0591E 01	5007.5
11	-2.1088E-20	1.0515E 01	5395.2	-2.2762E-20	1.0491E 01	4976.5
12	-2.1098E-20	1.0576E 01	5398.4	-2.2930E-20	1.0401E 01	4944.4
13	-2.1115E-20	1.0632E 01	5400.2	-2.3107E-20	1.0317E 01	4911.4
14	-2.1139E-20	1.0682E 01	5400.7	-2.3293E-20	1.0237E 01	4877.3
15	-2.1167E-20	1.0729E 01	5399.9	-2.3489E-20	1.0163E 01	4842.1
16	-2.1202E-20	1.0770E 01	5397.7	-2.3696E-20	1.0091E 01	4806.0
17	-2.1244E-20	1.0808E 01	5394.1	-2.3913E-20	1.0021E 01	4769.0
18	-2.1291E-20	1.0842E 01	5389.1	-2.4141E-20	9.9541E 00	4730.9
19	-2.1344E-20	1.0871E 01	5382.8	-2.4380E-20	9.8894E 00	4691.9
20	-2.1404E-20	1.0898E 01	5375.1	-2.4631E-20	9.8243E 00	4651.9
21	-2.1469E-20	1.0920E 01	5365.9	-2.4894E-20	9.7611E 00	4611.1
22	-2.1539E-20	1.0937E 01	5355.4	-2.5170E-20	9.6989E 00	4569.3
23	-2.1616E-20	1.0951E 01	5343.4	-2.5459E-20	9.6376E 00	4526.6
24	-2.1697E-20	1.0961E 01	5330.1	-2.5761E-20	9.5766E 00	4483.0
25	-2.1785E-20	1.0966E 01	5315.3	-2.6078E-20	9.5165E 00	4438.6
26	-2.1877E-20	1.0965E 01	5299.0	-2.6409E-20	9.4565E 00	4393.2
27	-2.1975E-20	1.0961E 01	5281.4	-2.6756E-20	9.3970E 00	4347.1
28	-2.2077E-20	1.0950E 01	5262.2	-2.7119E-20	9.3374E 00	4300.0
29	-2.2185E-20	1.0933E 01	5241.6	-2.7499E-20	9.2783E 00	4252.2
30	-2.2297E-20	1.0911E 01	5219.5	-2.7897E-20	9.2192E 00	4203.5
31	-2.2414E-20	1.0882E 01	5195.9	-2.8314E-20	9.1600E 00	4154.0
32	-2.2534E-20	1.0846E 01	5170.9	-2.8750E-20	9.1008E 00	4103.7
33	-2.2659E-20	1.0803E 01	5144.3	-2.9207E-20	9.0414E 00	4052.6
34	-2.2787E-20	1.0752E 01	5116.2	-2.9686E-20	8.9817E 00	4000.7
35	-2.2919E-20	1.0693E 01	5086.5	-3.0188E-20	8.9219E 00	3948.0

MATRIX ELEMENTS, EINSTEIN A'S AND ENERGIES FOR V= 2 TO 5 TRANSITIONS OF HCL

J	P-BRANCH <V J/MU/V' J+1> ESU-CM	P-BRANCH A SEC-1	P-BRANCH E CM-1	R-BRANCH <V J/MU/V' J-1> ESU-CM	R-BRANCH A SEC-1	R-BRANCH E CM-1
0	2.3325E-21	2.6447E-01	7749.0			
1	2.3451E-21	3.2305E-01	7755.0	2.3124E-21	7.6914E-01	7711.4
2	2.3587E-21	3.5236E-01	7770.2	2.3051E-21	5.0525E-01	7690.0
3	2.3740E-21	3.7225E-01	7791.6	2.2993E-21	4.4837E-01	7666.7
4	2.3941E-21	3.8811E-01	7802.1	2.2954E-21	4.2142E-01	7641.7
5	2.4143E-21	4.0209E-01	7810.7	2.2933E-21	4.0466E-01	7614.9
6	2.4364E-21	4.1512E-01	7817.5	2.2926E-21	3.9263E-01	7586.4
7	2.4607E-21	4.2779E-01	7822.4	2.2938E-21	3.8337E-01	7556.1
8	2.4868E-21	4.4028E-01	7825.4	2.2966E-21	3.7585E-01	7524.1
9	2.5152E-21	4.5300E-01	7826.5	2.3013E-21	3.6961E-01	7490.5
10	2.5459E-21	4.6595E-01	7825.7	2.3075E-21	3.6421E-01	7455.1
11	2.5786E-21	4.7929E-01	7823.0	2.3157E-21	3.5964E-01	7418.1
12	2.6138E-21	4.9311E-01	7818.3	2.3257E-21	3.5569E-01	7379.4
13	2.6515E-21	5.0746E-01	7811.8	2.3374E-21	3.5228E-01	7339.1
14	2.6916E-21	5.2246E-01	7803.3	2.3511E-21	3.4934E-01	7297.2
15	2.7344E-21	5.3810E-01	7792.9	2.3667E-21	3.4683E-01	7253.7
16	2.7797E-21	5.5442E-01	7780.4	2.3841E-21	3.4469E-01	7208.6
17	2.8274E-21	5.7146E-01	7766.1	2.4036E-21	3.4294E-01	7161.9
18	2.8785E-21	5.8934E-01	7749.8	2.4253E-21	3.4157E-01	7113.7
19	2.9324E-21	6.0804E-01	7731.5	2.4490E-21	3.4051E-01	7063.9
20	2.9892E-21	6.2762E-01	7711.2	2.4749E-21	3.3977E-01	7012.6
21	3.0492E-21	6.4810E-01	7689.0	2.5030E-21	3.3932E-01	6959.8
22	3.1123E-21	6.6948E-01	7664.7	2.5335E-21	3.3919E-01	6905.5
23	3.1788E-21	6.9196E-01	7638.5	2.5666E-21	3.3938E-01	6849.6
24	3.2488E-21	7.1526E-01	7610.2	2.6021E-21	3.3984E-01	6792.3
25	3.3224E-21	7.3969E-01	7579.9	2.6402E-21	3.4059E-01	6733.6
26	3.3996E-21	7.6514E-01	7547.6	2.6812E-21	3.4164E-01	6673.4
27	3.4810E-21	7.9179E-01	7513.2	2.7252E-21	3.4298E-01	6611.7
28	3.5660E-21	8.1944E-01	7476.8	2.7719E-21	3.4456E-01	6548.6
29	3.6556E-21	8.4835E-01	7438.3	2.8223E-21	3.4652E-01	6484.0
30	3.7495E-21	8.7843E-01	7397.7	2.8760E-21	3.4875E-01	6418.1
31	3.8480E-21	9.0972E-01	7355.0	2.9333E-21	3.5130E-01	6350.7
32	3.9512E-21	9.4217E-01	7310.2	2.9946E-21	3.5416E-01	6281.9
33	4.0587E-21	9.7606E-01	7263.2	3.0601E-21	3.5741E-01	6211.6
34	4.1734E-21	1.0111E 00	7214.1	3.1299E-21	3.6093E-01	6140.0
35	4.2927E-21	1.0475E 00	7162.8	3.2046E-21	3.6487E-01	6066.9

MATRIX ELEMENTS, EINSTEIN A'S AND ENERGIES FOR V= 2 TO 6 TRANSITIONS OF HCL

	P-BRANCH			R-BRANCH		
J	<V J/MU/V' J+1>	A	E	<V J/MU/V' J-1>	A	E
	ESU-CM	SEC-1	CM-1	ESU-CM	SEC-1	CM-1
0	-4.8259E-23	2.5247E-04	10121.4			
1	-5.1139E-23	3.4169E-04	10136.2	-4.3440E-23	6.0702E-04	10084.5
2	-5.4477E-23	4.1698E-04	10148.6	-4.1552E-23	5.4961E-04	10062.4
3	-5.8209E-23	4.9668E-04	10158.4	-4.0147E-23	5.0709E-04	10037.9
4	-6.2543E-23	5.8691E-04	10165.9	-3.9015E-23	4.7373E-04	10011.0
5	-6.7153E-23	6.9695E-04	10170.8	-3.8179E-23	4.5261E-04	9981.8
6	-7.2549E-23	8.1160E-04	10173.2	-3.7947E-23	4.4141E-04	9950.1
7	-7.8325E-23	9.5231E-04	10173.2	-3.7623E-23	4.3311E-04	9916.1
8	-8.4471E-23	1.1206E-03	10170.6	-3.7828E-23	4.3086E-04	9879.9
9	-9.1595E-23	1.3164E-03	10165.6	-3.8325E-23	4.3247E-04	9841.2
10	-9.9197E-23	1.5472E-03	10158.0	-3.9191E-23	4.3867E-04	9800.3
11	-1.0756E-22	1.8200E-03	10147.9	-4.0466E-23	4.4978E-04	9757.2
12	-1.1640E-22	2.1378E-03	10135.3	-4.2053E-23	4.6509E-04	9711.7
13	-1.2635E-22	2.5057E-03	10120.2	-4.3988E-23	4.8485E-04	9664.1
14	-1.3715E-22	2.9435E-03	10102.5	-4.6388E-23	5.1101E-04	9614.2
15	-1.4851E-22	3.4378E-03	10082.3	-4.8950E-23	5.3988E-04	9562.1
16	-1.6092E-22	4.0162E-03	10059.6	-5.2117E-23	5.7795E-04	9507.9
17	-1.7428E-22	4.6825E-03	10034.3	-5.5569E-23	6.2126E-04	9451.4
18	-1.8853E-22	5.4420E-03	10006.5	-5.9506E-23	6.7334E-04	9392.9
19	-2.0404E-22	6.3242E-03	9976.1	-6.3974E-23	7.3575E-04	9332.1
20	-2.2044E-22	7.3171E-03	9943.1	-6.8657E-23	8.0385E-04	9269.3
21	-2.3810E-22	8.4546E-03	9907.5	-7.3905E-23	8.8426E-04	9204.4
22	-2.5674E-22	9.7410E-03	9869.4	-7.9519E-23	9.7413E-04	9137.3
23	-2.7659E-22	1.1192E-02	9828.6	-8.5719E-23	1.0783E-03	9068.2
24	-2.9843E-22	1.2847E-02	9785.2	-9.2504E-23	1.1864E-03	8997.0
25	-3.2135E-22	1.4679E-02	9739.2	-9.9526E-23	1.2964E-03	8923.7
26	-3.4579E-22	1.6753E-02	9690.5	-1.0742E-22	1.4192E-03	8848.3
27	-3.7173E-22	1.9068E-02	9639.1	-1.1565E-22	1.5420E-03	8770.9
28	-3.9936E-22	2.1653E-02	9585.0	-1.2459E-22	1.6774E-03	8691.5
29	-4.2874E-22	2.4531E-02	9528.3	-1.3417E-22	1.8336E-03	8609.9
30	-4.6006E-22	2.7732E-02	9468.7	-1.4439E-22	2.0611E-03	8526.3
31	-4.9330E-22	3.1287E-02	9406.5	-1.5528E-22	2.3114E-03	8440.7
32	-5.2880E-22	3.5214E-02	9341.4	-1.6696E-22	2.5883E-03	8352.9
33	-5.6641E-22	3.9571E-02	9273.5	-1.7962E-22	2.8987E-03	8263.1
34	-6.0685E-22	4.4379E-02	9202.7	-1.9309E-22	3.2377E-03	8171.2
35	-6.4977E-22	4.9687E-02	9129.1	-2.0754E-22	3.6113E-03	8077.2

MATRIX ELEMENTS, EINSTEIN A'S AND ENERGIES FOR V= 2 TO 7 TRANSITIONS OF HCL

J	P-BRANCH <V J/MU/V' J+1> ESU-CM	P-BRANCH A SEC-1	P-BRANCH E CM-1	P-BRANCH <V J/MU/V' J-1> ESU-CM	P-BRANCH A SEC-1	P-BRANCH E CM-1
0	-1.3954E-22	3.8739E-03	12391.8			
1	-1.3985E-22	4.6847E-03	12405.3	-1.3879E-22	1.1397E-02	12355.5
2	-1.4015E-22	5.0534E-03	12415.7	-1.3841E-22	7.5138E-03	12332.9
3	-1.4035E-22	5.2651E-03	12423.0	-1.3797E-22	6.6779E-03	12307.0
4	-1.4045E-22	5.3980E-03	12427.3	-1.3750E-22	6.2727E-03	12279.2
5	-1.4062E-22	5.4954E-03	12428.4	-1.3713E-22	6.0183E-03	12246.4
6	-1.4047E-22	5.5419E-03	12426.3	-1.3652E-22	5.8062E-03	12211.6
7	-1.4041E-22	5.5767E-03	12421.2	-1.3610E-22	5.6438E-03	12173.7
8	-1.4007E-22	5.5753E-03	12412.9	-1.3551E-22	5.4867E-03	12133.0
9	-1.3969E-22	5.5582E-03	12401.6	-1.3500E-22	5.3471E-03	12089.3
10	-1.3911E-22	5.5176E-03	12387.0	-1.3435E-22	5.2045E-03	12042.7
11	-1.3827E-22	5.4476E-03	12369.4	-1.3365E-22	5.0628E-03	11993.2
12	-1.3726E-22	5.3576E-03	12348.6	-1.3297E-22	4.9260E-03	11940.8
13	-1.3605E-22	5.2471E-03	12324.7	-1.3220E-22	4.7861E-03	11885.6
14	-1.3451E-22	5.1069E-03	12297.6	-1.3137E-22	4.6439E-03	11827.5
15	-1.3287E-22	4.9555E-03	12267.3	-1.3059E-22	4.5074E-03	11766.6
16	-1.3077E-22	4.7703E-03	12234.0	-1.2954E-22	4.3540E-03	11702.9
17	-1.2834E-22	4.5609E-03	12197.4	-1.2852E-22	4.2052E-03	11636.4
18	-1.2573E-22	4.3411E-03	12157.7	-1.2742E-22	4.0534E-03	11567.2
19	-1.2260E-22	4.0893E-03	12114.8	-1.2610E-22	3.8902E-03	11495.2
20	-1.1919E-22	3.8255E-03	12068.7	-1.2487E-22	3.7362E-03	11420.5
21	-1.1535E-22	3.5427E-03	12019.4	-1.2347E-22	3.5744E-03	11343.1
22	-1.1106E-22	3.2447E-03	11966.9	-1.2202E-22	3.4137E-03	11262.9
23	-1.0639E-22	2.9386E-03	11911.2	-1.2045E-22	3.2501E-03	11180.1
24	-1.0104E-22	2.6136E-03	11852.2	-1.1868E-22	3.0805E-03	11094.5
25	-9.5428E-23	2.2964E-03	11789.9	-1.1702E-22	2.9219E-03	11006.3
26	-8.9053E-23	1.9680E-03	11724.4	-1.1506E-22	2.7532E-03	10915.3
27	-8.2265E-23	1.6510E-03	11655.5	-1.1313E-22	2.5917E-03	10821.7
28	-7.4685E-23	1.3365E-03	11583.2	-1.1087E-22	2.4217E-03	10725.4
29	-6.6513E-23	1.0400E-03	11507.6	-1.0870E-22	2.2624E-03	10626.3
30	-5.7598E-23	7.6430E-04	11428.6	-1.0636E-22	2.1031E-03	10524.6
31	-4.7833E-23	5.1604E-04	11345.1	-1.0385E-22	1.9450E-03	10420.0
32	-3.7260E-23	3.0620E-04	11260.0	-1.0123E-22	1.7906E-03	10312.8
33	-2.5821E-23	1.4363E-04	11170.4	-9.8441E-23	1.6389E-03	10202.7
34	-1.3274E-23	3.7029E-05	11077.2	-9.5340E-23	1.4862E-03	10089.8
35	3.1202E-25	1.9936E-08	10980.3	-9.2157E-23	1.3408E-03	9974.1

MATRIX ELEMENTS, EINSTEIN A'S AND ENERGIES FOR V= 3 TO 3 TRANSITIONS OF HCL

Pure Rotation

J	<V J/MU/V' J+1>	A	E
	ESU-CM	SEC-1	CM-1
0	1.1949E-18	1.0379E-03	19.1
1	1.1951E-18	9.9303E-03	38.1
2	1.1954E-18	3.5882E-02	57.2
3	1.1958E-18	8.0058E-02	76.2
4	1.1963E-18	1.7554E-01	95.1
5	1.1969E-18	3.0710E-01	114.0
6	1.1977E-18	4.9191E-01	132.8
7	1.1985E-18	7.3792E-01	151.5
8	1.1995E-18	1.0534E 00	170.2
9	1.2005E-18	1.4465E 00	188.7
10	1.2017E-18	1.9242E 00	207.1
11	1.2030E-18	2.4944E 00	225.4
12	1.2044E-18	3.1628E 00	243.5
13	1.2059E-18	3.9373E 00	261.5
14	1.2076E-18	4.8203E 00	279.3
15	1.2093E-18	5.8214E 00	296.9
16	1.2112E-18	6.9422E 00	314.3
17	1.2132E-18	8.1872E 00	331.6
18	1.2152E-18	9.5613E 00	348.6
19	1.2174E-18	1.1057E 01	365.4
20	1.2197E-18	1.2703E 01	382.0
21	1.2221E-18	1.4475E 01	398.3
22	1.2247E-18	1.6385E 01	414.4
23	1.2273E-18	1.8427E 01	430.2
24	1.2300E-18	2.0607E 01	445.8
25	1.2329E-18	2.2919E 01	461.0
26	1.2359E-18	2.5367E 01	476.0
27	1.2389E-18	2.7939E 01	490.7
28	1.2420E-18	3.0637E 01	505.0
29	1.2453E-18	3.3457E 01	519.1
30	1.2486E-18	3.6398E 01	532.8
31	1.2521E-18	3.9443E 01	546.2
32	1.2556E-18	4.2597E 01	559.2
33	1.2593E-18	4.5843E 01	571.9
34	1.2630E-18	4.9177E 01	584.2
35	1.2668E-18	5.2591E 01	596.1

MATRIX ELEMENTS, EINSTEIN A'S AND ENERGIES FOR V= 3 TO 4 TRANSITIONS OF HCL

J	P-BRANCH <V J/MU/V' J+1> ESU-CM	P-BRANCH A SEC-1	P-BRANCH E CM-1	R-BRANCH <V J/MU/V' J-1> ESU-CM	R-BRANCH A SEC-1	R-BRANCH E CM-1
0	1.3157E-19	3.1832E 01	2595.3			
1	1.2901E-19	3.7782E 01	2613.2	1.3609E-19	9.7212E 01	2557.9
2	1.2794E-19	3.9986E 01	2630.4	1.3816E-19	6.5262E 01	2538.1
3	1.2579E-19	4.0903E 01	2647.0	1.4022E-19	5.9071E 01	2517.9
4	1.2371E-19	4.1205E 01	2663.0	1.4229E-19	5.6507E 01	2497.1
5	1.2164E-19	4.1151E 01	2678.2	1.4437E-19	5.5112E 01	2475.7
6	1.1957E-19	4.0942E 01	2692.9	1.4645E-19	5.4216E 01	2453.9
7	1.1748E-19	4.0404E 01	2706.8	1.4853E-19	5.3558E 01	2431.4
8	1.1540E-19	3.9815E 01	2720.0	1.5062E-19	5.3022E 01	2408.5
9	1.1330E-19	3.9119E 01	2732.6	1.5271E-19	5.2541E 01	2385.1
10	1.1119E-19	3.8334E 01	2744.4	1.5481E-19	5.2081E 01	2361.2
11	1.0907E-19	3.7471E 01	2755.5	1.5692E-19	5.1618E 01	2336.8
12	1.0694E-19	3.6541E 01	2765.8	1.5903E-19	5.1139E 01	2311.9
13	1.0479E-19	3.5549E 01	2775.5	1.6114E-19	5.0636E 01	2286.6
14	1.0263E-19	3.4502E 01	2784.3	1.6327E-19	5.0100E 01	2260.9
15	1.0044E-19	3.3409E 01	2792.4	1.6540E-19	4.9531E 01	2234.7
16	9.8239E-20	3.2267E 01	2799.7	1.6753E-19	4.8927E 01	2208.1
17	9.6012E-20	3.1087E 01	2806.3	1.6968E-19	4.8274E 01	2181.2
18	9.3760E-20	2.9871E 01	2812.0	1.7183E-19	4.7585E 01	2153.8
19	9.1482E-20	2.8624E 01	2817.0	1.7398E-19	4.6855E 01	2126.1
20	8.9173E-20	2.7349E 01	2821.1	1.7614E-19	4.6094E 01	2098.0
21	8.6832E-20	2.6050E 01	2824.4	1.7831E-19	4.5275E 01	2069.6
22	8.4455E-20	2.4733E 01	2826.9	1.8048E-19	4.4427E 01	2040.8
23	8.2041E-20	2.3400E 01	2828.5	1.8265E-19	4.3541E 01	2011.7
24	7.9584E-20	2.2056E 01	2829.3	1.8483E-19	4.2619E 01	1982.2
25	7.7083E-20	2.0705E 01	2829.2	1.8701E-19	4.1661E 01	1952.5
26	7.4532E-20	1.9352E 01	2828.3	1.8920E-19	4.0671E 01	1922.5
27	7.1930E-20	1.8001E 01	2826.5	1.9139E-19	3.9649E 01	1892.2
28	6.9271E-20	1.6657E 01	2823.9	1.9357E-19	3.8598E 01	1861.6
29	6.6550E-20	1.5323E 01	2820.1	1.9575E-19	3.7521E 01	1830.7
30	6.3764E-20	1.4007E 01	2815.6	1.9794E-19	3.6419E 01	1799.6
31	6.0907E-20	1.2712E 01	2810.1	2.0012E-19	3.5292E 01	1768.2
32	5.7972E-20	1.1444E 01	2803.8	2.0229E-19	3.4146E 01	1736.6
33	5.4956E-20	1.0209E 01	2796.4	2.0446E-19	3.2981E 01	1704.7
34	5.1851E-20	9.0100E 00	2788.1	2.0662E-19	3.1901E 01	1672.6
35	4.8650E-20	7.8562E 00	2778.9	2.0878E-19	3.0607E 01	1640.3

MATRIX ELEMENTS, EINSTEIN A'S AND ENERGIES FOR V= 3 TO 5 TRANSITIONS OF HCL

	P-BRANCH			P-BRANCH		
J	<V J/MU/V' J+1>	A	E	<V J/MU/V' J-1>	A	E
	ESU-CM	SEC-1	CM-1	ESU-CM	SEC-1	CM-1
0	-2.9279E-20	1.1679E 01	5069.4			
1	-2.9183E-20	1.4060E 01	5086.3	-2.9500E-20	3.4795E 01	5032.7
2	-2.9096E-20	1.5111E 01	5101.7	-2.9626E-20	2.3113E 01	5012.4
3	-2.9018E-20	1.5717E 01	5115.9	-2.9761E-20	2.0723E 01	4991.0
4	-2.8950E-20	1.6120E 01	5128.8	-2.9907E-20	1.9661E 01	4968.4
5	-2.8890E-20	1.6412E 01	5140.4	-3.0063E-20	1.9038E 01	4944.6
6	-2.8839E-20	1.6636E 01	5150.8	-3.0230E-20	1.8616E 01	4919.7
7	-2.8797E-20	1.6816E 01	5159.9	-3.0407E-20	1.8300E 01	4893.6
8	-2.8763E-20	1.6964E 01	5167.7	-3.0596E-20	1.8048E 01	4866.4
9	-2.8738E-20	1.7088E 01	5174.2	-3.0797E-20	1.7837E 01	4838.2
10	-2.8722E-20	1.7194E 01	5179.4	-3.1010E-20	1.7653E 01	4808.8
11	-2.8713E-20	1.7285E 01	5183.3	-3.1235E-20	1.7488E 01	4778.4
12	-2.8713E-20	1.7364E 01	5185.8	-3.1472E-20	1.7338E 01	4746.9
13	-2.8721E-20	1.7432E 01	5187.0	-3.1722E-20	1.7198E 01	4714.4
14	-2.8737E-20	1.7490E 01	5186.9	-3.1986E-20	1.7066E 01	4680.8
15	-2.8761E-20	1.7539E 01	5185.4	-3.2264E-20	1.5940E 01	4646.3
16	-2.8793E-20	1.7580E 01	5182.5	-3.2556E-20	1.6819E 01	4610.7
17	-2.8832E-20	1.7613E 01	5178.3	-3.2863E-20	1.6701E 01	4574.1
18	-2.8878E-20	1.7638E 01	5172.7	-3.3186E-20	1.6586E 01	4536.6
19	-2.8933E-20	1.7655E 01	5165.7	-3.3524E-20	1.6475E 01	4498.1
20	-2.8994E-20	1.7664E 01	5157.3	-3.3879E-20	1.6364E 01	4458.6
21	-2.9062E-20	1.7665E 01	5147.5	-3.4251E-20	1.6255E 01	4418.3
22	-2.9138E-20	1.7658E 01	5136.2	-3.4641E-20	1.6148E 01	4377.0
23	-2.9219E-20	1.7641E 01	5123.6	-3.5050E-20	1.6041E 01	4334.7
24	-2.9308E-20	1.7617E 01	5109.5	-3.5479E-20	1.5935E 01	4291.6
25	-2.9402E-20	1.7582E 01	5093.9	-3.5927E-20	1.5829E 01	4247.6
26	-2.9503E-20	1.7538E 01	5076.8	-3.6398E-20	1.5724E 01	4202.6
27	-2.9609E-20	1.7483E 01	5058.3	-3.6890E-20	1.5619E 01	4156.8
28	-2.9721E-20	1.7417E 01	5038.3	-3.7406E-20	1.5513E 01	4110.1
29	-2.9838E-20	1.7340E 01	5016.8	-3.7946E-20	1.5407E 01	4062.6
30	-2.9959E-20	1.7251E 01	4993.8	-3.8513E-20	1.5301E 01	4014.2
31	-3.0085E-20	1.7149E 01	4969.2	-3.9107E-20	1.5195E 01	3964.9
32	-3.0213E-20	1.7033E 01	4943.1	-3.9729E-20	1.5087E 01	3914.8
33	-3.0346E-20	1.6902E 01	4915.4	-4.0383E-20	1.4979E 01	3863.8
34	-3.0480E-20	1.6756E 01	4886.1	-4.1068E-20	1.4870E 01	3811.9
35	-3.0615E-20	1.6593E 01	4855.2	-4.1787E-20	1.4760E 01	3759.3

MATRIX ELEMENTS, EINSTEIN A'S AND ENERGIES FOR V= 3 TO 6 TRANSITIONS OF HCL

J	R-BRANCH <V J/MU/V° J+1> ESU-CM	R-BRANCH A SEC-1	R-BRANCH E CM-1	P-BRANCH <V J/MU/V° J-1> ESU-CM	P-BRANCH A SEC-1	P-BRANCH E CM-1
0	3.8309E-21	6.3540E-01	7442.1			
1	3.8582E-21	7.7458E-01	7457.5	3.8108E-21	1.9501E 00	7405.8
2	3.8703E-21	8.4357E-01	7471.0	3.8001E-21	1.2161E 00	7384.9
3	3.8822E-21	8.8047E-01	7482.7	3.7910E-21	1.0798E 00	7362.2
4	3.8896E-21	9.2694E-01	7492.5	3.7863E-21	1.0151E 00	7337.7
5	3.8980E-21	9.5735E-01	7500.4	3.7831E-21	9.7475E-01	7311.4
6	3.9011E-21	9.8520E-01	7506.5	3.7824E-21	9.4574E-01	7283.4
7	4.0263E-21	1.0138E 00	7510.7	3.7844E-21	9.2318E-01	7253.7
8	4.0448E-21	1.0410E 00	7513.9	3.7892E-21	9.0681E-01	7222.2
9	4.1044E-21	1.0683E 00	7513.3	3.7964E-21	8.9921E-01	7189.0
10	4.1514E-21	1.0959E 00	7511.7	3.8063E-21	8.7572E-01	7154.0
11	4.2000E-21	1.1241E 00	7508.2	3.8193E-21	8.6411E-01	7117.5
12	4.2520E-21	1.1531E 00	7502.8	3.8349E-21	8.5378E-01	7079.2
13	4.3077E-21	1.1832E 00	7495.4	3.8535E-21	8.4481E-01	7039.3
14	4.3672E-21	1.2145E 00	7486.1	3.8751E-21	8.3690E-01	6997.8
15	4.4308E-21	1.2470E 00	7474.9	3.9000E-21	8.3003E-01	6954.7
16	4.4985E-21	1.2809E 00	7461.7	3.9280E-21	8.2410E-01	6909.9
17	4.5704E-21	1.3161E 00	7446.5	3.9593E-21	8.1901E-01	6863.6
18	4.6466E-21	1.3529E 00	7429.4	3.9942E-21	8.1484E-01	6815.8
19	4.7272E-21	1.3913E 00	7410.3	4.0327E-21	8.1146E-01	6766.3
20	4.8126E-21	1.4314E 00	7389.1	4.0749E-21	8.0883E-01	6715.3
21	4.9028E-21	1.4732E 00	7366.0	4.1210E-21	8.0700E-01	6662.8
22	4.9980E-21	1.5168E 00	7340.9	4.1711E-21	8.0590E-01	6608.8
23	5.0980E-21	1.5620E 00	7313.7	4.2253E-21	8.0549E-01	6553.3
24	5.2027E-21	1.6093E 00	7284.4	4.2841E-21	8.0589E-01	6496.2
25	5.3149E-21	1.6585E 00	7253.1	4.3473E-21	8.0691E-01	6437.7
26	5.4314E-21	1.7095E 00	7219.7	4.4152E-21	8.0862E-01	6377.6
27	5.5543E-21	1.7625E 00	7184.2	4.4884E-21	8.1107E-01	6316.1
28	5.6833E-21	1.8174E 00	7146.6	4.5669E-21	8.1428E-01	6253.0
29	5.8189E-21	1.8748E 00	7106.8	4.6512E-21	8.1821E-01	6188.5
30	5.9614E-21	1.9341E 00	7064.8	4.7414E-21	8.2283E-01	6122.4
31	6.1107E-21	1.9954E 00	7020.7	4.8380E-21	8.2822E-01	6054.9
32	6.2670E-21	2.0589E 00	6974.3	4.9420E-21	8.3453E-01	5985.8
33	6.4330E-21	2.1247E 00	6925.6	5.0532E-21	8.4163E-01	5915.3
34	6.6063E-21	2.1926E 00	6874.7	5.1727E-21	8.4964E-01	5843.2
35	6.7885E-21	2.2627E 00	6821.4	5.3011E-21	8.5869E-01	5769.5

MATRIX ELEMENTS, EINSTEIN A'S AND ENERGIES FOR V= 3 TO 7 TRANSITIONS OF HCL

J	P-BRANCH <V J/MU/V' J+1>	A	E	P-BRANCH <V J/MU/V' J-1>	A	E
	ESU-CM	SEC-1	CM-1	ESU-CM	SEC-1	CM-1
0	-2.5434E-22	6.1964E-03	9712.5			
1	-2.5983E-22	7.7944E-03	9726.6	-2.4503E-22	1.7065E-02	9676.8
2	-2.6577E-22	9.7688E-03	9738.2	-2.4112E-22	1.0943E-02	9655.3
3	-2.7254E-22	9.5896E-03	9747.3	-2.3781E-22	9.5087E-03	9631.3
4	-2.7980E-22	1.0358E-02	9753.9	-2.3480E-22	8.7556E-03	9604.9
5	-2.8794E-22	1.1152E-02	9758.0	-2.3251E-22	8.2721E-03	9576.1
6	-2.9686E-22	1.1991E-02	9759.7	-2.3052E-22	7.9057E-03	9544.9
7	-3.0658E-22	1.2894E-02	9758.7	-2.2908E-22	7.6262E-03	9511.3
8	-3.1717E-22	1.3876E-02	9755.3	-2.2819E-22	7.4099E-03	9475.3
9	-3.2898E-22	1.4979E-02	9749.3	-2.2786E-22	7.2458E-03	9437.0
10	-3.4165E-22	1.6183E-02	9740.7	-2.2789E-22	7.1131E-03	9396.4
11	-3.5556E-22	1.7531E-02	9729.7	-2.2873E-22	7.0341E-03	9353.5
12	-3.7062E-22	1.9026E-02	9716.1	-2.3009E-22	6.9876E-03	9308.3
13	-3.8717E-22	2.0715E-02	9699.9	-2.3225E-22	6.9873E-03	9260.8
14	-4.0511E-22	2.2600E-02	9681.2	-2.3496E-22	7.0170E-03	9211.1
15	-4.2445E-22	2.4696E-02	9659.9	-2.3839E-22	7.0844E-03	9159.1
16	-4.4545E-22	2.7048E-02	9636.0	-2.4268E-22	7.1963E-03	9105.0
17	-4.6803E-22	2.9662E-02	9609.6	-2.4768E-22	7.3441E-03	9048.6
18	-4.9260E-22	3.2607E-02	9580.6	-2.5373E-22	7.5455E-03	8990.1
19	-5.1879E-22	3.5856E-02	9549.0	-2.6036E-22	7.7736E-03	8929.4
20	-5.4713E-22	3.9498E-02	9514.8	-2.6809E-22	8.0587E-03	8866.6
21	-5.7756E-22	4.3551E-02	9477.9	-2.7676E-22	8.3906E-03	8801.6
22	-6.1006E-22	4.8033E-02	9438.4	-2.8643E-22	8.7732E-03	8734.4
23	-6.4479E-22	5.2988E-02	9396.3	-2.9705E-22	9.2036E-03	8665.2
24	-6.8200E-22	5.8484E-02	9351.4	-3.0878E-22	9.6920E-03	8593.8
25	-7.2185E-22	6.4572E-02	9303.9	-3.2162E-22	1.0239E-02	8520.3
26	-7.6397E-22	7.1211E-02	9253.6	-3.3542E-22	1.0834E-02	8444.6
27	-8.0921E-22	7.8579E-02	9200.6	-3.5071E-22	1.1511E-02	8366.8
28	-8.5719E-22	8.6631E-02	9144.8	-3.6697E-22	1.2238E-02	8286.9
29	-9.0843E-22	9.5494E-02	9086.2	-3.8472E-22	1.3046E-02	8204.9
30	-9.6294E-22	1.0519E-01	9024.7	-4.0363E-22	1.3914E-02	8120.7
31	-1.0209E-21	1.1577E-01	8960.3	-4.2410E-22	1.4868E-02	8034.3
32	-1.0829E-21	1.2739E-01	8892.9	-4.4629E-22	1.5918E-02	7945.7
33	-1.1488E-21	1.4008E-01	8822.6	-4.7003E-22	1.7050E-02	7854.9
34	-1.2192E-21	1.5393E-01	8749.1	-4.9581E-22	1.8297E-02	7761.8
35	-1.2945E-21	1.6907E-01	8672.6	-5.2373E-22	1.9664E-02	7666.5

MATRIX ELEMENTS, EINSTEIN A'S AND ENERGIES FOR V= 3 TO 0 TRANSITIONS OF HCL

J	R-BRANCH <V J/MU/V" J+1> ESU-CM	R-BRANCH A SEC-1	R-BRANCH E CM-1	P-BRANCH <V J/MU/V" J-1> ESU-CM	P-BRANCH A SEC-1	P-BRANCH E CM-1
0	-1.5760E-22	4.3526E-03	11878.8			
1	-1.5762E-22	5.2413E-03	11891.5	-1.5760E-22	1.2943E-02	11843.7
2	-1.5766E-22	5.6324E-03	11901.2	-1.5757E-22	9.5776E-03	11821.6
3	-1.5768E-22	5.8432E-03	11907.6	-1.5759E-22	7.6709E-03	11796.3
4	-1.5768E-22	5.9735E-03	11910.9	-1.5760E-22	7.2631E-03	11767.9
5	-1.5773E-22	6.0557E-03	11911.1	-1.5773E-22	7.0084E-03	11736.4
6	-1.5687E-22	6.0824E-03	11908.0	-1.5775E-22	6.8219E-03	11701.8
7	-1.5630E-22	6.0792E-03	11901.8	-1.5788E-22	6.6812E-03	11664.3
8	-1.5569E-22	6.0569E-03	11892.4	-1.5804E-22	6.5521E-03	11623.7
9	-1.5473E-22	5.9951E-03	11879.8	-1.5805E-22	6.4411E-03	11580.1
10	-1.5343E-22	5.8974E-03	11864.1	-1.5800E-22	6.3226E-03	11533.5
11	-1.5109E-22	5.7733E-03	11845.1	-1.5800E-22	6.2122E-03	11484.0
12	-1.4994E-22	5.6116E-03	11823.0	-1.5783E-22	6.0990E-03	11431.6
13	-1.4750E-22	5.4097E-03	11797.7	-1.5756E-22	5.9612E-03	11376.3
14	-1.4442E-22	5.1654E-03	11769.3	-1.5718E-22	5.8254E-03	11318.0
15	-1.4115E-22	4.8995E-03	11737.6	-1.5669E-22	5.6820E-03	11257.0
16	-1.3711E-22	4.5902E-03	11702.9	-1.5585E-22	5.5145E-03	11193.1
17	-1.3250E-22	4.2516E-03	11664.7	-1.5497E-22	5.3450E-03	11126.4
18	-1.2701E-22	3.8709E-03	11623.4	-1.5371E-22	5.1518E-03	11056.8
19	-1.2009E-22	3.4769E-03	11578.9	-1.5237E-22	4.9561E-03	10984.5
20	-1.1407E-22	3.0560E-03	11531.2	-1.5063E-22	4.7388E-03	10909.4
21	-1.0629E-22	2.6213E-03	11480.1	-1.4866E-22	4.5119E-03	10831.5
22	-9.7614E-23	2.1817E-03	11425.8	-1.4635E-22	4.2712E-03	10750.9
23	-8.8032E-23	1.7491E-03	11368.2	-1.4380E-22	4.0243E-03	10667.4
24	-7.7421E-23	1.3323E-03	11307.2	-1.4098E-22	3.7711E-03	10581.2
25	-6.5726E-23	9.4461E-04	11242.8	-1.3778E-22	3.5087E-03	10492.2
26	-5.3009E-23	6.0377E-04	11175.0	-1.3421E-22	3.2403E-03	10400.4
27	-3.8870E-23	3.1883E-04	11103.6	-1.3025E-22	2.9671E-03	10305.7
28	-2.3702E-23	1.1619E-04	11028.9	-1.2618E-22	2.7046E-03	10208.2
29	-7.1076E-24	1.0233E-05	10950.4	-1.2164E-22	2.4386E-03	10107.9
30	1.0926E-23	2.3655E-05	10869.4	-1.1686E-22	2.1809E-03	10004.7
31	3.0509E-23	1.9019E-04	10782.7	-1.1167E-22	1.9277E-03	9898.5
32	5.1842E-23	5.0769E-04	10693.3	-1.0613E-22	1.6835E-03	9789.4
33	7.4902E-23	1.0329E-03	10600.3	-1.0030E-22	1.4519E-03	9677.3
34	1.0003E-22	1.7925E-03	10502.8	-9.3865E-23	1.2261E-03	9562.1
35	1.2739E-22	2.8248E-03	10401.6	-8.7033E-23	1.0151E-03	9443.0

MATRIX ELEMENTS, EINSTEIN A'S AND ENERGIES FOR V= 4 TO 4 TRANSITIONS OF HCL

Pure Rotation

J	<V J/MU/V' J+1>	A	E
	ESU-CM	SEC-1	CM-1
0	1.2210E-18	9.8442E-04	18.5
1	1.2212E-18	9.4200E-03	36.9
2	1.2214E-18	3.4003E-02	55.3
3	1.2218E-18	8.3515E-02	73.8
4	1.2223E-18	1.6643E-01	92.1
5	1.2229E-18	2.9119E-01	110.4
6	1.2236E-18	4.6615E-01	128.6
7	1.2243E-18	6.9910E-01	146.7
8	1.2252E-18	9.9812E-01	164.8
9	1.2263E-18	1.3697E 00	182.7
10	1.2274E-18	1.8219E 00	200.5
11	1.2286E-18	2.3610E 00	218.2
12	1.2299E-18	2.9928E 00	235.7
13	1.2313E-18	3.7232E 00	253.1
14	1.2329E-18	4.5579E 00	270.3
15	1.2345E-18	5.5009E 00	287.4
16	1.2362E-18	6.5563E 00	304.2
17	1.2381E-18	7.7283E 00	320.9
18	1.2400E-18	9.0195E 00	337.3
19	1.2421E-18	1.0433E 01	353.6
20	1.2442E-19	1.1967E 01	369.5
21	1.2464E-19	1.3629E 01	385.3
22	1.2488E-18	1.5411E 01	400.8
23	1.2512E-18	1.7321E 01	416.1
24	1.2537E-18	1.9351E 01	431.0
25	1.2563E-18	2.1504E 01	445.7
26	1.2590E-18	2.3772E 01	460.1
27	1.2618E-18	2.6159E 01	474.2
28	1.2647E-18	2.8652E 01	488.0
29	1.2676E-18	3.1252E 01	501.4
30	1.2707E-18	3.3953E 01	514.6
31	1.2738E-18	3.6742E 01	527.3
32	1.2769E-18	3.9623E 01	539.8
33	1.2802E-18	4.2578E 01	551.9
34	1.2835E-18	4.5601E 01	563.6
35	1.2868E-18	4.8684E 01	575.0

MATRIX ELEMENTS, EINSTEIN A'S AND ENERGIES FOR V= 4 TO 5 TRANSITIONS OF HCL

	P-BRANCH			P-BRANCH		
J	<V J/MU/V' J+1>	A	E	<V J/MU/V' J-1>	A	E
	ESU-CM	SEC-1	CM-1	ESU-CM	SEC-1	CM-1
0	1.4216E-19	3.2730E 01	2492.8			
1	1.3979E-19	3.8768E 01	2510.0	1.4690E-19	1.0032E 02	2456.4
2	1.3740E-19	4.0937E 01	2526.6	1.4926E-19	6.7453E 01	2437.4
3	1.3502E-19	4.1772E 01	2542.6	1.5162E-19	6.1140E 01	2417.7
4	1.3262E-19	4.1966E 01	2557.9	1.5397E-19	5.8559E 01	2397.5
5	1.3021E-19	4.1789E 01	2572.6	1.5633E-19	5.7176E 01	2376.7
6	1.2778E-19	4.1365E 01	2586.6	1.5868E-19	5.6297E 01	2355.4
7	1.2536E-19	4.0761E 01	2599.9	1.6104E-19	5.5660E 01	2333.6
8	1.2291E-19	4.0019E 01	2612.5	1.6339E-19	5.5138E 01	2311.2
9	1.2045E-19	3.9163E 01	2624.3	1.6575E-19	5.4666E 01	2288.3
10	1.1798E-19	3.8213E 01	2635.5	1.6811E-19	5.4207E 01	2265.0
11	1.1549E-19	3.7181E 01	2646.0	1.7046E-19	5.3740E 01	2241.1
12	1.1298E-19	3.6077E 01	2655.7	1.7282E-19	5.3247E 01	2216.8
13	1.1046E-19	3.4908E 01	2664.7	1.7518E-19	5.2721E 01	2192.0
14	1.0791E-19	3.3684E 01	2672.9	1.7754E-19	5.2156E 01	2166.9
15	1.0535E-19	3.2409E 01	2680.3	1.7990E-19	5.1546E 01	2141.2
16	1.0276E-19	3.1088E 01	2687.0	1.8226E-19	5.0891E 01	2115.2
17	9.9989E-20	2.9732E 01	2692.9	1.8462E-19	5.0187E 01	2088.7
18	9.7179E-20	2.8340E 01	2698.0	1.8698E-19	4.9436E 01	2061.9
19	9.4328E-20	2.6921E 01	2702.3	1.8934E-19	4.8637E 01	2034.7
20	9.1434E-20	2.5479E 01	2705.7	1.9169E-19	4.7789E 01	2007.1
21	8.8502E-20	2.4018E 01	2708.4	1.9404E-19	4.6896E 01	1979.2
22	8.5000E-20	2.2545E 01	2710.1	1.9639E-19	4.5957E 01	1950.9
23	8.2054E-20	2.1066E 01	2711.1	1.9874E-19	4.4974E 01	1922.2
24	7.9047E-20	1.9584E 01	2711.2	2.0109E-19	4.3949E 01	1893.3
25	7.6870E-20	1.8107E 01	2710.3	2.0341E-19	4.2885E 01	1864.0
26	7.3741E-20	1.6639E 01	2708.6	2.0574E-19	4.1781E 01	1834.4
27	7.0530E-20	1.5188E 01	2706.0	2.0805E-19	4.0643E 01	1804.5
28	6.7240E-20	1.3759E 01	2702.5	2.1036E-19	3.9472E 01	1774.4
29	6.3866E-20	1.2358E 01	2698.1	2.1265E-19	3.8269E 01	1743.9
30	6.0399E-20	1.0993E 01	2692.7	2.1493E-19	3.7040E 01	1713.1
31	5.6834E-20	9.6698E 00	2686.4	2.1719E-19	3.5784E 01	1682.1
32	5.3163E-20	8.3963E 00	2679.1	2.1942E-19	3.4508E 01	1650.8
33	4.9378E-20	7.1795E 00	2670.8	2.2164E-19	3.3212E 01	1619.2
34	4.5470E-20	6.0273E 00	2661.6	2.2383E-19	3.1899E 01	1587.4
35	4.1428E-20	4.9476E 00	2651.3	2.2599E-19	3.0573E 01	1555.3

MATRIX ELEMENTS, EINSTEIN A'S AND ENERGIES FOR V= 4 TO 6 TRANSITIONS OF HCL

	R-BRANCH			P-BRANCH		
J	<V J/MU/V' J+1>	A	E	<V J/MU/V' J-1>	A	E
	ESU-CM	SEC-1	CM-1	ESU-CM	SEC-1	CM-1
0	-3.7917E-20	1.7311E 01	4965.2			
1	-3.7778E-20	2.0825E 01	4881.2	-3.8231E-20	5.1642E 01	4829.5
2	-3.7651E-20	2.2364E 01	4896.0	-3.8407E-20	3.4322E 01	4809.8
3	-3.7535E-20	2.3241E 01	4909.5	-3.8595E-20	3.0789E 01	4788.9
4	-3.7431E-20	2.3814E 01	4921.7	-3.8797E-20	2.9222E 01	4766.9
5	-3.7338E-20	2.4221E 01	4932.6	-3.9012E-20	2.8307E 01	4743.6
6	-3.7255E-20	2.4525E 01	4942.3	-3.9240E-20	2.7688E 01	4719.2
7	-3.7184E-20	2.4762E 01	4950.6	-3.9483E-20	2.7225E 01	4693.6
8	-3.7122E-20	2.4949E 01	4957.7	-3.9741E-20	2.6855E 01	4666.9
9	-3.7072E-20	2.5100E 01	4963.4	-4.0014E-20	2.6544E 01	4639.1
10	-3.7032E-20	2.5222E 01	4967.8	-4.0302E-20	2.6273E 01	4610.2
11	-3.7002E-20	2.5320E 01	4970.9	-4.0606E-20	2.6030E 01	4580.2
12	-3.6982E-20	2.5397E 01	4972.7	-4.0927E-20	2.5806E 01	4549.1
13	-3.6972E-20	2.5457E 01	4973.1	-4.1266E-20	2.5597E 01	4517.0
14	-3.6971E-20	2.5500E 01	4972.2	-4.1622E-20	2.5399E 01	4483.8
15	-3.6980E-20	2.5528E 01	4969.9	-4.1996E-20	2.5209E 01	4449.6
16	-3.6998E-20	2.5542E 01	4966.2	-4.2391E-20	2.5025E 01	4414.4
17	-3.7025E-20	2.5542E 01	4961.1	-4.2805E-20	2.4847E 01	4378.2
18	-3.7061E-20	2.5528E 01	4954.7	-4.3240E-20	2.4673E 01	4341.1
19	-3.7105E-20	2.5501E 01	4946.9	-4.3696E-20	2.4500E 01	4302.9
20	-3.7157E-20	2.5458E 01	4937.6	-4.4175E-20	2.4331E 01	4263.8
21	-3.7217E-20	2.5402E 01	4926.9	-4.4677E-20	2.4163E 01	4223.7
22	-3.7284E-20	2.5331E 01	4914.8	-4.5204E-20	2.3996E 01	4182.7
23	-3.7359E-20	2.5245E 01	4901.2	-4.5756E-20	2.3830E 01	4140.8
24	-3.7440E-20	2.5142E 01	4886.1	-4.6335E-20	2.3663E 01	4097.9
25	-3.7527E-20	2.5022E 01	4869.6	-4.6941E-20	2.3497E 01	4054.1
26	-3.7620E-20	2.4884E 01	4851.5	-4.7577E-20	2.3329E 01	4009.4
27	-3.7718E-20	2.4729E 01	4831.9	-4.8244E-20	2.3161E 01	3963.8
28	-3.7820E-20	2.4552E 01	4810.8	-4.8942E-20	2.2991E 01	3917.2
29	-3.7925E-20	2.4355E 01	4788.1	-4.9674E-20	2.2819E 01	3869.8
30	-3.8034E-20	2.4137E 01	4763.8	-5.0442E-20	2.2646E 01	3821.4
31	-3.8145E-20	2.3896E 01	4737.9	-5.1248E-20	2.2469E 01	3772.1
32	-3.8257E-20	2.3630E 01	4710.3	-5.2094E-20	2.2291E 01	3721.9
33	-3.8369E-20	2.3339E 01	4681.1	-5.2982E-20	2.2109E 01	3670.7
34	-3.8479E-20	2.3021E 01	4650.2	-5.3916E-20	2.1925E 01	3618.6
35	-3.8587E-20	2.2674E 01	4617.5	-5.4898E-20	2.1737E 01	3565.6

MATRIX ELEMENTS, EINSTEIN A'S AND ENERGIES FOR V= 4 TO 7 TRANSITIONS OF HCL

J	R-BRANCH <V J/MU/V' J+1> ESU-CM	R-BRANCH A SEC-1	R-BRANCH E CM-1	P-BRANCH <V J/MU/V' J-1> ESU-CM	P-BRANCH A SEC-1	P-BRANCH E CM-1
0	5.4728E-21	1.3101E 00	7135.6			
1	5.8867E-21	1.5548E 00	7150.3	5.8349E-21	3.8229E 00	7100.5
2	6.0243E-21	1.7341E 00	7163.1	5.8210E-21	2.5148E 00	7090.2
3	6.0655E-21	1.8256E 00	7174.1	5.8105E-21	2.2340E 00	7058.0
4	6.0805E-21	1.8343E 00	7183.1	5.8035E-21	2.1009E 00	7034.0
5	6.0860E-21	1.8560E 00	7190.2	5.7996E-21	2.0175E 00	7008.2
6	6.0879E-21	2.0104E 00	7195.4	5.7995E-21	1.9574E 00	6980.6
7	6.0886E-21	2.0515E 00	7198.7	5.8026E-21	1.9101E 00	6951.2
8	6.0888E-21	2.1111E 00	7200.0	5.8096E-21	1.8710E 00	6920.1
9	6.0256E-21	2.1602E 00	7199.4	5.8202E-21	1.8376E 00	6887.2
10	6.0860E-21	2.2055E 00	7196.9	5.8348E-21	1.8085E 00	6852.5
11	6.0851E-21	2.2537E 00	7192.4	5.8534E-21	1.7827E 00	6816.2
12	6.0841E-21	2.3110E 00	7186.0	5.8762E-21	1.7597E 00	6778.2
13	6.0826E-21	2.3838E 00	7177.6	5.9034E-21	1.7392E 00	6738.5
14	6.0808E-21	2.4185E 00	7167.2	5.9352E-21	1.7209E 00	6697.1
15	6.0660E-21	2.4751E 00	7154.9	5.9719E-21	1.7047E 00	6654.1
16	6.0592E-21	2.5341E 00	7140.5	6.0137E-21	1.6904E 00	6609.5
17	6.0587E-21	2.5955E 00	7124.2	6.0608E-21	1.6781E 00	6563.2
18	6.0647E-21	2.6596E 00	7105.9	6.1135E-21	1.6675E 00	6515.4
19	7.0773E-21	2.7262E 00	7085.6	6.1720E-21	1.6587E 00	6466.0
20	7.1370E-21	2.7558E 00	7063.2	6.2367E-21	1.6517E 00	6415.0
21	7.3239E-21	2.8685E 00	7038.8	6.3078E-21	1.6464E 00	6362.5
22	7.4594E-21	2.9442E 00	7012.3	6.3859E-21	1.6428E 00	6308.3
23	7.6006E-21	3.0230E 00	6983.9	6.4709E-21	1.6410E 00	6252.7
24	7.7503E-21	3.1050E 00	6953.1	6.5634E-21	1.6408E 00	6195.5
25	7.9091E-21	3.1901E 00	6920.4	6.6638E-21	1.6423E 00	6136.7
26	8.0761E-21	3.2784E 00	6885.4	6.7727E-21	1.6456E 00	6076.4
27	8.2520E-21	3.3699E 00	6848.3	6.8900E-21	1.6504E 00	6014.6
28	8.4369E-21	3.4643E 00	6809.0	7.0164E-21	1.6569E 00	5951.1
29	8.6313E-21	3.5619E 00	6767.4	7.1527E-21	1.6650E 00	5886.2
30	8.8356E-21	3.6624E 00	6723.6	7.2992E-21	1.6748E 00	5819.6
31	9.0503E-21	3.7658E 00	6677.5	7.4567E-21	1.6862E 00	5751.4
32	9.2756E-21	3.8718E 00	6629.0	7.6258E-21	1.6993E 00	5681.7
33	9.5123E-21	3.9806E 00	6578.0	7.8076E-21	1.7142E 00	5610.3
34	9.7606E-21	4.0916E 00	6524.6	8.0029E-21	1.7308E 00	5537.3
35	1.0022E-20	4.2051E 00	6468.7	8.2136E-21	1.7495E 00	5462.5

MATRIX ELEMENTS, EINSTEIN A'S AND ENERGIES FOR V= 4 TO 3 TRANSITIONS OF HCL

J	R-BRANCH <V J/MU/V' J+1> ESU-CM	R-BRANCH A SEC-1	R-BRANCH E CM-1	P-BRANCH <V J/MU/V' J-1> ESU-CM	P-BRANCH A SEC-1	P-BRANCH E CM-1
0	-6.5575E-22	3.6185E-02	8301.0			
1	-6.6460E-22	4.4795E-02	8315.3	-6.3997E-22	1.0225E-01	8267.5
2	-6.7415E-22	4.9556E-02	8326.1	-6.3294E-22	6.6226E-02	8246.5
3	-6.8466E-22	5.3147E-02	8334.4	-6.2663E-22	5.7976E-02	8223.0
4	-6.9602E-22	5.6276E-02	8340.1	-6.2082E-22	5.3740E-02	8197.0
5	-7.0820E-22	5.9220E-02	8343.2	-6.1555E-22	5.0888E-02	8168.5
6	-7.2153E-22	6.2165E-02	8343.8	-6.1097E-22	4.8725E-02	8137.6
7	-7.3616E-22	6.5212E-02	8341.8	-6.0701E-22	4.6961E-02	8104.2
8	-7.5207E-22	6.8408E-02	8337.2	-6.0369E-22	4.5466E-02	8068.4
9	-7.6943E-22	7.1815E-02	8330.0	-6.0112E-22	4.4185E-02	8030.2
10	-7.8836E-22	7.5478E-02	8320.2	-5.9929E-22	4.3074E-02	7989.7
11	-8.0915E-22	7.9489E-02	8307.9	-5.9843E-22	4.2134E-02	7946.8
12	-8.3170E-22	8.3837E-02	8292.9	-5.9838E-22	4.1329E-02	7901.5
13	-8.5649E-22	8.8641E-02	8275.4	-5.9950E-22	4.0686E-02	7853.9
14	-8.8337E-22	9.3805E-02	8255.3	-6.0157E-22	4.0164E-02	7804.1
15	-9.1275E-22	9.9710E-02	8232.6	-6.0499E-22	3.9808E-02	7752.0
16	-9.4473E-22	1.0613E-01	8207.3	-6.0964E-22	3.9587E-02	7697.6
17	-9.7965E-22	1.1322E-01	8179.3	-6.1567E-22	3.9516E-02	7641.0
18	-1.0170E-21	1.2103E-01	8148.7	-6.2321E-22	3.9603E-02	7582.1
19	-1.0578E-21	1.2967E-01	8115.5	-6.3247E-22	3.9864E-02	7521.1
20	-1.1019E-21	1.3921E-01	8079.6	-6.4335E-22	4.0281E-02	7457.8
21	-1.1498E-21	1.4976E-01	8041.0	-6.5614E-22	4.0883E-02	7392.4
22	-1.2009E-21	1.6135E-01	7999.7	-6.7076E-22	4.1654E-02	7324.8
23	-1.2561E-21	1.7410E-01	7955.7	-6.8753E-22	4.2629E-02	7254.9
24	-1.3155E-21	1.8813E-01	7908.0	-7.0644E-22	4.3797E-02	7182.9
25	-1.3793E-21	2.0355E-01	7859.2	-7.2769E-22	4.5180E-02	7108.6
26	-1.4477E-21	2.2043E-01	7806.7	-7.5131E-22	4.6773E-02	7032.2
27	-1.5209E-21	2.3888E-01	7751.4	-7.7752E-22	4.8599E-02	7953.4
28	-1.5996E-21	2.5913E-01	8693.0	-8.0651E-22	5.0676E-02	7872.5
29	-1.6834E-21	2.8113E-01	8631.7	-8.3802E-22	5.2962E-02	7789.2
30	-1.7732E-21	3.0517E-01	8567.4	-8.7282E-22	5.5548E-02	7703.6
31	-1.8691E-21	3.3128E-01	8499.9	-9.1064E-22	5.8388E-02	7615.7
32	-1.9715E-21	3.5964E-01	8429.3	-9.5102E-22	6.1527E-02	7525.5
33	-2.0812E-21	3.9049E-01	8355.4	-9.9682E-22	6.4974E-02	7432.8
34	-2.1982E-21	4.2384E-01	8278.3	-1.0454E-21	6.8726E-02	7337.6
35	-2.3235E-21	4.6002E-01	8197.6	-1.0984E-21	7.2851E-02	7240.0

MATRIX ELEMENTS, EINSTEIN A'S AND ENERGIES FOR V= 4 TO 0 TRANSITIONS OF HCL

J	R-BRANCH <V J/MU/V" J+1> ESU-CM	R-BRANCH A SEC-1	R-BRANCH E CM-1	P-BRANCH <V J/MU/V" J-1> ESU-CM	P-BRANCH A SEC-1	P-BRANCH E CM-1
0	-1.1097E-22	1.8884E-03	11362.1			
1	-1.1031E-22	2.2463E-03	11374.1	-1.1272E-22	5.7933E-03	11329.4
2	-1.0971E-22	2.3862E-03	11382.8	-1.1370E-22	3.9077E-03	11306.7
3	-1.0904E-22	2.4434E-03	11388.3	-1.1477E-22	3.5504E-03	11291.8
4	-1.0837E-22	2.4747E-03	11390.5	-1.1616E-22	3.4466E-03	11283.7
5	-1.0757E-22	2.4749E-03	11389.5	-1.1744E-22	3.3969E-03	11282.4
6	-1.0677E-22	2.4624E-03	11385.2	-1.1901E-22	3.3937E-03	11288.0
7	-1.0584E-22	2.4261E-03	11377.6	-1.2055E-22	3.4029E-03	11150.5
8	-1.0489E-22	2.3733E-03	11366.8	-1.2210E-22	3.4249E-03	11109.8
9	-1.0384E-22	2.2978E-03	11352.7	-1.2381E-22	3.4492E-03	11066.1
10	-1.0241E-22	2.2029E-03	11335.3	-1.2553E-22	3.4804E-03	11019.3
11	-1.0077E-22	2.0829E-03	11314.7	-1.2707E-22	3.5019E-03	10969.5
12	-9.9431E-23	1.9376E-03	11290.9	-1.2850E-22	3.5152E-03	10916.6
13	-9.8425E-23	1.7604E-03	11263.9	-1.2980E-22	3.5207E-03	10860.8
14	-9.5405E-23	1.5766E-03	11233.4	-1.3088E-22	3.5115E-03	10802.0
15	-7.9844E-23	1.3621E-03	11199.8	-1.3174E-22	3.4882E-03	10740.3
16	-7.3053E-23	1.1309E-03	11162.9	-1.3224E-22	3.4444E-03	10675.7
17	-6.5276E-23	8.9466E-04	11122.7	-1.3245E-22	3.383BE-03	10608.1
18	-5.6172E-23	6.5572E-04	11079.2	-1.3214E-22	3.2958E-03	10537.7
19	-4.5722E-23	4.2951E-04	11032.4	-1.3142E-22	3.1876E-03	10464.5
20	-3.3853E-23	2.3254E-04	10982.3	-1.3013E-22	3.0536E-03	10388.3
21	-2.0355E-23	8.2934E-05	10928.8	-1.2826E-22	2.8958E-03	10309.3
22	-5.3004E-24	5.5414E-06	10871.9	-1.2587E-22	2.7200E-03	10227.4
23	1.1633E-23	2.6271E-05	10811.6	-1.2270E-22	2.5183E-03	10142.7
24	3.0408E-23	1.7755E-04	10747.8	-1.1888E-22	2.3013E-03	10055.1
25	5.1554E-23	4.3826E-04	10680.5	-1.1418E-22	2.0642E-03	9964.6
26	7.4700E-23	1.0261E-03	10609.5	-1.0874E-22	1.8199E-03	9871.1
27	1.0027E-22	1.9114E-03	10535.0	-1.0241E-22	1.5651E-03	9774.7
28	1.2848E-22	2.9099E-03	10456.6	-9.5091E-23	1.3077E-03	9675.3
29	1.5927E-22	4.3635E-03	10374.5	-8.6913E-23	1.0575E-03	9572.8
30	1.9319E-22	6.2725E-03	10288.5	-7.7563E-23	8.1415E-04	9467.2
31	2.3011E-22	8.4729E-03	10198.4	-6.7273E-23	5.9129E-04	9358.5
32	2.7052E-22	1.1663E-02	10104.3	-5.5711E-23	3.9093E-04	9246.6
33	3.1468E-22	1.5329E-02	10004.0	-4.2992E-23	2.2409E-04	9131.3
34	3.6269E-22	1.9755E-02	9903.3	-2.9072E-23	9.8481E-05	9012.6
35	4.1510E-22	2.5056E-02	9796.1	-1.3876E-23	2.1527E-05	8890.5

MATRIX ELEMENTS, EINSTEIN A'S AND ENERGIES FOR V= 5 TO 5 TRANSITIONS OF HCL

Pure Rotation

J	<V J/MU/V' J+1>	A	E
	ESU-CM	SEC-1	CM-1
0	1.2451E-18	9.2505E-04	17.9
1	1.2452E-18	8.9564E-03	35.7
2	1.2454E-18	3.2020E-02	53.6
3	1.2458E-18	7.8513E-02	71.3
4	1.2462E-18	1.5642E-01	89.1
5	1.2467E-18	2.7385E-01	106.8
6	1.2474E-18	4.3810E-01	124.4
7	1.2481E-18	6.5705E-01	141.9
8	1.2489E-18	9.3760E-01	159.3
9	1.2498E-18	1.2865E 00	176.7
10	1.2508E-18	1.7109E 00	193.9
11	1.2519E-18	2.2158E 00	211.0
12	1.2531E-18	2.8081E 00	227.9
13	1.2544E-18	3.4911E 00	244.7
14	1.2558E-18	4.2728E 00	261.4
15	1.2573E-18	5.1528E 00	277.8
16	1.2589E-18	6.1383E 00	294.0
17	1.2605E-18	7.2319E 00	310.1
18	1.2623E-18	8.4331E 00	326.0
19	1.2641E-18	9.7466E 00	341.6
20	1.2660E-18	1.1174E 01	357.0
21	1.2680E-18	1.2709E 01	372.2
22	1.2701E-18	1.4362E 01	387.1
23	1.2722E-18	1.6123E 01	401.7
24	1.2745E-18	1.7994E 01	416.1
25	1.2768E-18	1.9971E 01	430.2
26	1.2791E-18	2.2052E 01	444.0
27	1.2815E-18	2.4230E 01	457.5
28	1.2840E-18	2.6505E 01	470.7
29	1.2866E-18	2.8866E 01	483.5
30	1.2891E-18	3.1310E 01	496.1
31	1.2918E-18	3.3828E 01	508.2
32	1.2944E-18	3.6410E 01	520.1
33	1.2971E-18	3.9050E 01	531.5
34	1.2998E-18	4.1735E 01	542.6
35	1.3025E-18	4.4455E 01	553.3

MATRIX ELEMENTS, EINSTEIN A'S AND ENERGIES FOR V= 5 TO 6 TRANSITIONS OF HCL

J	P-BRANCH <V J/MU/V' J+1>	P-BRANCH A	P-BRANCH E	R-BRANCH <V J/MU/V' J-1>	R-BRANCH A	R-BRANCH E
	ESU-CM	SEC-1	CM-1	ESU-CM	SEC-1	CM-1
0	1.4827E-19	3.1391E 01	2390.3			
1	1.4559E-19	3.0784E 01	2406.9	1.5359E-19	9.6658E 01	2355.2
2	1.4250E-19	3.0045E 01	2422.9	1.5623E-19	9.5118E 01	2336.7
3	1.4020E-19	2.9714E 01	2438.2	1.5886E-19	9.4127E 01	2317.7
4	1.3747E-19	2.9763E 01	2452.8	1.6148E-19	9.4710E 01	2298.0
5	1.3473E-19	2.9447E 01	2466.8	1.6410E-19	9.5455E 01	2277.8
6	1.3197E-19	2.9287E 01	2480.1	1.6671E-19	9.4668E 01	2257.0
7	1.2918E-19	2.9152E 01	2492.7	1.6931E-19	9.4102E 01	2235.7
8	1.2637E-19	2.7278E 01	2504.6	1.7191E-19	9.3439E 01	2213.8
9	1.2354E-19	2.6293E 01	2515.7	1.7450E-19	9.3214E 01	2191.4
10	1.2067E-19	2.5214E 01	2526.2	1.7709E-19	9.2793E 01	2168.6
11	1.1777E-19	2.4053E 01	2535.9	1.7966E-19	9.2353E 01	2145.2
12	1.1484E-19	2.2826E 01	2544.9	1.8224E-19	9.1880E 01	2121.3
13	1.1186E-19	2.1534E 01	2553.1	1.8480E-19	9.1365E 01	2097.0
14	1.0885E-19	2.0191E 01	2560.6	1.8736E-19	9.0805E 01	2072.3
15	1.0580E-19	1.8803E 01	2567.3	1.8991E-19	9.0191E 01	2047.1
16	1.0269E-19	1.7375E 01	2573.2	1.9245E-19	8.9526E 01	2021.5
17	9.9543E-20	1.5916E 01	2578.3	1.9498E-19	8.8808E 01	1995.5
18	9.6336E-20	1.4431E 01	2582.7	1.9749E-19	8.8033E 01	1969.0
19	9.3073E-20	1.2926E 01	2586.3	2.0000E-19	8.7205E 01	1942.2
20	8.9748E-20	1.1409E 01	2588.9	2.0249E-19	8.6325E 01	1915.1
21	8.6355E-20	9.8884E 00	2590.7	2.0497E-19	8.5392E 01	1887.6
22	8.2893E-20	8.3641E 00	2591.7	2.0743E-19	8.4410E 01	1859.7
23	7.9356E-20	6.8844E 00	2591.9	2.0987E-19	8.3378E 01	1831.4
24	7.5733E-20	5.4341E 00	2591.1	2.1230E-19	8.2302E 01	1802.9
25	7.2025E-20	4.0160E 00	2589.4	2.1470E-19	8.1182E 01	1774.0
26	6.8222E-20	2.6406E 00	2586.9	2.1707E-19	8.0020E 01	1744.8
27	6.4319E-20	1.3090E 00	2583.4	2.1942E-19	7.8820E 01	1715.2
28	6.0307E-20	9.6179E 00	2579.0	2.2174E-19	7.7586E 01	1685.4
29	5.6179E-20	8.2994E 00	2573.5	2.2402E-19	7.6318E 01	1655.2
30	5.1925E-20	7.0401E 00	2567.1	2.2627E-19	7.5021E 01	1624.7
31	4.7537E-20	5.8524E 00	2559.7	2.2848E-19	7.3698E 01	1593.9
32	4.3002E-20	4.7441E 00	2551.3	2.3065E-19	7.2352E 01	1562.8
33	3.8311E-20	3.7252E 00	2541.8	2.3276E-19	7.0987E 01	1531.4
34	3.3450E-20	2.8057E 00	2531.2	2.3483E-19	6.9605E 01	1499.7
35	2.8406E-20	1.9963E 00	2519.6	2.3684E-19	6.8213E 01	1467.6

MATRIX ELEMENTS, EINSTEIN A'S AND ENERGIES FOR V= 5 TO 7 TRANSITIONS OF HCL

J	P-BRANCH <V J/MU/V' J+1> ESU-CM	A SEC-1	E CM-1	P-BRANCH <V J/MU/V' J-1> ESU-CM	A SEC-1	E CM-1
0	-4.7366E-20	2.3748E 01	4660.7			
1	-4.7172E-20	2.9544E 01	4676.0	-4.7798E-20	7.0950E 01	4626.2
2	-4.6992E-20	3.0624E 01	4690.1	-4.8037E-20	4.7194E 01	4607.1
3	-4.6826E-20	3.1702E 01	4702.8	-4.8291E-20	4.2350E 01	4586.7
4	-4.6673E-20	3.2540E 01	4714.2	-4.8561E-20	4.0213E 01	4565.2
5	-4.6534E-20	3.3056E 01	4724.4	-4.8846E-20	3.8970E 01	4542.4
6	-4.6407E-20	3.3428E 01	4733.2	-4.9152E-20	3.8129E 01	4518.4
7	-4.6294E-20	3.3704E 01	4740.7	-4.9474E-20	3.7501E 01	4493.3
8	-4.6193E-20	3.3910E 01	4746.9	-4.9813E-20	3.6998E 01	4466.9
9	-4.6104E-20	3.4062E 01	4751.7	-5.0172E-20	3.6574E 01	4439.5
10	-4.6027E-20	3.4171E 01	4755.2	-5.0550E-20	3.6202E 01	4410.9
11	-4.5961E-20	3.4244E 01	4757.4	-5.0949E-20	3.5866E 01	4381.2
12	-4.5907E-20	3.4286E 01	4758.2	-5.1369E-20	3.5554E 01	4350.4
13	-4.5864E-20	3.4300E 01	4757.6	-5.1811E-20	3.5261E 01	4318.5
14	-4.5832E-20	3.4290E 01	4755.6	-5.2275E-20	3.4981E 01	4285.5
15	-4.5811E-20	3.4254E 01	4752.3	-5.2764E-20	3.4710E 01	4251.5
16	-4.5800E-20	3.4197E 01	4747.6	-5.3277E-20	3.4447E 01	4216.5
17	-4.5799E-20	3.4117E 01	4741.4	-5.3816E-20	3.4199E 01	4180.5
18	-4.5807E-20	3.4015E 01	4733.9	-5.4382E-20	3.3935E 01	4143.4
19	-4.5824E-20	3.3890E 01	4724.9	-5.4977E-20	3.3683E 01	4105.3
20	-4.5850E-20	3.3744E 01	4714.5	-5.5601E-20	3.3434E 01	4066.3
21	-4.5884E-20	3.3574E 01	4702.6	-5.6257E-20	3.3186E 01	4026.3
22	-4.5925E-20	3.3381E 01	4689.3	-5.6944E-20	3.2938E 01	3985.3
23	-4.5973E-20	3.3164E 01	4674.4	-5.7667E-20	3.2691E 01	3943.4
24	-4.6027E-20	3.2921E 01	4658.1	-5.8425E-20	3.2442E 01	3900.4
25	-4.6086E-20	3.2652E 01	4640.2	-5.9220E-20	3.2193E 01	3856.6
26	-4.6149E-20	3.2354E 01	4620.8	-6.0056E-20	3.1942E 01	3811.8
27	-4.6214E-20	3.2026E 01	4599.8	-6.0933E-20	3.1688E 01	3766.0
28	-4.6282E-20	3.1668E 01	4577.2	-6.1854E-20	3.1432E 01	3719.3
29	-4.6350E-20	3.1276E 01	4552.9	-6.2822E-20	3.1172E 01	3671.6
30	-4.6416E-20	3.0849E 01	4527.0	-6.3838E-20	3.0908E 01	3622.9
31	-4.6479E-20	3.0384E 01	4499.3	-6.4905E-20	3.0638E 01	3573.3
32	-4.6536E-20	2.9880E 01	4469.9	-6.6027E-20	3.0361E 01	3522.7
33	-4.6586E-20	2.9334E 01	4438.7	-6.7206E-20	3.0077E 01	3471.0
34	-4.6626E-20	2.8745E 01	4405.7	-6.8446E-20	2.9785E 01	3418.3
35	-4.6651E-20	2.8108E 01	4370.7	-6.9751E-20	2.9483E 01	3364.6

MATRIX ELEMENTS, EINSTEIN A'S AND ENERGIES FOR V= 5 TO 8 TRANSITIONS OF HCL

J	P-BRANCH <V J/MU/V" J+1> ESU-CM	P-BRANCH A SEC-1	P-BRANCH E CM-1	R-BRANCH <V J/MU/V" J-1> ESU-CM	R-BRANCH A SEC-1	R-BRANCH E CM-1
0	8.5561E-21	2.4255E 00	6827.0			
1	8.5340E-21	2.9603E 00	6841.0	8.5114E-21	7.1232E 00	6793.2
2	8.6196E-21	3.2137E 00	6853.0	8.4959E-21	4.6904E 00	6773.4
3	8.6566E-21	3.3770E 00	6863.1	8.4842E-21	4.1694E 00	6751.7
4	8.6897E-21	3.5006E 00	6871.2	8.4773E-21	3.9231E 00	6728.1
5	8.7479E-21	3.6036E 00	6877.4	8.4748E-21	3.7688E 00	6702.7
6	8.8012E-21	3.6950E 00	6881.6	8.4768E-21	3.6569E 00	6675.4
7	8.8600E-21	3.7707E 00	6883.8	8.4835E-21	3.5686E 00	6646.3
8	8.9246E-21	3.8606E 00	6884.0	8.4951E-21	3.4950E 00	6615.3
9	8.9953E-21	3.9397E 00	6882.3	8.5120E-21	3.4316E 00	6582.6
10	9.0724E-21	4.0185E 00	6878.6	8.5340E-21	3.3755E 00	6548.0
11	9.1550E-21	4.0974E 00	6872.8	8.5616E-21	3.3253E 00	6511.7
12	9.2467E-21	4.1773E 00	6865.1	8.5954E-21	3.2802E 00	6473.7
13	9.3446E-21	4.2600E 00	6855.4	8.6351E-21	3.2392E 00	6434.0
14	9.4499E-21	4.3444E 00	6843.7	8.6816E-21	3.2021E 00	6392.5
15	9.5636E-21	4.4316E 00	6830.0	8.7351E-21	3.1687E 00	6349.4
16	9.6856E-21	4.5221E 00	6814.3	8.7959E-21	3.1388E 00	6304.6
17	9.8157E-21	4.6157E 00	6796.5	8.8646E-21	3.1121E 00	6258.2
18	9.9556E-21	4.7134E 00	6776.7	8.9417E-21	3.0889E 00	6210.1
19	1.0104E-20	4.8144E 00	6754.9	9.0273E-21	3.0687E 00	6160.4
20	1.0263E-20	4.9199E 00	6730.9	9.1226E-21	3.0521E 00	6109.1
21	1.0431E-20	5.0295E 00	6704.9	9.2275E-21	3.0386E 00	6056.2
22	1.0611E-20	5.1436E 00	6676.7	9.3430E-21	3.0284E 00	6001.7
23	1.0801E-20	5.2621E 00	6646.4	9.4696E-21	3.0215E 00	5945.6
24	1.1002E-20	5.3851E 00	6613.8	9.6081E-21	3.0180E 00	5887.9
25	1.1214E-20	5.5124E 00	6579.1	9.7589E-21	3.0177E 00	5828.5
26	1.1442E-20	5.6447E 00	6542.1	9.9237E-21	3.0212E 00	5767.5
27	1.1681E-20	5.7814E 00	6502.8	1.0103E-20	3.0280E 00	5704.9
28	1.1934E-20	5.9222E 00	6461.2	1.0297E-20	3.0384E 00	5640.6
29	1.2200E-20	6.0673E 00	6417.2	1.0508E-20	3.0526E 00	5574.7
30	1.2481E-20	6.2164E 00	6370.7	1.0737E-20	3.0705E 00	5507.0
31	1.2777E-20	6.3690E 00	6321.8	1.0984E-20	3.0921E 00	5437.6
32	1.3089E-20	6.5247E 00	6270.3	1.1253E-20	3.1177E 00	5366.4
33	1.3417E-20	6.6831E 00	6216.1	1.1543E-20	3.1474E 00	5293.5
34	1.3762E-20	6.8430E 00	6159.3	1.1858E-20	3.1810E 00	5218.7
35	1.4125E-20	7.0037E 00	6099.7	1.2199E-20	3.2188E 00	5142.0

MATRIX ELEMENTS, EINSTEIN A'S AND ENERGIES FOR V= 5 TO 0 TRANSITIONS OF HCL

J	R-BRANCH <V J/MU/V" J+1> ESU-CM	A SEC-1	E CM-1	P-BRANCH <V J/MU/V" J-1> ESU-CM	A SEC-1	E CM-1
0	-1.3340E-21	1.3059E-01	8887.2			
1	-1.3473E-21	1.6053E-01	8899.8	-1.3097E-21	3.7343E-01	8854.1
2	-1.3615E-21	1.7625E-01	8909.7	-1.2986E-21	2.4308E-01	8833.6
3	-1.3766E-21	1.8731E-01	8917.0	-1.2881E-21	2.1356E-01	8810.5
4	-1.3930E-21	1.9644E-01	8921.7	-1.2784E-21	1.9840E-01	8784.8
5	-1.4104E-21	2.0469E-01	8923.7	-1.2694E-21	1.8853E-01	8756.6
6	-1.4289E-21	2.1258E-01	8923.0	-1.2611E-21	1.8079E-01	8725.8
7	-1.4505E-21	2.2039E-01	8919.6	-1.2535E-21	1.7430E-01	8692.5
8	-1.4732E-21	2.2836E-01	8913.6	-1.2469E-21	1.6872E-01	8656.7
9	-1.4979E-21	2.3665E-01	8905.0	-1.2413E-21	1.6379E-01	8618.4
10	-1.5250E-21	2.4543E-01	8893.7	-1.2368E-21	1.5936E-01	8577.6
11	-1.5547E-21	2.5478E-01	8879.7	-1.2335E-21	1.5540E-01	8534.4
12	-1.5872E-21	2.6480E-01	8863.1	-1.2317E-21	1.5187E-01	8488.8
13	-1.6229E-21	2.7586E-01	8843.8	-1.2315E-21	1.4875E-01	8440.8
14	-1.6619E-21	2.8780E-01	8821.9	-1.2329E-21	1.4602E-01	8390.5
15	-1.7047E-21	3.0090E-01	8797.2	-1.2363E-21	1.4373E-01	8337.7
16	-1.7515E-21	3.1526E-01	8769.9	-1.2418E-21	1.4186E-01	8282.7
17	-1.8026E-21	3.3102E-01	8739.9	-1.2496E-21	1.4042E-01	8225.4
18	-1.8582E-21	3.4832E-01	8707.2	-1.2600E-21	1.3943E-01	8165.7
19	-1.9189E-21	3.6740E-01	8671.8	-1.2731E-21	1.3894E-01	8103.8
20	-1.9846E-21	3.8826E-01	8633.6	-1.2890E-21	1.3888E-01	8039.6
21	-2.0559E-21	4.1120E-01	8592.6	-1.3082E-21	1.3937E-01	7973.1
22	-2.1332E-21	4.3638E-01	8548.9	-1.3307E-21	1.4034E-01	7904.4
23	-2.2166E-21	4.6393E-01	8502.3	-1.3567E-21	1.4183E-01	7833.4
24	-2.3067E-21	4.9408E-01	8452.8	-1.3866E-21	1.4390E-01	7760.0
25	-2.4037E-21	5.2699E-01	8400.3	-1.4205E-21	1.4653E-01	7684.4
26	-2.5084E-21	5.6302E-01	8344.9	-1.4590E-21	1.4979E-01	7606.5
27	-2.6210E-21	6.0226E-01	8286.4	-1.5019E-21	1.5366E-01	7526.1
28	-2.7419E-21	6.4488E-01	8224.9	-1.5499E-21	1.5818E-01	7443.4
29	-2.8721E-21	6.9139E-01	8160.0	-1.6035E-21	1.6346E-01	7358.2
30	-3.0122E-21	7.4197E-01	8091.8	-1.6627E-21	1.6947E-01	7270.6
31	-3.1626E-21	7.9683E-01	8020.3	-1.7284E-21	1.7629E-01	7180.4
32	-3.3247E-21	8.5651E-01	7945.3	-1.8014E-21	1.8406E-01	7087.5
33	-3.4989E-21	9.2116E-01	7866.7	-1.8819E-21	1.9276E-01	6992.0
34	-3.6864E-21	9.9112E-01	7784.3	-1.9709E-21	2.0255E-01	6893.7
35	-3.8882E-21	1.0668E 00	7698.1	-2.0693E-21	2.1352E-01	6792.5

MATRIX ELEMENTS, EINSTEIN A'S AND ENERGIES FOR V= 5 TO 10 TRANSITIONS OF HCL

	P-BRANCH			P-BRANCH		
J	<V J/MU/V' J+1>	A	E	<V J/MU/V' J-1>	A	E
	ESU-CM	SEC-1	CM-1	ESU-CM	SEC-1	CM-1
0	4.3475E-23	2.5145E-04	10836.4			
1	4.5652E-23	3.3375E-04	10847.5	3.8680E-23	5.9181E-04	10804.0
2	4.7370E-23	3.9600E-04	10855.3	3.5693E-23	3.3399E-04	10782.8
3	4.9199E-23	4.3199E-04	10859.6	3.2653E-23	2.4985E-04	10758.2
4	5.0896E-23	4.7312E-04	10860.6	2.9083E-23	1.8731E-04	10730.4
5	5.2538E-23	5.1155E-04	10858.3	2.5303E-23	1.3664E-04	10699.2
6	5.4406E-23	5.5378E-04	10852.5	2.1357E-23	9.4656E-05	10664.8
7	5.6550E-23	6.0180E-04	10843.4	1.7062E-23	5.9013E-05	10627.1
8	5.9029E-23	6.5775E-04	10830.9	1.2630E-23	3.1660E-05	10586.2
9	6.2102E-23	7.2867E-04	10815.0	8.2024E-24	1.3089E-05	10542.1
10	6.5759E-23	8.1620E-04	10795.7	3.6809E-24	2.5855E-06	10494.9
11	7.0346E-23	9.3155E-04	10773.1	-6.6462E-25	8.2686E-08	10444.4
12	7.5837E-23	1.0781E-03	10747.1	-4.9541E-24	4.5961E-06	10390.9
13	8.2597E-23	1.2715E-03	10717.8	-8.8720E-24	1.4169E-05	10334.2
14	9.0747E-23	1.5247E-03	10685.1	-1.2437E-23	2.7285E-05	10274.5
15	1.0033E-22	1.8449E-03	10649.0	-1.5583E-23	4.1951E-05	10211.7
16	1.1172E-22	2.2707E-03	10609.5	-1.8066E-23	5.5186E-05	10145.9
17	1.2507E-22	2.8161E-03	10566.6	-1.9905E-23	6.5511E-05	10077.1
18	1.4032E-22	3.5031E-03	10520.3	-2.0960E-23	7.0978E-05	10005.3
19	1.5821E-22	4.3963E-03	10470.6	-2.0805E-23	6.8275E-05	9930.5
20	1.7840E-22	5.5112E-03	10417.4	-1.9980E-23	6.1416E-05	9852.7
21	2.0150E-22	6.9241E-03	10360.6	-1.7804E-23	4.7517E-05	9771.9
22	2.2742E-22	8.6755E-03	10300.3	-1.4571E-23	3.0981E-05	9688.2
23	2.5647E-22	1.0839E-02	10236.4	-9.9172E-24	1.3956E-05	9601.3
24	2.8895E-22	1.3499E-02	10168.8	-3.8598E-24	2.0533E-06	9511.5
25	3.2511E-22	1.6744E-02	10097.5	3.6702E-24	1.8011E-06	9418.5
26	3.6514E-22	2.0667E-02	10022.3	1.2675E-23	2.0912E-05	9322.5
27	4.0943E-22	2.5392E-02	9943.3	2.3482E-23	6.9131E-05	9223.3
28	4.5822E-22	3.1032E-02	9860.2	3.6081E-23	1.5773E-04	9120.8
29	5.1206E-22	3.7755E-02	9773.0	5.0584E-23	2.9917E-04	9015.1
30	5.7121E-22	4.5715E-02	9681.6	6.7157E-23	5.0811E-04	8906.0
31	6.3629E-22	5.5082E-02	9585.8	8.6049E-23	8.0253E-04	8793.4
32	7.0820E-22	6.6127E-02	9485.4	1.0762E-22	1.2056E-03	8677.3
33	7.8703E-22	7.9018E-02	9380.3	1.3195E-22	1.7348E-03	8557.5
34	8.7390E-22	9.4076E-02	9270.3	1.5941E-22	2.4264E-03	8433.8
35	9.6969E-22	1.1161E-01	9155.1	1.9054E-22	3.3103E-03	8306.2

MATRIX ELEMENTS, EINSTEIN A'S AND ENERGIES FOR V= 6 TO 6 TRANSITIONS OF HCL

Pure Rotation

J	<V J/M /V' J+1>	A	E
	ESU-CM	SEC-1	CM-1
0	1.2667E-19	8.5580E-04	17.2
1	1.2668E-19	8.2509E-03	34.5
2	1.2670E-19	2.9778E-02	51.7
3	1.2673E-19	7.3025E-02	68.8
4	1.2677E-19	1.4567E-01	86.0
5	1.2681E-19	2.5462E-01	103.0
6	1.2687E-19	4.0757E-01	120.0
7	1.2693E-19	6.1104E-01	137.0
8	1.2700E-19	8.7158E-01	153.8
9	1.2707E-19	1.1959E 00	170.5
10	1.2716E-19	1.5894E 00	187.1
11	1.2725E-19	2.0579E 00	203.6
12	1.2736E-19	2.6066E 00	220.0
13	1.2747E-19	3.2399E 00	236.1
14	1.2758E-19	3.9621E 00	252.2
15	1.2771E-19	4.7766E 00	268.0
16	1.2784E-19	5.6858E 00	283.7
17	1.2798E-19	6.6926E 00	299.2
18	1.2813E-19	7.8000E 00	314.5
19	1.2828E-19	9.0072E 00	329.5
20	1.2844E-19	1.0313E 01	344.3
21	1.2861E-19	1.1721E 01	358.9
22	1.2878E-19	1.3229E 01	373.2
23	1.2896E-19	1.4833E 01	387.2
24	1.2914E-19	1.6532E 01	401.0
25	1.2932E-19	1.8322E 01	414.5
26	1.2951E-19	2.0199E 01	427.6
27	1.2970E-19	2.2157E 01	440.5
28	1.2990E-19	2.4192E 01	453.1
29	1.3010E-19	2.6295E 01	465.3
30	1.3029E-19	2.8461E 01	477.1
31	1.3049E-19	3.0679E 01	488.6
32	1.3069E-19	3.2940E 01	499.8
33	1.3088E-19	3.5237E 01	510.6
34	1.3107E-19	3.7555E 01	521.0
35	1.3125E-19	3.9883E 01	530.9

MATRIX ELEMENTS, EINSTEIN A'S AND ENERGIES FOR V= 6 TO 7 TRANSITIONS OF HCL

J	P-BRANCH <V J/MU/V' J+1>	A	F	P-BRANCH <V J/MU/V' J-1>	A	F
	ESU-CM	SEC-1	CM-1	ESU-CM	SEC-1	CM-1
0	1.5007E-19	2.9190E 01	2287.6			
1	1.4710E-19	3.3187E 01	2303.5	1.5594E-19	8.7321E 01	2253.8
2	1.4411E-19	3.4809E 01	2318.8	1.5285E-19	5.8979E 01	2235.9
3	1.4109E-19	3.5260E 01	2333.5	1.6174E-19	5.3675E 01	2217.4
4	1.3805E-19	3.5144E 01	2347.4	1.6461E-19	5.1595E 01	2198.3
5	1.3497E-19	3.4692E 01	2360.6	1.6746E-19	5.0534E 01	2178.6
6	1.3186E-19	3.4017E 01	2373.2	1.7030E-19	4.9895E 01	2158.4
7	1.2872E-19	3.3177E 01	2385.0	1.7313E-19	4.9442E 01	2137.6
8	1.2553E-19	3.2210E 01	2396.1	1.7594E-19	4.9072E 01	2116.2
9	1.2231E-19	3.1141E 01	2406.5	1.7873E-19	4.8726E 01	2094.3
10	1.1904E-19	2.9994E 01	2416.2	1.8151E-19	4.8370E 01	2071.8
11	1.1572E-19	2.8756E 01	2425.1	1.8428E-19	4.7987E 01	2048.9
12	1.1236E-19	2.7466E 01	2433.2	1.8702E-19	4.7563E 01	2025.4
13	1.0894E-19	2.6124E 01	2440.6	1.8975E-19	4.7089E 01	2001.5
14	1.0548E-19	2.4738E 01	2447.2	1.9247E-19	4.6563E 01	1977.1
15	1.0198E-19	2.3316E 01	2453.0	1.9516E-19	4.5979E 01	1952.3
16	9.8307E-20	2.1867E 01	2459.1	1.9783E-19	4.5336E 01	1927.0
17	9.4628E-20	2.0397E 01	2462.3	2.0048E-19	4.4635E 01	1901.3
18	9.0874E-20	1.8916E 01	2465.7	2.0310E-19	4.3875E 01	1875.2
19	8.7039E-20	1.7429E 01	2469.2	2.0570E-19	4.3056E 01	1848.6
20	8.3119E-20	1.5946E 01	2469.9	2.0827E-19	4.2180E 01	1821.7
21	7.9104E-20	1.4473E 01	2470.8	2.1080E-19	4.1250E 01	1794.4
22	7.4994E-20	1.3020E 01	2470.7	2.1330E-19	4.0266E 01	1766.8
23	7.0777E-20	1.1595E 01	2469.8	2.1577E-19	3.9232E 01	1738.7
24	6.6449E-20	1.0205E 01	2468.0	2.1819E-19	3.8149E 01	1710.3
25	6.2000E-20	8.8617E 00	2465.2	2.2057E-19	3.7022E 01	1681.6
26	5.7423E-20	7.5728E 00	2461.5	2.2289E-19	3.5852E 01	1652.5
27	5.2708E-20	6.3483E 00	2456.9	2.2517E-19	3.4643E 01	1623.1
28	4.7845E-20	5.1981E 00	2451.3	2.2739E-19	3.3400E 01	1593.4
29	4.2824E-20	4.1329E 00	2444.6	2.2954E-19	3.2124E 01	1563.3
30	3.7631E-20	3.1631E 00	2437.0	2.3162E-19	3.0821E 01	1532.9
31	3.2254E-20	2.3001E 00	2428.2	2.3362E-19	2.9493E 01	1502.2
32	2.6670E-20	1.5554E 00	2418.4	2.3554E-19	2.8145E 01	1471.2
33	2.0889E-20	9.4105E-01	2407.5	2.3737E-19	2.6780E 01	1439.8
34	1.4865E-20	4.6960E-01	2395.4	2.3910E-19	2.5403E 01	1408.1
35	8.5882E-21	1.5422E-01	2382.1	2.4072E-19	2.4017E 01	1376.0

MATRIX ELEMENTS, EINSTEIN A'S AND ENERGIES FOR V= 6 TO 8 TRANSITIONS OF HCL

	P-BRANCH			P-BRANCH		
J	<V J/MU/V' J+1>	A	E	<V J/MU/V' J-1>	A	E
	ESU-CM	SEC-1	CM-1	ESU-CM	SEC-1	CM-1
0	-5.7504E-20	3.0653E 01	4453.9			
1	-5.7341E-20	3.6808E 01	4468.5	-5.8184E-20	3.1740E 01	4420.7
2	-5.7094E-20	3.9448E 01	4491.9	-5.8502E-20	3.1054E 01	4402.2
3	-5.6863E-20	4.0905E 01	4493.8	-5.8838E-20	3.4836E 01	4382.4
4	-5.6640E-20	4.1815E 01	4504.4	-5.9194E-20	3.2099E 01	4361.3
5	-5.6450E-20	4.2421E 01	4513.6	-5.9571E-20	3.0513E 01	4338.9
6	-5.6267E-20	4.2838E 01	4521.4	-5.9969E-20	2.9445E 01	4315.4
7	-5.6098E-20	4.3126E 01	4528.1	-6.0388E-20	2.8647E 01	4290.6
8	-5.5943E-20	4.3319E 01	4533.3	-6.0830E-20	2.8008E 01	4264.5
9	-5.5803E-20	4.3439E 01	4537.1	-6.1296E-20	2.7469E 01	4237.3
10	-5.5675E-20	4.3499E 01	4539.5	-6.1786E-20	2.6991E 01	4209.0
11	-5.5561E-20	4.3508E 01	4540.5	-6.2302E-20	2.6557E 01	4179.4
12	-5.5460E-20	4.3473E 01	4540.2	-6.2845E-20	2.6154E 01	4148.8
13	-5.5370E-20	4.3398E 01	4538.5	-6.3415E-20	2.5770E 01	4117.0
14	-5.5292E-20	4.3285E 01	4535.3	-6.4014E-20	2.5401E 01	4084.1
15	-5.5225E-20	4.3137E 01	4530.8	-6.4643E-20	2.5040E 01	4050.1
16	-5.5167E-20	4.2954E 01	4524.8	-6.5303E-20	2.4686E 01	4015.1
17	-5.5120E-20	4.2737E 01	4517.4	-6.5997E-20	2.4337E 01	3979.0
18	-5.5081E-20	4.2486E 01	4508.5	-6.6724E-20	2.3989E 01	3941.9
19	-5.5051E-20	4.2202E 01	4498.2	-6.7488E-20	2.3642E 01	3903.7
20	-5.5028E-20	4.1892E 01	4486.3	-6.8289E-20	2.3293E 01	3864.6
21	-5.5008E-20	4.1527E 01	4473.0	-6.9130E-20	2.2944E 01	3824.4
22	-5.4996E-20	4.1135E 01	4458.2	-7.0011E-20	2.2591E 01	3783.2
23	-5.4986E-20	4.0704E 01	4441.7	-7.0937E-20	2.2234E 01	3741.0
24	-5.4978E-20	4.0233E 01	4423.7	-7.1908E-20	2.1873E 01	3697.7
25	-5.4977E-20	3.9721E 01	4404.1	-7.2927E-20	2.1506E 01	3653.5
26	-5.4965E-20	3.9166E 01	4382.9	-7.3997E-20	2.1132E 01	3608.3
27	-5.4955E-20	3.8565E 01	4359.9	-7.5121E-20	2.0752E 01	3562.0
28	-5.4940E-20	3.7917E 01	4335.3	-7.6301E-20	2.0364E 01	3514.7
29	-5.4918E-20	3.7220E 01	4308.9	-7.7543E-20	1.9966E 01	3466.4
30	-5.4885E-20	3.6471E 01	4280.7	-7.8849E-20	1.9559E 01	3417.0
31	-5.4840E-20	3.5667E 01	4250.7	-8.0224E-20	1.9141E 01	3366.5
32	-5.4777E-20	3.4806E 01	4218.8	-8.1672E-20	1.8711E 01	3314.9
33	-5.4693E-20	3.3885E 01	4184.9	-8.3198E-20	1.8268E 01	3262.3
34	-5.4581E-20	3.2901E 01	4149.1	-8.4808E-20	1.7810E 01	3208.4
35	-5.4435E-20	3.1849E 01	4111.1	-8.6507E-20	1.7335E 01	3153.4

MATRIX ELEMENTS, EINSTEIN A'S AND ENERGIES FOR V= 6 TO 9 TRANSITIONS OF HCL

	P-BRANCH			P-BRANCH		
J	<V J/MU/V' J+1>	A	E	<V J/MU/V' J-1>	A	E
	ESU-CM	SEC-1	CM-1	ESU-CM	SEC-1	CM-1
0	1.2007E-20	4.1668E 00	6514.1			
1	1.2039E-20	5.0573E 00	6527.3	1.1960E-20	1.2218E 01	6481.6
2	1.2077E-20	5.4806E 00	6538.5	1.1945E-20	8.0527E 00	6462.4
3	1.2120E-20	5.7488E 00	6547.7	1.1936E-20	7.1648E 00	6441.2
4	1.2170E-20	5.9474E 00	6554.8	1.1932E-20	6.7456E 00	6418.0
5	1.2227E-20	6.1090E 00	6559.9	1.1933E-20	6.4832E 00	6392.9
6	1.2290E-20	6.2495E 00	6562.9	1.1941E-20	6.2930E 00	6365.8
7	1.2360E-20	6.3772E 00	6563.9	1.1955E-20	6.1422E 00	6336.8
8	1.2438E-20	6.4972E 00	6562.9	1.1975E-20	6.0155E 00	6305.9
9	1.2524E-20	6.6129E 00	6559.8	1.2003E-20	5.9054E 00	6273.2
10	1.2619E-20	6.7259E 00	6554.6	1.2037E-20	5.8076E 00	6238.6
11	1.2721E-20	6.8387E 00	6547.4	1.2079E-20	5.7193E 00	6202.1
12	1.2834E-20	6.9534E 00	6538.2	1.2130E-20	5.6389E 00	6163.9
13	1.2957E-20	7.0679E 00	6526.8	1.2189E-20	5.5655E 00	6123.9
14	1.3090E-20	7.1841E 00	6513.4	1.2259E-20	5.4986E 00	6082.1
15	1.3234E-20	7.3077E 00	6497.9	1.2338E-20	5.4377E 00	6038.5
16	1.3390E-20	7.4334E 00	6480.4	1.2428E-20	5.3828E 00	5993.2
17	1.3559E-20	7.5638E 00	6460.7	1.2530E-20	5.3336E 00	5946.2
18	1.3738E-20	7.6990E 00	6439.0	1.2645E-20	5.2903E 00	5897.5
19	1.3931E-20	7.8395E 00	6415.1	1.2773E-20	5.2530E 00	5847.1
20	1.4138E-20	7.9854E 00	6389.0	1.2915E-20	5.2214E 00	5795.0
21	1.4359E-20	8.1371E 00	6360.8	1.3073E-20	5.1958E 00	5741.3
22	1.4595E-20	8.2938E 00	6330.3	1.3246E-20	5.1758E 00	5685.9
23	1.4845E-20	8.4561E 00	6297.6	1.3437E-20	5.1623E 00	5628.7
24	1.5111E-20	8.6237E 00	6262.7	1.3647E-20	5.1545E 00	5569.9
25	1.5393E-20	8.7957E 00	6225.4	1.3875E-20	5.1523E 00	5509.4
26	1.5691E-20	8.9721E 00	6185.7	1.4125E-20	5.1565E 00	5447.2
27	1.6006E-20	9.1527E 00	6143.5	1.4397E-20	5.1666E 00	5383.2
28	1.6338E-20	9.3363E 00	6098.9	1.4692E-20	5.1825E 00	5317.5
29	1.6689E-20	9.5224E 00	6051.7	1.5013E-20	5.2046E 00	5250.0
30	1.7059E-20	9.7105E 00	6001.8	1.5362E-20	5.2330E 00	5180.6
31	1.7449E-20	9.8994E 00	5949.2	1.5741E-20	5.2675E 00	5109.3
32	1.7860E-20	1.0088E 01	5893.8	1.6152E-20	5.3089E 00	5036.0
33	1.8292E-20	1.0276E 01	5835.5	1.6600E-20	5.3572E 00	4960.8
34	1.8747E-20	1.0461E 01	5774.1	1.7088E-20	5.4127E 00	4883.4
35	1.9225E-20	1.0641E 01	5709.5	1.7620E-20	5.4759E 00	4803.9

MATRIX ELEMENTS, EINSTEIN A'S AND ENERGIES FOR V= 6 TO 10 TRANSITIONS OF HCL
&

	P-BRANCH			P-BRANCH		
J	<V J/MU/V' J+1>	A	E	<V J/MU/V' J-1>	A	E
	ESU-CM	SEC-1	CM-1	ESU-CM	SEC-1	CM-1
0	-2.3254E-21	3.4372E-01	8463.3			
1	-2.4142E-21	4.4513E-01	8475.1	-2.3609E-21	1.0479E 00	8431.6
2	-2.4340E-21	4.8633E-01	8484.1	-2.3448E-21	6.9423E-01	8411.6
3	-2.4540E-21	5.1417E-01	8490.3	-2.3293E-21	6.0280E-01	8388.9
4	-2.4773E-21	5.3616E-01	8493.8	-2.3147E-21	5.6178E-01	8363.5
5	-2.5013E-21	5.5517E-01	8494.5	-2.3007E-21	5.3421E-01	8335.5
6	-2.5272E-21	5.7266E-01	8492.5	-2.2878E-21	5.1289E-01	8304.8
7	-2.5554E-21	5.8947E-01	8487.7	-2.2757E-21	4.9496E-01	8271.4
8	-2.5863E-21	6.0604E-01	8480.1	-2.2647E-21	4.7923E-01	8235.5
9	-2.6200E-21	6.2295E-01	8469.8	-2.2552E-21	4.6512E-01	8196.9
10	-2.6569E-21	6.4044E-01	8456.7	-2.2469E-21	4.5215E-01	8155.8
11	-2.6975E-21	6.5884E-01	8440.8	-2.2405E-21	4.4028E-01	8112.1
12	-2.7426E-21	6.7863E-01	8422.2	-2.2363E-21	4.2946E-01	8065.9
13	-2.7930E-21	6.9991E-01	8400.8	-2.2341E-21	4.1952E-01	8017.3
14	-2.8466E-21	7.2295E-01	8376.7	-2.2349E-21	4.1044E-01	7966.1
15	-2.9067E-21	7.4797E-01	8349.7	-2.2386E-21	4.0274E-01	7912.5
16	-2.9731E-21	7.7560E-01	8320.0	-2.2458E-21	3.9594E-01	7856.4
17	-3.0459E-21	8.0580E-01	8287.5	-2.2566E-21	3.9015E-01	7798.0
18	-3.1261E-21	8.3918E-01	8252.1	-2.2718E-21	3.8562E-01	7737.1
19	-3.2139E-21	8.7579E-01	8213.9	-2.2916E-21	3.8224E-01	7673.8
20	-3.3101E-21	9.1623E-01	8172.8	-2.3169E-21	3.8021E-01	7608.1
21	-3.4151E-21	9.6060E-01	8128.7	-2.3472E-21	3.7941E-01	7540.1
22	-3.5295E-21	1.0093E 00	8081.8	-2.3838E-21	3.8004E-01	7469.6
23	-3.6540E-21	1.0628E 00	8031.8	-2.4269E-21	3.8211E-01	7396.7
24	-3.7894E-21	1.1214E 00	7978.7	-2.4772E-21	3.8571E-01	7321.4
25	-3.9356E-21	1.1851E 00	7922.5	-2.5346E-21	3.9073E-01	7243.6
26	-4.0941E-21	1.2547E 00	7863.1	-2.6005E-21	3.9747E-01	7163.2
27	-4.2652E-21	1.3304E 00	7800.4	-2.6747E-21	4.0576E-01	7080.4
28	-4.4498E-21	1.4124E 00	7734.3	-2.7583E-21	4.1579E-01	6994.9
29	-4.6487E-21	1.5011E 00	7664.8	-2.8513E-21	4.2761E-01	6906.8
30	-4.8633E-21	1.5971E 00	7591.6	-2.9562E-21	4.4134E-01	6816.0
31	-5.0942E-21	1.7005E 00	7514.7	-3.0721E-21	4.5702E-01	6722.4
32	-5.3432E-21	1.8120E 00	7433.9	-3.2012E-21	4.7491E-01	6625.8
33	-5.6117E-21	1.9319E 00	7349.1	-3.3446E-21	4.9515E-01	6526.3
34	-5.9016E-21	2.0608E 00	7260.0	-3.5039E-21	5.1796E-01	6423.6
35	-6.2150E-21	2.1991E 00	7166.5	-3.6815E-21	5.4372E-01	6317.6

MATRIX ELEMENTS, EINSTEIN A'S AND ENERGIES FOR V= 6 TO 11 TRANSITIONS OF HCL

J	P-BRANCH <V J/MU/V' J+1> ESU-CM	P-BRANCH A SEC-1	P-BRANCH E CM-1	R-BRANCH <V J/MU/V' J-1> ESU-CM	R-BRANCH A SEC-1	R-BRANCH E CM-1
0	3.75225E-22	1.6045E-02	10298.8			
1	3.79445E-22	1.9775E-02	10306.0	3.6532E-22	4.5276E-02	10264.8
2	3.83337E-22	2.1669E-02	10312.7	3.5955E-22	2.9060E-02	10244.1
3	3.87104E-22	2.2925E-02	10315.9	3.5321E-22	2.5062E-02	10219.9
4	3.90788E-22	2.3850E-02	10315.6	3.4633E-22	2.2762E-02	10192.2
5	3.94385E-22	2.4618E-02	10311.7	3.3900E-22	2.1009E-02	10161.1
6	3.97737E-22	2.5288E-02	10304.3	3.3111E-22	1.9478E-02	10126.5
7	4.01131E-22	2.5926E-02	10293.4	3.2283E-22	1.8074E-02	10088.6
8	4.05469E-22	2.6556E-02	10279.9	3.1421E-22	1.6751E-02	10047.3
9	4.10778E-22	2.7229E-02	10261.0	3.0543E-22	1.5503E-02	10002.6
10	4.16638E-22	2.7996E-02	10239.5	2.9653E-22	1.4319E-02	9954.6
11	4.24238E-22	2.8876E-02	10214.5	2.8754E-22	1.3194E-02	9903.3
12	4.33190E-22	2.9838E-02	10186.0	2.7846E-22	1.2157E-02	9848.7
13	4.43778E-22	3.1219E-02	10153.9	2.7057E-22	1.1207E-02	9790.9
14	4.56666E-22	3.2787E-02	10118.4	2.6280E-22	1.0347E-02	9729.9
15	4.71018E-22	3.4680E-02	10079.3	2.5580E-22	9.5861E-03	9665.6
16	4.90125E-22	3.7001E-02	10036.7	2.4987E-22	8.9372E-03	9598.2
17	5.11345E-22	3.9787E-02	9990.5	2.4500E-22	8.3883E-03	9527.5
18	5.36268E-22	4.3164E-02	9940.7	2.4165E-22	7.9589E-03	9453.8
19	5.65088E-22	4.7223E-02	9887.2	2.3998E-22	7.6478E-03	9376.8
20	5.98132E-22	5.2090E-02	9830.1	2.4025E-22	7.4599E-03	9296.7
21	6.36278E-22	5.7883E-02	9769.3	2.4265E-22	7.3983E-03	9213.4
22	6.79947E-22	6.4770E-02	9704.7	2.4756E-22	7.4772E-03	9127.0
23	7.28926E-22	7.2907E-02	9636.2	2.5501E-22	7.6950E-03	9037.3
24	7.83208E-22	8.2520E-02	9563.8	2.6559E-22	8.0941E-03	8944.3
25	8.44788E-22	9.3774E-02	9487.4	2.7924E-22	8.6436E-03	8848.0
26	9.13564E-22	1.0696E-01	9406.8	2.9639E-22	9.4049E-03	8748.4
27	9.89855E-22	1.2229E-01	9321.9	3.1712E-22	1.0393E-02	8645.3
28	1.07465E-21	1.4000E-01	9232.6	3.4192E-22	1.1621E-02	8538.6
29	1.16882E-21	1.6067E-01	9138.7	3.7041E-22	1.3137E-02	8428.3
30	1.27178E-21	1.8440E-01	9040.1	4.0435E-22	1.4987E-02	831 .2
31	1.38508E-21	2.1146E-01	8936.5	4.4286E-22	1.7214E-02	8196.3
32	1.51178E-21	2.4280E-01	8827.8	4.8479E-22	1.9873E-02	8074.3
33	1.65088E-21	2.7865E-01	8713.6	5.3676E-22	2.3036E-02	7948.1
34	1.80435E-21	3.1946E-01	8593.8	5.9354E-22	2.6789E-02	7817.4
35	1.97431E-21	3.6609E-01	8467.8	6.5815E-22	3.1244E-02	7682.1

MATRIX ELEMENTS, EINSTEIN A'S AND ENERGIES FOR V= 7 TO 7 TRANSITIONS OF HCL

Pure Rotation

J	<V J/MU/V' J+1>	A	E
	ESU-CM	SEC-1	CM-1
0	1.2851E-18	7.0117E-04	16.6
1	1.2852E-18	7.5774E-03	33.2
2	1.2854E-18	2.7347E-02	49.7
3	1.2856E-18	6.7112E-02	66.3
4	1.2859E-18	1.3377E-01	82.8
5	1.2862E-18	2.3384E-01	99.2
6	1.2866E-18	3.7423E-01	115.6
7	1.2871E-18	5.4001E-01	131.9
8	1.2876E-18	7.3990E-01	148.1
9	1.2883E-18	1.0071E 00	164.2
10	1.2890E-18	1.3574E 00	180.2
11	1.2898E-18	1.7862E 00	196.0
12	1.2906E-18	2.3880E 00	211.8
13	1.2913E-18	2.9665E 00	227.3
14	1.2921E-18	3.6250E 00	242.8
15	1.2931E-18	4.3670E 00	258.0
16	1.2941E-18	5.1944E 00	273.1
17	1.2951E-18	6.1092E 00	287.9
18	1.2962E-18	7.1122E 00	302.6
19	1.2974E-18	8.2038E 00	317.0
20	1.2986E-18	9.3833E 00	331.2
21	1.2997E-18	1.0651E 01	345.1
22	1.3009E-18	1.2003E 01	358.8
23	1.3022E-18	1.3438E 01	372.3
24	1.3034E-18	1.4952E 01	385.4
25	1.3046E-18	1.6541E 01	398.2
26	1.3059E-18	1.8200E 01	410.9
27	1.3071E-18	1.9922E 01	423.0
28	1.3083E-18	2.1702E 01	434.9
29	1.3094E-18	2.3530E 01	446.4
30	1.3105E-18	2.5400E 01	457.6
31	1.3115E-18	2.7299E 01	468.4
32	1.3125E-18	2.9217E 01	478.8
33	1.3133E-18	3.1144E 01	488.9
34	1.3140E-18	3.3067E 01	498.5
35	1.3145E-18	3.4970E 01	507.7

MATRIX ELEMENTS, EINSTEIN A'S AND ENERGIES FOR V= 7 TO 8 TRANSITIONS OF HCL

J	P-BRANCH <V J/MU/V' J+1> ESU-CM	P-BRANCH A SEC-1	P-BRANCH E CM-1	R-BRANCH <V J/MU/V' J-1> ESU-CM	R-BRANCH A SEC-1	R-BRANCH E CM-1
0	1.4709E-19	2.3529E 01	2187.9			
1	1.4388E-19	2.7569E 01	2198.2	1.5349E-19	7.3478E 01	2150.4
2	1.4054E-19	2.8767E 01	2212.7	1.5664E-19	4.9802E 01	2133.1
3	1.3721E-19	2.9974E 01	2226.6	1.5977E-19	4.5464E 01	2115.2
4	1.3394E-19	2.9698E 01	2239.8	1.6287E-19	4.3823E 01	2096.7
5	1.3043E-19	2.9134E 01	2252.2	1.6594E-19	4.3026E 01	2077.5
6	1.2696E-19	2.7380E 01	2264.0	1.6899E-19	4.2571E 01	2057.9
7	1.2345E-19	2.6484E 01	2275.0	1.7201E-19	4.2261E 01	2037.4
8	1.1987E-19	2.5479E 01	2285.2	1.7500E-19	4.2006E 01	2016.5
9	1.1624E-19	2.4388E 01	2294.7	1.7797E-19	4.1759E 01	1995.0
10	1.1255E-19	2.3225E 01	2303.5	1.8091E-19	4.1491E 01	1972.9
11	1.0878E-19	2.2005E 01	2311.5	1.8382E-19	4.1187E 01	1950.4
12	1.0495E-19	2.0738E 01	2318.7	1.8670E-19	4.0836E 01	1927.3
13	1.0104E-19	1.9433E 01	2325.2	1.8955E-19	4.0430E 01	1903.7
14	9.7044E-20	1.8100E 01	2330.9	1.9237E-19	3.9967E 01	1879.6
15	9.2963E-20	1.6748E 01	2335.7	1.9515E-19	3.9444E 01	1855.1
16	8.8789E-20	1.5385E 01	2339.8	1.9789E-19	3.8859E 01	1830.1
17	8.4516E-20	1.4020E 01	2343.0	2.0059E-19	3.8212E 01	1804.7
18	8.0139E-20	1.2662E 01	2345.4	2.0324E-19	3.7505E 01	1778.8
19	7.5650E-20	1.1320E 01	2346.9	2.0585E-19	3.6737E 01	1752.5
20	7.1044E-20	1.0003E 01	2347.6	2.0840E-19	3.5911E 01	1725.8
21	6.6310E-20	8.7213E 00	2347.4	2.1090E-19	3.5029E 01	1698.7
22	6.1443E-20	7.4944E 00	2346.2	2.1333E-19	3.4092E 01	1671.3
23	5.6432E-20	6.3021E 00	2344.2	2.1569E-19	3.3104E 01	1643.4
24	5.1268E-20	5.1456E 00	2341.1	2.1799E-19	3.2068E 01	1615.2
25	4.5930E-20	4.1455E 00	2337.1	2.2020E-19	3.0987E 01	1586.5
26	4.0436E-20	3.1933E 00	2332.1	2.2233E-19	2.9865E 01	1557.5
27	3.4743E-20	2.3406E 00	2326.0	2.2437E-19	2.8704E 01	1528.1
28	2.8848E-20	1.5999E 00	2319.9	2.2631E-19	2.7510E 01	1498.3
29	2.2735E-20	9.8372E-01	2310.7	2.2814E-19	2.6286E 01	1468.2
30	1.6386E-20	5.0511E-01	2301.4	2.2986E-19	2.5037E 01	1437.6
31	9.7828E-21	1.7747E-01	2290.9	2.3144E-19	2.3767E 01	1406.7
32	2.9052E-21	1.5438E-02	2279.2	2.3289E-19	2.2481E 01	1375.4
33	-4.2714E-21	3.2823E-02	2266.3	2.3418E-19	2.1183E 01	1343.6
34	-1.1772E-20	2.4477E-01	2252.1	2.3530E-19	1.9878E 01	1311.5
35	-1.9625E-20	6.6659E-01	2236.6	2.3622E-19	1.8572E 01	1278.9

MATRIX ELEMENTS, EINSTEIN A'S AND ENERGIES FOR V= 7 TO 9 TRANSITIONS OF HCL

J	P-BRANCH <V J/MU/V' J+1> ESU-CM	A SEC-1	F CM-1	R-BRANCH <V J/MU/V' J-1> ESU-CM	A SEC-1	F CM-1
0	-6.25898E-21	3.7586E 01	4243.1			
1	-6.8247E-20	4.5079E 01	4256.9	-6.9365E-20	1.1271E 02	4211.2
2	-6.7914E-20	4.8251E 01	4269.4	-6.9780E-20	7.5075E 01	4193.3
3	-6.7601E-20	4.9965E 01	4280.5	-7.0218E-20	6.7479E 01	4174.0
4	-6.7306E-20	5.1003E 01	4290.2	-7.0680E-20	6.4153E 01	4153.4
5	-6.7028E-20	5.1656E 01	4298.5	-7.1166E-20	6.2235E 01	4131.4
6	-6.6768E-20	5.2074E 01	4305.3	-7.1678E-20	6.0945E 01	4108.2
7	-6.6524E-20	5.2327E 01	4310.8	-7.2216E-20	5.9983E 01	4083.7
8	-6.6295E-20	5.2457E 01	4314.8	-7.2782E-20	5.9210E 01	4057.9
9	-6.6082E-20	5.2491E 01	4317.4	-7.3376E-20	5.8553E 01	4030.8
10	-6.5883E-20	5.2465E 01	4318.6	-7.4000E-20	5.7967E 01	4002.6
11	-6.5697E-20	5.2330E 01	4318.4	-7.4656E-20	5.7431E 01	3973.1
12	-6.5525E-20	5.2156E 01	4316.7	-7.5344E-20	5.6925E 01	3942.4
13	-6.5366E-20	5.1925E 01	4313.5	-7.6067E-20	5.6438E 01	3910.6
14	-6.5215E-20	5.1642E 01	4309.0	-7.6826E-20	5.5965E 01	3877.6
15	-6.5074E-20	5.1309E 01	4302.9	-7.7622E-20	5.5499E 01	3843.5
16	-6.4946E-20	5.0927E 01	4295.4	-7.8457E-20	5.5036E 01	3808.2
17	-6.4824E-20	5.0498E 01	4286.4	-7.9334E-20	5.4573E 01	3771.9
18	-6.4708E-20	5.0020E 01	4275.9	-8.0255E-20	5.4110E 01	3734.4
19	-6.4598E-20	4.9493E 01	4263.9	-8.1221E-20	5.3643E 01	3695.9
20	-6.4492E-20	4.8919E 01	4250.3	-8.2236E-20	5.3171E 01	3656.3
21	-6.4386E-20	4.8291E 01	4235.2	-8.3301E-20	5.2693E 01	3615.7
22	-6.4282E-20	4.7612E 01	4218.4	-8.4419E-20	5.2209E 01	3573.9
23	-6.4174E-20	4.6878E 01	4200.1	-8.5594E-20	5.1715E 01	3531.2
24	-6.4062E-20	4.6087E 01	4180.1	-8.6827E-20	5.1211E 01	3487.3
25	-6.3942E-20	4.5237E 01	4158.4	-8.8123E-20	5.0696E 01	3442.4
26	-6.3810E-20	4.4323E 01	4134.9	-8.9484E-20	5.0167E 01	3396.4
27	-6.3664E-20	4.3344E 01	4109.6	-9.0914E-20	4.9623E 01	3349.3
28	-6.3498E-20	4.2297E 01	4082.5	-9.2417E-20	4.9062E 01	3301.1
29	-6.3309E-20	4.1178E 01	4053.5	-9.3997E-20	4.8480E 01	3251.8
30	-6.3091E-20	3.9984E 01	4022.5	-9.5659E-20	4.7877E 01	3201.2
31	-6.2838E-20	3.8713E 01	3989.4	-9.7409E-20	4.7249E 01	3149.5
32	-6.2542E-20	3.7361E 01	3954.2	-9.9251E-20	4.6594E 01	3096.4
33	-6.2196E-20	3.5927E 01	3916.8	-1.0119E-19	4.5910E 01	3042.1
34	-6.1790E-20	3.4406E 01	3877.1	-1.0324E-19	4.5193E 01	2986.5
35	-6.1312E-20	3.2798E 01	3835.1	-1.0541E-19	4.4441E 01	2929.5

MATRIX ELEMENTS, EINSTEIN A'S AND ENERGIES FOR V= 7 TO 10 TRANSITIONS OF HCL

J	R-BRANCH <V J/MU/V" J+1> ESU-CM	R-BRANCH A SEC-1	R-BRANCH E CM-1	P-BRANCH <V J/MU/V" J-1> ESU-CM	P-BRANCH A SEC-1	P-BRANCH E CM-1
0	1.6404E-20	6.6903E 00	6102.3			
1	1.6436E-20	8.0956E 00	6204.7	1.6363E-20	1.9642E 01	6161.2
2	1.6474E-20	8.7583E 00	6215.0	1.6353E-20	1.2960E 01	6142.5
3	1.6521E-20	9.1704E 00	6223.1	1.6351E-20	1.1543E 01	6121.7
4	1.6576E-20	9.4686E 00	6229.2	1.6356E-20	1.0877E 01	6098.9
5	1.6639E-20	9.7057E 00	6233.1	1.6368E-20	1.0462E 01	6074.1
6	1.6710E-20	9.9067E 00	6234.9	1.6388E-20	1.0161E 01	6047.2
7	1.6792E-20	1.0086E 01	6234.5	1.6417E-20	9.9225E 00	6018.3
8	1.6883E-20	1.0260E 01	6232.0	1.6454E-20	9.7212E 00	5987.4
9	1.6983E-20	1.0404E 01	6227.4	1.6500E-20	9.5451E 00	5954.6
10	1.7095E-20	1.0553E 01	6220.7	1.6556E-20	9.3872E 00	5919.8
11	1.7218E-20	1.0698E 01	6211.8	1.6622E-20	9.2433E 00	5883.1
12	1.7353E-20	1.0843E 01	6200.7	1.6700E-20	9.1111E 00	5844.5
13	1.7502E-20	1.0988E 01	6187.5	1.6790E-20	8.9895E 00	5804.0
14	1.7664E-20	1.1135E 01	6172.2	1.6893E-20	8.8767E 00	5761.6
15	1.7840E-20	1.1286E 01	6154.7	1.7009E-20	8.7729E 00	5717.4
16	1.8031E-20	1.1437E 01	6135.0	1.7142E-20	8.6779E 00	5671.4
17	1.8238E-20	1.1595E 01	6113.1	1.7291E-20	8.5918E 00	5623.6
18	1.8462E-20	1.1759E 01	6089.0	1.7459E-20	8.5145E 00	5574.0
19	1.8704E-20	1.1927E 01	6062.7	1.7645E-20	8.4466E 00	5522.6
20	1.8963E-20	1.2102E 01	6034.0	1.7853E-20	8.3879E 00	5469.4
21	1.9242E-20	1.2283E 01	6003.1	1.8083E-20	8.3391E 00	5414.5
22	1.9540E-20	1.2469E 01	5969.9	1.8339E-20	8.3002E 00	5357.7
23	1.9859E-20	1.2661E 01	5934.2	1.8621E-20	8.2718E 00	5299.1
24	2.0199E-20	1.2858E 01	5896.1	1.8932E-20	8.2538E 00	5238.8
25	2.0561E-20	1.3059E 01	5855.5	1.9274E-20	8.2463E 00	5176.6
26	2.0944E-20	1.3263E 01	5812.3	1.9649E-20	8.2495E 00	5112.5
27	2.1351E-20	1.3469E 01	5766.5	2.0060E-20	8.2637E 00	5046.5
28	2.1781E-20	1.3674E 01	5717.9	2.0509E-20	8.2883E 00	4978.6
29	2.2234E-20	1.3876E 01	5666.6	2.1000E-20	8.3235E 00	4908.6
30	2.2711E-20	1.4072E 01	5612.3	2.1536E-20	8.3690E 00	4836.7
31	2.3211E-20	1.4260E 01	5554.9	2.2119E-20	8.4244E 00	4762.5
32	2.3736E-20	1.4436E 01	5494.3	2.2755E-20	8.4895E 00	4686.2
33	2.4284E-20	1.4596E 01	5430.5	2.3447E-20	8.5642E 00	4607.6
34	2.4855E-20	1.4735E 01	5363.1	2.4203E-20	8.6479E 00	4526.6
35	2.5450E-20	1.4848E 01	5292.1	2.5027E-20	8.7410E 00	4443.1

MATRIX ELEMENTS, EINSTEIN A'S AND ENERGIES FOR V= 7 TO 11 TRANSITIONS OF HCL

J	P-BRANCH <V J/MU/V' J+1> ESU-CM	P-BRANCH A SEC-1	P-BRANCH E CM-1	R-BRANCH <V J/MU/V' J-1> ESU-CM	R-BRANCH A SEC-1	R-BRANCH E CM-1
0	-3.0714E-21	9.5225E-01	8024.0			
1	-4.0344E-21	1.0338E 00	8035.6	-3.9251E-21	9.6630E 00	7994.4
2	-4.0334E-21	1.1335E 00	8043.5	-3.9029E-21	1.6163E 00	7975.0
3	-4.0513E-21	1.1634E 00	8049.7	-3.8834E-21	1.4275E 00	7952.7
4	-4.0824E-21	1.2400E 00	8050.9	-3.8641E-21	1.3334E 00	7927.6
5	-4.1156E-21	1.2702E 00	8050.3	-3.8461E-21	1.2707E 00	7899.6
6	-4.1500E-21	1.3140E 00	8046.7	-3.8292E-21	1.2223E 00	7868.9
7	-4.1848E-21	1.3468E 00	8040.2	-3.8140E-21	1.1818E 00	7835.5
8	-4.2196E-21	1.3785E 00	8030.9	-3.8002E-21	1.1461E 00	7799.2
9	-4.2538E-21	1.4099E 00	8018.6	-3.7884E-21	1.1138E 00	7760.3
10	-4.2870E-21	1.4420E 00	8003.5	-3.7790E-21	1.0841E 00	7718.6
11	-4.3189E-21	1.4753E 00	7985.4	-3.7718E-21	1.0564E 00	7674.3
12	-4.3493E-21	1.5104E 00	7964.5	-3.7673E-21	1.0308E 00	7627.3
13	-4.3780E-21	1.5474E 00	7940.7	-3.7653E-21	1.0072E 00	7577.6
14	-4.4048E-21	1.5861E 00	7913.9	-3.7707E-21	9.8548E-01	7525.4
15	-4.4298E-21	1.6319E 00	7884.3	-3.7786E-21	9.6557E-01	7470.6
16	-4.4526E-21	1.6797E 00	7851.7	-3.7918E-21	9.4824E-01	7413.2
17	-4.4737E-21	1.7321E 00	7816.1	-3.8100E-21	9.3299E-01	7353.2
18	-4.4934E-21	1.7907E 00	7777.6	-3.8365E-21	9.2009E-01	7290.7
19	-5.1145E-21	1.8530E 00	7736.0	-3.8695E-21	9.0978E-01	7225.6
20	-5.2520E-21	1.9225E 00	7691.4	-3.9107E-21	9.0220E-01	7159.0
21	-5.4031E-21	1.9992E 00	7643.7	-3.9610E-21	8.9753E-01	7087.8
22	-5.5686E-21	2.0833E 00	7592.8	-4.0213E-21	8.9586E-01	7015.1
23	-5.7493E-21	2.1757E 00	7538.7	-4.0928E-21	8.9753E-01	6939.7
24	-5.9467E-21	2.2767E 00	7481.2	-4.1763E-21	9.0260E-01	6861.7
25	-6.1620E-21	2.3871E 00	7420.4	-4.2731E-21	9.1112E-01	6781.0
26	-6.3964E-21	2.5075E 00	7356.0	-4.3845E-21	9.2355E-01	6697.6
27	-6.6511E-21	2.6384E 00	7288.0	-4.5119E-21	9.4001E-01	6611.4
28	-6.9273E-21	2.7801E 00	7216.2	-4.6566E-21	9.6066E-01	6522.2
29	-7.2270E-21	2.9333E 00	7140.5	-4.8204E-21	9.8583E-01	6430.1
30	-7.5515E-21	3.0981E 00	7060.7	-5.0050E-21	1.0157E 00	6334.9
31	-7.9026E-21	3.2747E 00	6976.7	-5.2126E-21	1.0505E 00	6236.5
32	-8.2813E-21	3.4631E 00	6888.2	-5.4452E-21	1.0906E 00	6134.7
33	-8.6917E-21	3.6633E 00	6795.0	-5.7050E-21	1.1364E 00	6029.4
34	-9.1342E-21	3.8745E 00	6696.8	-5.9977E-21	1.1882E 00	5920.5
35	-9.6119E-21	4.0962E 00	6593.4	-6.3245E-21	1.2466E 00	5807.6

MATRIX ELEMENTS, EINSTEIN A'S AND ENERGIES FOR V= 7 TO 12 TRANSITIONS OF HCL

J	P-BRANCH <V J/MU/V' J+1> ESU-CM	P-BRANCH A SEC-1	P-BRANCH E CM-1	R-BRANCH <V J/MU/V' J-1> ESU-CM	R-BRANCH A SEC-1	R-BRANCH E CM-1
0	9.6078E-22	8.8989E-02	9733.1			
1	9.6857E-22	1.0984E-01	9742.4	9.4336E-22	2.5504E-01	9703.6
2	9.7603E-22	1.1862E-01	9747.9	9.3374E-22	1.6554E-01	9683.3
3	9.8308E-22	1.2487E-01	9749.8	9.2335E-22	1.4461E-01	9659.4
4	9.8989E-22	1.2946E-01	9748.0	9.1236E-22	1.3332E-01	9631.9
5	9.9728E-22	1.3314E-01	9742.6	9.0071E-22	1.2510E-01	9600.8
6	1.0047E-21	1.3625E-01	9733.4	8.8836E-22	1.1819E-01	9566.1
7	1.0127E-21	1.3904E-01	9720.5	8.7554E-22	1.1198E-01	9527.8
8	1.0216E-21	1.4169E-01	9703.9	8.6241E-22	1.0620E-01	9485.9
9	1.0317E-21	1.4435E-01	9683.6	8.4902E-22	1.0071E-01	9440.5
10	1.0434E-21	1.4720E-01	9659.6	8.3559E-22	9.5481E-02	9391.6
11	1.0570E-21	1.5022E-01	9631.9	8.2227E-22	9.0490E-02	9339.3
12	1.0732E-21	1.5392E-01	9600.6	8.0944E-22	8.5785E-02	9283.4
13	1.0920E-21	1.5805E-01	9565.4	7.9705E-22	8.1324E-02	9224.2
14	1.1143E-21	1.6294E-01	9526.6	7.8575E-22	7.7212E-02	9161.5
15	1.1405E-21	1.6873E-01	9484.0	7.7572E-22	7.3454E-02	9095.3
16	1.1711E-21	1.7564E-01	9437.6	7.6740E-22	7.0100E-02	9025.8
17	1.2067E-21	1.8381E-01	9387.4	7.6089E-22	6.7132E-02	8952.9
18	1.2481E-21	1.9355E-01	9333.4	7.5689E-22	6.4635E-02	8876.6
19	1.2958E-21	2.0502E-01	9275.5	7.5554E-22	6.2593E-02	8796.9
20	1.3507E-21	2.1860E-01	9213.7	7.5780E-22	6.1117E-02	8713.9
21	1.4133E-21	2.3448E-01	9147.9	7.6362E-22	6.0156E-02	8627.3
22	1.4845E-21	2.5306E-01	9077.9	7.7372E-22	5.9779E-02	8537.4
23	1.5653E-21	2.7474E-01	9003.8	7.8857E-22	6.0018E-02	8443.9
24	1.6565E-21	2.9996E-01	8925.3	8.0877E-22	6.0924E-02	8346.8
25	1.7589E-21	3.2911E-01	8842.4	8.3487E-22	6.2545E-02	8246.1
26	1.8738E-21	3.6281E-01	8754.9	8.6784E-22	6.4996E-02	8141.7
27	2.0025E-21	4.0162E-01	8662.6	9.0804E-22	6.8305E-02	8033.4
28	2.1458E-21	4.4606E-01	8565.3	9.5633E-22	7.2583E-02	7921.1
29	2.3054E-21	4.9700E-01	8462.9	1.0139E-21	7.7988E-02	7804.7
30	2.4833E-21	5.5506E-01	8354.8	1.0813E-21	8.4604E-02	7684.0
31	2.6807E-21	6.2104E-01	8241.0	1.1601E-21	9.2646E-02	7558.8
32	2.8998E-21	6.9576E-01	8121.1	1.2514E-21	1.0228E-01	7428.8
33	3.1429E-21	7.8008E-01	7994.6	1.3567E-21	1.1373E-01	7293.7
34	3.4125E-21	8.7477E-01	7861.3	1.4781E-21	1.2729E-01	7153.4
35	3.7116E-21	9.8057E-01	7720.4	1.6178E-21	1.4328E-01	7007.3

MATRIX ELEMENTS, EINSTEIN A'S AND ENERGIES FOR V= 0 TO 0 TRANSITIONS OF HCL

Pure Rotation

J	<V J/M(1)/V' J+1>	A	E
	ESU-CM	SEC-1	CM-1
0	1.2954E-18	7.1516E-04	15.9
1	1.2955E-18	6.3485E-03	31.8
2	1.2956E-18	2.4723E-02	47.8
3	1.2957E-18	6.0662E-02	63.6
4	1.2959E-18	1.2084E-01	79.5
5	1.3001E-18	2.1131E-01	95.2
6	1.3003E-18	3.3801E-01	110.9
7	1.3006E-18	5.0645E-01	126.6
8	1.3009E-18	7.2210E-01	142.1
9	1.3013E-18	9.8597E-01	157.6
10	1.3017E-18	1.3147E 00	172.9
11	1.3021E-18	1.7007E 00	188.2
12	1.3025E-18	2.1519E 00	203.3
13	1.3030E-18	2.6713E 00	218.2
14	1.3035E-18	3.2621E 00	233.0
15	1.3040E-18	3.9266E 00	247.6
16	1.3045E-18	4.6661E 00	262.1
17	1.3051E-18	5.4816E 00	276.3
18	1.3057E-18	6.3742E 00	290.3
19	1.3062E-18	7.3423E 00	304.1
20	1.3068E-18	8.3857E 00	317.7
21	1.3073E-18	9.5017E 00	331.0
22	1.3079E-18	1.0688E 01	344.0
23	1.3084E-18	1.1941E 01	356.8
24	1.3089E-18	1.3257E 01	369.2
25	1.3092E-18	1.4630E 01	381.4
26	1.3095E-18	1.6053E 01	393.2
27	1.3097E-18	1.7521E 01	404.7
28	1.3099E-18	1.9024E 01	415.9
29	1.3098E-18	2.0555E 01	426.7
30	1.3097E-18	2.2104E 01	437.1
31	1.3093E-18	2.3660E 01	447.1
32	1.3087E-18	2.5210E 01	456.7
33	1.3079E-18	2.6743E 01	465.9
34	1.3068E-18	2.8243E 01	474.7
35	1.3053E-18	2.9695E 01	483.0

MATRIX ELEMENTS, EINSTEIN A'S AND ENERGIES FOR V= 8 TO 9 TRANSITIONS OF HCL

J	R-BRANCH <V J/MU/V' J+1>	R-BRANCH A	R-BRANCH E	P-BRANCH <V J/MU/V' J-1>	P-BRANCH A	P-BRANCH E
	ESU-CM	SEC-1	CM-1	ESU-CM	SEC-1	CM-1
0	1.3947E-19	1.7939E 01	2076.1			
1	1.3494E-19	2.0876E 01	2090.6	1.4538E-19	5.6689E 01	2044.9
2	1.3136E-19	2.1619E 01	2104.4	1.4876E-19	3.8615E 01	2028.3
3	1.2772E-19	2.1592E 01	2117.5	1.5210E-19	3.5410E 01	2011.0
4	1.2402E-19	2.1199E 01	2129.9	1.5540E-19	3.4266E 01	1993.1
5	1.2026E-19	2.0561E 01	2141.5	1.5865E-19	3.3761E 01	1974.4
6	1.1643E-19	1.9783E 01	2152.3	1.6187E-19	3.3504E 01	1955.2
7	1.1252E-19	1.8897E 01	2162.4	1.6504E-19	3.3346E 01	1935.3
8	1.0854E-19	1.7928E 01	2171.7	1.6817E-19	3.3216E 01	1914.8
9	1.0447E-19	1.6895E 01	2180.3	1.7127E-19	3.3077E 01	1893.7
10	1.0031E-19	1.5813E 01	2188.1	1.7432E-19	3.2908E 01	1872.0
11	9.6061E-20	1.4693E 01	2195.0	1.7732E-19	3.2696E 01	1849.8
12	9.1709E-20	1.3547E 01	2201.2	1.8028E-19	3.2432E 01	1826.9
13	8.7251E-20	1.2385E 01	2206.6	1.8319E-19	3.2112E 01	1803.6
14	8.2679E-20	1.1215E 01	2211.1	1.8604E-19	3.1733E 01	1779.7
15	7.7987E-20	1.0049E 01	2214.8	1.8884E-19	3.1292E 01	1755.3
16	7.3166E-20	8.8950E 00	2217.7	1.9158E-19	3.0789E 01	1730.5
17	6.8210E-20	7.7639E 00	2219.7	1.9425E-19	3.0226E 01	1705.1
18	6.3109E-20	6.6657E 00	2220.8	1.9685E-19	2.9601E 01	1679.3
19	5.7854E-20	5.6109E 00	2221.0	1.9937E-19	2.8918E 01	1653.1
20	5.2437E-20	4.6126E 00	2220.3	2.0180E-19	2.8178E 01	1626.4
21	4.6846E-20	3.6757E 00	2218.7	2.0414E-19	2.7383E 01	1599.2
22	4.1071E-20	2.8183E 00	2216.2	2.0638E-19	2.6537E 01	1571.7
23	3.5098E-20	2.0502E 00	2212.7	2.0850E-19	2.5642E 01	1543.8
24	2.8915E-20	1.3841E 00	2208.2	2.1051E-19	2.4701E 01	1515.4
25	2.2507E-20	8.3295E-01	2202.6	2.1238E-19	2.3720E 01	1486.7
26	1.5858E-20	4.1008E-01	2196.0	2.1412E-19	2.2700E 01	1457.6
27	8.9504E-21	1.2935E-01	2188.3	2.1569E-19	2.1648E 01	1428.0
28	1.7635E-21	4.9635E-03	2179.5	2.1710E-19	2.0567E 01	1398.1
29	-5.7236E-21	5.1597E-02	2169.4	2.1832E-19	1.9461E 01	1367.7
30	-1.3537E-20	2.8428E-01	2158.2	2.1936E-19	1.8337E 01	1336.9
31	-2.1703E-20	7.1847E-01	2145.6	2.2019E-19	1.7198E 01	1305.7
32	-3.0254E-20	1.3698E 00	2131.7	2.2072E-19	1.6049E 01	1274.0
33	-3.9223E-20	2.2543E 00	2116.5	2.2103E-19	1.4897E 01	1241.8
34	-4.8652E-20	3.3881E 00	2099.7	2.2109E-19	1.3747E 01	1209.1
35	-5.8584E-20	4.7874E 00	2081.4	2.2075E-19	1.2604E 01	1175.8

MATRIX ELEMENTS, EINSTEIN A'S AND ENERGIES FOR V= 8 TO 10 TRANSITIONS OF HCL

J	R-BRANCH <V J/MU/V' J+1> ESU-CM	R-BRANCH A SEC-1	R-BRANCH E CM-1	P-BRANCH <V J/MU/V' J-1> ESU-CM	P-BRANCH A SEC-1	P-BRANCH E CM-1
0	-8.0210E-20	4.3891E 01	4025.3			
1	-7.9766E-20	5.2574E 01	4038.4	-8.1227E-20	1.3194E 02	3994.9
2	-7.9326E-20	5.4139E 01	4050.0	-8.1765E-20	9.7970E 01	3977.5
3	-7.8890E-20	5.8064E 01	4060.2	-8.2330E-20	7.9142E 01	3958.8
4	-7.8511E-20	6.0139E 01	4068.9	-8.2924E-20	7.5302E 01	3938.6
5	-7.8134E-20	5.9852E 01	4076.1	-8.3547E-20	7.3103E 01	3917.1
6	-7.7775E-20	6.0218E 01	4081.9	-8.4202E-20	7.1632E 01	3894.2
7	-7.7434E-20	6.0381E 01	4086.2	-8.4888E-20	7.0537E 01	3869.9
8	-7.7110E-20	6.0206E 01	4089.0	-8.5609E-20	6.9656E 01	3844.3
9	-7.6801E-20	6.0288E 01	4090.3	-8.6364E-20	6.8902E 01	3817.4
10	-7.6504E-20	6.0079E 01	4090.1	-8.7156E-20	6.8227E 01	3789.2
11	-7.6224E-20	5.9780E 01	4088.4	-8.7987E-20	6.7599E 01	3759.7
12	-7.5958E-20	5.9401E 01	4085.3	-8.8857E-20	6.7000E 01	3729.0
13	-7.5692E-20	5.8966E 01	4080.6	-8.9770E-20	6.6416E 01	3697.0
14	-7.5440E-20	5.8429E 01	4074.3	-9.0726E-20	6.5838E 01	3663.8
15	-7.5196E-20	5.7824E 01	4066.6	-9.1729E-20	6.5260E 01	3629.3
16	-7.4958E-20	5.7163E 01	4057.3	-9.2779E-20	6.4677E 01	3593.7
17	-7.4721E-20	5.6436E 01	4046.4	-9.3881E-20	6.4086E 01	3556.9
18	-7.4477E-20	5.5637E 01	4033.9	-9.5035E-20	6.3483E 01	3518.9
19	-7.4227E-20	5.4772E 01	4019.8	-9.6246E-20	6.2867E 01	3479.8
20	-7.3962E-20	5.3838E 01	4004.1	-9.7515E-20	6.2237E 01	3439.5
21	-7.3686E-20	5.2843E 01	3986.7	-9.8846E-20	6.1589E 01	3398.0
22	-7.3398E-20	5.1756E 01	3967.5	-1.0024E-19	6.0923E 01	3355.5
23	-7.3104E-20	5.0603E 01	3946.9	-1.0171E-19	6.0237E 01	3311.7
24	-7.2804E-20	4.9373E 01	3924.2	-1.0325E-19	5.9530E 01	3266.9
25	-7.2502E-20	4.8063E 01	3899.8	-1.0487E-19	5.8800E 01	3220.8
26	-7.2198E-20	4.6670E 01	3873.4	-1.0657E-19	5.8044E 01	3173.6
27	-7.1892E-20	4.5191E 01	3845.2	-1.0835E-19	5.7260E 01	3125.2
28	-7.1588E-20	4.3623E 01	3816.0	-1.1023E-19	5.6445E 01	3075.5
29	-7.0989E-20	4.1964E 01	3782.5	-1.1221E-19	5.5597E 01	3024.6
30	-7.0344E-20	4.0209E 01	3748.0	-1.1429E-19	5.4712E 01	2972.4
31	-6.9713E-20	3.8357E 01	3711.1	-1.1648E-19	5.3784E 01	2918.9
32	-6.9096E-20	3.6405E 01	3671.9	-1.1880E-19	5.2809E 01	2863.8
33	-6.8496E-20	3.4354E 01	3630.1	-1.2124E-19	5.1782E 01	2807.3
34	-6.7911E-20	3.2201E 01	3585.7	-1.2381E-19	5.0697E 01	2749.2
35	-6.7107E-20	2.9940E 01	3538.4	-1.2652E-19	4.9547E 01	2689.5

MATRIX ELEMENTS, EINSTEIN A'S AND ENERGIES FOR V= 8 TO 11 TRANSITIONS OF HCL

	P-BRANCH			P-BRANCH		
J	<V J/MU/V' J+1>	A	E	<V J/MU/V' J-1>	A	E
	ESU-CM	SEC-1	CM-1	ESU-CM	SEC-1	CM-1
0	2.1866E-20	1.0048E 01	5857.8			
1	2.1892E-20	1.2159E 01	5869.3	2.1844E-20	2.9627E 01	5828.1
2	2.1929E-20	1.3132E 01	5878.6	2.1847E-20	1.9574E 01	5810.0
3	2.1975E-20	1.3726E 01	5885.8	2.1861E-20	1.7455E 01	5789.7
4	2.2033E-20	1.4147E 01	5890.6	2.1885E-20	1.6467E 01	5767.3
5	2.2101E-20	1.4473E 01	5893.3	2.1920E-20	1.5856E 01	5742.7
6	2.2182E-20	1.4744E 01	5893.7	2.1965E-20	1.5416E 01	5715.9
7	2.2274E-20	1.4979E 01	5891.9	2.2022E-20	1.5066E 01	5687.1
8	2.2380E-20	1.5188E 01	5887.8	2.2091E-20	1.4773E 01	5656.1
9	2.2499E-20	1.5382E 01	5881.5	2.2173E-20	1.4516E 01	5623.1
10	2.2632E-20	1.5564E 01	5872.9	2.2269E-20	1.4285E 01	5588.1
11	2.2780E-20	1.5738E 01	5862.1	2.2379E-20	1.4074E 01	5550.9
12	2.2944E-20	1.5908E 01	5849.0	2.2506E-20	1.3880E 01	5511.8
13	2.3124E-20	1.6075E 01	5833.7	2.2649E-20	1.3698E 01	5470.7
14	2.3322E-20	1.6240E 01	5816.1	2.2811E-20	1.3530E 01	5427.5
15	2.3538E-20	1.6406E 01	5796.2	2.2993E-20	1.3374E 01	5382.5
16	2.3773E-20	1.6574E 01	5773.9	2.3196E-20	1.3230E 01	5335.4
17	2.4028E-20	1.6743E 01	5749.4	2.3423E-20	1.3098E 01	5286.5
18	2.4305E-20	1.6915E 01	5722.5	2.3677E-20	1.2978E 01	5235.6
19	2.4603E-20	1.7090E 01	5693.2	2.3957E-20	1.2870E 01	5182.8
20	2.4923E-20	1.7266E 01	5661.5	2.4268E-20	1.2775E 01	5128.1
21	2.5267E-20	1.7445E 01	5627.3	2.4612E-20	1.2693E 01	5071.4
22	2.5634E-20	1.7624E 01	5590.6	2.4991E-20	1.2625E 01	5012.8
23	2.6027E-20	1.7803E 01	5551.3	2.5409E-20	1.2571E 01	4952.3
24	2.6445E-20	1.7980E 01	5509.3	2.5868E-20	1.2531E 01	4889.8
25	2.6888E-20	1.8154E 01	5464.6	2.6373E-20	1.2505E 01	4825.3
26	2.7358E-20	1.8320E 01	5417.1	2.6927E-20	1.2494E 01	4758.7
27	2.7855E-20	1.8478E 01	5366.6	2.7536E-20	1.2499E 01	4690.0
28	2.8378E-20	1.8622E 01	5313.1	2.8203E-20	1.2518E 01	4619.2
29	2.8928E-20	1.8748E 01	5256.4	2.8934E-20	1.2552E 01	4546.1
30	2.9504E-20	1.8852E 01	5196.4	2.9736E-20	1.2601E 01	4470.6
31	3.0105E-20	1.8926E 01	5132.9	3.0615E-20	1.2663E 01	4392.7
32	3.0729E-20	1.8962E 01	5065.7	3.1578E-20	1.2740E 01	4312.2
33	3.1371E-20	1.8953E 01	4994.6	3.2635E-20	1.2828E 01	4229.1
34	3.2030E-20	1.8885E 01	4919.4	3.3793E-20	1.2927E 01	4143.1
35	3.2699E-20	1.8749E 01	4839.7	3.5065E-20	1.3034E 01	4054.0

MATRIX ELEMENTS, EINSTEIN A'S AND ENERGIES FOR V= 8 TO 12 TRANSITIONS OF HCL

J	R-BRANCH <V J/MU/V' J+1> ESU-CM	R-BRANCH A SEC-1	R-BRANCH E CM-1	P-BRANCH <V J/MU/V' J-1> ESU-CM	P-BRANCH A SEC-1	P-BRANCH E CM-1
0	-6.2061E-21	1.7442E 00	7556.1			
1	-6.2288E-21	2.1245E 00	7576.1	-6.1479E-21	5.0763E 00	7537.2
2	-6.2741E-21	2.3073E 00	7583.0	-6.1219E-21	3.3304E 00	7518.3
3	-6.3123E-21	2.4257E 00	7586.9	-6.0979E-21	2.9481E 00	7496.4
4	-6.3538E-21	2.5144E 00	7587.7	-6.0760E-21	2.7599E 00	7471.6
5	-6.3991E-21	2.5874E 00	7585.6	-6.0563E-21	2.6362E 00	7443.8
6	-6.4485E-21	2.6513E 00	7580.4	-6.0389E-21	2.5417E 00	7413.0
7	-6.5033E-21	2.7100E 00	7572.1	-6.0242E-21	2.4630E 00	7379.4
8	-6.5626E-21	2.7657E 00	7560.8	-6.0120E-21	2.3939E 00	7342.8
9	-6.6285E-21	2.8204E 00	7546.5	-6.0032E-21	2.3313E 00	7303.4
10	-6.7014E-21	2.8753E 00	7529.1	-5.9981E-21	2.2737E 00	7261.1
11	-6.7820E-21	2.9315E 00	7508.6	-5.9971E-21	2.2202E 00	7215.9
12	-6.8713E-21	2.9903E 00	7485.1	-6.0011E-21	2.1705E 00	7168.0
13	-6.9702E-21	3.0523E 00	7458.4	-6.0106E-21	2.1243E 00	7117.2
14	-7.0800E-21	3.1188E 00	7428.7	-6.0266E-21	2.0818E 00	7063.6
15	-7.2014E-21	3.1906E 00	7395.9	-6.0497E-21	2.0430E 00	7007.2
16	-7.3362E-21	3.2688E 00	7359.9	-6.0815E-21	2.0083E 00	6946.1
17	-7.4849E-21	3.3540E 00	7320.7	-6.1223E-21	1.9777E 00	6886.2
18	-7.6494E-21	3.4474E 00	7278.3	-6.1741E-21	1.9519E 00	6821.5
19	-7.8307E-21	3.5499E 00	7232.7	-6.2377E-21	1.9309E 00	6754.1
20	-8.0302E-21	3.6620E 00	7183.8	-6.3147E-21	1.9153E 00	6683.9
21	-8.2497E-21	3.7851E 00	7131.4	-6.4067E-21	1.9053E 00	6610.9
22	-8.4901E-21	3.9194E 00	7075.7	-6.5151E-21	1.9011E 00	6535.1
23	-8.7534E-21	4.0660E 00	7016.4	-6.6420E-21	1.9035E 00	6456.5
24	-9.0414E-21	4.2257E 00	6953.4	-6.7889E-21	1.9125E 00	6374.9
25	-9.3553E-21	4.3985E 00	6886.7	-6.9583E-21	1.9286E 00	6290.4
26	-9.6974E-21	4.5852E 00	6816.0	-7.1526E-21	1.9523E 00	6202.9
27	-1.0070E-20	4.7861E 00	6741.3	-7.3741E-21	1.9840E 00	6112.1
28	-1.0474E-20	5.0011E 00	6662.3	-7.6261E-21	2.0241E 00	6018.1
29	-1.0912E-20	5.2300E 00	6578.7	-7.9119E-21	2.0733E 00	5920.7
30	-1.1388E-20	5.4726E 00	6490.5	-8.2353E-21	2.1320E 00	5819.7
31	-1.1903E-20	5.7273E 00	6397.2	-8.6009E-21	2.2010E 00	5715.0
32	-1.2459E-20	5.9926E 00	6298.6	-9.0140E-21	2.2810E 00	5606.3
33	-1.3060E-20	6.2657E 00	6194.3	-9.4807E-21	2.3728E 00	5493.4
34	-1.3709E-20	6.5423E 00	6083.8	-1.0009E-20	2.4770E 00	5375.9
35	-1.4403E-20	6.8162E 00	5966.7	-1.0604E-20	2.5944E 00	5253.7

MATRIX ELEMENTS, EINSTEIN A'S AND ENERGIES FOR V= 0 TO 0 TRANSITIONS OF HCL

Pure Rotation

J	<V J/MU/V' J+1>	A	E
	ESU-CM	SEC-1	CM-1
0	1.3080E-18	6.3298E-04	15.2
1	1.3081E-18	9.0673E-03	30.5
2	1.3081E-18	2.1901E-02	45.7
3	1.3081E-18	5.3707E-02	60.9
4	1.3081E-18	1.0700E-01	76.0
5	1.3081E-18	1.8704E-01	91.1
6	1.3082E-18	2.9907E-01	106.1
7	1.3082E-18	4.4795E-01	121.0
8	1.3082E-18	6.3837E-01	135.9
9	1.3083E-18	8.7477E-01	150.7
10	1.3083E-18	1.1610E 00	165.4
11	1.3083E-18	1.5009E 00	179.9
12	1.3083E-18	1.8974E 00	194.3
13	1.3083E-18	2.3534E 00	208.6
14	1.3083E-18	2.8710E 00	222.7
15	1.3082E-18	3.4518E 00	236.7
16	1.3081E-18	4.0969E 00	250.5
17	1.3080E-18	4.8064E 00	264.1
18	1.3078E-18	5.5798E 00	277.4
19	1.3076E-18	6.4166E 00	290.6
20	1.3073E-18	7.3139E 00	303.4
21	1.3069E-18	8.2695E 00	316.1
22	1.3064E-18	9.2802E 00	328.4
23	1.3058E-18	1.0340E 01	340.5
24	1.3051E-18	1.1446E 01	352.2
25	1.3042E-18	1.2590E 01	363.7
26	1.3032E-18	1.3765E 01	374.8
27	1.3019E-18	1.4963E 01	385.5
28	1.3004E-18	1.6175E 01	395.9
29	1.2987E-18	1.7391E 01	405.8
30	1.2966E-18	1.8599E 01	415.4
31	1.2942E-18	1.9789E 01	424.5
32	1.2913E-18	2.0945E 01	433.2
33	1.2879E-18	2.2056E 01	441.5
34	1.2840E-18	2.3105E 01	449.2
35	1.2794E-18	2.4076E 01	456.4

MATRIX ELEMENTS, EINSTEIN A'S AND ENERGIES FOR V= 9 TO 10 TRANSITIONS OF HCL

	R-BRANCH			P-BRANCH		
J	<V J/MU/V' J+1>	A	E	<V J/MU/V' J-1>	A	E
	ESU-CM	SEC-1	CM-1	ESU-CM	SEC-1	CM-1
0	1.2215E-19	1.2030E 01	1964.4			
1	1.1936E-19	1.3935E 01	1978.2	1.3053E-19	3.8701E 01	1934.7
2	1.1568E-19	1.4152E 01	1991.2	1.3412E-19	3.6570E 01	1918.7
3	1.1152E-19	1.3943E 01	2003.5	1.3764E-19	3.4535E 01	1902.1
4	1.0749E-19	1.3474E 01	2015.0	1.4110E-19	3.3990E 01	1884.7
5	1.0336E-19	1.2853E 01	2025.7	1.4450E-19	3.3566E 01	1866.7
6	9.9120E-20	1.2131E 01	2035.6	1.4784E-19	3.3596E 01	1847.9
7	9.4780E-20	1.1330E 01	2044.8	1.5111E-19	3.3579E 01	1828.5
8	9.0351E-20	1.0497E 01	2053.1	1.5433E-19	3.3566E 01	1808.5
9	8.5878E-20	9.6211E 00	2060.7	1.5747E-19	3.3531E 01	1787.9
10	8.1372E-20	8.7233E 00	2067.4	1.6056E-19	3.3460E 01	1766.5
11	7.6836E-20	7.8150E 00	2073.3	1.6357E-19	3.3343E 01	1744.6
12	7.1273E-20	6.9070E 00	2078.4	1.6651E-19	3.3175E 01	1722.1
13	6.6783E-20	6.0092E 00	2082.6	1.6938E-19	3.2951E 01	1699.1
14	6.1036E-20	5.1322E 00	2086.0	1.7216E-19	3.2671E 01	1675.4
15	5.5626E-20	4.2866E 00	2088.5	1.7496E-19	3.2333E 01	1651.2
16	5.0041E-20	3.4833E 00	2090.1	1.7746E-19	3.1937E 01	1626.5
17	4.4269E-20	2.7331E 00	2090.8	1.7995E-19	3.1484E 01	1601.3
18	3.8300E-20	2.0460E 00	2090.5	1.8234E-19	3.0975E 01	1575.5
19	3.2120E-20	1.4308E 00	2089.4	1.8460E-19	3.0412E 01	1549.3
20	2.5717E-20	9.2114E-01	2087.2	1.8673E-19	2.9796E 01	1522.6
21	1.9075E-20	5.0501E-01	2084.0	1.8871E-19	2.9131E 01	1495.4
22	1.2179E-20	2.0483E-01	2079.8	1.9054E-19	2.8419E 01	1467.7
23	5.0109E-21	3.4443E-02	2074.6	1.9219E-19	2.7665E 01	1439.5
24	-2.4470E-21	8.1459E-03	2068.3	1.9365E-19	2.6871E 01	1410.9
25	-1.0218E-20	1.4061E-01	2060.9	1.9491E-19	2.6043E 01	1381.9
26	-1.8323E-20	4.4691E-01	2052.2	1.9594E-19	2.5184E 01	1352.4
27	-2.6790E-20	9.4210E-01	2042.4	1.9672E-19	2.4299E 01	1322.4
28	-3.5647E-20	1.6420E 00	2031.3	1.9723E-19	2.3394E 01	1291.9
29	-4.4925E-20	2.5521E 00	2018.9	1.9744E-19	2.2473E 01	1261.0
30	-5.4663E-20	3.7182E 00	2005.2	1.9731E-19	2.1543E 01	1229.6
31	-6.4900E-20	5.1258E 00	1990.0	1.9682E-19	2.0608E 01	1197.7
32	-7.5683E-20	6.8001E 00	1973.4	1.9591E-19	1.9675E 00	1165.3
33	-8.7066E-20	8.7553E 00	1955.1	1.9455E-19	1.8749E 00	1132.3
34	-9.9110E-20	1.1007E 01	1935.2	1.9269E-19	1.7838E 00	1098.7
35	-1.1188E-19	1.3565E 01	1913.4	1.9026E-19	1.6946E 00	1064.5

MATRIX ELEMENTS, EINSTEIN A'S AND ENERGIES FOR V= 0 TO 11 TRANSITIONS OF HCL

	R-BRANCH			P-BRANCH		
J	<V J/MU/V' J+1>	A	F	<V J/MU/V' J-1>	A	F
	ESU-CM	SEC-1	CM-1	ESU-CM	SEC-1	CM-1
0	-8.2262E-20	4.8717E 01	3796.9			
1	-8.1658E-20	5.8258E 01	3809.1	-8.3550E-20	1.4684E 02	3767.9
2	-8.1083E-20	6.2158E 01	3819.9	-8.4240E-20	8.8029E 01	3751.2
3	-8.0530E-20	6.4142E 01	3829.1	-8.4961E-20	8.8284E 01	3733.0
4	-8.0001E-20	6.5225E 01	3836.7	-8.5716E-20	8.4080E 01	3713.4
5	-7.9493E-20	6.5797E 01	3842.8	-8.6507E-20	8.1691E 01	3692.2
6	-7.9005E-20	6.6040E 01	3847.4	-8.7335E-20	8.0101E 01	3669.7
7	-7.8534E-20	6.6048E 01	3850.5	-8.8202E-20	7.8921E 01	3645.7
8	-7.8079E-20	6.5877E 01	3851.9	-8.9109E-20	7.7969E 01	3620.3
9	-7.7638E-20	6.5561E 01	3851.9	-1.0006E-19	7.7148E 01	3593.5
10	-7.7210E-20	6.5120E 01	3850.2	-1.0105E-19	7.6405E 01	3565.3
11	-7.6792E-20	6.4568E 01	3847.0	-1.0210E-19	7.5703E 01	3535.8
12	-7.6381E-20	6.3915E 01	3842.2	-1.0319E-19	7.5024E 01	3504.9
13	-7.5975E-20	6.3165E 01	3835.7	-1.0433E-19	7.4349E 01	3472.7
14	-7.5571E-20	6.2325E 01	3827.7	-1.0552E-19	7.3672E 01	3439.2
15	-7.5167E-20	6.1396E 01	3818.1	-1.0678E-19	7.2983E 01	3404.4
16	-7.4759E-20	6.0377E 01	3806.7	-1.0809E-19	7.2276E 01	3368.3
17	-7.4343E-20	5.9271E 01	3793.8	-1.0946E-19	7.1548E 01	3330.9
18	-7.3915E-20	5.8076E 01	3779.1	-1.1090E-19	7.0796E 01	3292.2
19	-7.3471E-20	5.6791E 01	3762.7	-1.1241E-19	7.0015E 01	3252.3
20	-7.3005E-20	5.5415E 01	3744.6	-1.1399E-19	6.9203E 01	3211.1
21	-7.2512E-20	5.3945E 01	3724.6	-1.1564E-19	6.8358E 01	3168.7
22	-7.1987E-20	5.2380E 01	3702.8	-1.1738E-19	6.7477E 01	3125.1
23	-7.1420E-20	5.0717E 01	3679.1	-1.1920E-19	6.6557E 01	3080.1
24	-7.0805E-20	4.8955E 01	3653.4	-1.2110E-19	6.5594E 01	3033.9
25	-7.0131E-20	4.7091E 01	3625.7	-1.2310E-19	6.4586E 01	2986.3
26	-6.9390E-20	4.5123E 01	3595.9	-1.2520E-19	6.3530E 01	2937.5
27	-6.8567E-20	4.3051E 01	3563.8	-1.2740E-19	6.2420E 01	2887.2
28	-6.7650E-20	4.0874E 01	3529.5	-1.2971E-19	6.1254E 01	2835.6
29	-6.6621E-20	3.8591E 01	3492.9	-1.3214E-19	6.0027E 01	2782.5
30	-6.5461E-20	3.6204E 01	3453.7	-1.3470E-19	5.8734E 01	2727.8
31	-6.4145E-20	3.3715E 01	3411.8	-1.3739E-19	5.7370E 01	2671.6
32	-6.2646E-20	3.1127E 01	3367.2	-1.4021E-19	5.5927E 01	2613.7
33	-6.0930E-20	2.8446E 01	3319.6	-1.4319E-19	5.4399E 01	2554.1
34	-5.8957E-20	2.5682E 01	3268.9	-1.4633E-19	5.2778E 01	2492.5
35	-5.6677E-20	2.2846E 01	3214.7	-1.4964E-19	5.1053E 01	2429.0

MATRIX ELEMENTS, EINSTEIN A'S AND ENERGIES FOR V= 9 TO 12 TRANSITIONS OF HCL

J	R-BRANCH <V J/MU/V' J+1>	R-BRANCH A	R-BRANCH F	P-BRANCH <V J/MU/V' J-1>	P-BRANCH A	P-BRANCH F
	ESU-CM	SEC-1	CM-1	ESU-CM	SEC-1	CM-1
0	2.8572E-20	1.4241E 01	5505.2			
1	2.8584E-20	1.7203E 01	5515.9	2.8583E-20	4.2118E 01	5477.1
2	2.8611E-20	1.8550E 01	5524.2	2.8617E-20	2.7957E 01	5459.5
3	2.8651E-20	1.9354E 01	5530.2	2.8660E-20	2.4983E 01	5439.7
4	2.8706E-20	1.9910E 01	5533.8	2.8718E-20	2.3505E 01	5417.7
5	2.8776E-20	2.0329E 01	5535.1	2.8790E-20	2.2660E 01	5393.4
6	2.8862E-20	2.0666E 01	5534.1	2.8878E-20	2.2055E 01	5366.8
7	2.8963E-20	2.0947E 01	5530.7	2.8982E-20	2.1578E 01	5338.0
8	2.9080E-20	2.1191E 01	5525.0	2.9103E-20	2.1178E 01	5307.0
9	2.9215E-20	2.1406E 01	5516.9	2.9243E-20	2.0828E 01	5273.8
10	2.9369E-20	2.1602E 01	5506.4	2.9401E-20	2.0513E 01	5238.4
11	2.9541E-20	2.1781E 01	5493.5	2.9580E-20	2.0223E 01	5200.8
12	2.9733E-20	2.1949E 01	5478.2	2.9782E-20	1.9954E 01	5161.1
13	2.9945E-20	2.2107E 01	5460.5	3.0007E-20	1.9703E 01	5119.2
14	3.0180E-20	2.2259E 01	5440.4	3.0259E-20	1.9468E 01	5075.2
15	3.0437E-20	2.2404E 01	5417.8	3.0540E-20	1.9247E 01	5029.1
16	3.0718E-20	2.2545E 01	5392.7	3.0851E-20	1.9041E 01	4980.9
17	3.1024E-20	2.2681E 01	5365.1	3.1197E-20	1.8850E 01	4930.6
18	3.1356E-20	2.2812E 01	5335.0	3.1579E-20	1.8674E 01	4878.2
19	3.1713E-20	2.2938E 01	5302.2	3.2002E-20	1.8514E 01	4823.6
20	3.2097E-20	2.3057E 01	5266.9	3.2469E-20	1.8370E 01	4767.0
21	3.2509E-20	2.3168E 01	5228.8	3.2984E-20	1.8242E 01	4708.2
22	3.2949E-20	2.3268E 01	5187.9	3.3551E-20	1.8132E 01	4647.4
23	3.3416E-20	2.3353E 01	5144.2	3.4176E-20	1.8039E 01	4584.3
24	3.3910E-20	2.3419E 01	5097.5	3.4861E-20	1.7963E 01	4519.0
25	3.4431E-20	2.3460E 01	5047.7	3.5615E-20	1.7905E 01	4451.4
26	3.4976E-20	2.3472E 01	4994.8	3.6441E-20	1.7862E 01	4381.6
27	3.5545E-20	2.3447E 01	4938.5	3.7347E-20	1.7835E 01	4309.3
28	3.6135E-20	2.3376E 01	4878.7	3.8340E-20	1.7822E 01	4234.5
29	3.6742E-20	2.3250E 01	4815.1	3.9[illegible]E-20	1.7822E 01	4157.1
30	3.7366E-20	2.3059E 01	4747.7	4.06[illegible]E-20	1.7833E 01	4077.0
31	3.7992E-20	2.2790E 01	4676.1	4.1928E-20	1.7853E 01	3993.9
32	3.8620E-20	2.2429E 01	4600.1	4.3364E-20	1.7878E 01	3907.8
33	3.9235E-20	2.1961E 01	4519.3	4.4943E-20	1.7907E 01	3818.4
34	3.9823E-20	2.1366E 01	4433.3	4.6690E-20	1.7933E 01	3725.4
35	4.0361E-20	2.0623E 01	4341.7	4.8594E-20	1.7950E 01	3628.6

MATRIX ELEMENTS, EINSTEIN A'S AND ENERGIES FOR V= 10 TO 10 TRANSITIONS OF HCL

Pure Rotation

J	<V J/MU/V' J+1>	A	E
	ESU-CM	SEC-1	CM-1
0	1.3087E-18	5.4682E-04	14.5
1	1.3087E-18	5.2405E-03	29.0
2	1.3086E-18	1.8917E-02	43.5
3	1.3084E-18	4.6378E-02	57.9
4	1.3083E-18	9.2362E-02	72.3
5	1.3081E-18	1.6140E-01	86.7
6	1.3079E-18	2.5793E-01	101.0
7	1.3075E-18	3.8616E-01	115.2
8	1.3071E-18	5.4996E-01	129.4
9	1.3067E-18	7.5301E-01	143.5
10	1.3062E-18	9.9854E-01	157.4
11	1.3057E-18	1.2896E 00	171.3
12	1.3051E-18	1.6285E 00	185.0
13	1.3044E-18	2.0172E 00	198.6
14	1.3037E-18	2.4574E 00	212.0
15	1.3028E-18	2.9496E 00	225.2
16	1.3019E-18	3.4944E 00	238.3
17	1.3009E-18	4.0910E 00	251.2
18	1.2998E-18	4.7386E 00	263.8
19	1.2982E-18	5.4347E 00	276.2
20	1.2967E-18	6.1774E 00	288.4
21	1.2949E-18	6.9621E 00	300.3
22	1.2930E-18	7.7853E 00	311.9
23	1.2909E-18	8.6412E 00	323.2
24	1.2884E-18	9.5233E 00	334.2
25	1.2857E-18	1.0425E 01	344.8
26	1.2826E-18	1.1337E 01	355.1
27	1.2791E-18	1.2252E 01	364.9
28	1.2751E-18	1.3159E 01	374.4
29	1.2706E-18	1.4046E 01	383.5
30	1.2655E-18	1.4901E 01	392.1
31	1.2597E-18	1.5711E 01	400.2
32	1.2532E-18	1.6462E 01	407.9
33	1.2457E-18	1.7137E 01	415.0
34	1.2371E-18	1.7722E 01	421.5
35	1.2273E-18	1.8196E 01	427.4

MATRIX ELEMENTS, EINSTEIN A'S AND ENERGIES FOR V= 10 TO 11 TRANSITIONS OF HCL

	R-BRANCH			P-BRANCH		
J	<V J/MU/V' J+1>	A	E	<V J/MU/V' J-1>	A	E
	ESU-CM	SEC-1	CM-1	ESU-CM	SEC-1	CM-1
0	9.9480E-20	6.5193E 00	1847.0			
1	9.5419E-20	7.3501E 00	1860.0	1.0730E-19	2.1725E 01	1818.7
2	9.1248E-20	7.3440E 00	1872.1	1.1106E-19	1.5129E 01	1803.5
3	8.6963E-20	7.0446E 00	1883.5	1.1472E-19	1.4146E 01	1787.5
4	8.2556E-20	6.6035E 00	1894.1	1.1830E-19	1.3926E 01	1770.7
5	7.8030E-20	6.0827E 00	1903.9	1.2179E-19	1.3928E 01	1753.3
6	7.3368E-20	5.5143E 00	1912.8	1.2517E-19	1.4002E 01	1735.1
7	6.8564E-20	4.9154E 00	1920.9	1.2847E-19	1.4090E 01	1716.2
8	6.3612E-20	4.3102E 00	1928.2	1.3168E-19	1.4165E 01	1696.6
9	5.8503E-20	3.7017E 00	1934.6	1.3479E-19	1.4211E 01	1676.3
10	5.3225E-20	3.1039E 00	1940.2	1.3780E-19	1.4220E 01	1655.4
11	4.7771E-20	2.5278E 00	1944.9	1.4071E-19	1.4186E 01	1633.8
12	4.2129E-20	1.9837E 00	1948.8	1.4351E-19	1.4105E 01	1611.5
13	3.6296E-20	1.4822E 00	1951.7	1.4619E-19	1.3976E 01	1588.7
14	3.0270E-20	1.0343E 00	1953.7	1.4875E-19	1.3798E 01	1565.2
15	2.3950E-20	6.5162E-01	1954.8	1.5117E-19	1.3571E 01	1541.1
16	1.7428E-20	3.4576E-01	1955.0	1.5345E-19	1.3294E 01	1516.5
17	1.0652E-20	1.2920E-01	1954.2	1.5556E-19	1.2968E 01	1491.3
18	3.6036E-21	1.4768E-02	1952.4	1.5751E-19	1.2596E 01	1465.5
19	-3.7340E-21	1.5809E-02	1949.6	1.5926E-19	1.2179E 01	1439.2
20	-1.1390E-20	1.4615E-01	1945.8	1.6081E-19	1.1718E 01	1412.3
21	-1.9356E-20	4.2001E-01	1940.8	1.6213E-19	1.1218E 01	1385.0
22	-2.7684E-20	8.5204E-01	1934.8	1.6320E-19	1.0682E 01	1357.1
23	-3.6389E-20	1.4571E 00	1927.7	1.6399E-19	1.0135E 01	1328.7
24	-4.5500E-20	2.2504E 00	1919.3	1.6448E-19	9.5146E 00	1299.8
25	-5.5048E-20	3.2471E 00	1909.7	1.6464E-19	8.8920E 00	1270.3
26	-6.5047E-20	4.4623E 00	1898.7	1.6443E-19	8.2499E 00	1240.3
27	-7.5567E-20	5.9111E 00	1886.4	1.6382E-19	7.5934E 00	1209.8
28	-8.6692E-20	7.6077E 00	1872.7	1.6277E-19	6.9279E 00	1178.7
29	-9.8373E-20	9.5661E 00	1857.4	1.6121E-19	6.2591E 00	1147.0
30	-1.1073E-19	1.1790E 01	1840.6	1.5911E-19	5.5930E 00	1114.7
31	-1.2381E-19	1.4317E 01	1822.0	1.5639E-19	4.9358E 00	1081.8
32	-1.3769E-19	1.7131E 01	1801.7	1.5297E-19	4.2938E 00	1048.2
33	-1.5246E-19	2.0245E 01	1779.5	1.4876E-19	3.6733E 00	1013.9
34	-1.6822E-19	2.3661E 01	1755.2	1.4365E-19	3.0808E 00	978.9
35	-1.8509E-19	2.7376E 01	1729.7	1.3751E-19	2.5228E 00	943.0

MATRIX ELEMENTS, EINSTEIN A'S AND ENERGIES FOR V= 10 TO 12 TRANSITIONS OF HCL

J	R-BRANCH <V J/MU/V" J+1> ESU-CM	R-BRANCH A SEC-1	R-BRANCH E CM-1	P-BRANCH <V J/MU/V" J-1> ESU-CM	P-BRANCH A SEC-1	P-BRANCH E CM-1
0	-1.0436E-19	5.1176E 01	3555.3			
1	-1.0358E-19	6.1077E 01	3566.7	-1.0602E-19	1.5479E 02	3527.9
2	-1.0282E-19	6.5024E 01	3576.4	-1.0689E-19	1.0348E 02	3511.8
3	-1.0210E-19	6.6939E 01	3584.6	-1.0781E-19	9.3315E 01	3494.2
4	-1.0140E-19	6.7892E 01	3591.2	-1.0876E-19	8.8971E 01	3475.1
5	-1.0072E-19	6.8293E 01	3596.2	-1.0976E-19	8.6526E 01	3454.4
6	-1.0005E-19	6.8333E 01	3599.5	-1.1078E-19	8.4908E 01	3432.2
7	-9.9401E-20	6.8112E 01	3601.2	-1.1188E-19	8.3709E 01	3408.5
8	-9.8765E-20	6.7688E 01	3601.3	-1.1301E-19	8.2735E 01	3383.3
9	-9.8137E-20	6.7095E 01	3599.7	-1.1419E-19	8.1886E 01	3356.6
10	-9.7516E-20	6.6355E 01	3596.4	-1.1543E-19	8.1102E 01	3328.4
11	-9.6903E-20	6.5484E 01	3591.4	-1.1672E-19	8.0349E 01	3298.8
12	-9.6298E-20	6.4489E 01	3584.8	-1.1807E-19	7.9601E 01	3267.7
13	-9.5702E-20	6.3377E 01	3576.5	-1.1948E-19	7.8843E 01	3235.2
14	-9.5116E-20	6.2153E 01	3566.4	-1.2096E-19	7.8064E 01	3201.2
15	-9.4365E-20	6.0819E 01	3554.5	-1.2250E-19	7.7254E 01	3165.9
16	-9.3692E-20	5.9374E 01	3540.9	-1.2412E-19	7.6409E 01	3129.1
17	-9.2992E-20	5.7821E 01	3525.5	-1.2580E-19	7.5522E 01	3091.0
18	-9.2267E-20	5.6159E 01	3508.2	-1.2757E-19	7.4589E 01	3051.4
19	-9.1479E-20	5.4387E 01	3489.1	-1.2942E-19	7.3607E 01	3010.5
20	-9.0649E-20	5.2504E 01	3468.1	-1.3135E-19	7.2571E 01	2968.2
21	-8.9757E-20	5.0510E 01	3445.0	-1.3337E-19	7.1479E 01	2924.5
22	-8.8791E-20	4.8404E 01	3419.9	-1.3549E-19	7.0326E 01	2879.4
23	-8.7737E-20	4.6185E 01	3392.8	-1.3770E-19	6.9108E 01	2832.9
24	-8.6581E-20	4.3853E 01	3363.4	-1.4002E-19	6.7822E 01	2784.9
25	-8.5304E-20	4.1409E 01	3331.7	-1.4245E-19	6.6461E 01	2735.4
26	-8.3897E-20	3.8856E 01	3297.6	-1.4498E-19	6.5021E 01	2684.4
27	-8.2306E-20	3.6198E 01	3261.1	-1.4764E-19	6.3496E 01	2631.9
28	-8.0533E-20	3.3439E 01	3221.8	-1.5042E-19	6.1879E 01	2577.6
29	-7.8535E-20	3.0587E 01	3179.7	-1.5333E-19	6.0163E 01	2521.7
30	-7.6272E-20	2.7655E 01	3134.6	-1.5638E-19	5.8339E 01	2463.9
31	-7.3697E-20	2.4656E 01	3086.3	-1.5957E-19	5.6399E 01	2404.1
32	-7.0752E-20	2.1611E 01	3034.6	-1.6291E-19	5.4336E 01	2342.3
33	-6.7364E-20	1.8545E 01	2979.1	-1.6640E-19	5.2138E 01	2278.2
34	-6.3445E-20	1.5490E 01	2919.7	-1.7004E-19	4.9796E 01	2211.8
35	-5.8883E-20	1.2490E 01	2855.7	-1.7384E-19	4.7298E 01	2142.7

MATRIX ELEMENTS, EINSTEIN A'S AND ENERGIES FOR V= 11 TO 11 TRANSITIONS OF HCL

Pure Rotation

J	<V J/MU/V' J+1>	A	E
	ESU-CM	SEC-1	CM-1
0	1.2382E-18	4.5689E-04	13.7
1	1.2980E-18	4.3796E-03	27.5
2	1.2978E-18	1.5906E-02	41.2
3	1.2975E-18	3.4745E-02	54.9
4	1.2970E-18	7.7102E-02	68.5
5	1.2965E-18	1.3466E-01	82.1
6	1.2958E-18	2.1504E-01	95.6
7	1.2950E-18	3.2164E-01	109.1
8	1.2941E-18	4.5762E-01	122.5
9	1.2931E-18	6.2583E-01	135.8
10	1.2919E-18	8.2891E-01	149.0
11	1.2906E-18	1.0688E 00	162.1
12	1.2891E-18	1.3473E 00	175.1
13	1.2875E-18	1.6659E 00	187.9
14	1.2857E-18	2.0240E 00	200.6
15	1.2836E-18	2.4247E 00	213.1
16	1.2814E-18	2.8647E 00	225.4
17	1.2789E-18	3.3439E 00	237.5
18	1.2762E-18	3.8600E 00	249.4
19	1.2731E-18	4.4104E 00	261.0
20	1.2698E-18	4.9918E 00	272.4
21	1.2661E-18	5.5994E 00	283.5
22	1.2619E-18	6.2279E 00	294.3
23	1.2573E-18	6.8715E 00	304.7
24	1.2523E-18	7.5224E 00	314.8
25	1.2466E-18	8.1727E 00	324.5
26	1.2402E-18	8.8136E 00	333.8
27	1.2332E-18	9.4352E 00	342.8
28	1.2252E-18	1.0026E 01	351.2
29	1.2163E-18	1.0575E 01	359.2
30	1.2063E-18	1.1049E 01	366.6
31	1.1949E-18	1.1434E 01	373.6
32	1.1820E-18	1.1736E 01	379.9
33	1.1673E-18	1.2079E 01	385.6
34	1.1505E-18	1.2205E 01	390.7
35	1.1311E-18	1.2158E 01	395.0

MATRIX ELEMENTS, EINSTEIN A'S AND ENERGIES FOR V= 11 TO 12 TRANSITIONS OF HCL

	R-BRANCH			P-BRANCH		
J	<V J/MU/V' J+1>	A	E	<V J/MU/V' J-1>	A	E
	ESU-CM	SEC-1	CM-1	ESU-CM	SEC-1	CM-1
0	6.5184E-20	2.2687E 00	1722.1			
1	6.0963E-20	2.4239E 00	1736.2	7.3390E-20	8.2226E 00	1695.4
2	5.6387E-20	2.2730E 00	1745.5	7.7278E-20	5.9303E 00	1680.9
3	5.1751E-20	2.0215E 00	1756.0	8.1028E-20	5.7089E 00	1665.6
4	4.6948E-20	1.7296E 00	1765.6	8.4642E-20	5.7627E 00	1649.5
5	4.1970E-20	1.4246E 00	1774.4	8.8121E-20	5.8884E 00	1632.6
6	3.6809E-20	1.1228E 00	1782.3	9.1462E-20	6.0287E 00	1615.0
7	3.1452E-20	8.3660E-01	1789.4	9.4666E-20	6.1607E 00	1596.7
8	2.5893E-20	5.7667E-01	1795.6	9.7728E-20	6.2727E 00	1577.6
9	2.0118E-20	3.5305E-01	1800.8	1.0064E-19	6.3581E 00	1557.7
10	1.4114E-20	1.7579E-01	1805.2	1.0341E-19	6.4127E 00	1537.2
11	7.8678E-21	5.5140E-02	1808.7	1.0602E-19	6.4339E 00	1516.0
12	1.3750E-21	1.6718E-03	1811.2	1.0846E-19	6.4199E 00	1494.0
13	-5.4111E-21	2.6408E-02	1812.7	1.1072E-19	6.3698E 00	1471.4
14	-1.2470E-20	1.4091E-01	1813.3	1.1279E-19	6.2834E 00	1448.1
15	-1.9356E-20	3.5719E-01	1812.8	1.1466E-19	6.1609E 00	1424.2
16	-2.7562E-20	6.8782E-01	1811.4	1.1630E-19	6.0027E 00	1399.6
17	-3.6621E-20	1.1459E 00	1808.8	1.1770E-19	5.8102E 00	1374.3
18	-4.6056E-20	1.7448E 00	1805.2	1.1883E-19	5.5847E 00	1348.4
19	-5.5893E-20	2.4987E 00	1800.5	1.1967E-19	5.3284E 00	1321.9
20	-6.2161E-20	3.4215E 00	1794.7	1.2018E-19	5.0437E 00	1294.8
21	-7.1881E-20	4.5275E 00	1787.6	1.2034E-19	4.7333E 00	1267.1
22	-8.2117E-20	5.8311E 00	1779.4	1.2010E-19	4.4006E 00	1238.8
23	-9.2873E-20	7.3464E 00	1769.8	1.1942E-19	4.0494E 00	1209.9
24	-1.0422E-19	9.0870E 00	1758.9	1.1825E-19	3.6837E 00	1180.4
25	-1.1618E-19	1.1066E 01	1746.6	1.1654E-19	3.3081E 00	1150.3
26	-1.2882E-19	1.3294E 01	1732.8	1.1422E-19	2.9275E 00	1119.6
27	-1.4220E-19	1.5782E 01	1717.4	1.1122E-19	2.5471E 00	1088.2
28	-1.5639E-19	1.8537E 01	1700.3	1.0746E-19	2.1724E 00	1056.2
29	-1.7147E-19	2.1563E 01	1681.5	1.0294E-19	1.8092E 00	1023.4
30	-1.8754E-19	2.4862E 01	1660.7	9.7256E-20	1.4635E 00	989.9
31	-2.0469E-19	2.8428E 01	1637.9	9.0569E-20	1.1412E 00	955.7
32	-2.2307E-19	3.2248E 01	1612.8	8.2621E-20	8.4823E-01	920.5
33	-2.4280E-19	3.6302E 01	1585.3	7.3219E-20	5.9052E-01	884.4
34	-2.6407E-19	4.0553E 01	1555.1	6.2121E-20	3.7356E-01	847.2
35	-2.8709E-19	4.4950E 01	1522.0	4.9023E-20	2.0242E-01	809.0

MATRIX ELEMENTS, EINSTEIN A'S AND ENERGIES FOR V= 12 TO 12 TRANSITIONS OF HCL

Pure Rotation

J	<V J/MU/V' J+1>	A	E
	ESU-CM	SEC-1	CM-1
0	1.2712E-18	3.5618E-04	12.9
1	1.2709E-18	3.5058E-03	25.9
2	1.2704E-18	1.2643E-02	38.8
3	1.2698E-18	3.0375E-02	51.7
4	1.2690E-18	6.1592E-02	64.5
5	1.2679E-18	1.0746E-01	77.3
6	1.2667E-18	1.7138E-01	90.0
7	1.2652E-18	2.5596E-01	102.7
8	1.2635E-18	3.6355E-01	115.3
9	1.2616E-18	4.9619E-01	127.8
10	1.2594E-18	6.5564E-01	140.2
11	1.2570E-18	8.4332E-01	152.5
12	1.2542E-18	1.0601E 00	164.6
13	1.2512E-18	1.3064E 00	176.6
14	1.2478E-18	1.5824E 00	188.5
15	1.2440E-18	1.8873E 00	200.2
16	1.2399E-18	2.2198E 00	211.6
17	1.2353E-18	2.5782E 00	222.9
18	1.2302E-18	2.9597E 00	233.9
19	1.2245E-18	3.3610E 00	244.7
20	1.2183E-18	3.7776E 00	255.2
21	1.2114E-18	4.2046E 00	265.4
22	1.2038E-18	4.6363E 00	275.2
23	1.1953E-18	5.0650E 00	284.7
24	1.1859E-18	5.4837E 00	293.8
25	1.1754E-18	5.8835E 00	302.5
26	1.1636E-18	6.2548E 00	310.7
27	1.1505E-18	6.5872E 00	318.5
28	1.1357E-18	6.8698E 00	325.7
29	1.1190E-18	7.0907E 00	332.4
30	1.1000E-18	7.2381E 00	338.4
31	1.0785E-18	7.2991E 00	343.8
32	1.0538E-18	7.2611E 00	348.5
33	1.0253E-18	7.1116E 00	352.4
34	9.9226E-19	6.8385E 00	355.5
35	9.5350E-19	6.4308E 00	357.6

REFERENCES

1. R. E. Meredith and F. G. Smith, Investigations of Fundamental Laser Processes, Vol. II, Computation of Electric Dipole Matrix Element for Hydrogen Fluoride and Deuterium Fluoride, Report No. 8413-39-T(II), Willow Run Laboratories of the Institute of Science and Technology, The University of Michigan, Ann Arbor, November 1971.

2. R. A. Toth, R. H. Hunt, and E. K. Plyler, Line Intensities in the 3 - 0 Band of CO and Dipole Matrix Elements for the CO Molecule, J. Mol. Spectr., Vol. 32, 1969, pp. 85-96.

3. P. W. Anderson, "Pressure Broadening in the Microwave and Infrared Regions," Phys. Rev., Vol. 76, 1949, p. 647.

4. L. Pauling and E. B. Wilson, Introduction to Quantum Mechanics, McGraw-Hill, New York, 1935.

5. J. L. Dunham, "The Energy Levels of a Rotating Vibration," Phy. Rev., Vol. 41, 1932, p. 721.

6. R. A. Toth, R. H. Hunt, and E. K. Plyler, "Dipole Moment Matrix Elements for the 1-0, 2-0 and 3-0 Vibration-Rotation Bands of Diatomic Molecules," J. Mol. Spectr., Vol. 32, 1969, p. 74.

7. R. Rydberg, "Graphic Representations of Some Results in Band Spectroscopy," Zeitschrift fur Physik, Vol. 73, 1931, p. 376.

8. O. Klein, "Calculation of Potential Curves for Diatomic Molecules by Means of Spectral Terms," Zeitschrift fur Physik, Vol. 76, 1932, p. 226.

9. J. T. Vanderslice et al., "Ground State of Hydrogen by the Rydberg-Klein-Rees Method," J. Mol. Spectr., Vol. 3, 1959, p. 17.

10. R. J. LeRoy and G. Burns, "A Method for Testing and Improving Molecular Constants of Diatomic Molecules with Special Reference to $Br_2'\left(^1\Sigma_g^+\right)$, J. Mol. Spectr., Vol. 25, 1968, p. 75.

11. R. N. Zare, Programs for Calculating Relative Intensities in the Vibrational Structure of Electronic Band Systems, Report No. UCRL-10925, University of California, November 1963.

12. D. H. Rank, D. P. Eastman, B. S. Rao, and T. A Wiggins, "Rotational and Vibrational Constants of the HCl^{35} and DCl^{35} Molecules," J. Opt. Soc. Am., Vol. 52, 1962, p. 1.

13. D. H. Rank, B. S. Rao, and T. A. Wiggins, "Molecular Constants of HCl," J. Mol. Spectr., Vol. 17, 1965, p. 122.

14. G. Herzberg, Spectra of Diatomic Molecules, D. Van Nostrand Co., Princeton, 1950.

15. R. H. Pennington, Introductory Computer Methods and Numerical Analysis, MacMillan Company, Toronto, 1965.

16. J. Trischka and H. Salwen, "Dipole Moment Function of Diatomic Molecules," J. Chem. Phys., Vol. 31, 1959, p. 218.

17. E. W. Kaiser, "Dipole Moment and Hyperfine Parameters of HCl^{35} and DCl^{35}," J. Chem. Phys., Vol. 53, 1970, p. 1686.

18. W. S. Benedict et al., "Infrared Line and Band Strengths and Dipole Moment Function in HCl and DCl," J. Chem. Phys., Vol. 26, 1957, p. 1671.

19. R. A. Toth, R. H. Hunt, and E. K. Plyler, "Line Strengths, Line Widths, and Dipole Moment Function for HCl," J. Mol. Spectr., Vol. 35, 1970, p. 110.

20. S. S. Penner and D. Weber, "Infrared Intensity Measurements on Nitric Oxide, Hydrogen Chloride, and Hydrogen Bromide," J. Chem. Phys., Vol. 21, 1953, p. 649.

21. H. Babrov, G. Ameer, and W. Benesch, "Line Strengths and Widths in the HCl Fundamental Band," J. Mol. Spectr., Vol. 3, 1959, p. 185.

22. J. H. Jaffe, S. Kimel, and M. A. Hirshfeld, "Refraction Spectrum of Gases in the Infrared; Intensities and Widths of Lines in the 2 → 0 Band of HCl," J. Chem. Phys., Vol. 40, 1962, p. 113.

23. R. E. Meredith, A New Method for The Direct Measurement of Spectral Line Strengths and Widths, JQSRT, Vol. 12, 1972, pp. 455-484.

24. Plyler and Thibault, "Self Broadening of Carbon Monoxide in the 2ν and 3ν Bands," J. of Research NBS Physics and Chem., Vol. 67A, No. 3, June 1963.

25. R. R. Stephens and T. A. Cool, "Vibrational Energy Transfer and De-excitation on the HF, DF, HF-CO_2 and DF_2 Systems," J. Chem. Phys., Vol. 56, 1972, p. 5863.

26. J. J. Hinchen, "Vibrational Relaxation of Hydrogen Fluoride and Deuterium Fluoride," Paper given at 3rd Conference on Chemical and Molecular Lasers, St. Louis, 1, 2, 3, May 1972.

27. M. A. Kwok, "HF Deactivation Kinetics Using a Medium Pressure Flow Tube: HF + H_2 Systems," Paper given at 3rd Conference on Chemical and Molecular Lasers, St. Louis, 1, 2, 3, May 1972.

28. T. F. Deutsch, "Laser Emission from HF Rotational Transitions," Appl. Phys. Lett., Vol. 11, 1967, p. 18.

29. R. L. Wilkins, "Monte Carlo Calculations of Reaction Rates and Energy Distributions Among Reaction Products I. F + H_2 = HF + H," J. Chem. Phys., Vol. 57, 1972, p. 912.

30. N. Jonathan et al., "Initial Vibrational Energy Level Distributions Determined by Infrared Chemi-Luminescence, II," Molecular Physics, Vol. 22, 1971, p. 561.

31. L. Henry, "Chemical Laser Probing of Reactions." Paper given at 3rd Conference on Chemical and Molecular Lasers, St. Louis, 1, 2, 3, May 1972.

32. R. D. Sharma and C. A. Brau, "Energy Transfer in Near-Resonant Molecular Collisions due to Long Range Forces with Application to Transfer of Vibrational Energy from ν_3 Mode of CO_2 to N_2^*," J. Chem. Phys., Vol. 50, 1969, p. 924.

33. E. L. Steele, Optical Lasers in Electronics, John Wiley and Sons, Inc., New York, 1968.

34. K. J. Pettiplece, "A TEM_{00} Short Pulse HF Oscillator," submitted to Chemical Physics Letters, February 1972.

35. B. A. Lippmann and J. Schwinger, "Variational Principles for Scattering I," Phys. Rev., Vol. 79, 1950, p. 469.

36. M. Gell-Mann and M. L. Goldberger, "The Formal Theory of Scattering," Phys. Rev., Vol. 91, 1953, p. 398.

37. C. J. Tsao and B. Curnutte, "Line Width of Pressure Broadened Spectral Lines," J. Quant. Spectrosc. Radiat. Transfer, Vol. 2, 1961, p. 41.

38. W. S. Benedict and R. Herman, "The Calculation of Self Broadened Line Width in Linear Molecules," J. Quant. Spectrosc. Radiat. Transfer, Vol. 3, 1963, p. 265.

39. W. F. Herget et al., "Infrared Spectrum of Hydrogen Fluoride: Line Positions and Line Shapes: Treatment of Data Results," J. Opt. Soc. Am., Vol. 52, 1962, p. 113.

40. R. Lovell and W. F. Herget, "Lorentz Parameters and Vibration-Rotation Interactions Constants for the Fundamental Band of HF," J. Opt. Soc. Am., Vol. 52, 1962, p. 1374.

41. R. F. Meredith, "Strengths and Widths in the First Overtone Band of Hydrogen Fluoride," J. Quant. Spectrosc. Radiat. Transfer, Vol. 12. 1972, p. 485.

42. A. A. Mason and A. H. Nielsen, "Rotational Spectrum of Hydrogen Fluoride: Frequencies and Line Widths," J. Opt. Soc. Amer., Vol. 57, 1967, p. 1464.

43. W. S. Benedict et al., "The Strengths, Widths and Shapes of Infrared Lines," Can. J. Phys., Vol. 34, 1956, p. 830.

44. R. Herman and R. F. Wallis, "Influence of Vibration-Rotation Interaction on Line Intensities in Vibration-Rotation Bands of Diatomic Molecules," J. Chem. Phys., Vol. 23, 1955, p. 637.

45. W. S. Benedict et al., "The Strengths, Widths and Shapes of Infrared Lines, The HCl Fundamental," Can. J. Phys., Vol. 34, 1956, p. 850.

46. H. W. Marshall, A High Resolution Infrared Spectrometer, Ph.D Dissertation, The University of Michigan, Ann Arbor, 1960 (unpublished).

47. E. S. Fishburne and K. Narahari Rao, "Vibration-Rotation Bands of HF," J. Molec. Spectr., Vol. 19, 1966, p. 290.

48. J. W. C. Johns and R. F. Barrow, The Ultraviolet Spectra of HF and DF, Proc. Roy. Soc., A251, London, 1959, p. 504.

49. A. C. G. Mitchell and M. W. Zemansky, Resonance Radiation and Excited Atoms, The MacMillan Company, New York, 1934.

DISTRIBUTION LIST

Commanding General
U. S. Army Missile Command
Redstone Arsenal, Alabama 35809
ATTN: AMSMI-RMS (1)

MITRE Corporation
P. O. Box 208
Bedford, Massachusetts 01730
ATTN: Dr. John Connally (1)

Air Force Weapons Laboratory
Albuquerque, New Mexico 87117
ATTN: SAL/LT D. Fuller (3)

Rome Air Development Center
Griffiss Air Force Base, New York 13440
ATTN: Mr. Bill Fontana/OCSS (1)

Headquarters, Air Force Aeronautical Systems Division
Wright-Patterson Air Force Base, Ohio 45433
ATTN: ASBX/Mr. Ira Bowker (1)

Department of the Navy
Naval Ordnance Systems Command
Washington, D. C. 20360
ATTN: ORD-912 (1)
ATTN: ORD-0832 (2)

Johns Hopkins University
Applied Physics Laboratory
8621 Georgia Avenue
Silver Spring, Maryland 20910
ATTN: Dr. W. Good (1)

The Boeing Company
P. O. Box 3999
MS 8A19 Org 2-5091
Seattle, Washington 98124
ATTN: Mr. L. W. Holinson (1)

McDonnell-Douglas Astronautics Company
Western Division, Dept. A-830, M89
5301 Bolsa Avenue
Huntington Beach, California 92647
ATTN: Mr. R. E. Hanna (1)

AVCO-Missile Systems Division
201 Lowell Street
Wilmington, Massachusetts 01887
ATTN: Mr. Walter Schafer (1)

General Research Corporation
1501 Wilson Boulevard
Suite 500
Arlington, Virginia 22209
ATTN: Dr. Giles Crimi (1)

Headquarters, U. S. Army Combat Development Command
Fort Belvoir, Virginia 22060
ATTN: CDCCD-C MJR Knapp (1)

Headquarters, Air Force Systems Command
Andrews Air Force Base, Virginia 20331
ATTN: SCTSW/COL O. R. Cunningham (1)

Air Force Weapons Laboratory
Albuquerque, New Mexico 87117
ATTN: SAL MJR R. Feaster (1)
ATTN: LR COL D. L. Lamberson (1)
ATTN: LRL MJR D. Haycock (1)
ATTN: SYT MJR R. Roland (1)
ATTN: LRT MJR R. Ogluktan (1)
ATTN: CL Mr. John Walsh (1)

Advanced Research Projects Agency
1400 Wilson Boulevard
Arlington, Virginia 22209
ATTN: Dr. S. J. Lukasik (1)
ATTN: Director, STO (1)
ATTN: Director, Laser Division, STO (1)
ATTN: CPT Stoessell (1)

ODDR&E
Washington, D. C. 26301
ATTN: Mr. Edward Myers (E&IS) (1)
ATTN: Mr. Ben T. Plymate (SW) (1)

Joint Continental Defense Systems
Integration Planning Staff
1320 Wilson Boulevard
Arlington, Virginia 22209
ATTN: Mr. L. Katz (1)

U. S. Arms Control & Disarmament Agency
Washington, D. C. 20451
ATTN: Mr. Charles Henkie (1)

Department of the Army
Chief of Research & Development
Washington, D. C. 20310
ATTN: COL F. O. Cornay (CRDPES) (1)
ATTN: Chief, Air Defense & Missiles Division (1)

U. S. Army SAFEGUARD Systems Office
Commonwealth Building
1320 Wilson Boulevard
Arlington, Virginia 22209
ATTN: Mr. Albert J. Basl, Jr. (1)

U. S. Army Missile Command
Redstone Arsenal, Alabama 35809
ATTN: Dr. J. P. Hallowes, Jr. (1)
ATTN: Mr. Walter Jennings (1)
ATTN: Dr. Tom Barr (1)

Commanding General
U. S. Army Weapons Command
Rock Island, Illinois 61201
ATTN: Dr. Leonard B. Gardner (1)
I&E Directorate

Director
U. S. Army Advanced Ballistic Missile Defense Agency
P. O. Box 1500
Huntsville, Alabama 35807
ATTN: CRDABH-O (1)

Commanding General
U. S. Army Materiel Command
Washington, D. C. 20315
ATTN: Mr. Paul Chernoff (AMCHD-TP) (1)

Commanding General
U. S. Army Munitions Command
Dover, New Jersey 07801
ATTN: Mr. G. F. Chesnov (1)
(AMSMU-RE-R)

Director
U. S. Army Ballistic Research Laboratories
Aberdeen Proving Ground, Maryland 21005
ATTN: Dr. Robert Eichelberger (1)
ATTN: Mr. Frank Allen (1)
ATTN: Dr. E. C. Alcarez (1)

Commanding Officer
U. S. Army Combat Development Command
Air Defense Agency
Fort Bliss, Texas 79916 (1)

Commanding Officer
U. S. Army Frankford Arsenal
Philadelphia, Pennsylvania 19137
ATTN: Dr. Sidney Ross (1)

Commanding General
U. S. Army Electronics Command
Fort Monmouth, New Jersey 07703
ATTN: AMSEL-XL-D, Dr. R. G. Buser (1)

Department of the Navy
Deputy Chief of Naval Operation Development OP-723
Pentagon 5C739
Washington, D. C. 20350
ATTN: CPT J. G. Wilson, U. S. Navy (1)

Office of Naval Research
495 Summer Street
Boston, Massachusetts 02210
ATTN: Dr. Fred Quelle (1)

Office of Naval Research
800 N. Quincy Street
Arlington, Virginia 22217
ATTN: Dr. W. J. Condell (421) (1)

Department of the Navy
Deputy Chief of Naval Materiel (Development)
Washington, D. C. 20360
ATTN: Mr. R. Gaylord (MAT 032B) (1)

Naval Research Laboratory
Washington, D. C. 20390
ATTN: Dr. W. R. Sooy (Code 6500) (1)
ATTN: Dr. H. W. Gandy (Code 6506) (1)
ATTN: Dr. A. L. Schindler (Code 6330) (1)
ATTN: Dr. H. Shenker (Code 6530) (1)
ATTN: Mr. D. J. McLaughlin (Code 6507) (1)

Naval Ordnance Laboratory
White Oak, Silver Spring, Maryland 20910
ATTN: Dr. Leon H. Schindel (Code 310) (1)
ATTN: Dr. E. Leroy Herrs (Code 313) (1)

U. S. Naval Weapons Center
China Lake, California 93557
ATTN: Mr. A. L. Bi-tell (Code 3042) (1)

Headquarters, U. S. Air Force (AF/RDPS)
The Pentagon
Washington, D. C. 20330
ATTN: LT C. Parsons (1)

Headquarters, AFSC (DLTW)
Andrews Air Force Base
Washington, D. C. 20331
ATTN: MAJ A. J. Chiota (1)

Headquarters, SAMSO (XRTD)
Los Angeles Air Force Station
Air Force Unit Post Office
Los Angeles, California 90045
ATTN: LT Dartan De Maie (1)

Air Force Avionics Laboratories (TEL)
Wright-Patterson Air Force Base, Ohio 45433
ATTN: Mr. K. Hulchinson (1)

Headquarters, Electronic Systems Division (ESL)
L. G. Hanscom Field
Bedford, Massachusetts 01730
ATTN: Mr. A. E. Anderson (XRT) (2)

Air Force Rocket Propulsion Laboratory
Edwards Air Force Base, California 93523
ATTN: XP-James Edwards (1)

Air Force Aero-Space Propulsion Laboratory
Wright-Patterson Air Force Base, Ohio 45433
ATTN: COL Tipton Motl-Smith (APG) (1)

Air Force Foreign Technology Division
Wright-Patterson Air Force Base, Ohio 45433
ATTN: LT R. J. Faehl (PDTR) (1)

USAF/INAKA/LTC W. M. Trueadell
Washington, D. C. 20330 (1)

Aerospace Research Labs (AP)
Wright-Patterson Air Force Base, Ohio 45433
ATTN: MAJ M. R. Fossett, Jr. (1)

Defense Intelligence Agency
Washington, D. C. 20301
ATTN: Mr. Seymour Berler (DT-1D) (1)

Central Intelligency Agency
Washington, D. C. 20505
ATTN: Mr. J. C. Nall (1)

Aerospace Corporation
P. O. Box 95085
Los Angeles, California 90045
ATTN: Dr. G. P. Millburn (1)

Atlantic Research Corporation
Propulsion Division
Shirley Highway and Edsall Road
Alexandria, Virginia 22314
ATTN: Mr. R. F. Hoglund (1)

AVCO-Everett Research Laboratories
2385 Revere Beach Parkway
Everett, Massachusetts 02149
ATTN: Dr. George Sutton (1)
ATTN: Dr. Jack Daugherty (1)

Battelle Memorial Institute
505 King Avenue
Columbus, Ohio 43201
ATTN: Mr. Robert Kohn (STOIAC) (1)

Electro-Optical Systems
300 North Halstead
Pasadena, California 91107
ATTN: Dr. Andrew Jensen (1)

General Electric Company
Space Division
Valley Forge Space Center
P. O. Box 8555
Philadelphia, Pennsylvania 19101
ATTN: Mr. W. J. East (1)

General Research Corporation
P. O. Box 3587
Santa Barbara, California 93105
ATTN: Dr. R. Holbrook (1)

Hercules, Inc.
Explosives & Chemical Propulsion Division
Wilmington, Delaware 19899
ATTN: Mr. J. E. Greer (1)

Hercules, Inc.
P. O. Box 210
Cumberland, Maryland 21502
ATTN: Dr. R. F. Preckel (1)

Hughes Research Laboratories
3011 Malibu Canyon Road
Malibu, California 90265
ATTN: Dr. D. Forster (2)

Hughes Aircraft Company
Centinella & Teale Streets
Culver City, California 90230
ATTN: Mr. Stan Novak (2)

Hughes Aircraft Company
P. O. Box 3310
Fullerton, California 90230
ATTN: Dr. William Yates (1)

Institute for Defense Analyses
400 Army Navy Drive
Arlington, Virginia 22202
ATTN: Dr. John Asmus (1)

Lawrence Livermore Laboratory
University of California
P. O. Box 808
Livermore, California 94551

ATTN: Dr. R. L. Kidder (1)
ATTN: Dr. Edward Teller (1)

Lulejian & Associates
1650 South Pacific Coast Highway
Redondo Beach, California 90277

ATTN: COL Robert Bowers (1)

MIT Lincoln Laboratory
P. O. Box 73
Lexington, Massachusetts 02173

ATTN: Dr. S. Edelberg (1)
ATTN: Dr. R. Kingston (1)
ATTN: Dr. J. Freedman (1)
ATTN: Dr. G. P. Dinneen (1)
ATTN: Dr. R. S. Cooper (1)

Mathematical Sciences Northwest, Incorporation
4545 15th Avenue, NE
Seattle, Washington 98105

ATTN: Mr. P. H. Rose (1)
ATTN: Dr. Abraham Hertzberg (1)

McDonnell Douglas Research Laboratories
Department 220, Box 516
St. Louis, Missouri 63166

ATTN: Dr. D. P. Ames (1)

North American Rockwell Corporation
Autonetics Division
3370 Miraloma Avenue
Anaheim, California 92803

ATTN: Mr. T. T. Kumagai (1)
D/476 Mail Code HA18

Northrop Corporation Laboratories
3401 W. Broadway
Hawthorne, California 90250

ATTN: Mr. G. R. Hasserjian (1)

Physics International
2700 Merced Street
San Leandro, California 94577

ATTN: Dr. G. Yonas (1)
Electron Beam Research & Technical Department

RAND Corporation
1700 Main Street
Santa Monica, California 90406

ATTN: Dr. C. R. Culp (1)
Dr. R. Huntley

ATTN: Dr. Allen Shapiro (1)

Raytheon Company
Foundry Avenue
Waltham, Massachusetts 02154

ATTN: Dr. Frank Horrigan (1)

Riverside Research Institute
80 West End
New York, New York 10023

ATTN: Dr. L. H. O'Neill (1)
ATTN: Dr. John Bose (1)
ATTN: Miss Helen Cressman (1)
ATTN: Hp-EGL Project Library (1)

R&D Associates
P. O. Box 3580
Santa Monica, California 90431

ATTN: Dr. R. E. Lelevier (1)

Thiokol Chemical Corporation
WASATCH Division
P. O. Box 524
Brigham City, Utah 84302

ATTN: Mr. J. M. Stone (1)

TRW Systems Group
One Space Park
Redondo Beach, California 90278

ATTN: Mr. Norman Campbell (1)

United Aircraft Research Laboratories
400 Main Street
East Hartford, Connecticut 06108

ATTN: Mr. G. H. McLafferty (3)
ATTN: Mr. Albert Angelbeck (1)

United Aircraft Corporation
Pratt & Whitney Aircraft Division
Florida Research and Development Center
West Palm Beach, Florida 33402

ATTN: Mr. R. Mulready (1)
ATTN: Mr. Ed Pinsley (1)

Westinghouse Electric Corporation
Defense and Space Center
Friendship International Airport
P. O. Box 746
Baltimore, Maryland 21203

ATTN: Mr. R. A. Lee (1)

Stanford Research Institute
Menlo Park, California 94025

ATTN: Classified Documents Services (1)

A. F. Avionics Laboratory
Wright Patterson Air Force Base, Ohio 45433

ATTN: AFAL/TEO (CPT Wm Boney) (1)

UNCLASSIFIED

Security Classification

DOCUMENT CONTROL DATA - R & D

(Security classification of title, body of abstract and indexing annotation must be entered when the overall report is classified)

1 ORIGINATING ACTIVITY *(Corporate author)*

Environmental Research Institute of Michigan,
Ann Arbor

2a. REPORT SECURITY CLASSIFICATION

UNCLASSIFIED

2b. GROUP

N/A

3 REPORT TITLE

INVESTIGATIONS OF CHEMICAL LASER PROCESSES

4 DESCRIPTIVE NOTES *(Type of report and inclusive dates)*

Semiannual Technical Report 1 January 1972 Through 30 June 1972

5 AUTHOR(S) *(First name, middle initial, last name)*

George H. Lindquist
Robert E. Meredith
Charles B. Arnold
Frederick G. Smith
Robert L. Spellicy

6 REPORT DATE

February 1973

7a. TOTAL NO. OF PAGES

xvi + 183

7b. NO. OF REFS

49

8a CONTRACT OR GRANT NO

DAAH 01-72-C-0572

b PROJECT NO

ARPA Order No. 1108-72

c

d

9a ORIGINATOR'S REPORT NUMBER(S)

191300-1-P

9b OTHER REPORT NO(S) *(Any other numbers that may be assigned this report)*

10 DISTRIBUTION STATEMENT

Initial distribution is indicated at the end of this document.

11 SUPPLEMENTARY NOTES

This contract is monitored by the ARPA Support Office, Army Missile Command, Huntsville, Alabama

12 SPONSORING MILITARY ACTIVITY

Advanced Research Projects Agency
Department of Defense
Washington, D. C. 20301

13 ABSTRACT

A complete set of electric dipole transition probabilities for HCl has been computed by means of a numerical procedure developed previously. To produce these computations, the dipole moment and internuclear potential for the HCl molecule were modeled with the available experimental data. The results are presented in tabular form for vibrational quantum states from 1 to 12, for changes in vibrational states between 0 and 5, and for all rotational states between 0 and 35. Progress on experimental measurements of the intensity of the v = 0 to v' = 4 band of CO are included as well as progress on an experiment to measure rotational relaxation in an excited cell of HF.

Measurements of the strengths and widths of lines in the v = 0 to v' = 3 band of HF are reported. This work was begun under an earlier contract with the Advanced Research Projects Agency, and was completed under the current contract. The electric dipole matrix element for the band has been determined from the measured strengths to be 1.628×10^{-21} esu-cm. The rotational dependence of the measured half widths agrees with the Anderson theory of collision broadening if off-resonant collisions are taken into account. A complete code has been written to compute line widths resulting from collision broadening. A section describing this program is included. Sample calculations which show good agreement with available experimental data are presented.

DD FORM 1 NOV 68 1473

UNCLASSIFIED

Security Classification

14 KEY WORDS	LINK A		LINK B		LINK C	
	ROLE	WT	ROLE	WT	ROLE	WT
Probe laser						
Pump laser						
Hydrogen fluoride						
Line widths						
Hydrogen chloride						
Dipole moment						
Transition probabilities						
Molecular rotation						
Molecular vibration						
HF laser						
Rotational relaxation						
Laser stimulation						
Laser absorption						
Fluorescence						